REFERENCES

[1] Watson, J. D.; Crick, F. H. C., A Structure for deoxyribose nucleic acid. *Nature*, **1953**, *171*, 737-738.

[2] http://spatial.maine.edu~cbultproject.thml.

[3] Uhlmann, E.; Peyman, A. Antisense ODNs: A New Therapeutic Principle. *Chem. Rev.* **1990**, *90*, 544-584.

[4] Zamecnik, P. C.; Stephensen, M. L., Inhibition of Rous sarcoma virus replication and cell transformation by a specific oligodeoxynucleotide. *Proc. Natl. Acad. Sci. USA* **1978**, *75*, 280-284.

[5] Milligan, J. F.; Matteucci, M. D.; Martin, J. C., Current Concept in Antisense Drug Design. *J. Med. Chem.* **1993**, *36*, 1923-1937.

[6] Mesmaeker, A.D; Waldner, A.; Sanghvi, Y. S.; Lebreton, J., Comparison of Rigid and Flexible Backbones in Antisense Oligonucleotides *Bioorg. Med. Chem. Lett.* **1994**, *4*, 395-398.

[7] Nielsen, P. E., DNA analogues with nonphosphodiester backbones. *Annu. Rev. Biophys. Biomol. Struct.* **1995**, *24*, 167-183.

[8] Mesmaeker, A.D.; Altmann, K.-H..; Waldner, A.; Wendeborn, S., Backbone modifications in oligonucleotides and peptide nucleic acid systems. *Curr. Opin. Struc. Bio.* **1995**, *5*, 343-355.

[9] Wengel, J., Synthesis of 3'-C-and 4'-C-branched oligodeoxynucleotides and the development of LNA (locked nucleic acid) *Acc. Chem. Res.* **1999**, *32*, 301-310.

[10] Håkansson, A. E.; Koshkin, A. A.; Sørensen, M. D.; Wengel, J., Convenient syntheses of 7-hydroxy-1-hydroxy-methyl-3-(thymin-1-yl)-2,5-dioxa bicyclo[2.2.1]-heptanes: α-L-ribo- and α-L-xylo-configured LNA nucleosides *J. Org. Chem.* **2000**, *65*, 5161-5166.

[11] Stirchak, E. P.; Summerton, J. E.; Weller, D. D., Uncharged stereoregular nucleic acid analogs: Morpholino nucleoside oligomers with carbamate internucleoside linkages. *Nucleic Acids Res.* **1989**, *17*, 6129-6141.

[12] Nielsen, P. E.; Egholm, M.; Berg, R. H.; Buchardt, O. Sequence-Selective Recognition of DNA by Strand Displacement with a Thymine-Substituted Polyamide. *Science*, **1991**, *254*, 1497-1500.

[13] Egholm, M.; Buchardt, O.; Christensen, L.; Behrens, C.; Freier, S. M.; Driver, D. A.; Berg, R. H.; Kim, S. K.; Norden, B.; Nielsen, P. E. PNA Hybridizes to Complementary Oligonucleotides Obeying the Watson-Crick Hydrogen-Bonding Rules. *Nature* **1993**, *365*, 566-568.

[14] Nielsen, P. E.; Egholm, M.; Buchardt, O., Evidence for $(PNA)_2$/DNA triplex structure upon binding of PNA to dsDNA by strand displacement. *J. Mol. Recog.* **1994**, *7*, 165-170.

[15] Nielsen, P. E.; Haaima, G. Peptide Nucleic Acid (PNA). A DNA Mimic with a Pseudopeptide Backbone. *Chem. Soc. Rev.* **1997**, 73-78.

[16] Brown, S. C.; Thomson, S. A.; Veal, J. M.; Davis, D. G. NMR Solution Structure of a Peptide Nucleic Acid Complexed with RNA. *Science* **1994**, *265*, 777-780.

[17] Erikson, M.; Nielsen, P. E. Solution Structure of a Peptide Nucleic acid-DNA Duplex. *Nat. Struct. Biol.* **1996**, 3410-3413.

[18] Rasmussen, H.; Kastrup, J. S.; Nielsen, J. N.; Nielsen, J. M.; Nielsen, P. E. Crystal Structure of a Peptide Nucleic Acid (PNA) duplex at 1.7Å Resolution. *Nat. Struct. Biol.* **1997**, *4*, 98-101.

[19] Betts, L.; Josey, J. A.; Veal, J. M.; Jordan, S. R. A Nucleic Acid Triple Helix Formed by a Peptide Nucleic Acid-DNA Complex. *Science* **1995**, *270*, 1838-1841.

[20] Soliva, R.; Sherer,E.; Langhton, C. A.; Orozco, M. Molecular Dynamic Simulation of PNA-DNA and PNA-RNA Duplexes in Aqueous Solution. *J. Am. Soc.* **2000**, *122*, 5997-6008.

[21] Peffer, N. J.; Hanvey, J. C.; Bisi, J. E.; Thomson, S. A.; Hassman, C. F.; Noble, S. A.; Basbiss, L. E. Strand-Invasion of Duplex DNA by Peptide Nucleic Acid Oligomer. *Proc. Natl. Acad. Sci. USA.* **1993**, *90*, 10648-10652.

[22] Lesnik, E. A.; Risen, M. R.; Driver, D. A.; Griffith, M. C.; Sprankle, K.; Freier, S. M., Evaluation of pyrimidine PNA binding to ssDNA targets from nonequilibrium melting experiments. *Nucleic Acids Res.* **1997**, *25*, 568-574.

[23] Hyrup, B.; Nielsen, P. E., Peptide nucleic acids (PNA): Synthesis, properties and potential applications. *Bioorg. Med. Chem.* **1996**, *4*, 5-23.

[24] Uhlmann, E.; Peyman, A.; Breipohl, G.; Will, D. W., PNA: synthetic polyamide nucleic acids with unusual binding properties. *Angew. Chem. Int. Ed.* **1998**, *37*, 2796-2823.

[25] Hyrup, B.; Egholm, M.; Nielsen, P. E.; Wittung, P.; Norden, P. B.; Buchardt, O., Structure-Activity Studies of the Binding of Modified Peptide Nucleic Acids (PNAs) to DNA. *J. Am. Chem. Soc.* **1994**, *116*, 7964-7970.

[26] Hyrup, B.; Egholm, M.; Buchardt, O.; Nielsen, P. E., A flexible and positively charged PNA analogue with an ethylene-linker to the nucleobase: Synthesis and hybridization properties. *Bioorg. Med. Chem. Lett.* **1996**, *6*, 1083-1088.

[27] Krotz, A. H.; Buchardt, O.; Nielsen, P. E., Synthesis of 'retro-inverso' peptide nucleic acids: 2. Oligomerization and stability. *Tetrahedron Lett.* **1995**, *36*, 6941-6944.

[28] Vilaivan, T.; Suparpprom, C.; Harnyuttanakorn, P.; Lowe, G., Synthesis and properties of novel pyrrolidinyl PNA carrying β-amino acid spacers. *Tetrahedron Lett.* **2001**, *42*, 5533-5536.

[29] Haaima, G.; Lohse, A.; Buchardt, O.; Nielsen, P. E., P. Peptide nucleic acids (PNAs) containing thymine monomers derived from chiral amino acids: Hybridization and solubility properties of D-lysine PNA. *Angew. Chem. Int. Ed. Engl.* **1996**, *35*, 1939-1942.

[30] Lagriffoule, P.; Wittung, P.; Eriksson, M.; Jensen, K. K.; Norden, B.; Buchardt, O.; Nielsen, P. E., Peptide nucleic acids with a conformationally contrained chiral cyclohexyl-derived backbone. *Chem. Eur. J.* **1997**, *3*, 912-919.

[31] Govindaraju, T.; Kumar, V. A.; Ganesh, K. N. Synthesis and Evaluation of (1*S*,2*R*/1*R*,2*S*)-Aminocyclohexylglycyl PNAs as Conformationally Preorganized PNA Analogues for DNA/RNA Recognition. *J. Org. Chem.* **2004**, *69*, 1858-1865.

[32] Govindaraju, T.; Kumar, V. A.; Ganesh, K. N. (*SR/RS*)-Cyclohexanyl PNAs: Conformationally Preorganized PNA Analogs with Unprecedented Preference for Duplex Formation with RNA. *J. Am. Chem. Soc.* **2005**, *127*, 4144-4145.

[33] Pokorski, J. K.; Myers, M. C.; Appella, D. H., Cyclopropane PNA: observable triplex melting in a PNA constrained with a 3-membered ring. *Tetrahedron Lett.* **2005**, *46*(6), 915-917.

[34] Maison, W.; Schlemminger, I.; Westerhoff, O.; Martens, J., Modified PNAs:a simple method for the synthesis of monomeric building blocks *Bioorg. Med. Chem. Lett.* **1999**, *9*, 581-584.

[35] Gellman, S.H. Foldamers: A Manifesto. *Acc. Chem. Res.* **1998**, *31*, 173-180.

[36] Kirshenbaum, K.; Zuckermann, R. N.; Dill, K. A., Designing polymers that mimic biomolecules. *Curr. Opin. In Struc. Bio.* **1999**, *9*, 530-535.

[37] Appella, D. H.; Christianson, L. A.; Karle, I. L.; Powell, D. R.; Gellman, S. H., *β*-Peptide Foldamers: Robust Helix Formation in a New Family of *β*-Amino Acid Oligomers, *J. Am. Chem.. Soc.*, **1996,** *118,* 13071-13072.

[38] Appella, D. H.; Christianson, L. A.; Klein, D. A.; Richards, M. R.; Powell, D. R.; Gellman, S. H. Synthesis and Structural Characterization of Helix-Forming *β*-Peptides: *trans*-2-Aminocyclopentanecarboxylic Acid Oligomers. *J. Am. Chem. Soc.* **1999**, *121*, 7574-7581.

[39] Appella, D. H.; Christianson, L. A.; Karle, I. L.; Powell, D. R.; Gellman, S. H. Synthesis and Characterization of *trans*-2-minocyclohexanecarboxylic Acid Oligomers: An Unnatural Helical Secondary Structure and Implications for *β*-Peptide Tertiary Structure *J. Am. Chem. Soc.* **1999**, *121*, 6206-6212.

[40] Barchi, J. J. Jr.; Huang, X.; Appella, D. H.; Christianson, L. A.; Durell, S. R.; Gellman, S. H. Solution Conformation of Helix-Forming *β*-Amino Acid Homooligomers. *J. Am. Chem. Soc.* **2000**, *112*, 2711-2718.

[41] Cheng, R. P.; Gellman, S. H.; Degrado, W. F.; β-peptides: From Structure to Function. *Chem. Rev.* **2001**, *101*, 3219-3232.

[42] Abele, S.; Guichard, G.; Seebach, D., (*S*)-β^3-Homolysine and (*S*)-β^3-Homo serine-Containing β-peptides: CD Spectra in aqueous Solution. *Helv. Chim. Acta.* **1998**, *81*, 2141-2156.

[43] Gademann, K.; Jaun, B.; Seebach, D.; Perozzo, R.; Folkers, G., Temperature-Dependent NMR and CD Spectra of β-peptides: On the Thermal Stability of β-peptides Helices - Is the Folding Process of β-peptides Non-Cooperative? *Helv. Chim. Acta.* **1998**, *82*, 1-11.

[44] Daura, X.; van Gunsteren, W. F.; Rigo, D.; Jaun, B.; Seebach, D. Studying the Stability of a Helical β-Heptapeptides by Molecular Dynamics Simulations. *Chem. Eur. J.* **1997**, **3**, 1410-1417.

[45] Pokorski, J. K.; Witschi, M. A.; Purnell, B. L.; Appella, D. H. (*S,S*)-*trans*-Cyclopentane-Constrained Peptide Nucleic Acids. A General Backbone Modification that Improves Binding Affinity and Sequence Specificity. *J. Am. Chem. Soc.* **2004**, *126*, 15067-15073.

[46] Englund, E. A.; Xu, Q.; Witschi, M. A.; Appella, D. H. PNA·DNA Duplexes, Triplexes, and Quadruplexes Are Stabilized with *trans*-Cyclopentane Units. *J. Am. Chem. Soc.* **2006**, *128*, 16456-16457.

[47] Schmitt, M. A.; Weisblum, B.; Gellman, S. H. Unexpected Relationships between Structure and Function in α,β-Peptides: Antimicrobial Foldamers with Heterogeneous Backbones. *J. Am. Chem. Soc.* **2004**, *126*, 6848-6849.

[48] Schmitt, M. A.; Choi, S. H.; Guzei, I. A.; Gellman, S., Residue Requirements for Helical Folding in Short α:β-Peptides: Crystallographic Characterization of the 11-Helix in an Optimized Sequence. *J. Am. Chem. Soc.* **2005**, *127*, 13130-13131.

[49] Schmitt, M. A.; Choi, S. H.; Guzei, I. A.; Gellman, S. H. New Helical Foldamers: Heterogeneous Backbones with 1:2 and 2:1 α:β-Amino Acid Residue Patterns. *J. Am. Chem. Soc.* **2006**, *128*, 4538-4539.

[50] D'Costa, M.; Kumar, V. A.; Ganesh, K. N., Aminoethylprolyl Peptide Nucleic Acids (*aep*PNA): Chiral PNA Analogues That Form Highly Stable DNA:*aep*PNA_2 Triplexes. *Org. Lett.* **1999**, *1*(10), 1513-1516.

[51] Lowe, G.; Vilaivan, T.; Westwell, M. S., Hybridization Studies with Chiral Peptide Nucleic Acids. *Bioorg. Chem.* **1997**, *25*, 321-329.

[52] Jordan, S.; Schwemler, C.; Kosch, W.; Kretschmer, A.; Schwenner, E.; Stropp, U.; Mielke, B. Synthesis of new building blocks for peptide nucleic acids containing monomers with variations in the backbone. *Bioorg. & Med. Chem. Lett.* **1997**, *7*, 687-690.

[53] Vilaivan, T.; Khongdeesameor, C.; Harnyuttanakorn, P.; Westwell, M. S.; Lowe, G. Synthesis and Properties of Chiral Peptide Nucleic Acids with a *N*-Aminoethyl-D-proline Backbone. *Bioorg. & Med. Chem. Lett.* **2000**, *10*, 2541-2545.

[54] Liu, Y.; Jin, T.; L, K., Synthesis and Binding Affinity of a Chiral PNA analogue. *Nucleosides, Nucleotides & Nucleic Acids*, **2001**, *20*(9), 1705-1721.

[55] Sharma, N. K.; Ganesh, K. N., Expanding the repertoire of pyrrolidyl PNA analogues for DNA/RNA hybridization selectivity: aminoethyl pyrrolidinone PNA (*aepone*PNA). *Chem. Commun.* **2003**, 2484-2485.

[56] Altmann, K. H.; Husken, D.; Cuenoud, B.; Garcia-Echeverria, C., Synthesis and Hybridization Properties of Polyamide Based Nucleic Acid Analogues Incorporating Pyrrolidine-derived Nucleoamino Acids. *Bioorg. & Med. Chem. Lett.* **2000**, *10*, 929-933.

[57] Altmann, K.-H.; Chiesi, C. S.; Garcia-Echeverria, C., Polyamide based nucleic acid analogs - synthesis of .delta.-amino acids with nucleic acid bases bearing side chains. *Bioorg. & Med. Chem. Lett.* **1997**, *7(9)*, 1119-1122.

[58] García-Echeverría, C.; Hüsken, D.; Chiesi, C. S.; Altmann, K. H., Novel Polyamide Based Nucleic Acid Analogs - Synthesis of Oligomers and RNA-Binding Properties, *Bioorg. Med. Chem. Lett.*, **1997**, *7*(9), 1123-1126.

[59] Hickman. D. T.; King, P. M.; Cooper, M. A.; Slater, J. M.; Micklefield, J., Unusual RNA and DNA binding properties of a novel pyrrolidine-amide oligonucleotides mimic (POM). *Chem. Commun.* **2000**, 2251-2252.

[60] Hickman, D. T.; Samuel Tan, T. H.; Morral, J.; King, P. M.; Cooper, M. A.; Micklefield, J. Design, synthesis, conformational analysis and nucleic acid hybridization properties of thymidyl pyrrolidine-amide oligo nucleotide mimics (POM)., *Org. Biomol. Chem.* **2003**, *1*, 3277-3292.

[61] Samuel Tan, T. H.; Hickman, D. T.; Morral, J.; Beadham, I. G.; Micklefield, J., Nucleic acid binding properties of thyminyl and adeninyl pyrrolidine-amide oligonucleotide mimics (POM). *Chem.Commun.* **2004**, 516-517.

[62] Worthington, R. J.; O'Rourke, A. P.; Morral, J.; Samuel Tan, T. H.; Micklefield, J., Mixed-sequence pyrrolidine-amide oligonucleotide mimics: Boc(Z) synthesis and DNA/RNA binding properties. *Org. Biomol. Chem.*, **2007**, *5*, 249-259.

[63] Govindaraju, T.; Kumar, V. A., Backbone Extended Pyrrolidine Peptide Nucleic Acids (*bep*PNA): Design, Synthesis and DNA/RNA binding Studies. *Chem. Commun.* **2002**, 1-2.

[64] Govindaraju, T.; Kumar, V. A., Backbone extended pyrrolidine PNA (*bep*PNA): a chiral PNA for selective RNA recognition. *Tetrahedron*, **2006**, *62*, 2321-2330.

[65] D'Costa, M.; Kumar, V. A.; Ganesh, K. N., Synthesis of 4(*S*)-(*N*-Boc-amino)-2-(*S*/*R*)-(thymin-1-ylmethyl)-pyrrolidine-*N*-1-acetic acid: a novel cyclic PNA with constrained flexibility. *Tetrahedron Lett.* **2002**, *43*, 883-886.

[66] Lonkar, P. S.; Ganesh, K. N.; Kumar, V. A., Chimeric (*aeg*-pyrrolidine)PNAs: synthesis and stereo-discriminative duplex binding with DNA/RNA. *Org. Biomol. Chem.* **2004**, *2*, 2604-2611.

[67] Püschi, A.; Tedeschi, T.; Nielsen, P. E., Pyrrolidine PNA: A Novel Conformationally Restricted PNA Analogue. *Org. Lett.* **2000**, *2*(26), 4161-4163.

[68] Püschi, A.; Boesen, T.; Zuccarello, G.; Dahl, O.; Pitsch, S.; Nielsen, P. E., Synthesis of Pyrrolidinone PNA: A Novel Conformationally Restricted PNA Analogue. *J. Org. Chem.* **2001**, *66*, 707-712.

[69] Norden, B.; Ray, A. Peptide Nucleic Acid (PNA): Its Medical and Biotechnical Applications and Promise for the Future. *The FASEB Journal* **2000**, *14*, 1041-1059.

[70] Mologni, L.; IeCoutre, P., Nielsen, P. E.; Gambacorti-Passerini, C., Additive antisense effects of different PNAs on the *in vitro* translation of the PML/RARα gene. *Nucleic Acids Res.* **1998**, *26*, 1934-1938.

[71] Taylor, R. W.; Chinnery, P. F.; Turnbull, D. M.; Lightowlers, R. N., Selective inhibition of mutant human mitochondrial DNA replication *in vitro* by peptide nucleic acids. *Nature Genet.* **1997**, *15*, 212-215.

[72] Winssinger, N. *et al.* From split-pool libraries to spatially addressable microarrays and its application to functional proteomic profiling. *Angew. Chem. Int. Ed. Engl.* **2001**, *40*, 3152–3155.

[73] Komiyama, M.; Ye, S.; Liang, X.; Yamamoto, Y.; Tomita, T.; Zhou, J; Aburatani, H. PNA for One-base Differentiating Protection of DNA from Nuclease and Its Use for SNPs Detection. *J. Am. Chem. Soc.* **2003**, *125*, 3758-3762.

[74] Lutz, M. J.; Benner, S. A.; Hein, S.; Breipohl, G; Uhlmann, E., Recognition of uncharged polyamide-linked nucleic acid analogs by DNA polymerases and reverse transcriptases, *J. Am. Chem. Soc.* **1997**, *119*, 3177-3178.

[75] Thiede, C.; Bayerdörffer, E.; Blasczyk, R.; Wittig, B., A. Neubauer, Simple and sensitive detection of mutations in the rat proto-oncogenes using PNA-mediated PCR clamping, *Nucleic Acids Res.* **1996**, *24*, 983-984.

[76] Svanvik, N.; Stahlberg, A.; Sehlstedt, U.; Sjöback, R.; Kubiska, M.; Detection of PCR products in real time using light-up probes, *Anal. Biochem.* **2000**, *287*, 179-183.

[77] Khongdeesameor, C., Synthesis of novel peptide nucleic acids carrying hydrophilic side chain and their properties. Master degree Thesis, Chulalongkorn University, **1999**.

[78] Croce P. D.; La Rosa C., Stereoselective synthesis of (1*R*,4*R*)-*N*-acyl-2-oxa-5-aza-bicyclo[2.2.1]heptan-3-ones via mesoionic compounds. An improved synthesis of *cis*-4-hydroxy-D-proline. *Tetrahedron Asym.*; **2002**, 13, 197-201.

[79] Lowe, G.; Vilaivan, T., Amino Acids Bearing Nucleobases for the Synthesis of Novel Peptide Nucleic Acids. *J. Chem. Soc., Perkin Trans. 1* **1997**, 539-546.

[80] Lowe, G.; Vilaivan, T., Dipeptides Bearing Nucleobases for the Synthesis of Novel Peptide Nucleic Acids. *J. Chem. Soc.; Perkin Trans. 1* **1997**, 547-554.

[81] Lowe, G.; Vilaivan, T. Solid Phase Synthesis of Novel Peptide Nucleic Acids. *J. Chem. Soc.; Perkin Trans. I.* **1997**, 555-560.

[82] Tozuka, Z.; Takoya, T.; Studies on Tomaymycin I: The Structure Determination of Tomaymycin on the basis of NMR Spectra. *J. Antibiotics*, **1983**, *36*, 142.

[83] Miller, J. B.; Preparation of crystalline Diphenyldiazomethane. *J. Org. Chem.*, **1959**, 24, 560-561.

[84] Cruickshank, K. A.; Jiriony, J.; Reese, C. B., The Benzoylation of Uracil and Thymine. *Tetrahedron*, **1984**, 25(6), 681-684.

[85] Peterson, M. L.; Vince, R., Synthesis and Biological Evaluation of 4-Purinylpyrrolidine Nucleosides. *J. Med. Chem.*, **1991**, 34, 2787-2797.

[86] Mitsunobu, O. The Use of Diethylazodicarboxylate and Triphenylphosphine in Synthesis and Transformation of Natural Products. *Synthesis* 1, **1981**, 1-28.

[87] Zijlmans, M. J. M.; Martens, U. M.; Poon, S. S. S.; Raap, A. K.; Tanke, H. J.; Ward, R. K.; Lansdorp, P. M.; Telomeres in the Mouse Have Large Inter-Chromosomal Variation in the Number of T_2AG_3 Repeats. *Proc. Natl. Acad. Sci.* **1997**, *94*, 7423-7428.

[88] Bullock, M. W.; Hand, J. J.; Stockstad, E. L. R. Reduction of 6-Aroylaminopurines with Lithium Aluminum Hydride. *J. Org. Chem.* **1957**, *22*, 568-569.

[89] Stelakatos, G. C.; Paganou, A.; Zervas, L., New methods in peptide synthesis. Part III. Protection of carboxyl group. *J. Chem. Soc. C*, **1966**, 1191-1199.

[90] Brown, D.; Todd, A.; Varadarajan, S. The structures of some acylcytosines, *J. Chem. Soc.* **1956**, 2384-2387.

[91] Porter, N. A.; Caldwell, S. E.; Lowe, J. R. Preparation of Unsymmetrically Labelel Hydroperoxides. A Hydroxamate Ester-Nitrosation Approch. *J.Org. Chem.* **1998**, *63*, 5547-5554.

[92] Takeda, K.; Akiyama, A.; Nakamura, H.; Takizawa, S.; Mizuno, Y.; Takayanagi, H.; Harigaya, Y.; Dicarbonates: Convenient 4-Dimethyl aminopyridine Catalyzed Esterification Reagents. *Synthesis*, **1994**, 1063-1066.

[93] Murata, M.; Hara T.; Mori, K.; Ooe M.; Mizugaki, T.; Ebitani, K.; Kaneda K. Efficient deprotection of *N*-benzyloxycarbonyl group from amino acids by hydroxyapatite-bound Pd catalyst in the presence of molecular hydrogen. *Tetrahedron Asym.*, **2003**, 44, 4981-4984.

[94] Klosterman, H. J.; Lamoureux, G. L.; Parsons, J. L. Isolation, Characterization and Synthesis of Linatine. A Vitamin B_6 Antagonist from Flaxseed (Linum usitatissimum). *Biochemistry*. **1967**, *6*, 170-177.

[95] LePlae, P, R.; Umezawa, N.; Lee, H.–S.; Gellman, S. H. An Efficient Route to Either Enantiomer of *trans*-2-Aminocyclopentanecarboxylic Acid. *J. Org. Chem.* **2001**, *66*, 5629-5632.

[96] Cimarelli, C.; Palmieri, G.; Diastereo and Enantioselective Entry to β-Amino Esters by Hydride Reduction of Homochiral β-Enamino Esters. *Tetrahedron Asym*, **1994**, *5*(8), 1455-1458.

[97] Cassani, G. R.; Bollum, F., Oligodeoxythymidylate:polydeoxyadenylate and oligodeoxyadenylate:polydeoxythymidylate interactions. *J. Biochemistry*, **1969**, *8*, 3928-3936.

[98] Sambrook, J., Fritsh, E. F., Maniatis, T. Molecular Cloning: A Laboratory Manual. 2nd ed. New York: Cold spring harbor laboratory press, **1989**.

[99] Greenstein, J. P.; Winitz, M. Chemistry of the Amino Acids. New York: John Wiley & Sons, **1961**.

[100] Baker, G. L.; Fritschel, S. J.; Stille, J. R.; Stille, J. K. Transition-Metal-Catalyzed Asymmetric Organic Synthesis *via* Polymer-Attached Optically Active Phosphine Ligand: Preparation of Amino Acids in High Optical Yield *via* Catalytic Hydrogenation. *J. Org. Chem.* **1981**, *46*, 2954-2960.

[101] Vilaivan, T. Synthesis and Properties of Novel Nucleopeptides. Doctoral Dissertation, University of Oxford, **1996**.

[102] Borcherding, D. R.; Butler, B. T.; Linnik, M. D.; Mehdi, S.; Dudley, M. W.; Edward, C. K., *cis*-(1*S*,3*R*)-1-(9-Adenyl)-3-Hydroxy-Cyclopentane Inhibits the Respiratory Burst from Polymorphonuclear Leukocytes and has *in vivo* Efficacy in an Acute and Chronic Model of Imflammation. *Nucleosides Nucleotides*. **1996**, *15*, 967-969.

[103] Verheggen, I.; Aerschot, A. V.; Toppet, S.; Snoeck, R.; Janssen, G.; Balzarini, J.; Clercq, E. D.; Herdewijn, P. Synthesis and Antiherpes Virus Activity of 1,5-Anhydrohexitol Nucleosides. *J. Med. Chem.*, **1993**, *36*, 2033-2040.

[104] Verheggen, I.; Aerschot, A. V.; Meervelt, L. V.; Rozenski, J.; Wiebe, L.; Snoeck, R.; Andrei, G.; Balzarini, J.; Claes, P.; De Clercq, E.; Herdewijn, P. Synthesis, Biological Evaluation, and Structure Analysis of a Series of New l,5-Anhydrohexitol Nucleosides. *J. Med. Chem.*, **1995**, *38*, 826-835.

[105] Perez-Perez, M. J.; Rozenski, J.; Busson, R.; Herdewijn, P. Application of the Mitsunobu-Type Condensation Reaction to the Synthesis of Phosphonate Derivatives of Cyclohexenyl and Cyclohexanyl Nucleosides. *J. Org. Chem.*, **1995**, *60*, 1531-1537.

[106] Büchi H, Khorana HG. CV. Total synthesis of the structural gene for an alanine transfer ribonucleic acid from yeast. Chemical synthesis of an icosadeoxyribonucleotide corresponding to the nucleotide sequence 31 to 50. *J Mol Biol.* **1972**, *72*(2), 251–288.

[107] Jenny, T. F.; Schneider, K. C.; Benner, S. A., N^2-isobutyrl-O^6-[2-(para-nitrophenyl)ethyl]guanine: A new building block for the efficient synthesis of carbocyclic guanosine analogs. *Nucleosides & Nucleotides*, **1992**, *11*, 12571261.

[108] Green, G. R.; Grinter, T. J.; Kincey, P. M., Jarvest, R. L., The effect of the C-6 substituent on the regioselectivity of n-alkylation of 2-aminopurines. *Tetrahedron*, **1990**, 46, 6903-6914.

[109] United States Patent: 6,133,444.

[110] Greene, T. W.; Wuts, P. G. M. Protective Groups in Organic Synthesis, 3rd ed., New York: John Wiley & sons, **1999**, 506-507.

[111] Srisuwannaket, C.; Synthesis and DNA-Binding Properties of Pyrrolidinyl Peptide Nucleic Acids Bearing (1*S*,2*S*)-2-Aminocyclopentane Carboxylic Acids Spacer. Doctoral Dissertation. Chulalongkorn University, **2005**.

[112] Vilaivan, T.; Suparpprom, C.; Duanglaor, P.; Harnyuttanakorn, P.; Lowe, G. Synthesis and Nucleic Acid Binding Studies of Novel Pyrrolidinyl PNA Carrying an *N*-amino-*N*-methylglycine Spacer. *Tetrahedron Lett.* **2003**, *44*, 1663-1666.

[113] Dhaon, M. K.; Olsen, R. K.; Ramasamy, K. Esterification of *N*-Protected α-Amino Acids with Alcohol/Carbodiimde/4-(Dimethylamino)-pyridine. Racemization of aspartic and Glutamic Acid Derivatives. *J. Org. Chem.* **1982**, *47*, 1962-1965.

[114] Thorsett, E. D.; Conversion of α-aminoesters to α-ketoesters. *Tetrahedron Lett.* **1982**, *23*, 1875-1876.

[115] Guy, L.; Vidal, J.; Collet, A. Design and Synthesis of Hydrazinopeptides and Their Evaluation as Human Leukocyte Elastase Inhibitors. *J. Med. Chem.* **1998**, *41*, 4833-4843.

[116] Vidal, J.; Guy, L.; Sterin, S.; Collet, A. Electrophilic Amination: Preparation and Use of *N*-Boc-3-(4-cyanophenyl)oxaziridine, a New Reagent that Transfer a N-Boc Group to *N*- and *C*-Nucleophiles. *J. Org. Chem.* **1993**, *58*, 4791-4793.

[117] Vidal, J.; Damestoy, S.; Guy, L.; Hannachi, J. C.; Aubry, A.; Collet, A. *N*-Alkyloxycarbonyl-3-aryloxaziridines: Their Preparation, Structure and Utilization as Electrophilic Amination Reagents. *Chem. Eur. J.* **1997**, *3*(10), 1691-1709.

[118] Yamazaki, T.; Zhu, Y.-F.; Probstl, A.; Chadha, R. K.; Goodman, M. Probing a Molecular Model of Taste Utilizing Peptidomimetic Stereoisomers of 2-Aminocyclopentanecarboxylic Acid Methyl Ester. *J. Org. Chem.*, **1991**, *56*, 6644-6655.

[119] Merrifield, R. B. Solid Phase Peptide Synthesis of a Tetrapeptide. *J. Am. Chem. Soc.* **1963**, *85*, 2149-2154.

[120] TentaGel is a trademark of Rapp Polymer GmbH, Tubingen, Germany.

[121] Rink, H. Solid-phase synthesis of protected peptide fragments using a trialkoxy-diphenyl-methylester resin. *Tetrahedron Lett.* **1987**, *28*, 3787-3790.

[122] Wang, S.; *p*-Alkoxybenzyl Alcohol Resin and *p*-Alkoxybenzyloxycarbonyl hydrazide Resin for Solid Phase Synthesis of Protected Peptide Fragments. *J. Am. Chem. Soc.*, **1972**, *95*, 1328-1333.

[123] Vilaivan, T.; Lowe, G. A Novel Pyrrolidinyl PNA Showing High Sequence Specificity and Preferential Binding to DNA over RNA. *J. Am. Chem. Soc.* **2002**, *124*, 9326-9327.

[124] Eghlom, M.; Buchardt, O.; Nielsen, P. E.; Berg, R. H. Peptide Nucleic Acid (PNA). Oligonucleotide Analogues with an Achiral Peptide Backbone. *J. Am. Chem. Soc.* **1992**, *114*, 1895-1897.

[125] Carpino, L. A. 1-Hydroxy-7-azabenzotriazole. An Efficient Peptide Coupling Additive. *J. Am. Chem. Soc.* **1993**, *115*, 4397-4398.

[126] Bodanszky, M. Peptide Chemistry. A Practical Text Book, 2nd ed., New York: Springer-Verlag Berlin Heidelberg. **1993**, 60-68.

[127] Nudelman, A.; Bechor, Y.; Falb, E.; Fisher, B.; Wexler, B. A.; Nudelman, A., Acetyl chloride-methanol as a convenient reagent for: a) quantitative formation of amine hydrochlorides b) carboxylate ester formation c) mild removal of *N-tert*-Boc-protective group, *Synth. Commun.* **1998**, *28*, 471-474.

[128] Lilley, D. M. J. Methods in Enzymology, Volume 211, DNA Structures Part A: Synthesis and Physical Analysis of DNA, Academic press, 389-405.

[129] Blackburn, G. M.; Gart, M. S. Nucleic Acids in Chemistry and Biology, 2nd ed., New York: Oxford University Press. 446-451.

[130] Voet, D.; Voet, J. G. Biochemistry, 2nd ed., New York: John Wiley & Sons, 862-870.

[131] Tomac, S.; Sarrkar, M.; Ratilainem, P.; Nielsen, P. E.; Norden, B.; Gräslund, A. Ionic Effect on the Stability and Conformation of Peptide Nucleic Acid Complexes. *J. Am. Chem. Soc.* **1996**, *118*, 5544-5552.

[132] Suparpprom, C.; Srisuwannaket, C.; Sangvanich, P.; Vilaivan, T. Synthesis and Oligodeoxynucleotide Binding Properties of Pyrrolidinyl Peptide Nucleic Acids Bearing Prolyl-2-aminocyclopentanecarboxylic Acid (ACPC) Backbones. *Tetrahedron Lett.* **2005**, *46*, 2833-2837.

[133] Egholm, M.; Buchardt, O.; Nielsen, P. E.; Berg, R. H. Peptide Nucleic Acids (PNA). Oligonucleotide Analogues with an Achiral Peptide Backbone. *J. Am. Chem. Soc.* **1992**, *114*, 1895-1897.

[134] Job, P. Formation and stability of inorganic complexes in solution. *Ann. Chim.* **1928**, *9*, 113-203.

[135] Vilaivan, T.; Srisuwannaket, C. Hybridization of Pyrrolidinyl Peptide Nucleic Acids and DNA: Selectivity, Base-Pairing Specificity and Direction of Binding. *Org. Lett.* **2006**, *8*(9), 1879-1900.

[136] Schütz, R.; Cantin, M.; Roberts, C.; Greiner, B.; Uhlmann, E.; Leumann, C. Olifinic Peptide Nucleic Acids (OPNAs) : New Aspects of the Molecular Recognition of DNA by PNA. *Angew. Chem. Int. Ed.* **2000**, *39*. 1250-1253.

[137] Chiuchay, P.; Saen-Oon, S.; Vilaivan, T.; Hannongbua, S., Structure and Dynamic Properties of Pyrrolidinyl Peptide Nucleic Acids Binding to DNA in Water. *31st Congress on Science and Technology of Thailand*, **2005**.

[138] Noteberg, D.; Branalt, J.; Kvarnstrom, I.; Classon, B.; Samuelsson, B.; Nillroth, U.; Helena Danielson, U.; Karlsen, A.; Hallberg, A., Synthesis of enantiomerically pure *cis* and *trans* 2-aminocyclopentane carboxylic acids. Use of proline replacements in potential HIV-protease inhibitors. *Tetrahedron*, **1997**, *53*(23), 7975-7984.

[139] Sugimura, T.; Iguchi, H.; Tsuchida, R.; Tai, A.; Nishiyama, N.; Hakushi, T., Diastereoface-differentiating oxidation of 1-cyclohexenyl ether using a 2,4-pentanediol tether. *Tetrahedron Asym.* **1998**, *9*(6), 1007-1013.

APPENDICES

APPENDIX A

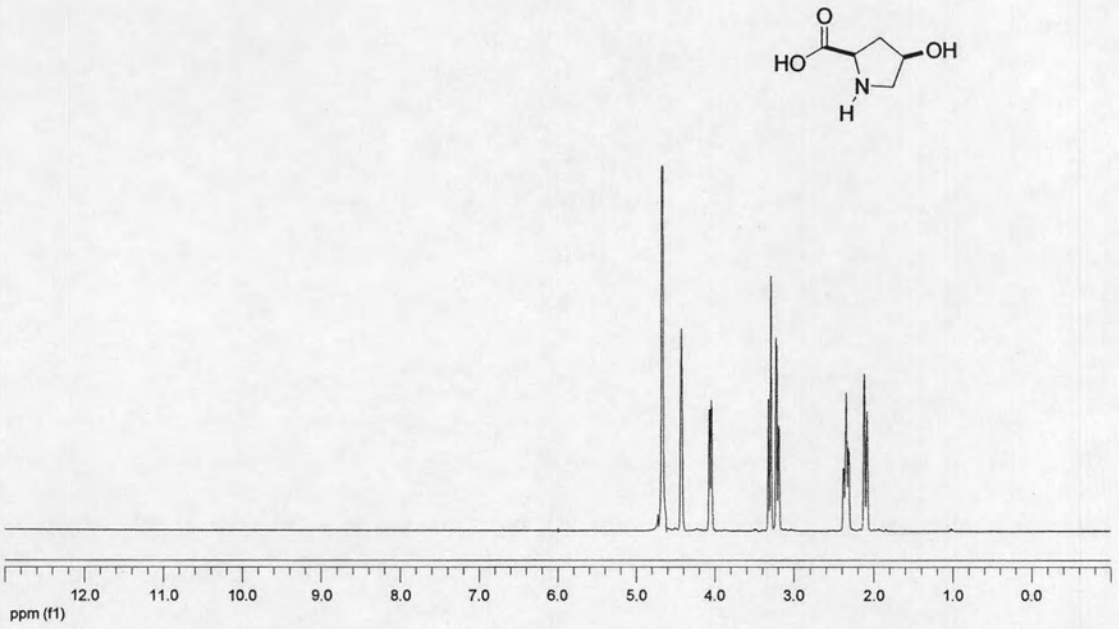

Figure A-1: ^{1}H NMR (400 MHz, D_2O) of *cis*-4-Hydroxy-D-proline (**1**)

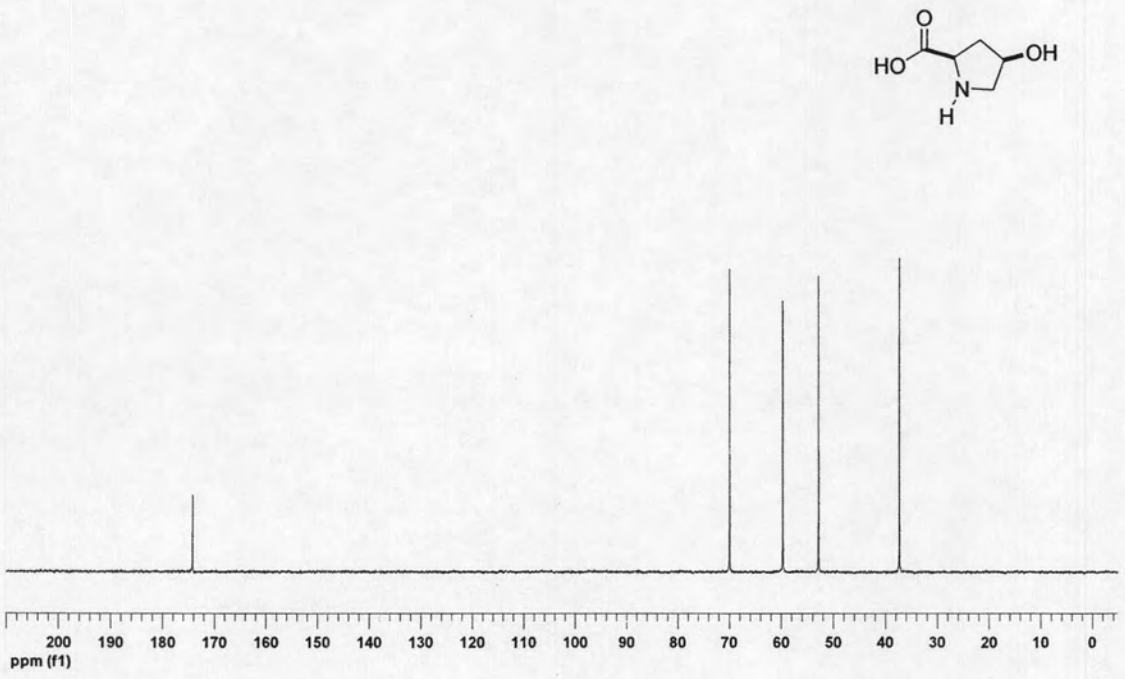

Figure A-2: ^{13}C NMR (100 MHz, D_2O) of *cis*-4-Hydroxy-D-proline (**1**)

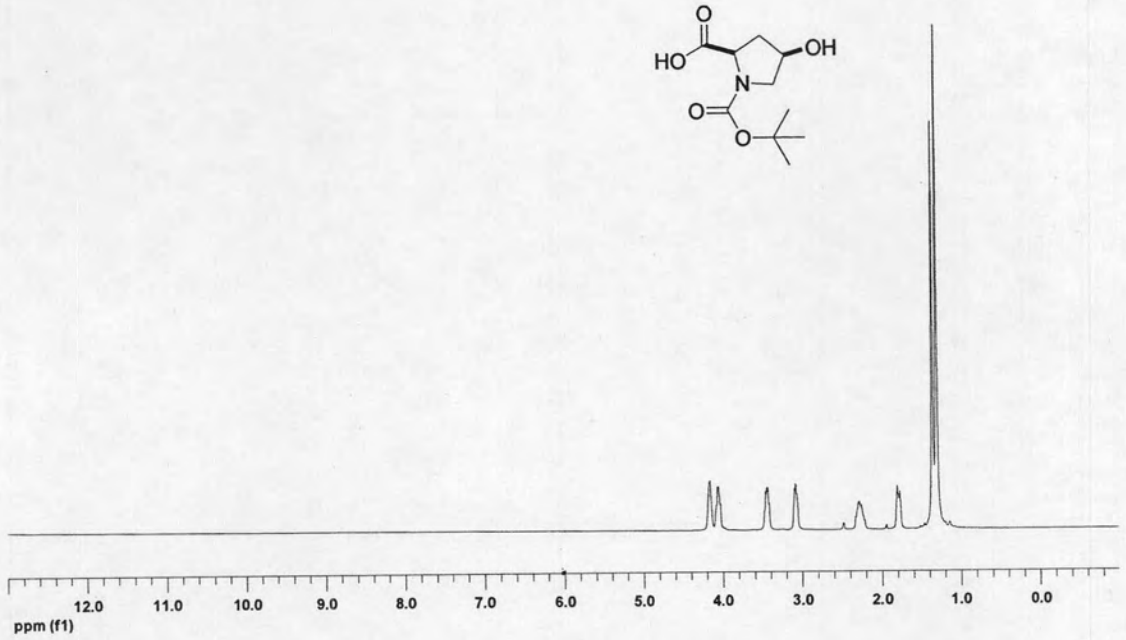

Figure A-3: ^{1}H NMR (400 MHz, DMSO-d_6) of *N-tert*-Butoxycarbonyl-*cis*-4-hydroxy-D-proline (**2**)

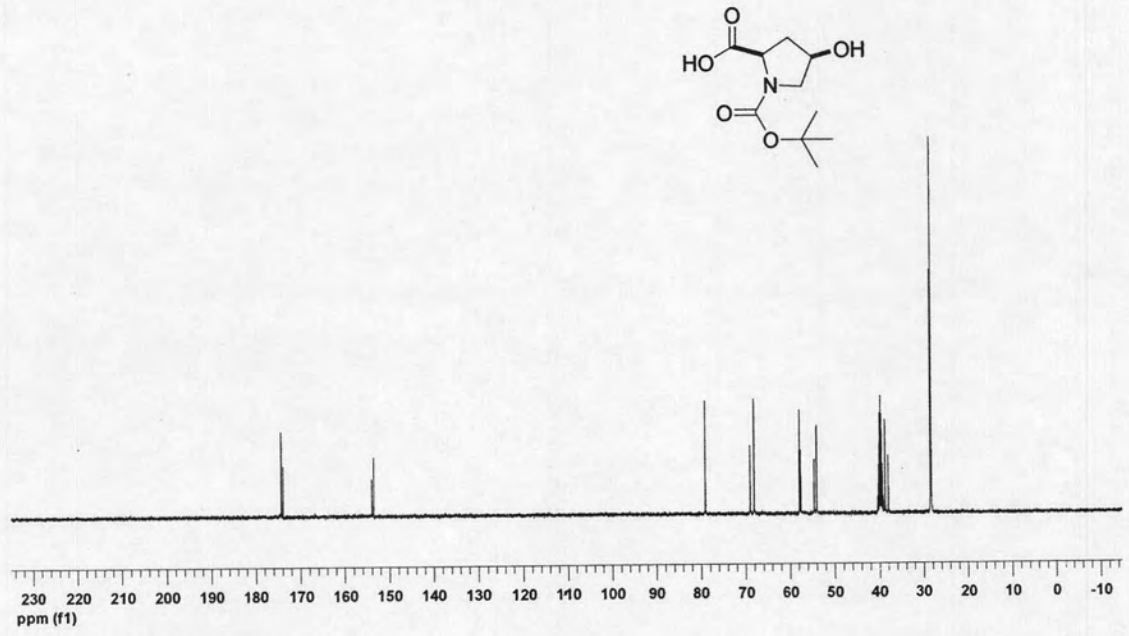

Figure A-4: ^{13}C NMR (100 MHz, DMSO-d_6) of *N-tert*-Butoxycarbonyl-*cis*-4-hydroxy-D-proline (**2**)

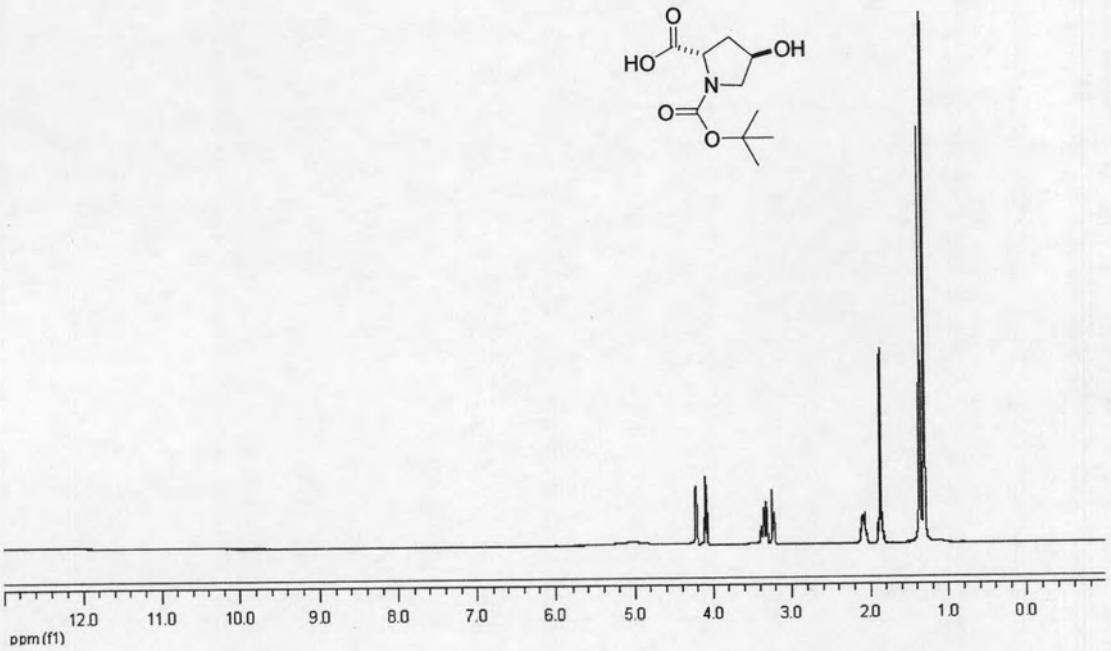

Figure A-5: ^{1}H NMR (200 MHz, DMSO-d_6) of *N-tert*-Butoxycarbonyl-*trans*-4-hydroxy-L-proline (**3**)

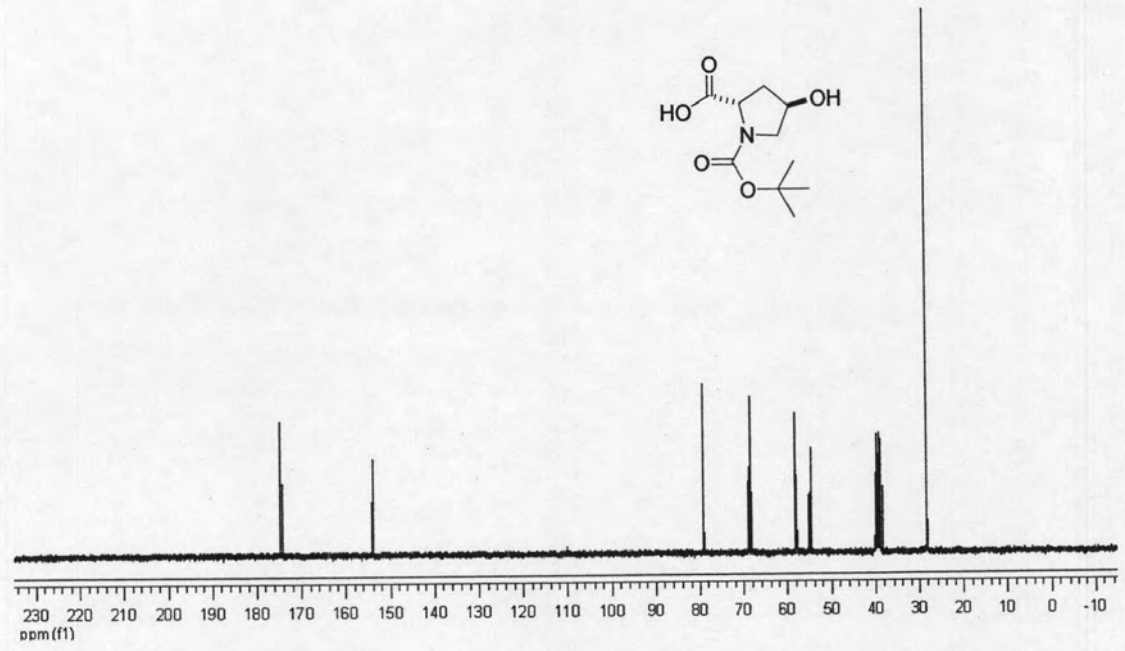

Figure A-6: ^{13}C NMR (50 MHz, DMSO-d_6) of *N-tert*-Butoxycarbonyl-*trans*-4-hydroxy-L-proline (**3**)

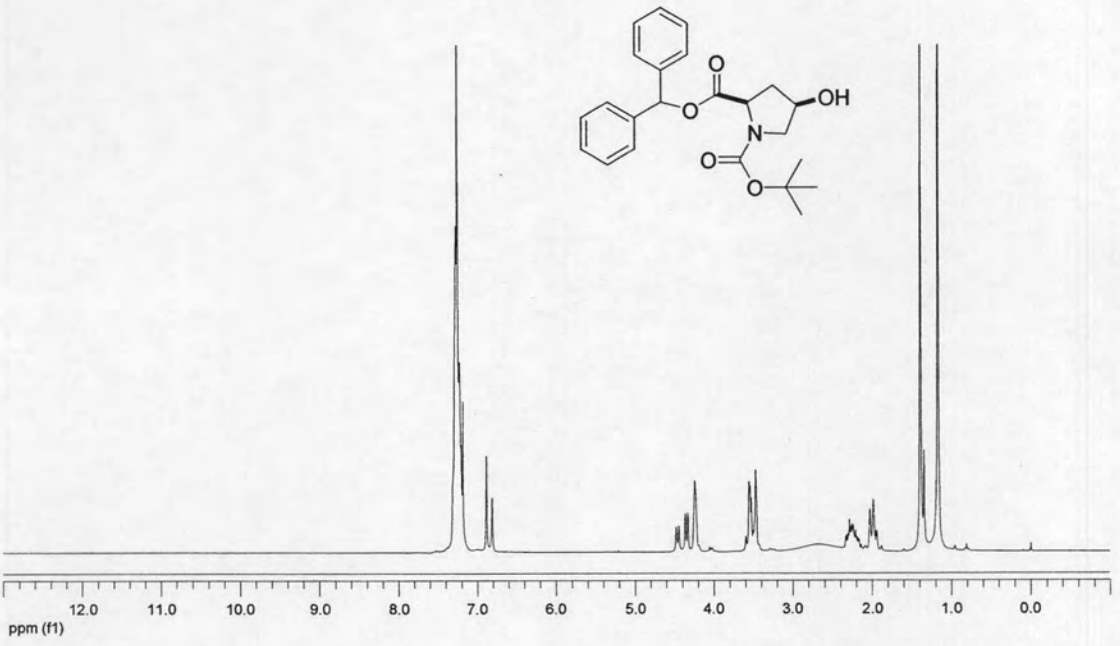

Figure A-7: ^{1}H NMR (300 MHz, $CDCl_3$) of *N-tert*-Butoxycarbonyl-*cis*-4-hydroxy-D-proline diphenylmethyl ester (**5**)

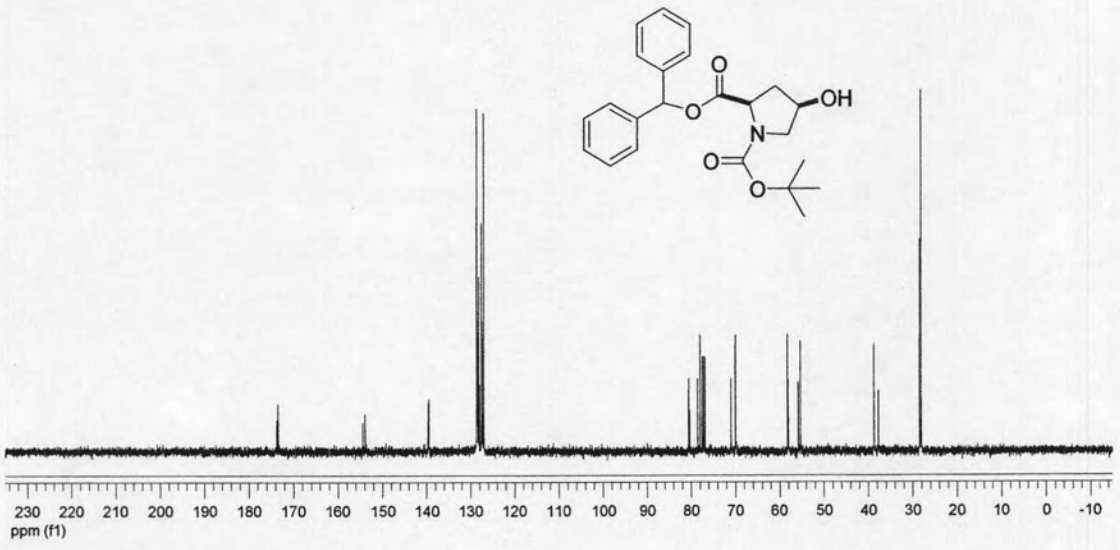

Figure A-8: ^{13}C NMR (75 MHz, $CDCl_3$) of *N-tert*-Butoxycarbonyl-*cis*-4-hydroxy-D-proline diphenylmethyl ester (**5**)

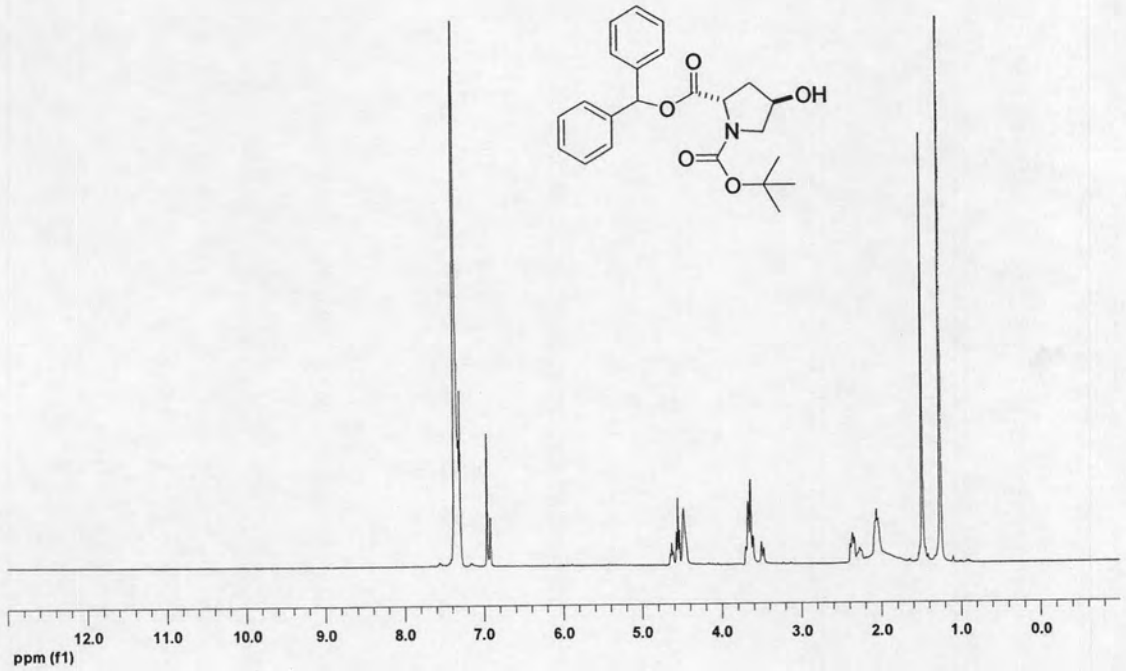

Figure A-9: ^{1}H NMR (400 MHz, $CDCl_3$) of *N-tert*-Butoxycarbonyl-*trans*-4-hydroxy-L-proline diphenylmethyl ester (**6**)

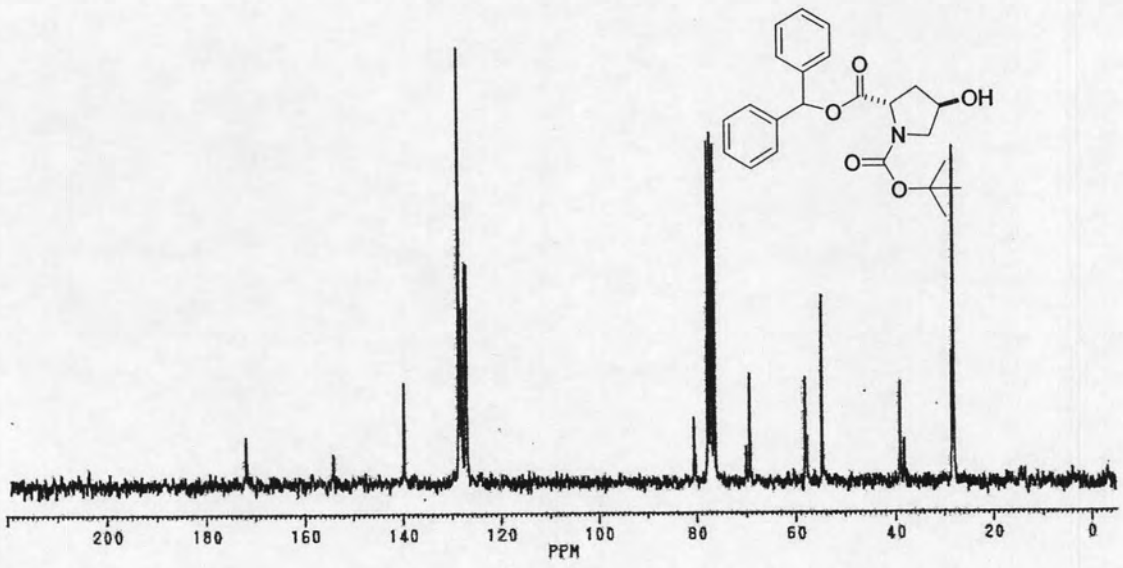

Figure A-10: ^{13}C NMR (50 MHz, $CDCl_3$) of *N-tert*-Butoxycarbonyl-*trans*-4-hydroxy-L-proline diphenylmethyl ester (**6**)

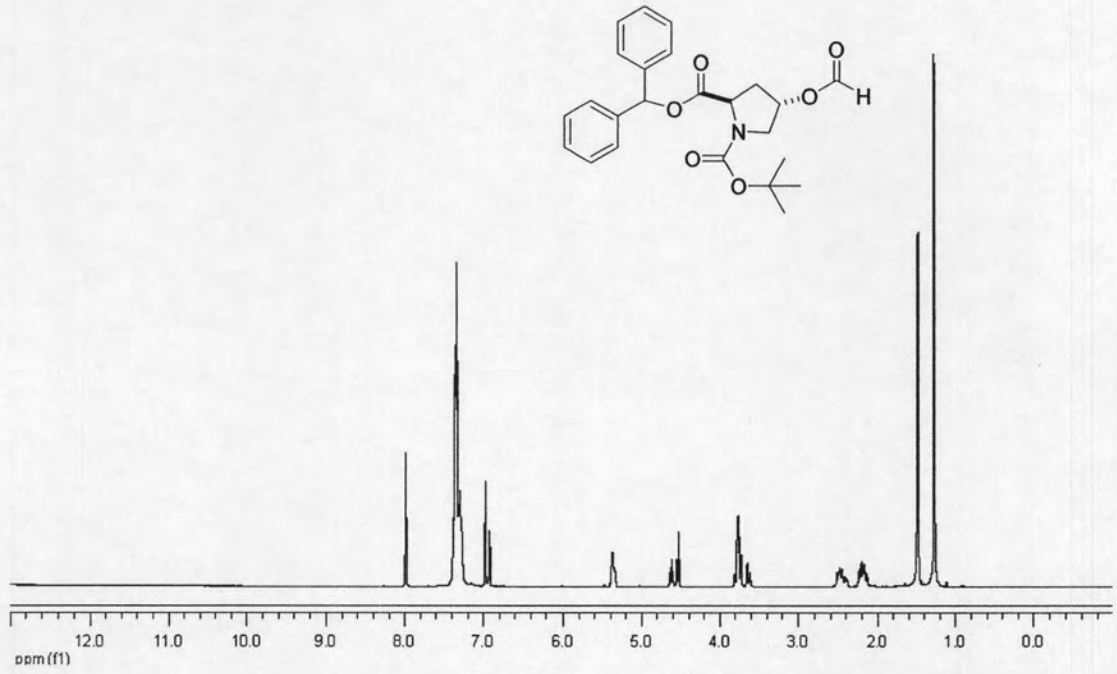

Figure A-11: ^{1}H NMR (400 MHz, $CDCl_3$) of *N-tert*-Butoxycarbonyl-*trans*-4-formyl-D-proline diphenylmethyl ester (**7**)

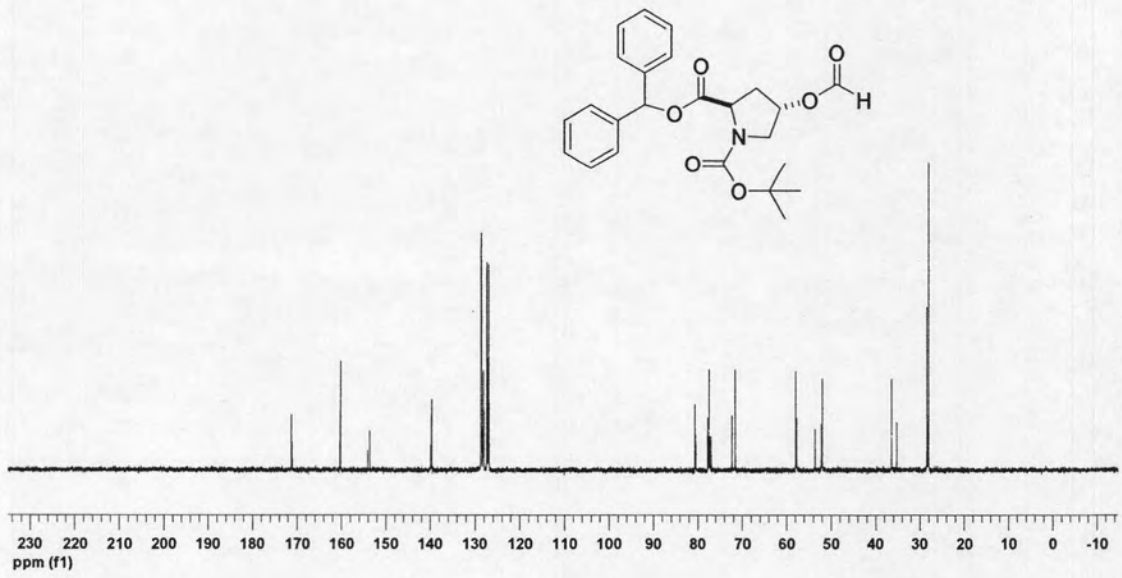

Figure A-12: ^{13}C NMR (100 MHz, $CDCl_3$) of *N-tert*-Butoxycarbonyl-*trans*-4-formyl-D-proline diphenylmethyl ester (**7**)

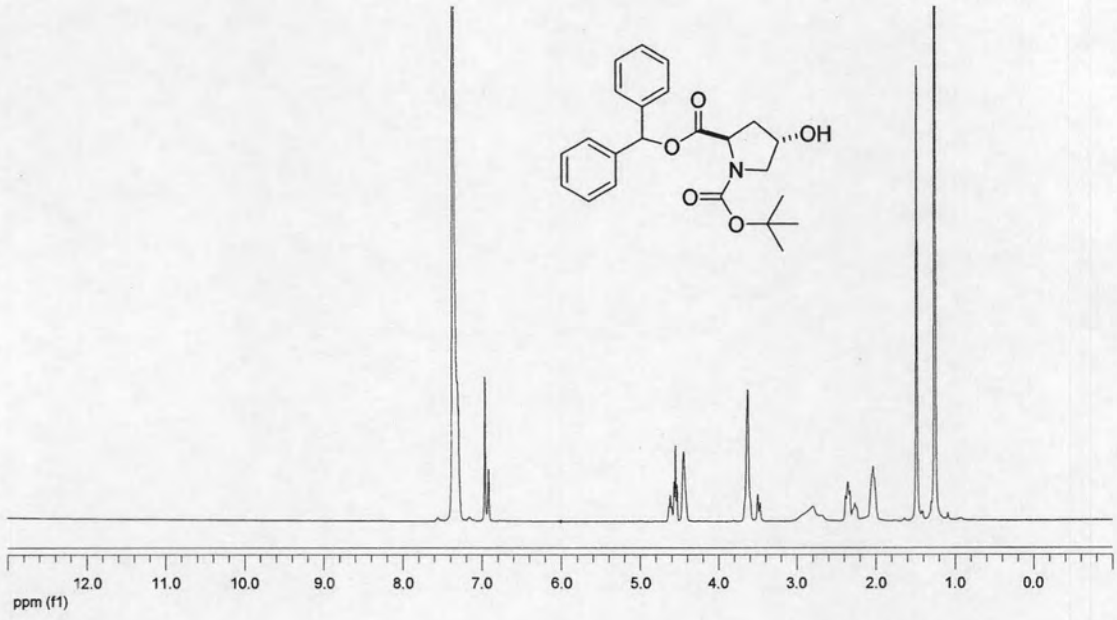

Figure A-13: ^{1}H NMR (400 MHz, $CDCl_3$) of *N*-tert-Butoxycarbonyl-trans-4-hydroxy-D-proline diphenylmethyl ester (**8**)

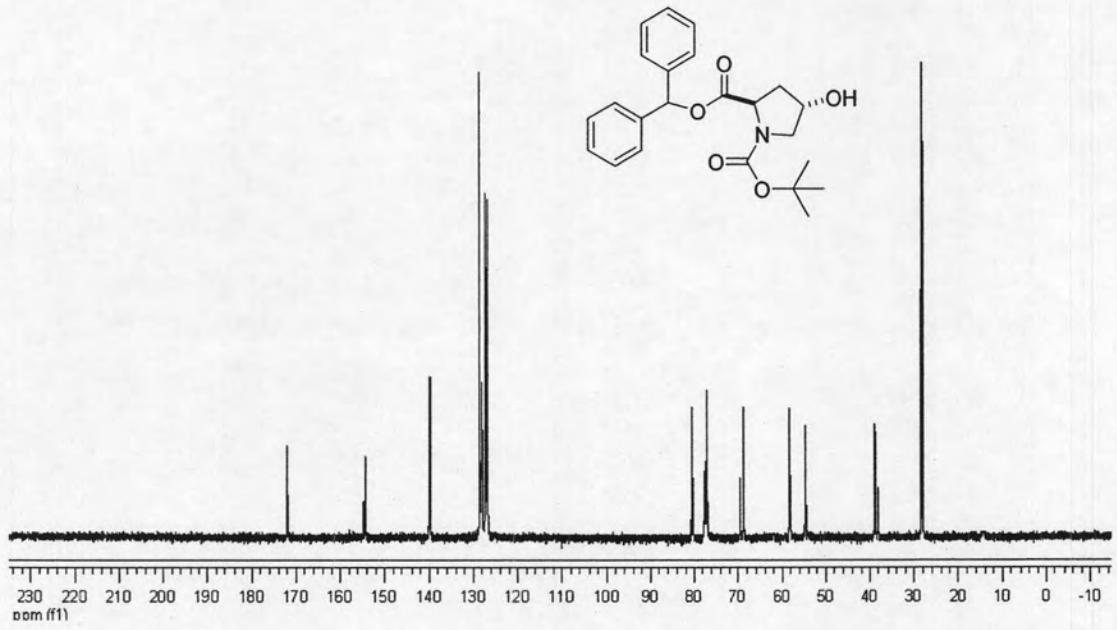

Figure A-14: ^{13}C NMR (100 MHz, $CDCl_3$) of *N*-tert-Butoxycarbonyl-trans-4-hydroxy-D-proline diphenylmethyl ester (**8**)

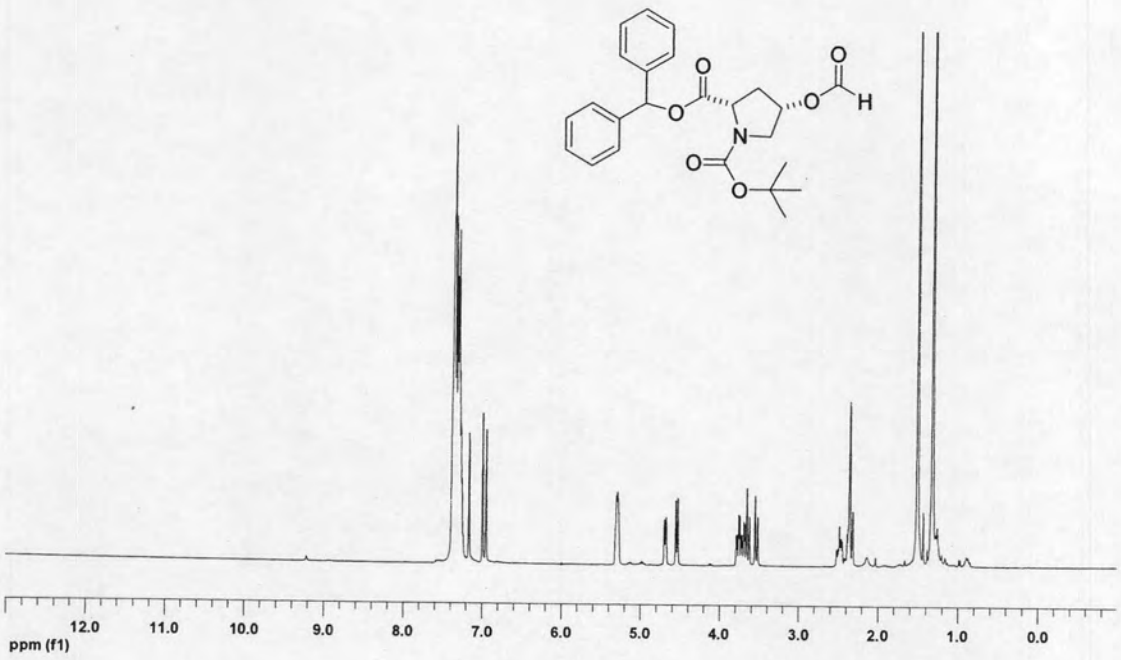

Figure A-15: ^{1}H NMR (400 MHz, $CDCl_3$) of *N-tert*-Butoxycarbonyl-*cis*-4-formyl-L-proline diphenylmethyl ester (**9**)

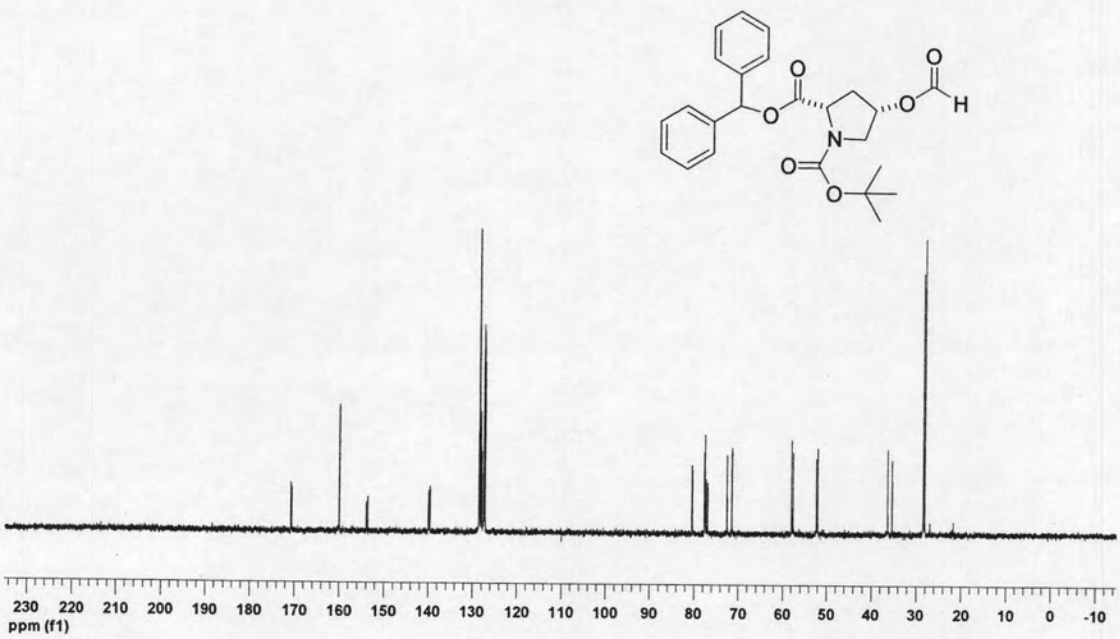

Figure A-16: ^{13}C NMR (100 MHz, $CDCl_3$) of *N-tert*-Butoxycarbonyl-*cis*-4-formyl-L-proline diphenylmethyl ester (**9**)

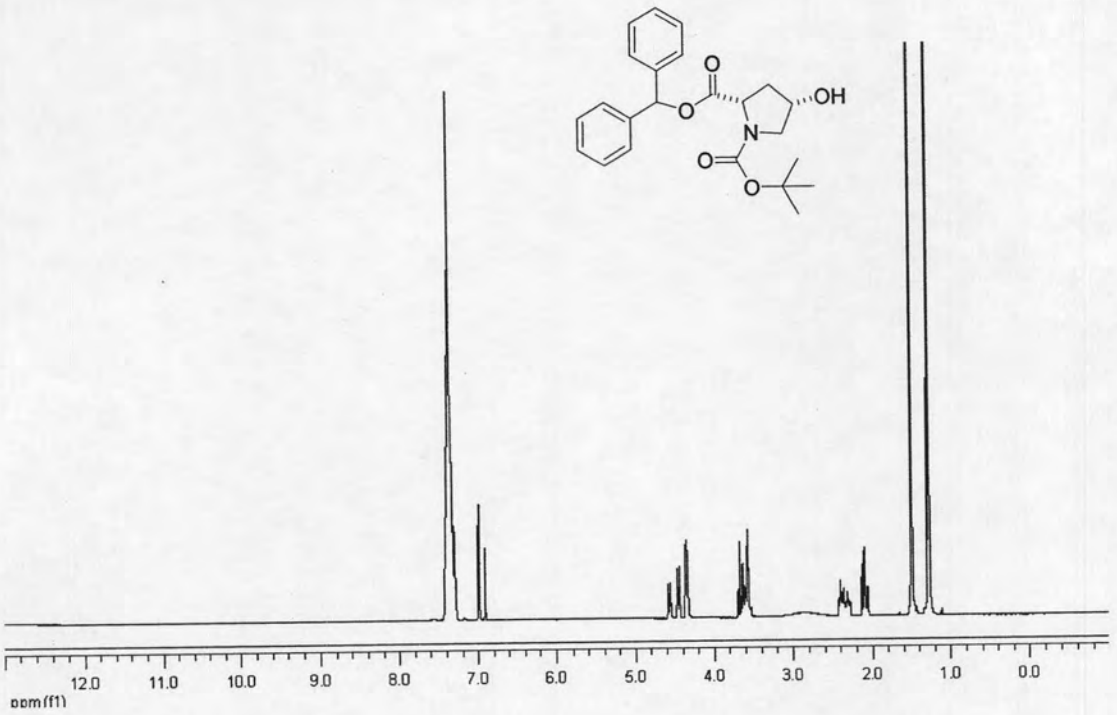

Figure A-17: ^{1}H NMR (400 MHz, $CDCl_3$) of *N-tert*-Butoxycarbonyl-*cis*-4-hydroxy-L-proline diphenylmethyl ester (**10**)

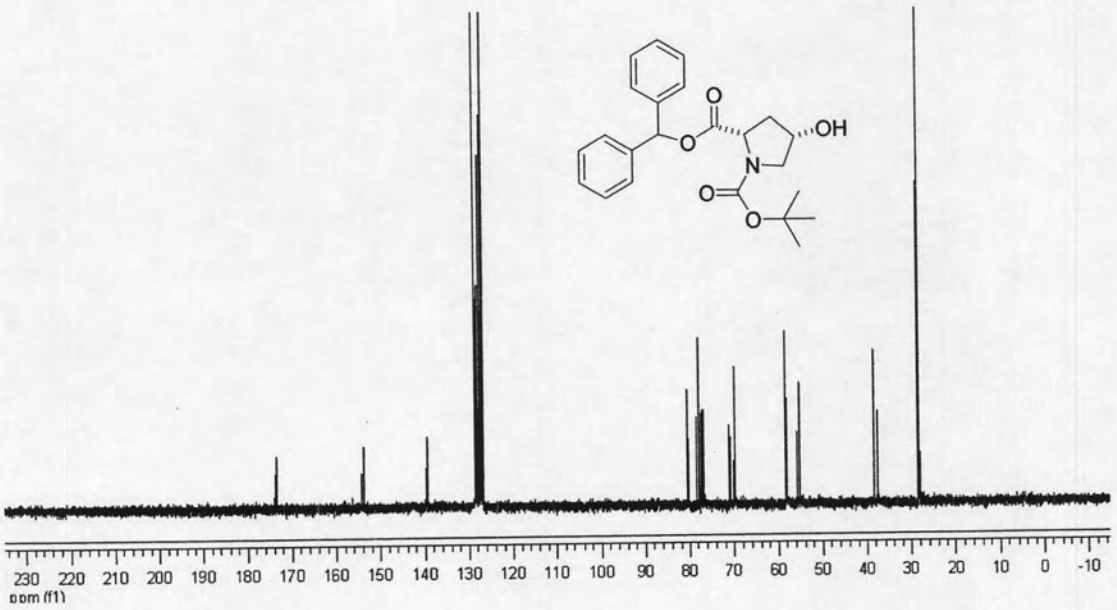

Figure A-18: ^{13}C NMR (100 MHz, $CDCl_3$) of *N-tert*-Butoxycarbonyl-*cis*-4-hydroxy-L-proline diphenylmethyl ester (**10**)

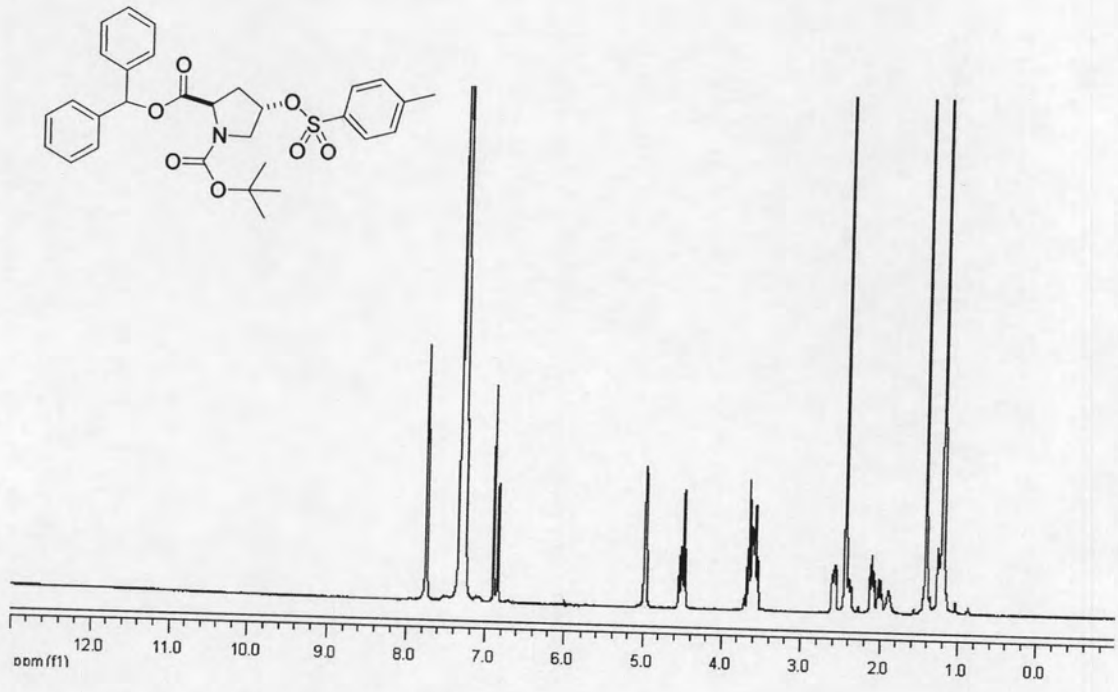

Figure A-19: ^{1}H NMR (400 MHz, $CDCl_3$) of *N-tert*-Butoxycarbonyl-*trans*-4-tosyl-D-proline diphenylmethyl ester (**11**)

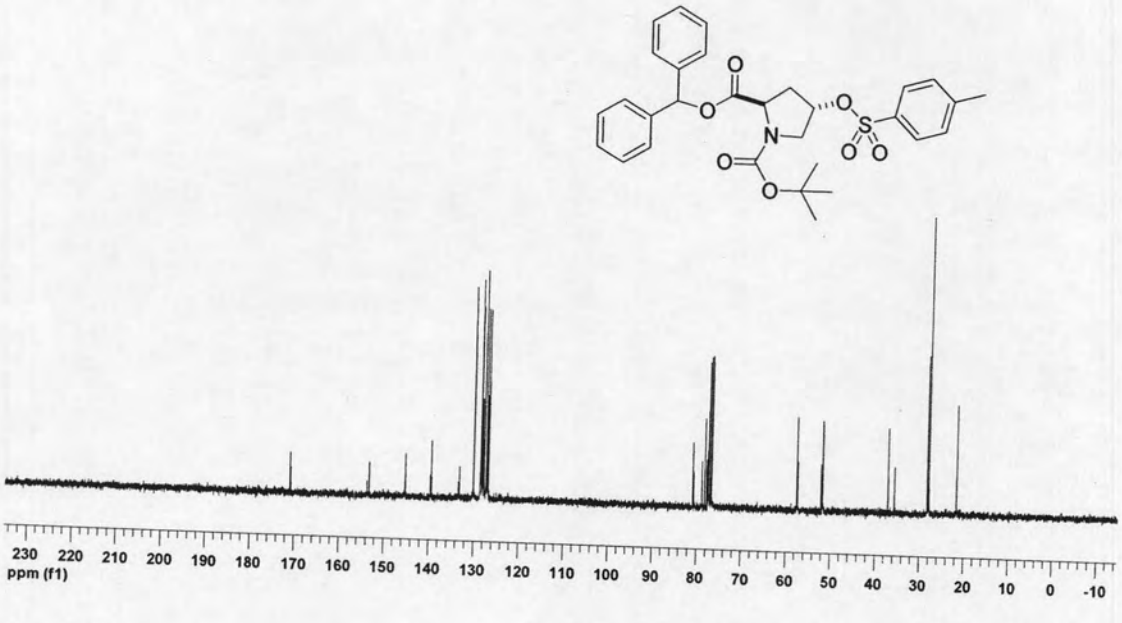

Figure A-20: ^{13}C NMR (100 MHz, $CDCl_3$) of *N-tert*-Butoxycarbonyl-*trans*-4-tosyl-D-proline diphenylmethyl ester (**11**)

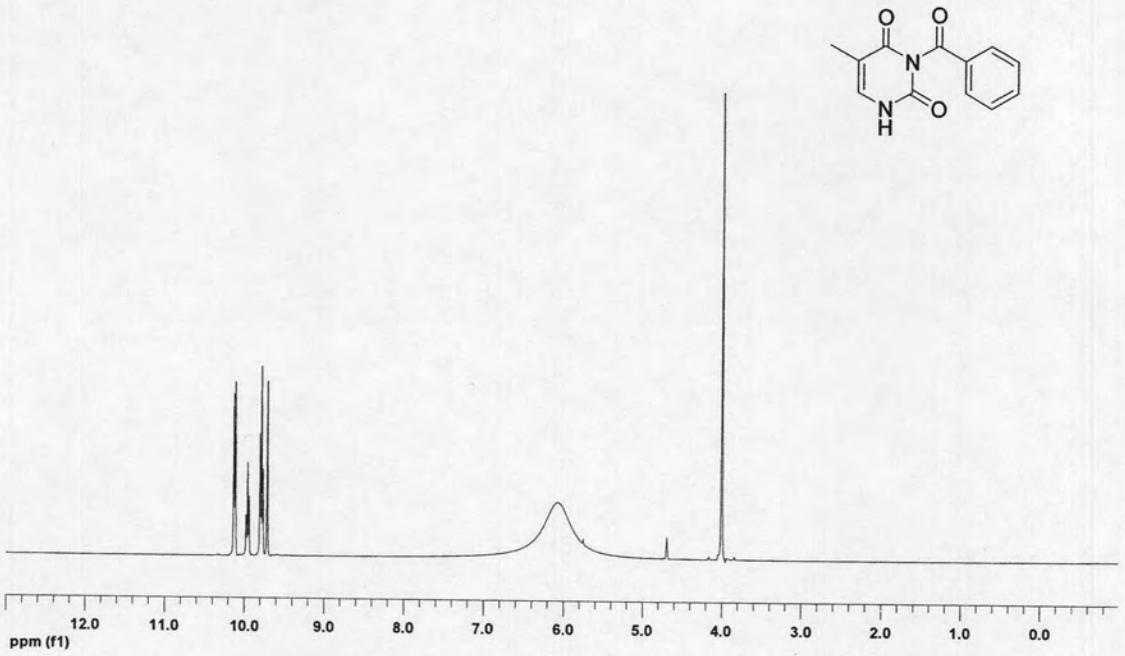

Figure A-21: ^{1}H NMR (400 MHz, DMSO-d_6) of N^3-Benzoylthymine (**12**)

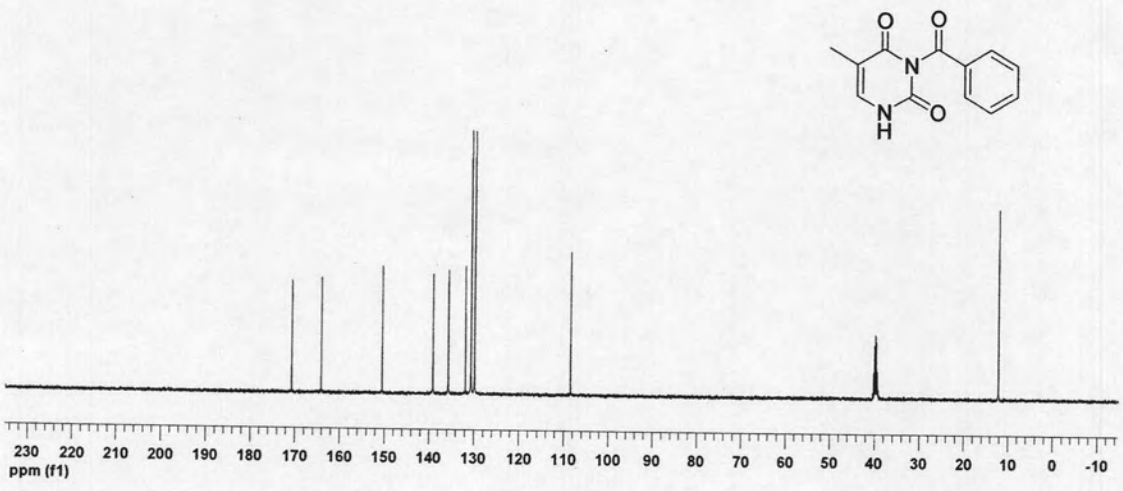

Figure A-22: ^{13}C NMR (100 MHz, DMSO-d_6) of N^3-Benzoylthymine (**12**)

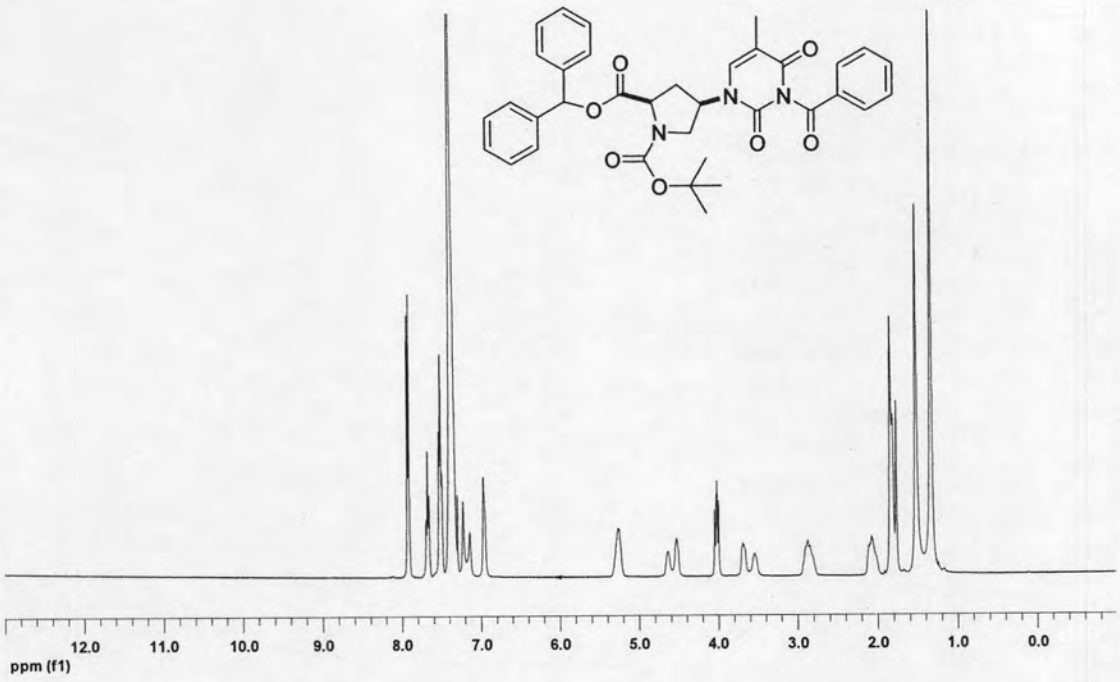

Figure A-23: ^{1}H NMR (400 MHz, $CDCl_3$) of *N-tert*-Butoxycarbonyl-*cis*-4-(N^3-benzoylthymin-1-yl)-D-proline diphenylmethyl ester (**13**)

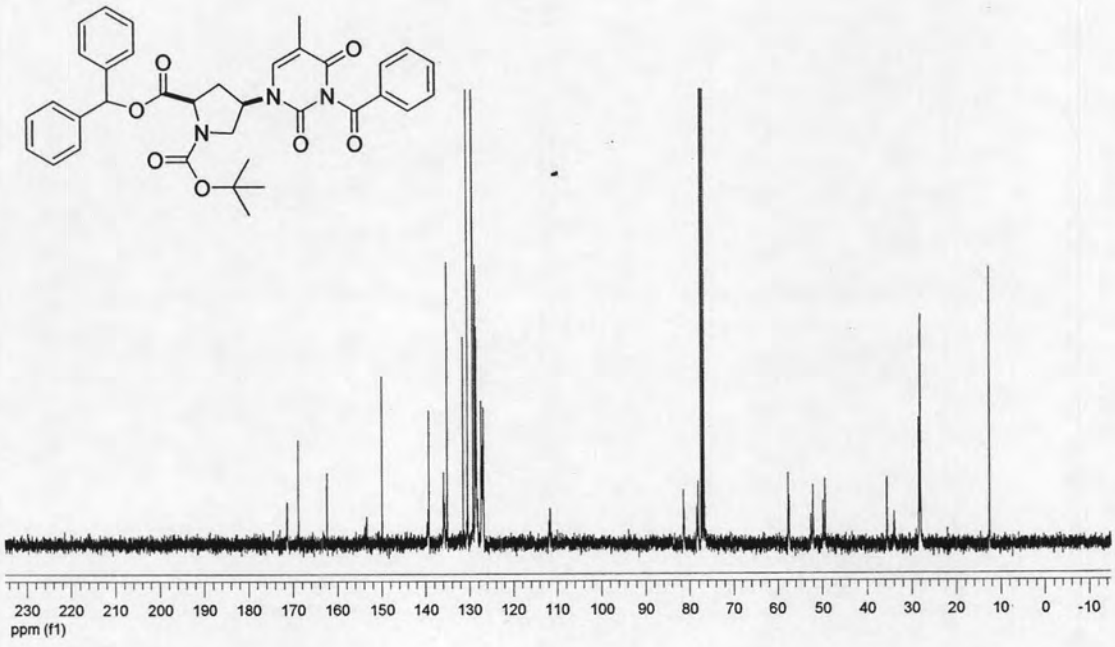

Figure A-24: ^{13}C NMR (100 MHz, $CDCl_3$) of *N-tert*-Butoxycarbonyl-*cis*-4-(N^3-benzoylthymin-1-yl)-D-proline diphenylmethyl ester (**13**)

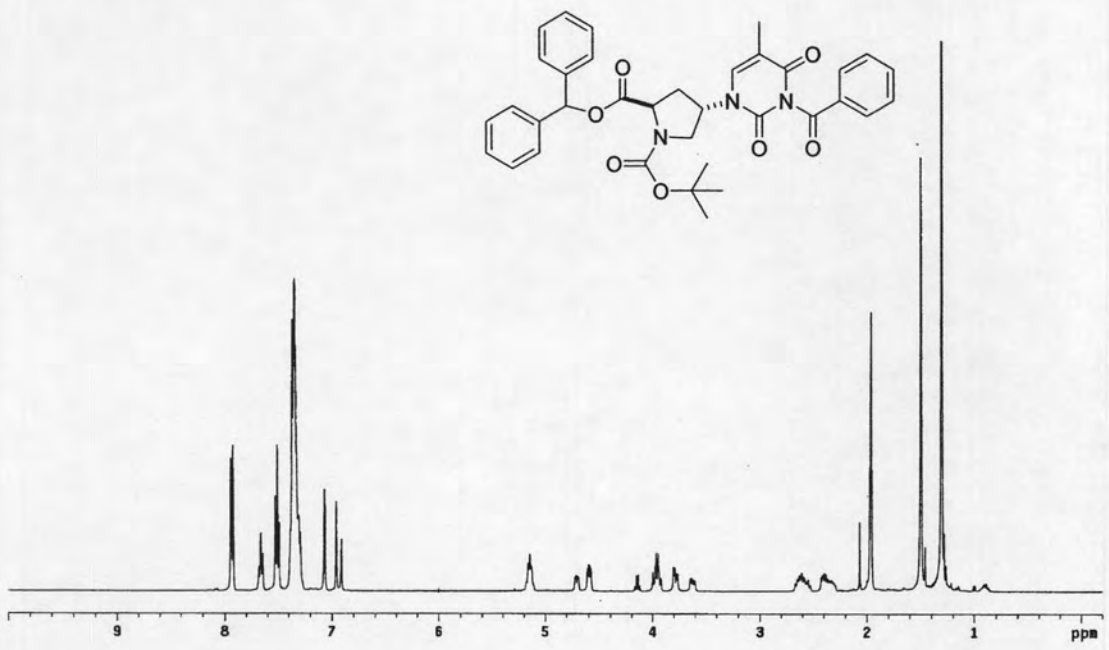

Figure A-25: ^{1}H NMR (200 MHz, $CDCl_3$) of *N-tert*-Butoxycarbonyl-*trans*-4-(N^3-benzoylthymin-1-yl)-D-proline diphenylmethyl ester (**14**)

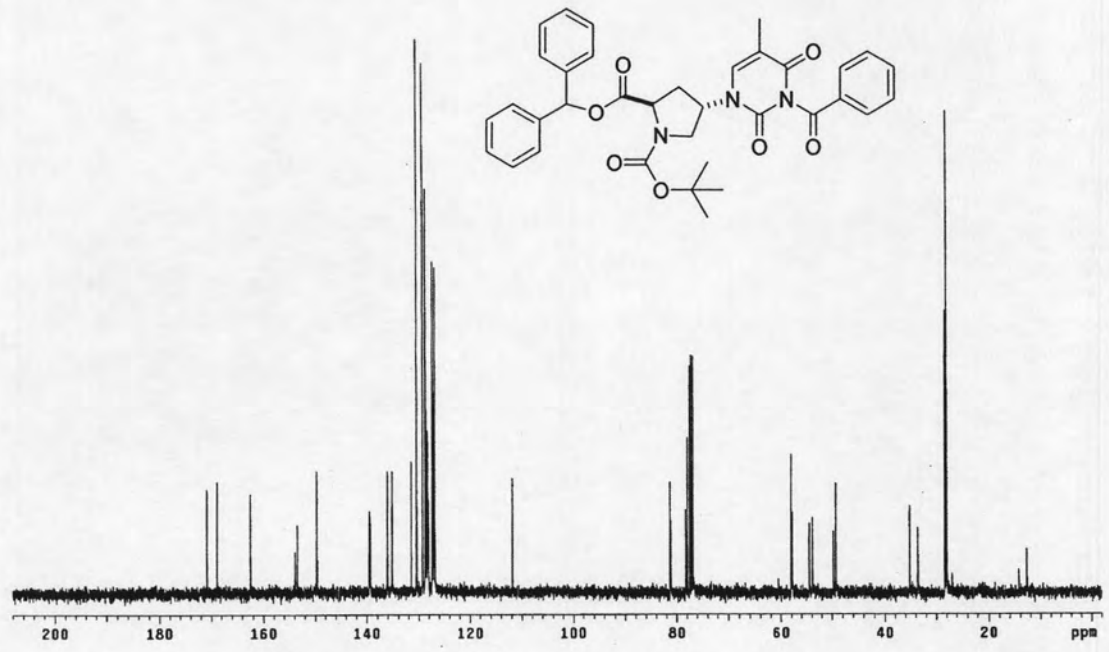

Figure A-26: ^{13}C NMR (50 MHz, $CDCl_3$) of *N-tert*-Butoxycarbonyl-*trans*-4-(N^3-benzoylthymin-1-yl)-D-proline diphenylmethyl ester (**14**)

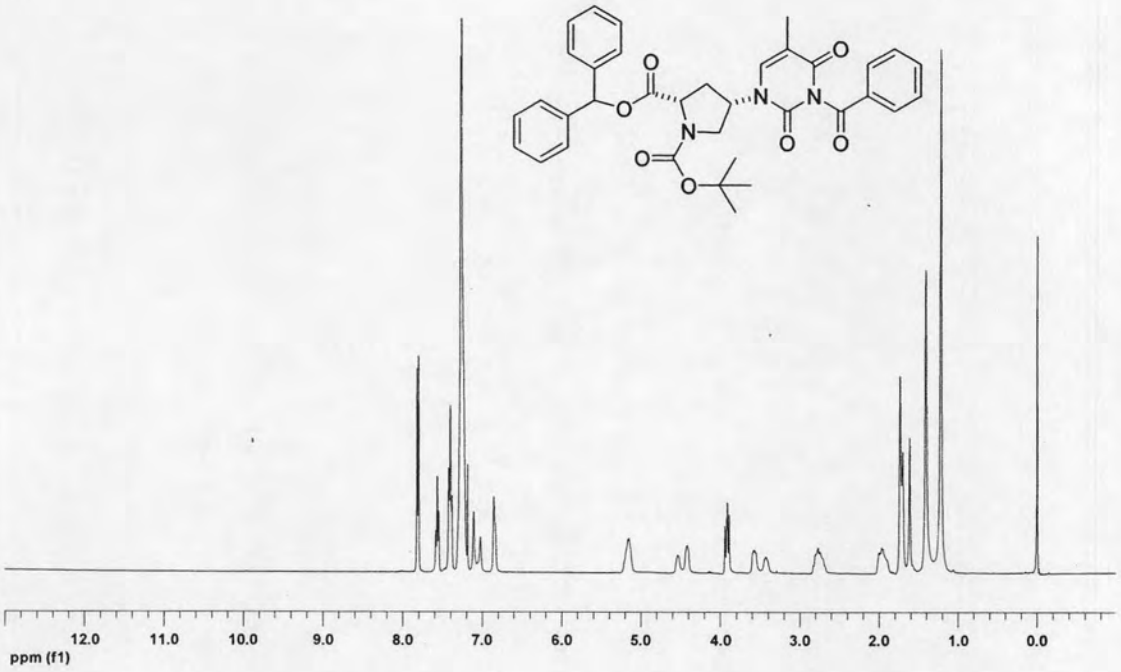

Figure A-27: ^{1}H NMR (400 MHz, $CDCl_3$) of *N-tert*-Butoxycarbonyl-*cis*-4-(N^3-benzoylthymin-1-yl)-L-proline diphenylmethyl ester (**15**)

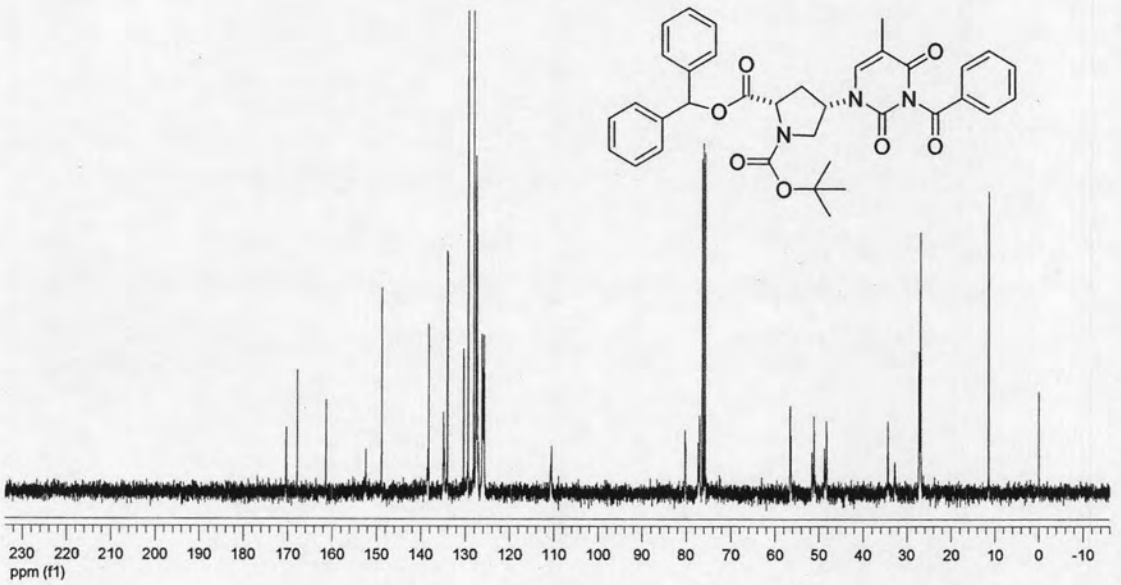

Figure A-28: ^{13}C NMR (100 MHz, $CDCl_3$) of *N-tert*-Butoxycarbonyl-*cis*-4-(N^3-benzoylthymin-1-yl)-L-proline diphenylmethyl ester (**15**)

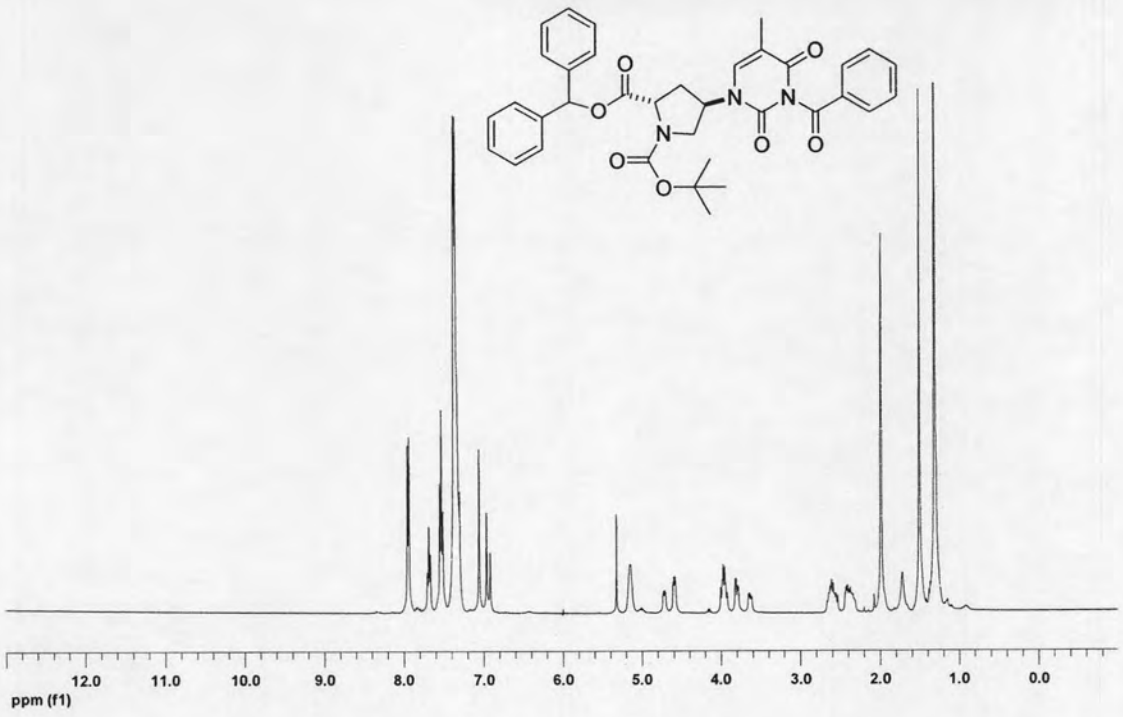

Figure A-29: ^{1}H NMR (400 MHz, $CDCl_3$) of *N-tert*-Butoxycarbonyl-*trans*-4-(N^3-benzoylthymin-1-yl)-L-proline diphenylmethyl ester (**16**)

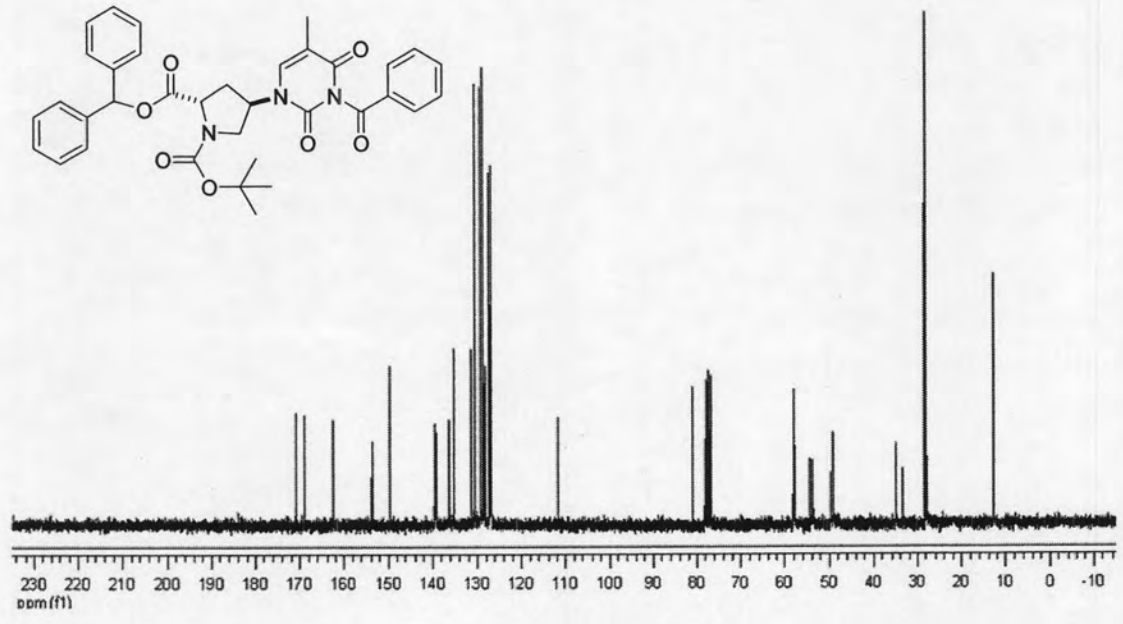

Figure A-30: ^{13}C NMR (100 MHz, $CDCl_3$) of *N-tert*-Butoxycarbonyl-*trans*-4-(N^3-benzoylthymin-1-yl)-L-proline diphenylmethyl ester (**16**)

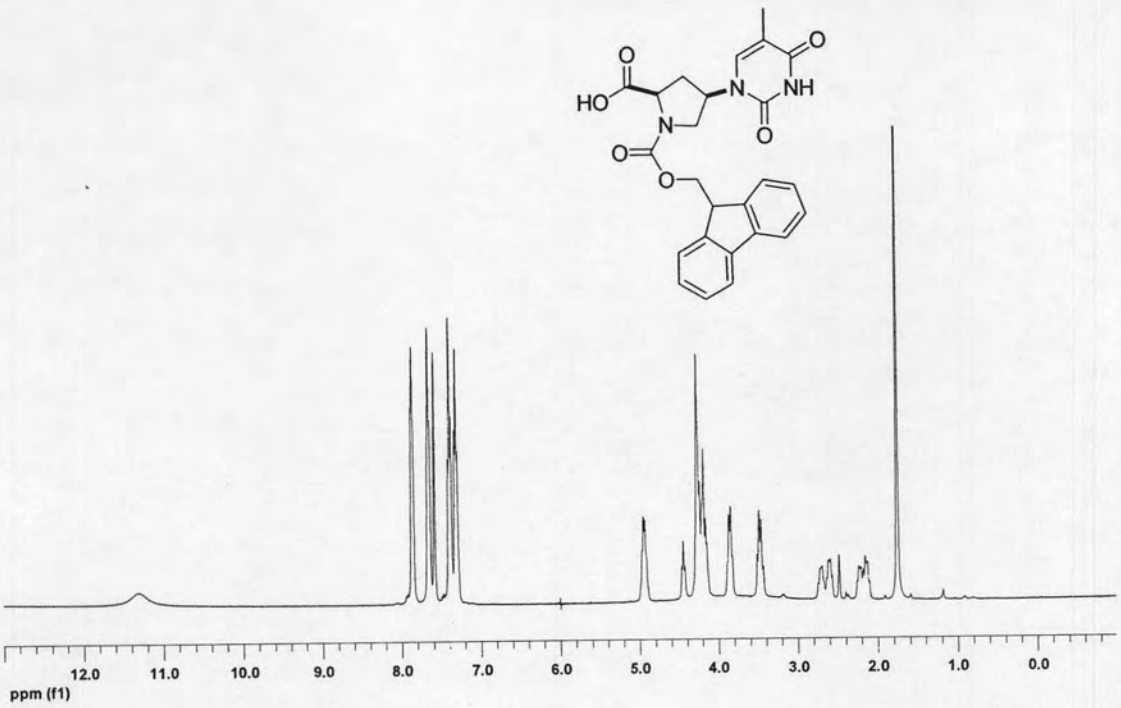

Figure A-31: ^{1}H NMR (400 MHz; DMSO-d_6) of (*N*-fluoren-9-ylmethoxycarbonyl)-*cis*-4-(thymin-1-yl)-D-proline (**17**)

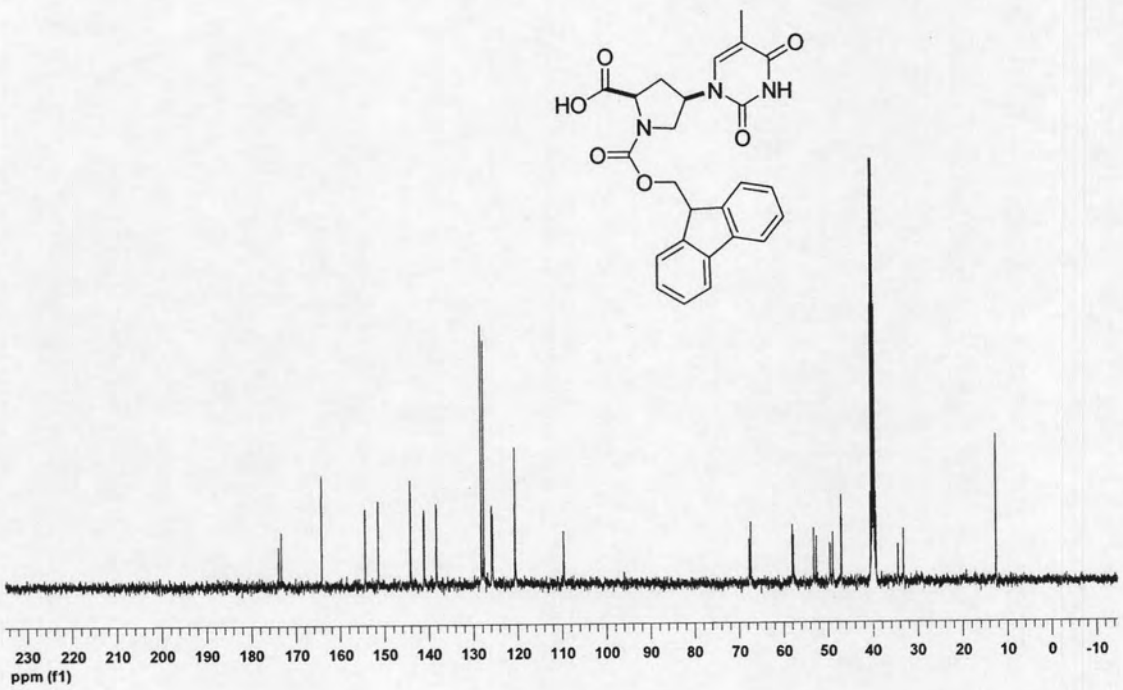

Figure A-32: ^{13}C NMR (100 MHz; DMSO-d_6) of (*N*-fluoren-9-ylmethoxycarbonyl)-*cis*-4-(thymin-1-yl)-D-proline (**17**)

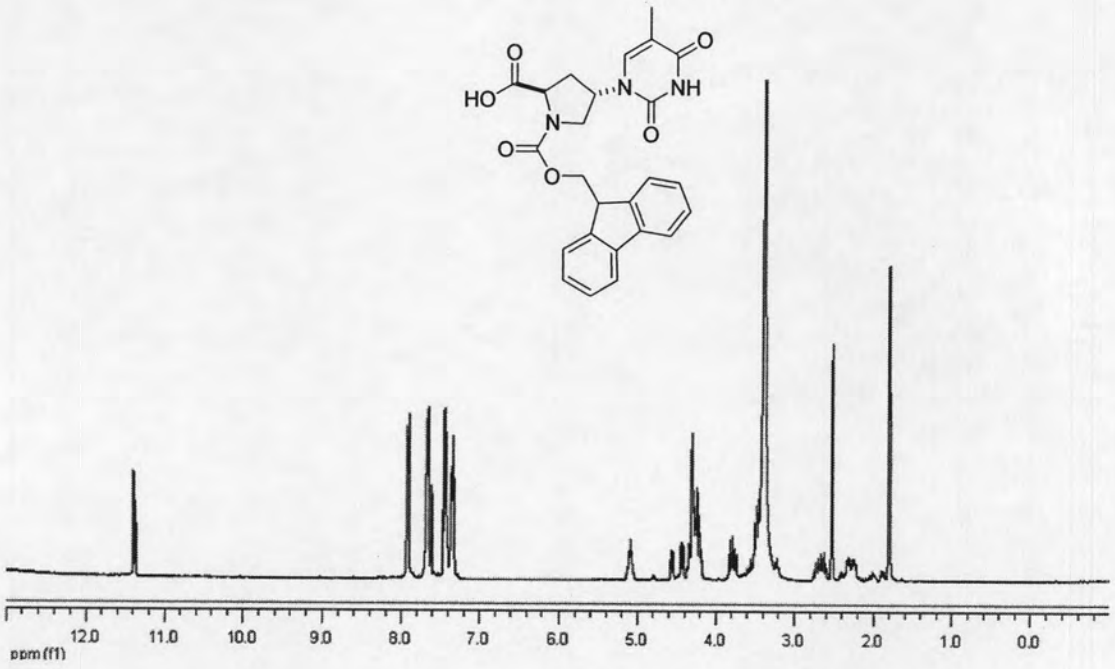

Figure A-33: ^{1}H NMR (400 MHz, DMSO-d_6) of (*N*-Fluoren-9-ylmethoxycarbonyl)-*trans*-4-(thymin-1-yl)-D-proline (**18**)

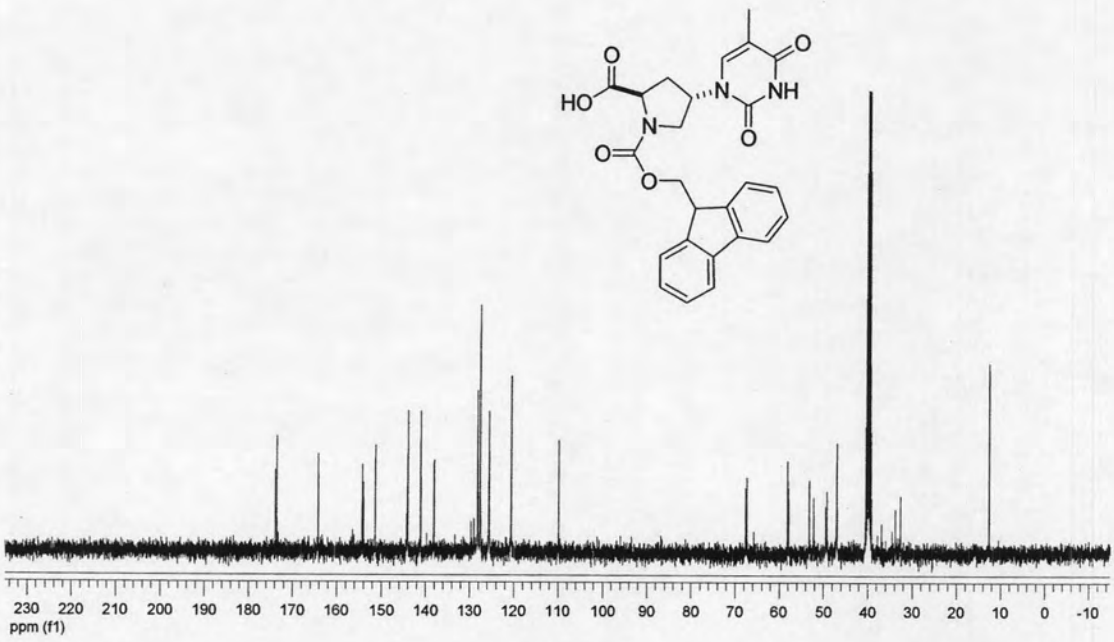

Figure A-34: ^{13}C NMR (100 MHz, DMSO-d_6) of (*N*-Fluoren-9-ylmethoxycarbonyl)-*trans*-4-(thymin-1-yl)-D-proline (**18**)

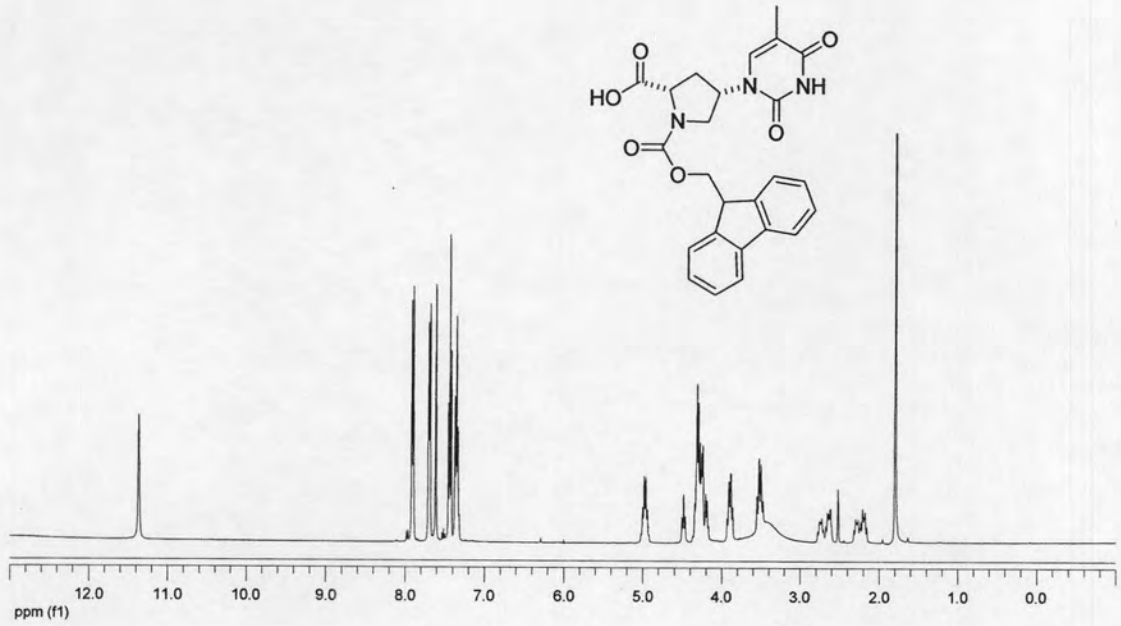

Figure A-35: ^{1}H NMR (400 MHz, DMSO-d_6) of (*N*-Fluoren-9-ylmethoxycarbonyl)-*cis*-4-(thymin-1-yl)-L-proline (**19**)

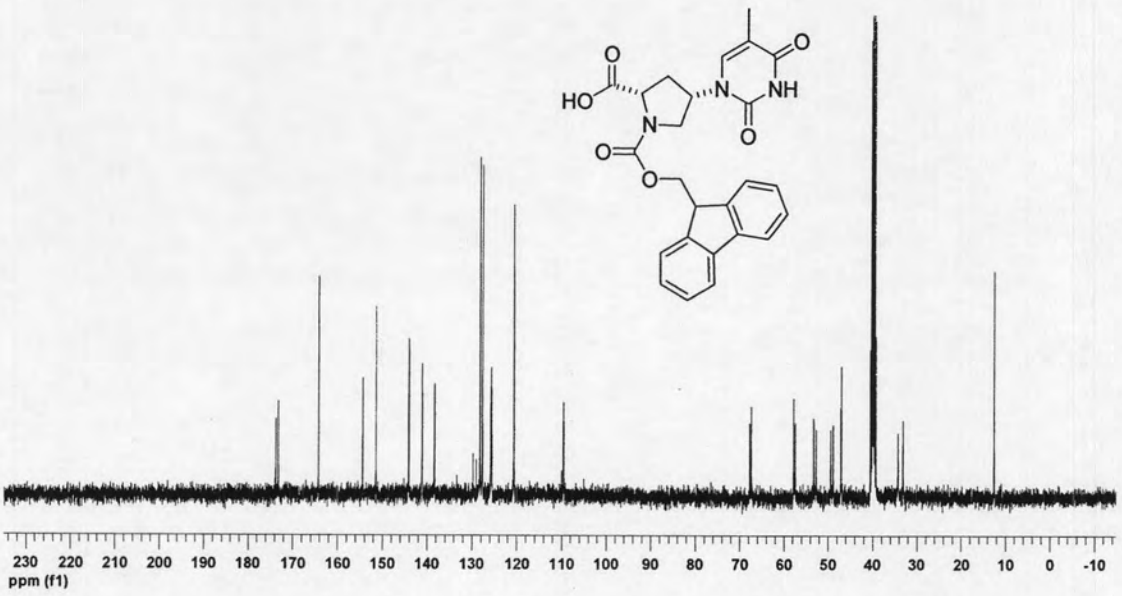

Figure A-36: ^{13}C NMR (100 MHz, DMSO-d_6) of (*N*-Fluoren-9-ylmethoxycarbonyl)-*cis*-4-(thymin-1-yl)-L-proline (**19**)

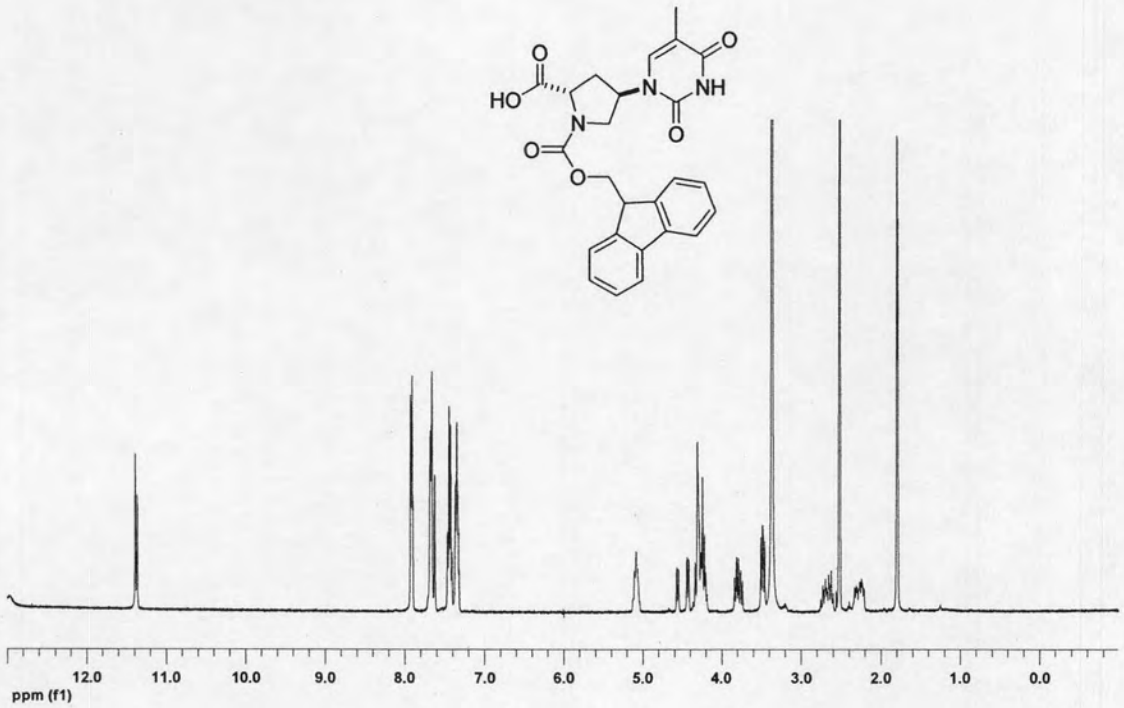

Figure A-37: ^{1}H NMR (400 MHz, DMSO-d_6) of (*N*-Fluoren-9-ylmethoxycarbonyl)-*trans*-4-(thymin-1-yl)-L-proline (**20**)

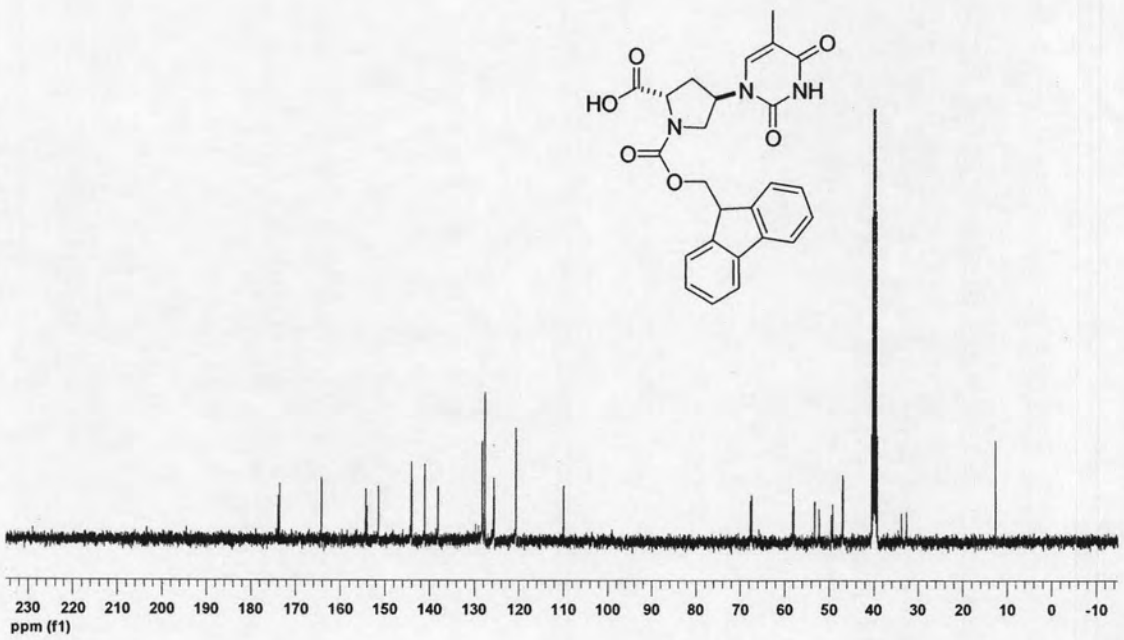

Figure A-38: ^{13}C NMR (100 MHz, DMSO-d_6) of (*N*-Fluoren-9-ylmethoxycarbonyl)-*trans*-4-(thymin-1-yl)-L-proline (**20**)

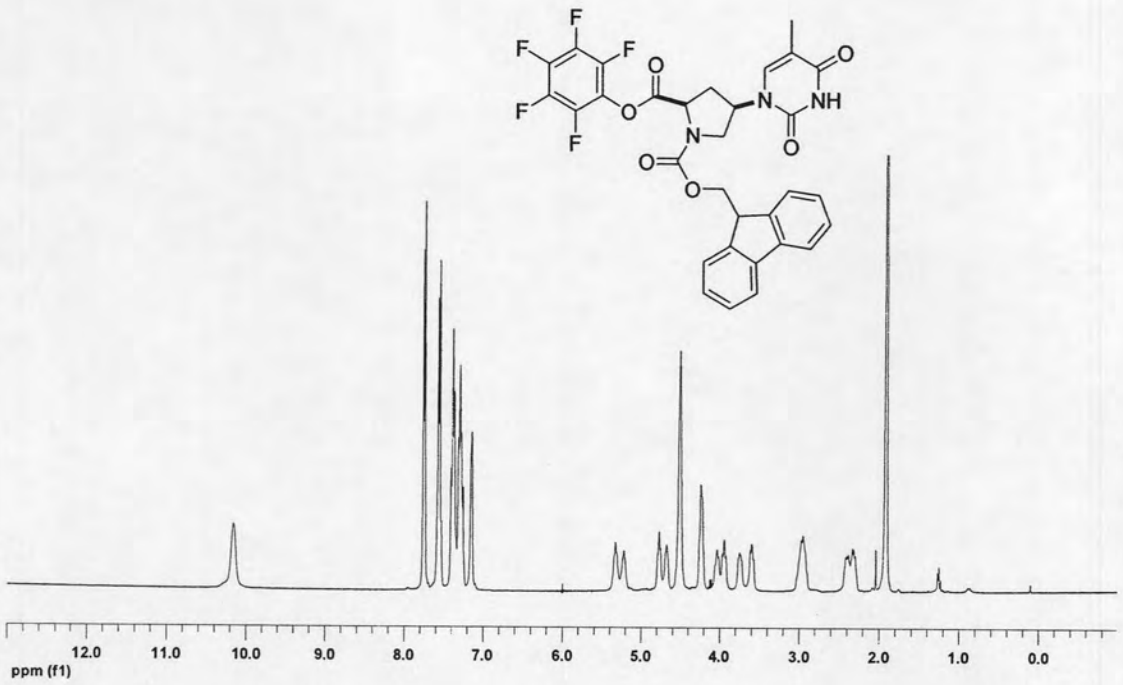

Figure A-39: ^{1}H NMR (400 MHz, $CDCl_3$) of (*N*-Fluoren-9-ylmethoxycarbonyl)-*cis*-4-(thymin-1-yl)-D-proline pentafluorophenyl ester (**21**)

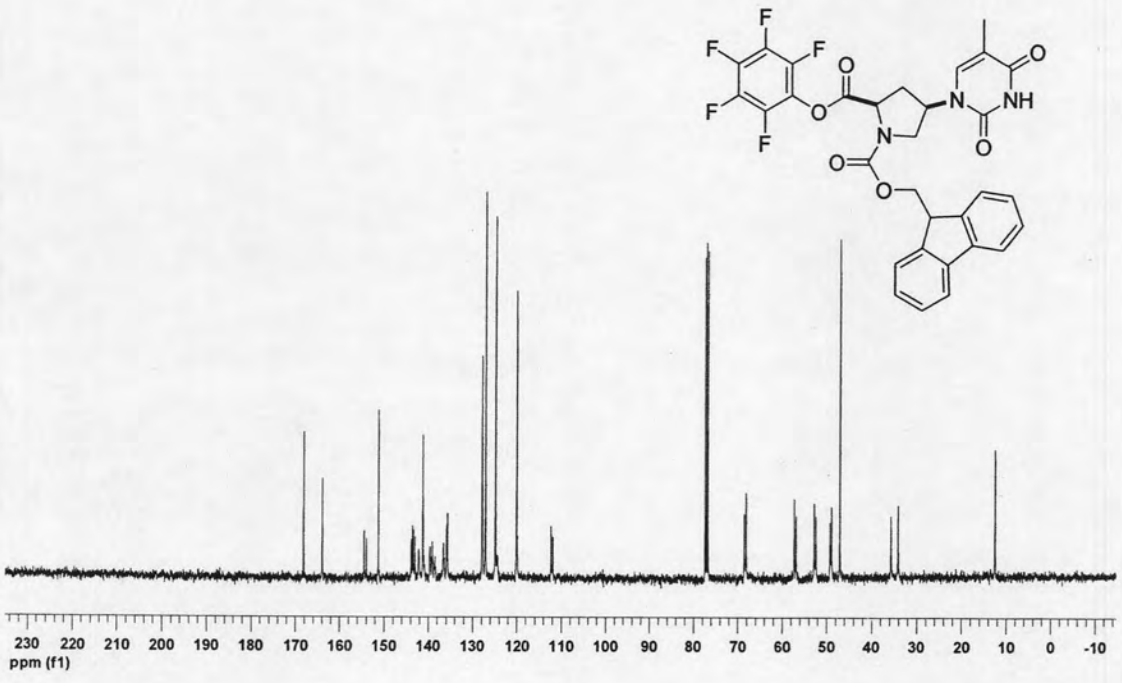

Figure A-40: ^{13}C NMR (100 MHz, $CDCl_3$) of (*N*-Fluoren-9-ylmethoxycarbonyl)-*cis*-4-(thymin-1-yl)-D-proline pentafluorophenyl ester (**21**)

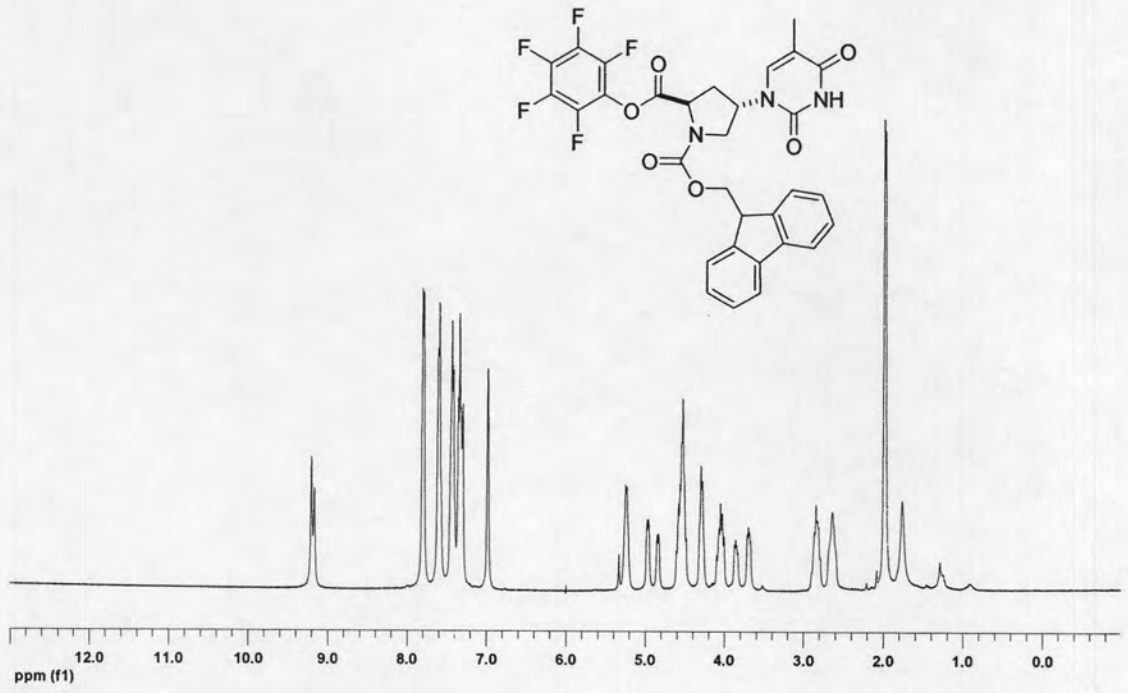

Figure A-41: ^{1}H NMR (400 MHz, $CDCl_3$) of (*N*-Fluoren-9-ylmethoxycarbonyl)-*trans*-4-(thymin-1-yl)-D-proline pentafluorophenyl ester (**22**)

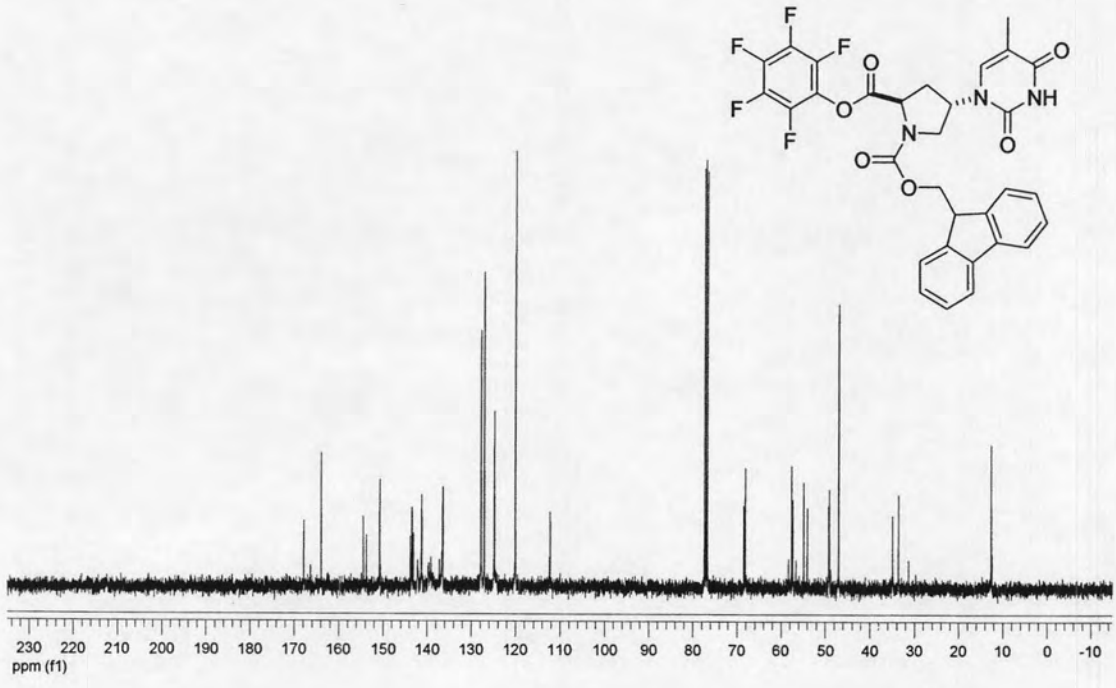

Figure A-42: ^{13}C NMR (100 MHz, $CDCl_3$) of (*N*-Fluoren-9-ylmethoxycarbonyl)-*trans*-4-(thymin-1-yl)-D-proline pentafluorophenyl ester (**22**)

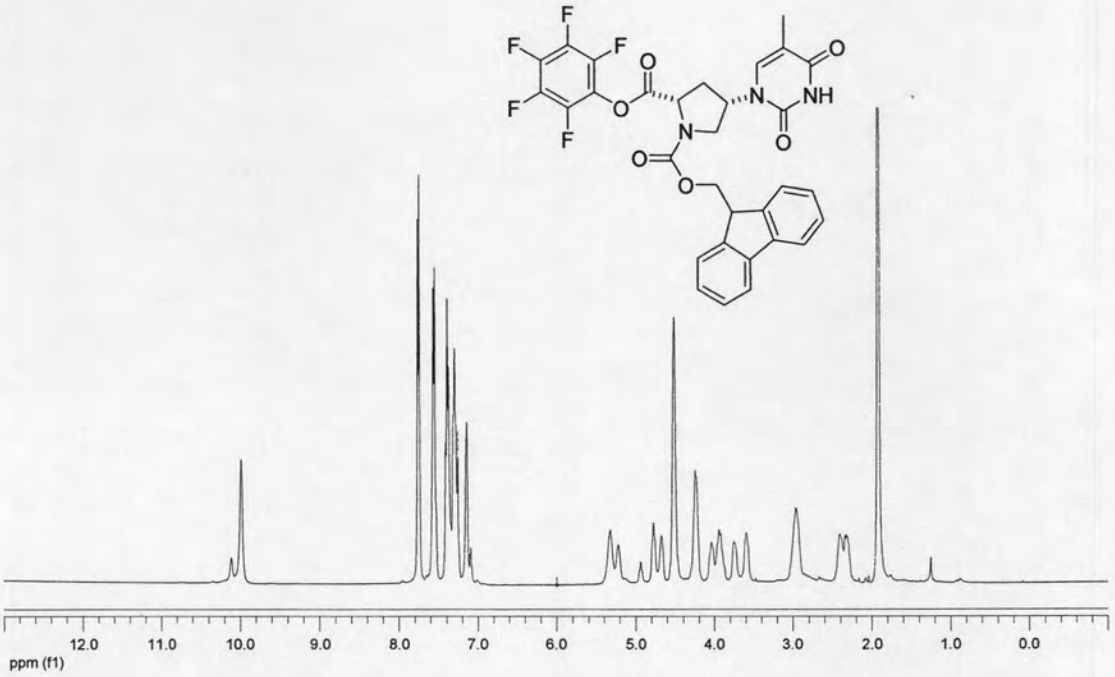

Figure A-43: ^{1}H NMR (400 MHz, $CDCl_3$) of (*N*-Fluoren-9-ylmethoxycarbonyl)-*cis*-4-(thymin-1-yl)-L-proline pentafluorophenyl ester (**23**)

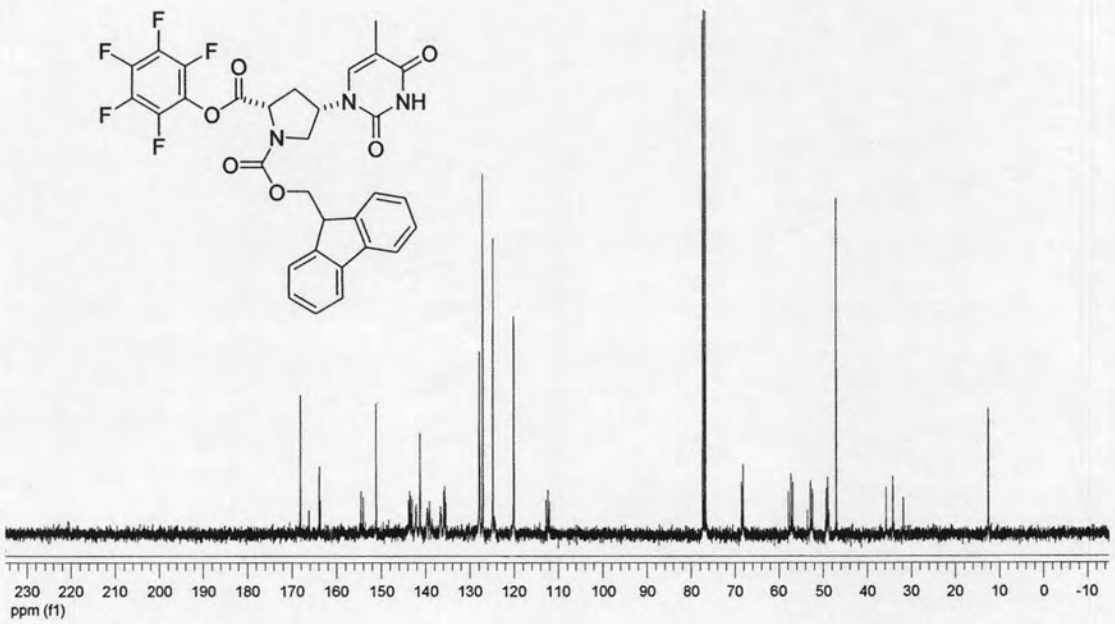

Figure A-44: ^{13}C NMR (100 MHz, $CDCl_3$) of (*N*-Fluoren-9-ylmethoxycarbonyl)-*cis*-4-(thymin-1-yl)-L-proline pentafluorophenyl ester (**23**)

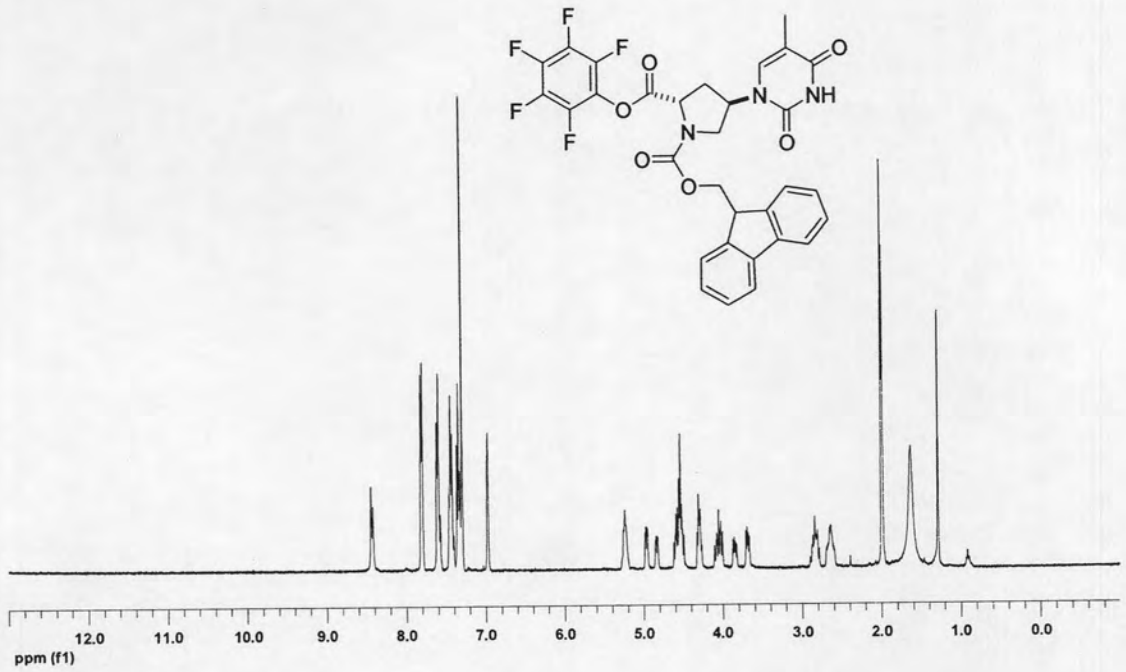

Figure A-45: ^{1}H NMR (400 MHz, $CDCl_3$) of (*N*-Fluoren-9-ylmethoxycarbonyl)-*trans*-4-(thymin-1-yl)-L-proline pentafluorophenyl ester (**24**)

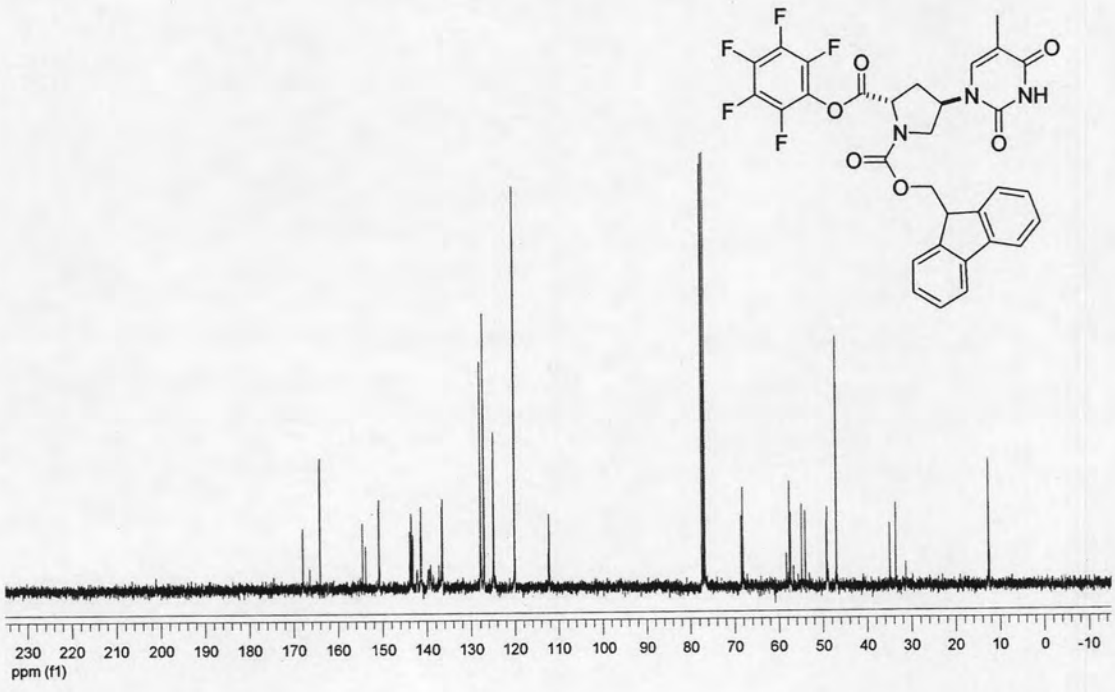

Figure A-46: ^{13}C NMR (100 MHz, $CDCl_3$) of (*N*-Fluoren-9-ylmethoxycarbonyl)-*trans*-4-(thymin-1-yl)-L-proline pentafluorophenyl ester (**24**)

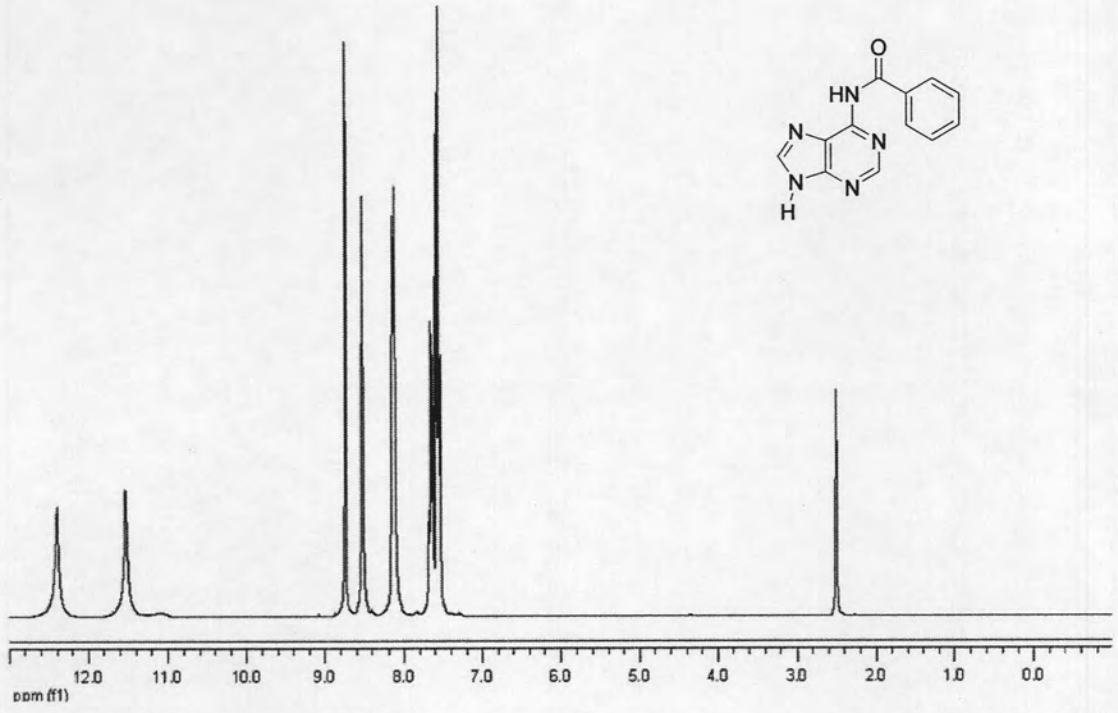

Figure A-47: ^{1}H NMR (400 MHz, DMSO-d_6) of N^6-Benzoyladenine (**25**)

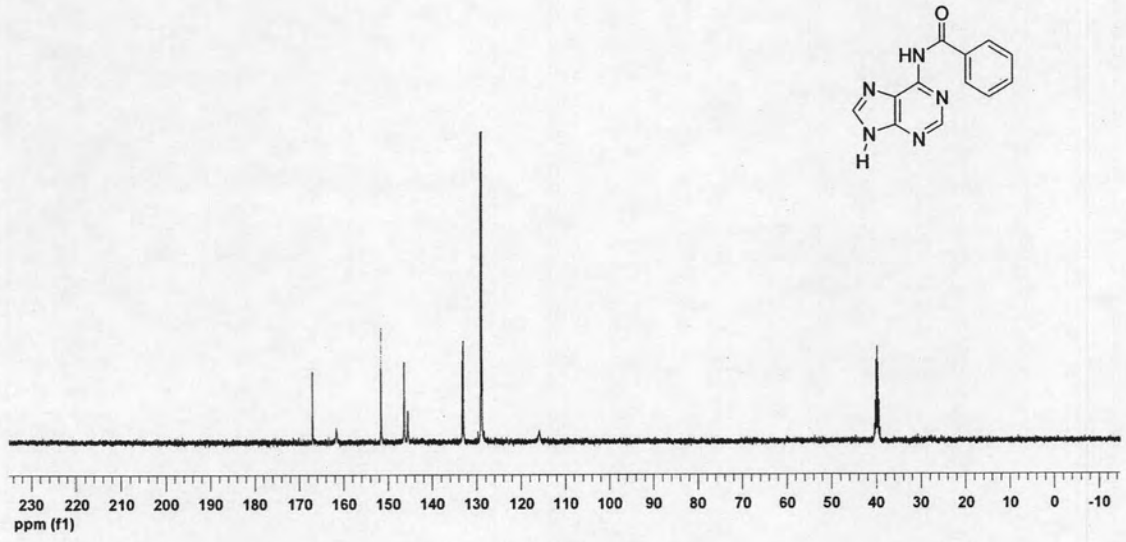

Figure A-48: ^{13}C NMR (100 MHz, DMSO-d_6) of N^6-Benzoyladenine (**25**)

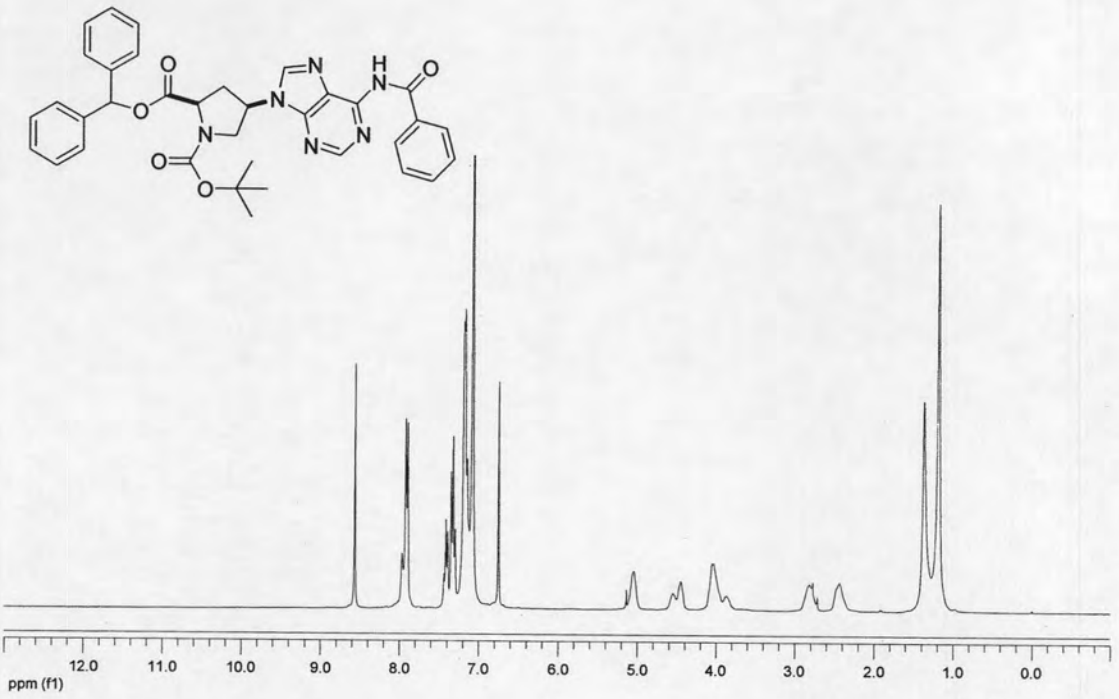

Figure A-49: ^{1}H NMR (300 MHz, $CDCl_3$) of (*N-tert*-butyloxycarbonyl)-*cis*-4-(N^6-benzoyladenin-9-yl)-D-proline diphenylmethyl ester (**26**)

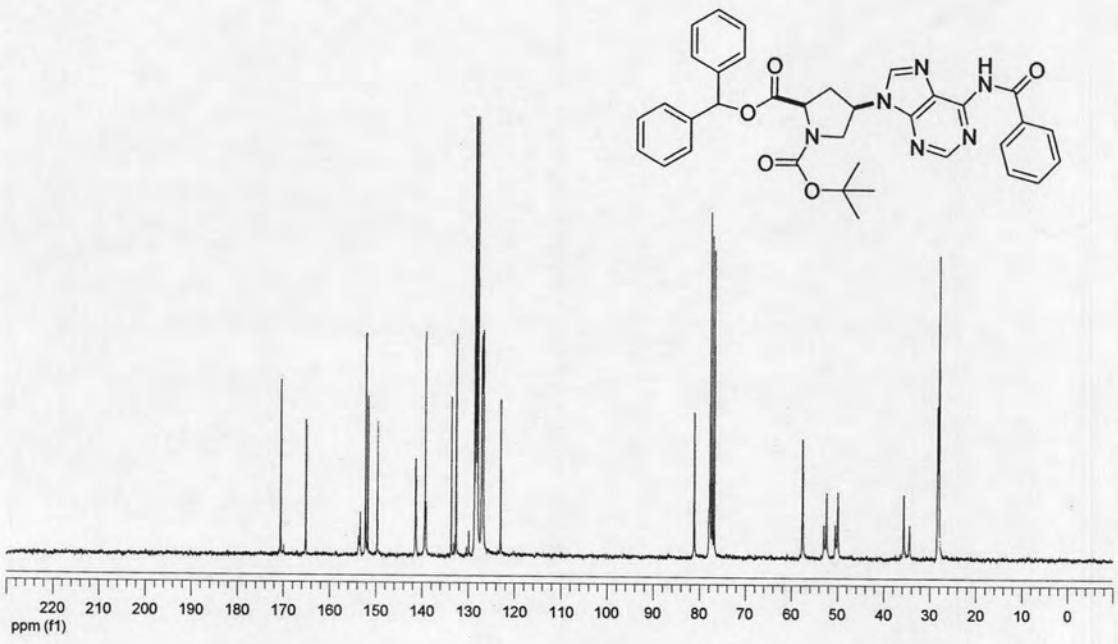

Figure A-50: ^{13}C NMR (75 MHz, $CDCl_3$) of (*N-tert*-butyloxycarbonyl)-*cis*-4-(N^6-benzoyladenin-9-yl)-D-proline diphenylmethyl ester (**26**)

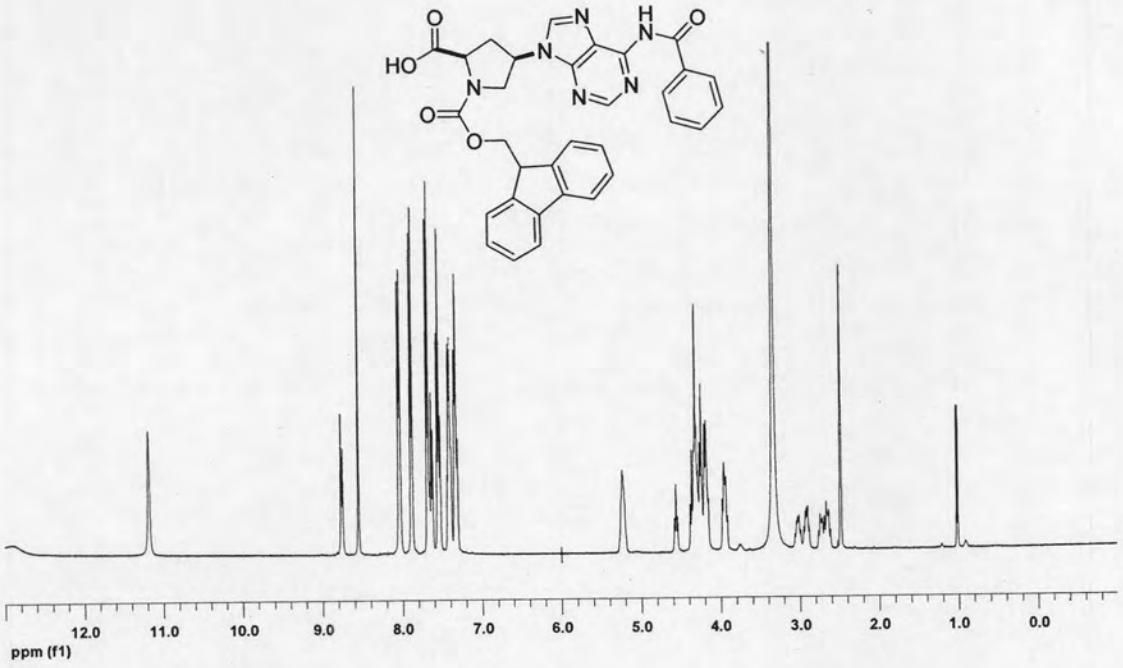

Figure A-51: ^{1}H NMR (400 MHz, DMSO-d_6) of (*N*-fuoren-9-ylmethoxycarbonyl)-*cis*-4-(N^4- benzoyladenin-9-yl)-D-proline (**27**)

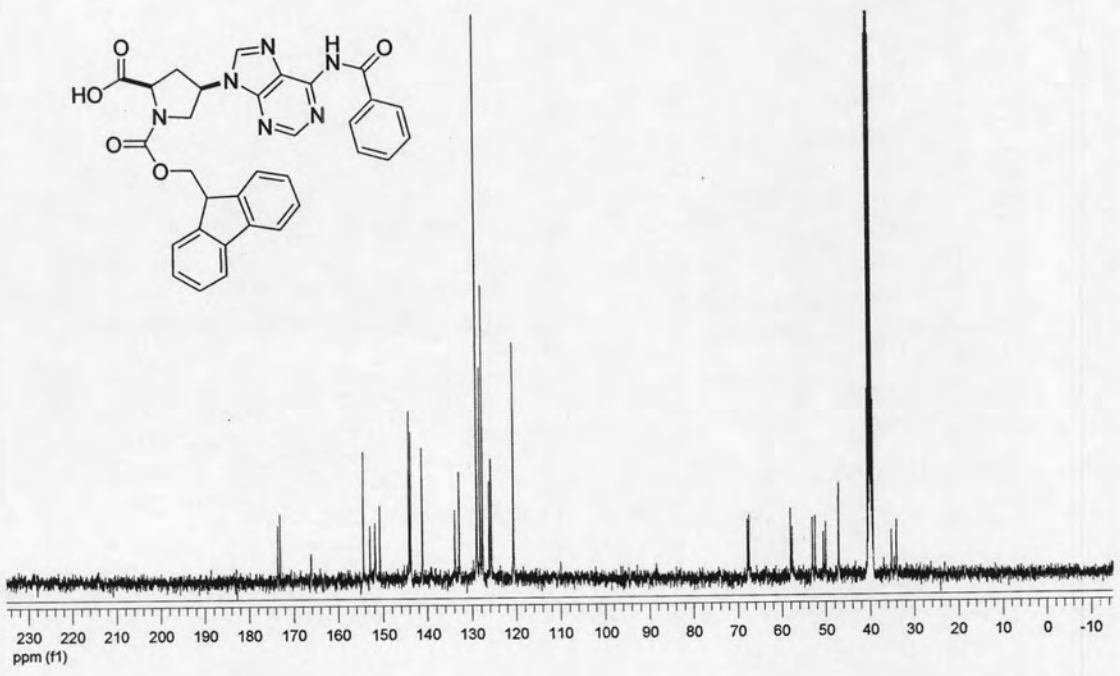

Figure A-52: ^{13}C NMR (100 MHz, DMSO-d_6) of (*N*-Fluoren-9-ylmethoxycarbonyl)-*cis*-4-(N^6-benzoyladenin-9-yl)-D-proline (**27**)

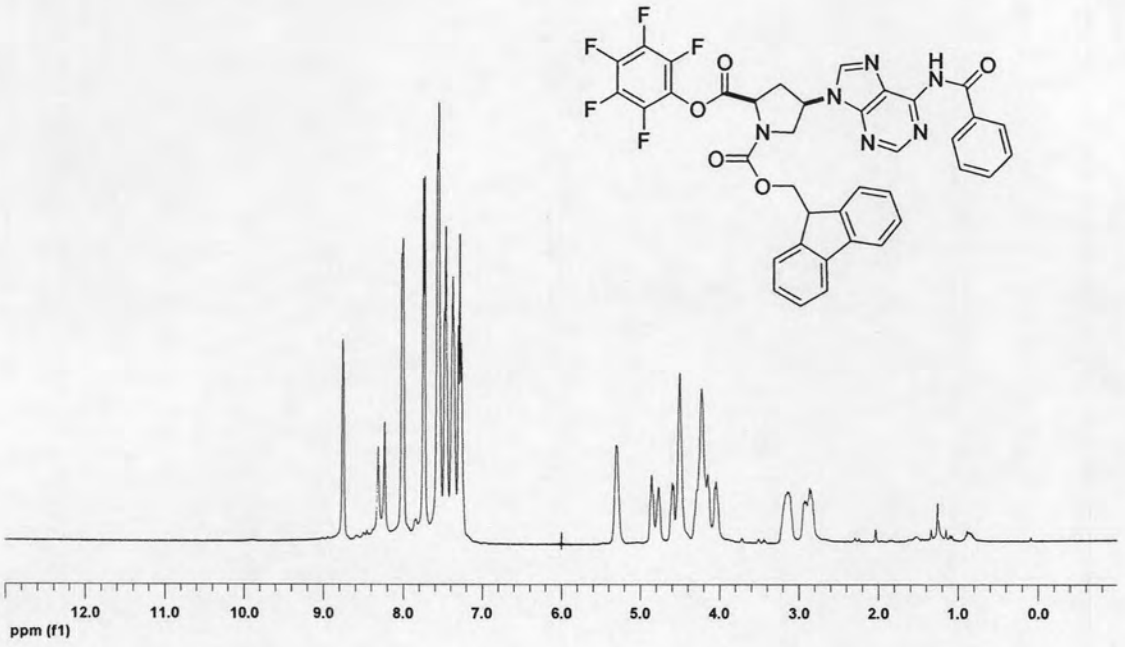

Figure A-53: ^{1}H NMR (400 MHz, $CDCl_3$) of (*N*-Fluoren-9-ylmethoxycarbonyl)-*cis*-4-(N^6-benzoyladenin-9-yl)-D-proline pentafluorophenyl ester (**28**)

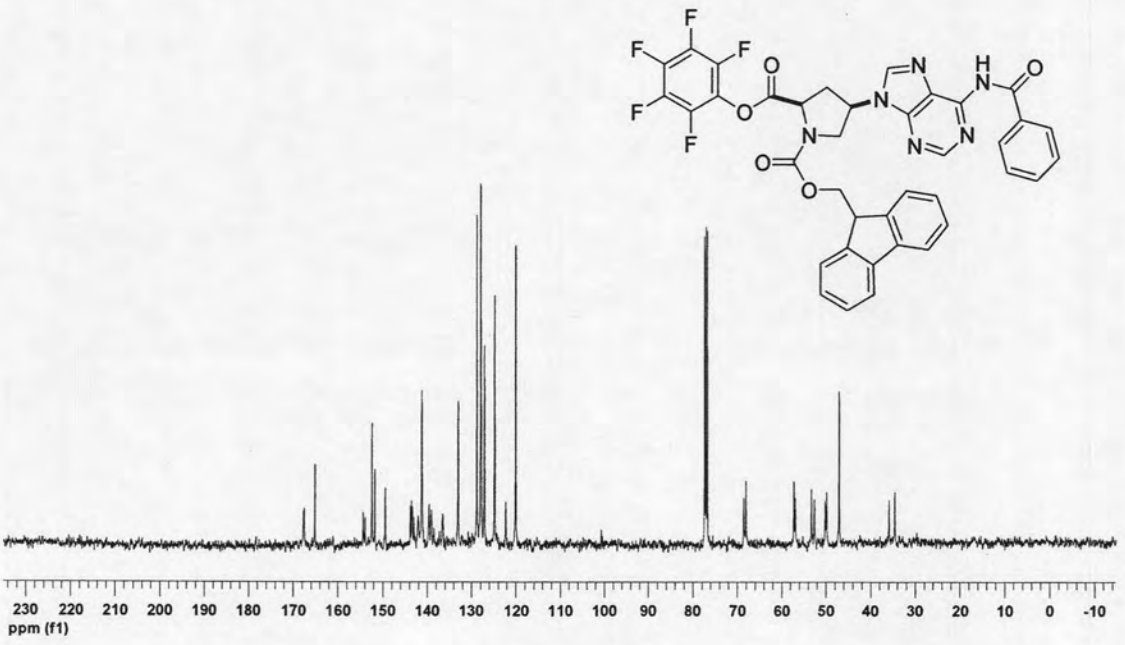

Figure A-54: ^{13}C NMR (100 MHz, $CDCl_3$) of (*N*-Fluoren-9-ylmethoxycarbonyl)-*cis*-4-(N^6-benzoyladenin-9-yl)-D-proline pentafluorophenyl ester (**28**)

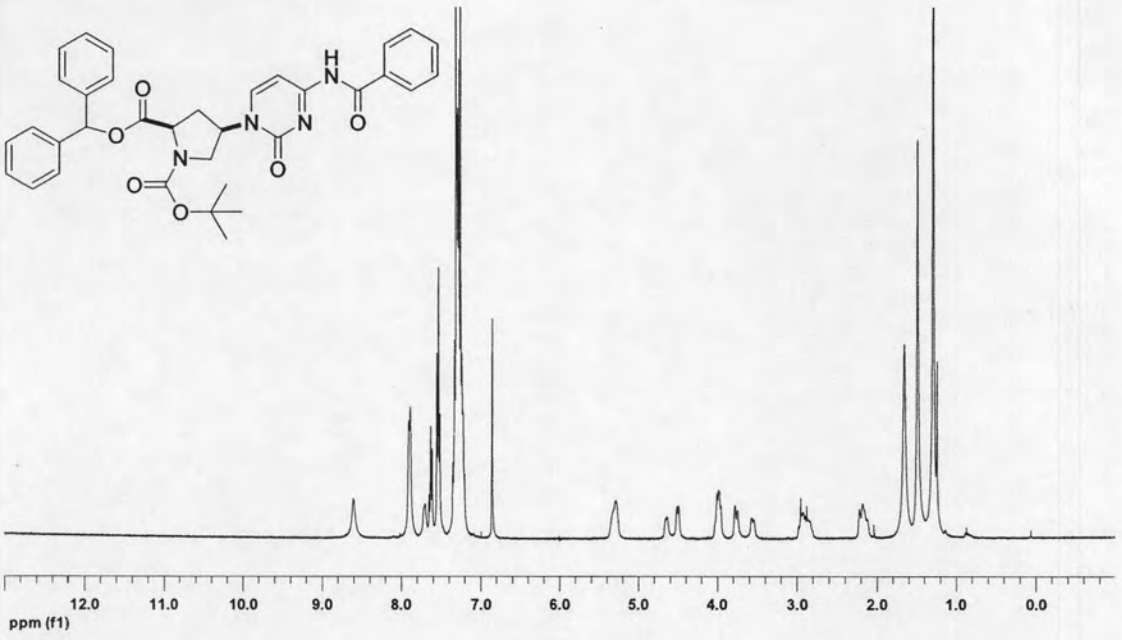

Figure A-55: ^{1}H NMR (400 MHz, $CDCl_3$) of (*N-tert*-butyloxycarbonyl)-*cis*-4-(N^4-benzoylcytosin-9-yl)-D-proline diphenylmethyl ester (**29**)

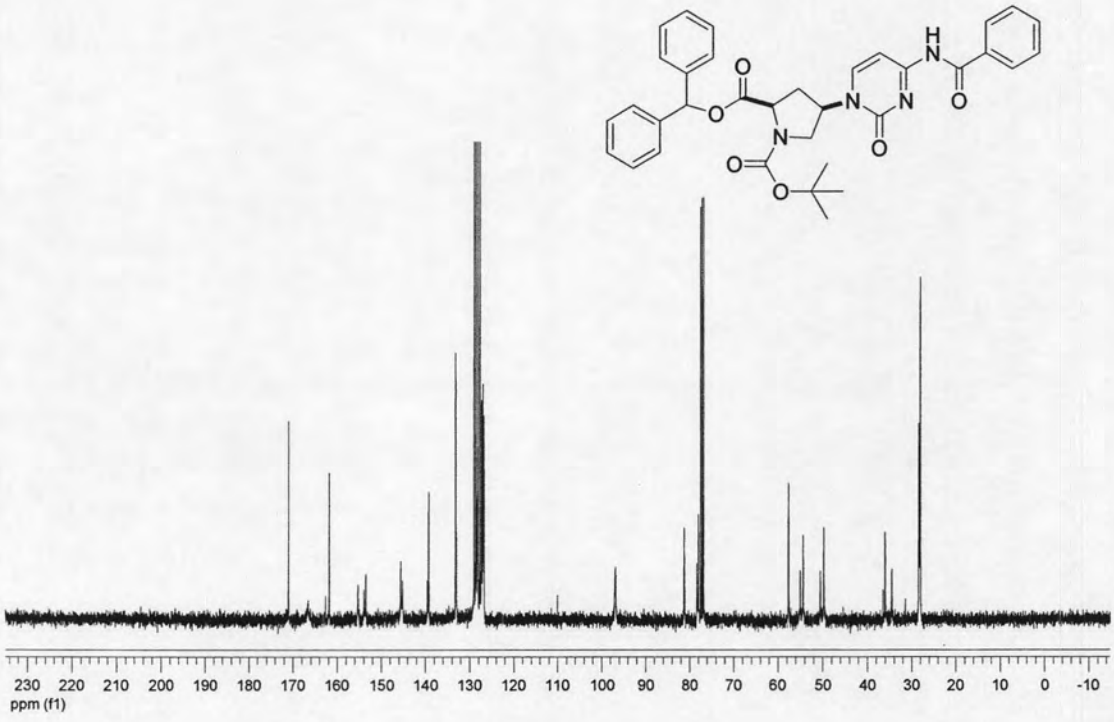

Figure A-56: ^{13}C NMR (100 MHz, $CDCl_3$) of (*N-tert*-butyloxycarbonyl)-*cis*-4-(N^4-benzoylcytosin-9-yl)-D-proline diphenylmethyl ester (**29**)

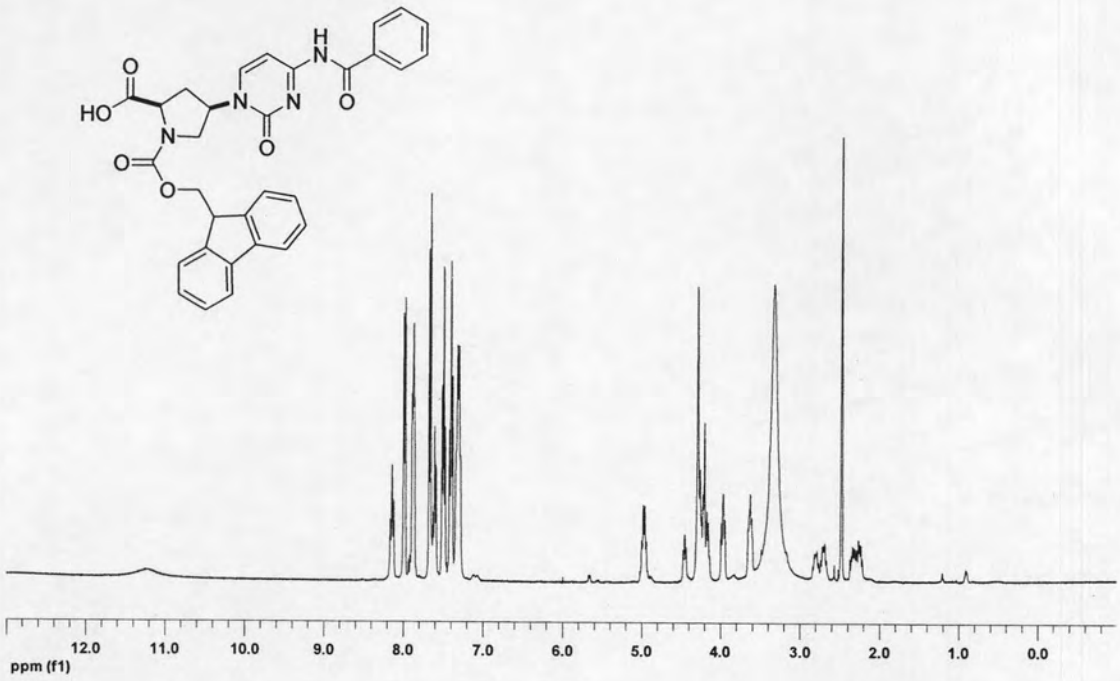

Figure A-57: ^{1}H NMR (400 MHz, $CDCl_3$) of (*N*-fluoren-9-ylmethoxycarbonyl)-*cis*-4-(N^4-benzoylcytosin-1-yl)-D-proline (**30**)

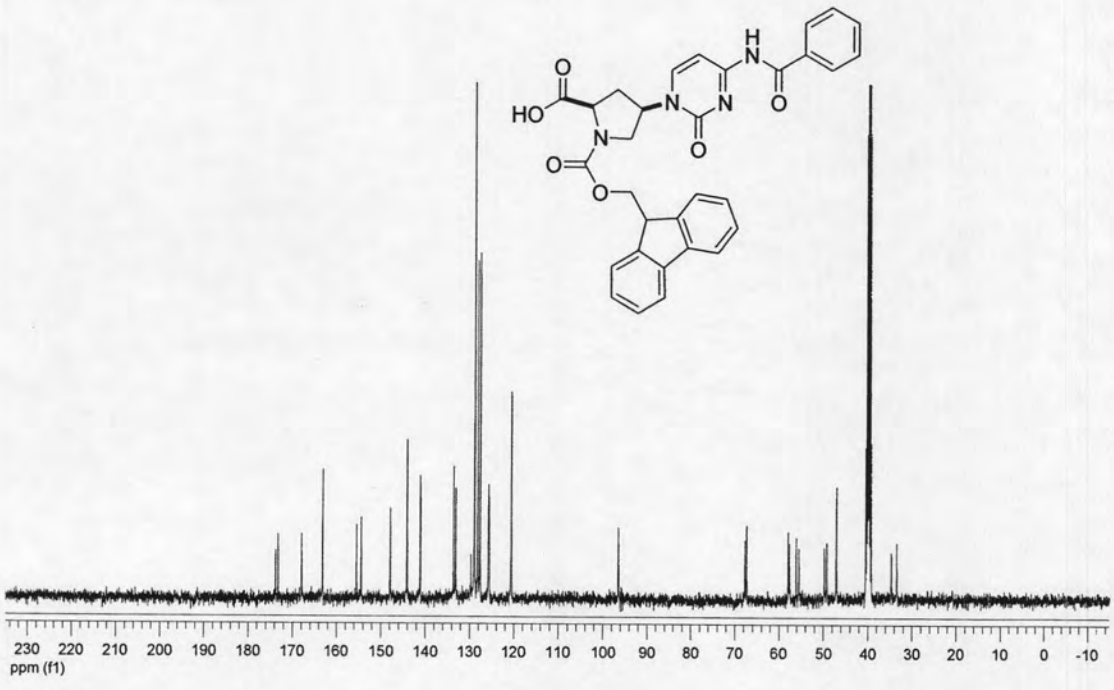

Figure A-58: ^{13}C NMR (100 MHz, $CDCl_3$) of (*N*-Fluoren-9-ylmethoxycarbonyl)-*cis*-4-(N^4-benzoylcytosin-1-yl)-D-proline (**30**)

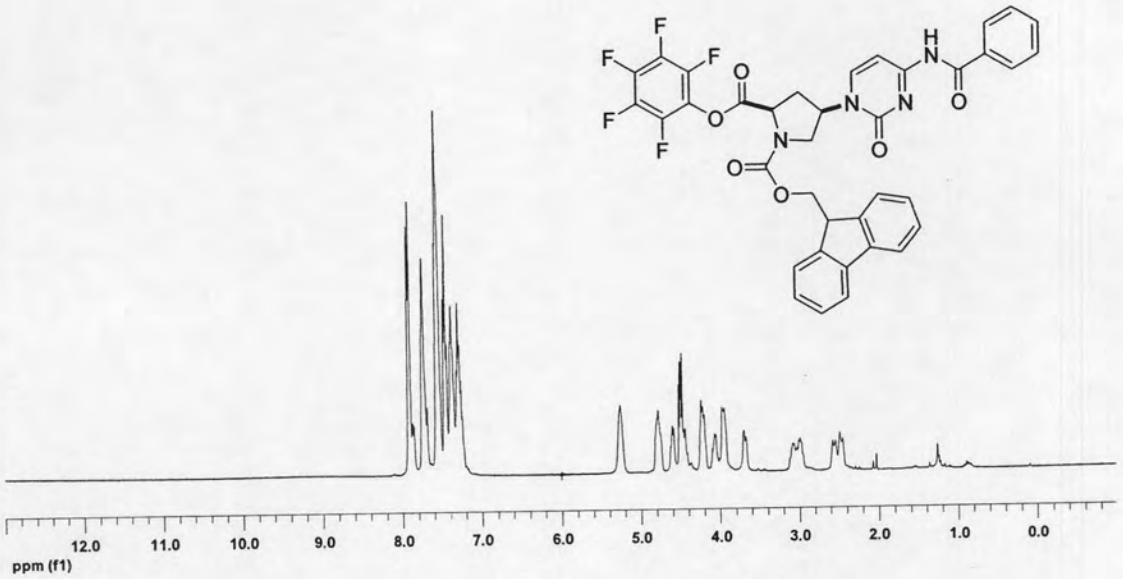

Figure A-59: ^{1}H NMR (400 MHz, $CDCl_3$) of (*N*-Fluoren-9-ylmethoxycarbonyl)-*cis*-4-(N^4-benzoylcytosin-1-yl)-D-proline pentafluorophenyl ester (**31**)

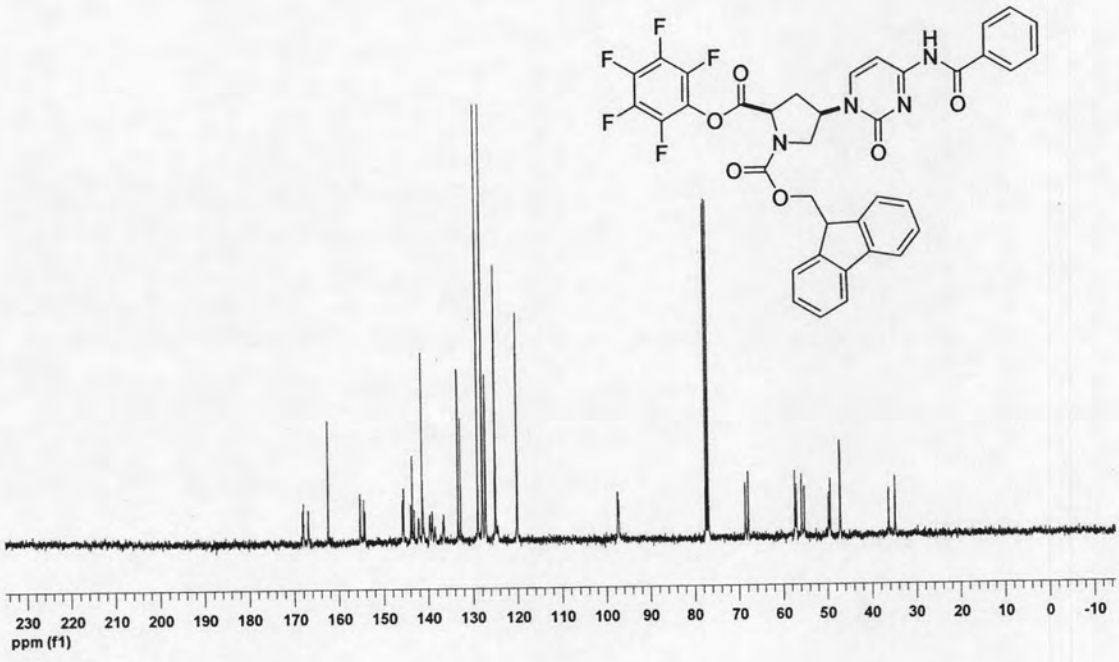

Figure A-60: ^{13}C NMR (100 MHz, $CDCl_3$) of (*N*-Fluoren-9-ylmethoxycarbonyl)-*cis*-4-(N^4-benzoylcytosin-1-yl)-D-proline pentafluorophenyl ester (**31**)

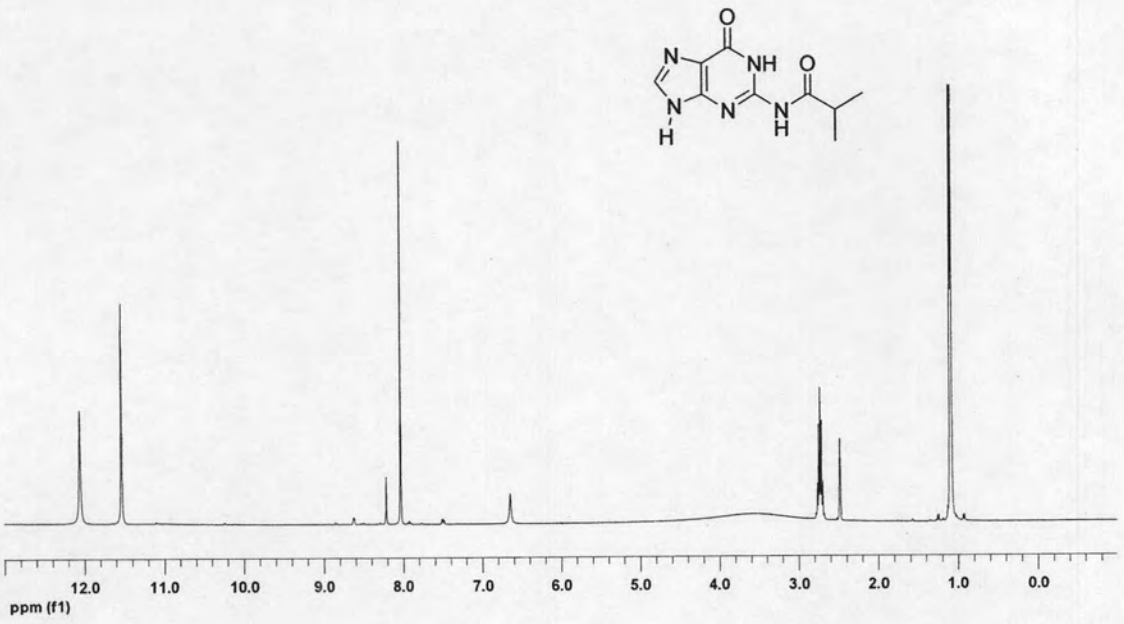

Figure A-61: ^{1}H NMR (400 MHz, DMSO-d_6) of N^2-Isobutyrylguanine (**32**)

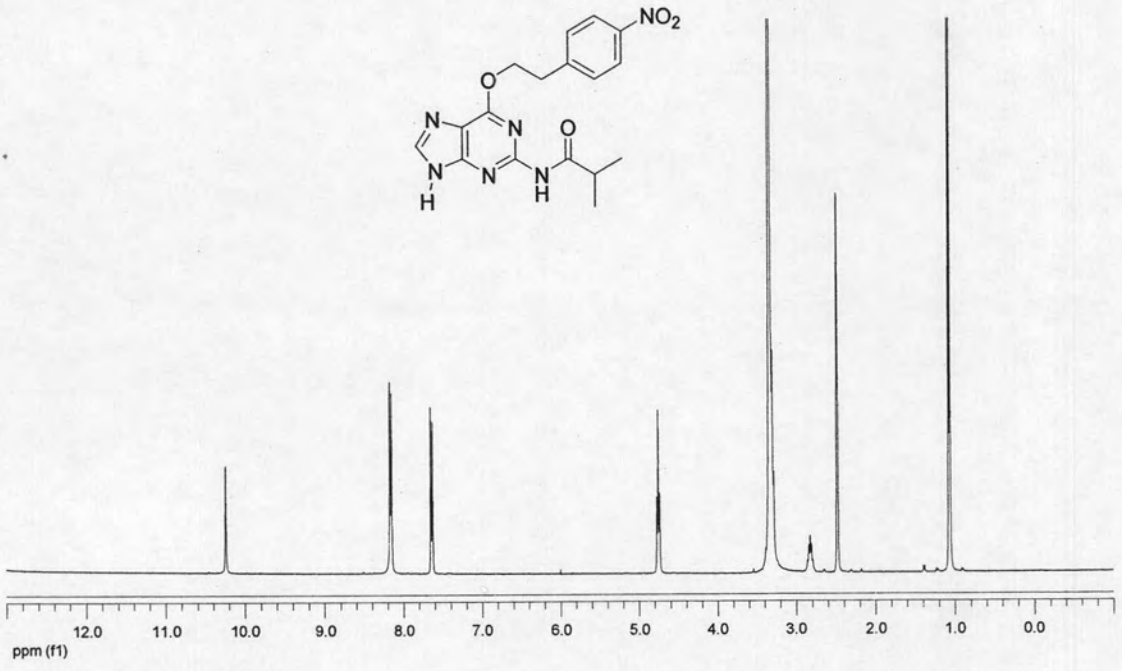

Figure A-62: ^{1}H NMR (400 MHz, DMSO-d_6) of N^2-Isobutyryl-O^7-(*p*-nitroethyl) guanine

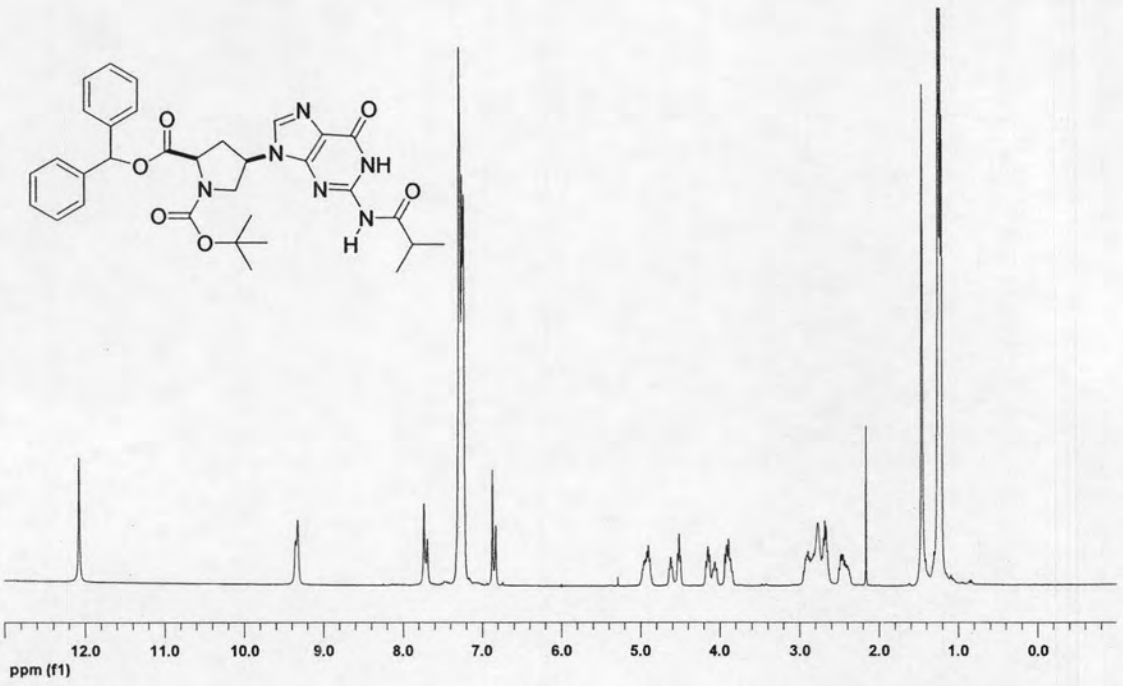

Figure A-63: ^{1}H NMR (400 MHz, $CDCl_3$) of (*N-tert*-butyloxycarbonyl)-*cis*-4-(N^2-isobutylguanin-9-yl)-D-proline diphenylmethyl ester (**33**)

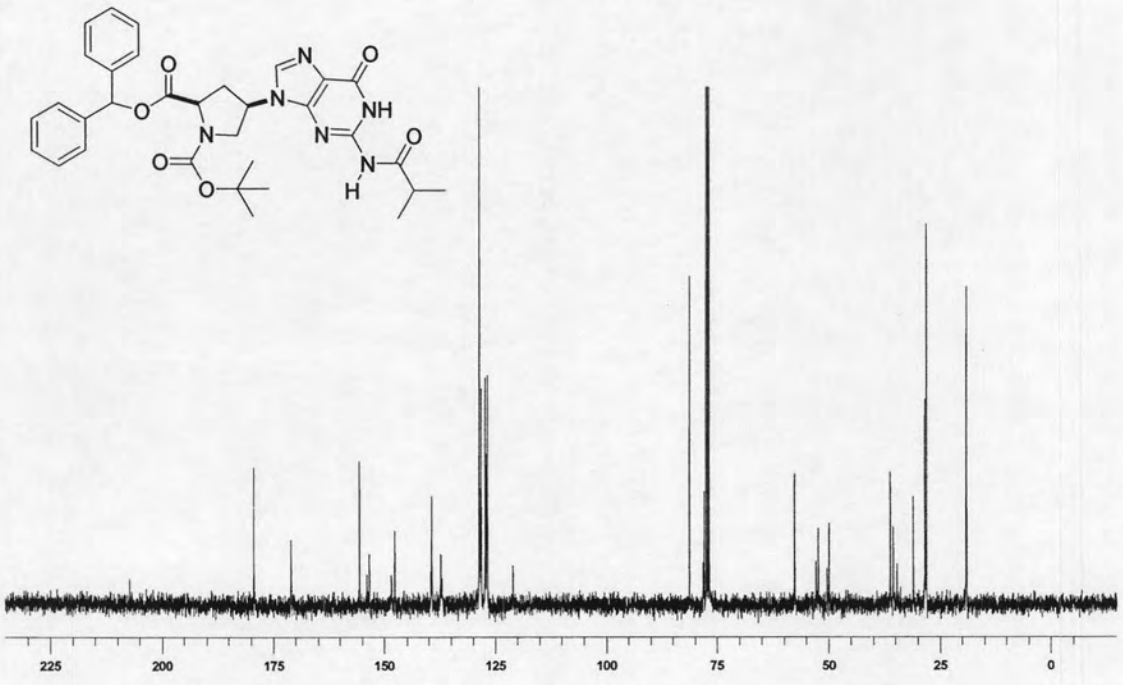

Figure A-64: ^{13}C NMR (100 MHz, $CDCl_3$) of (*N-tert*-butyloxycarbonyl)-*cis*-4-(N^2-isobutylguanin-9-yl)-D-proline diphenylmethyl ester (**33**)

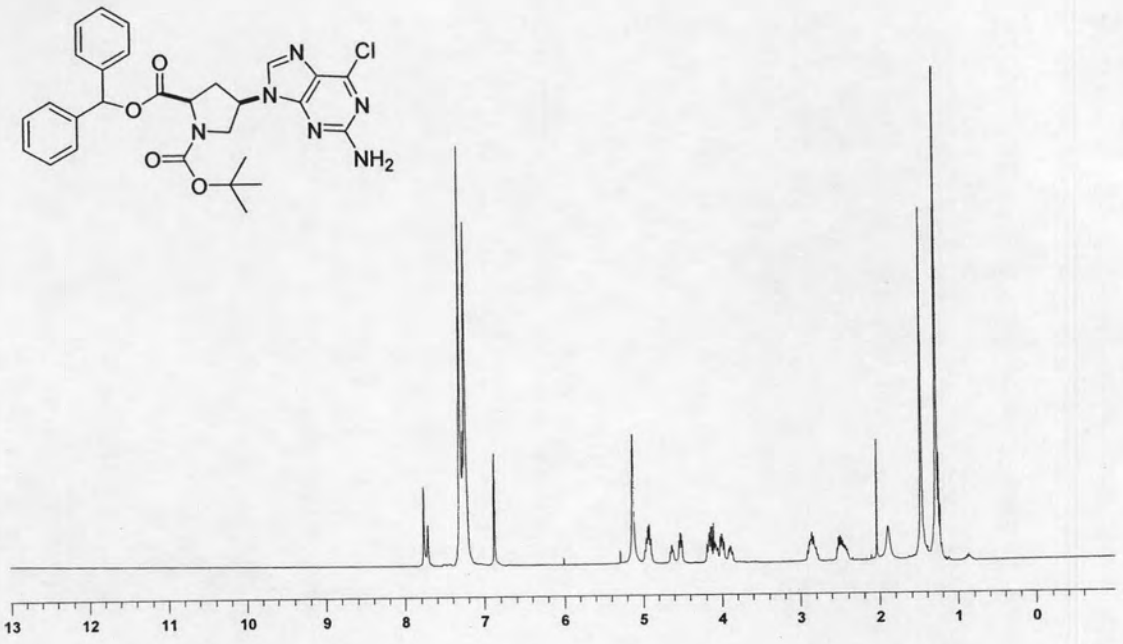

Figure A-65: ^{1}H NMR (400 MHz, $CDCl_3$) of (*N-tert*-butyloxycarbonyl)-*cis*-4-(6-chloroguanin-9-yl)-D-proline diphenylmethyl ester (**34**)

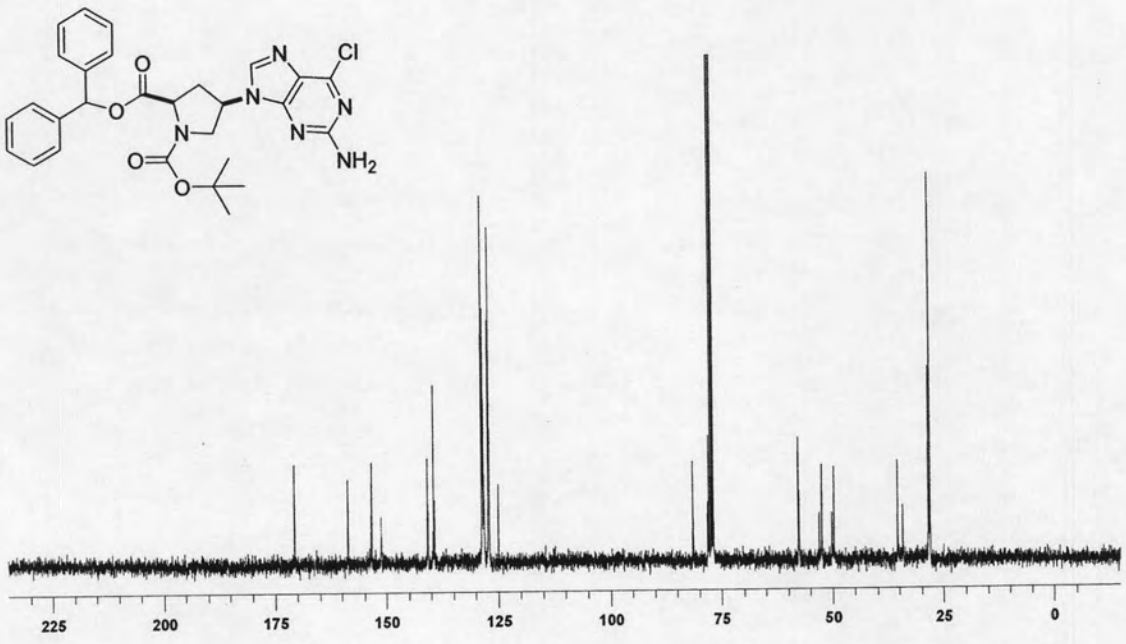

Figure A-66: ^{13}C NMR (100 MHz, $CDCl_3$) of (*N-tert*-butyloxycarbonyl)-*cis*-4-(6-chloroguanin-9-yl)-D-proline diphenylmethyl ester (**34**)

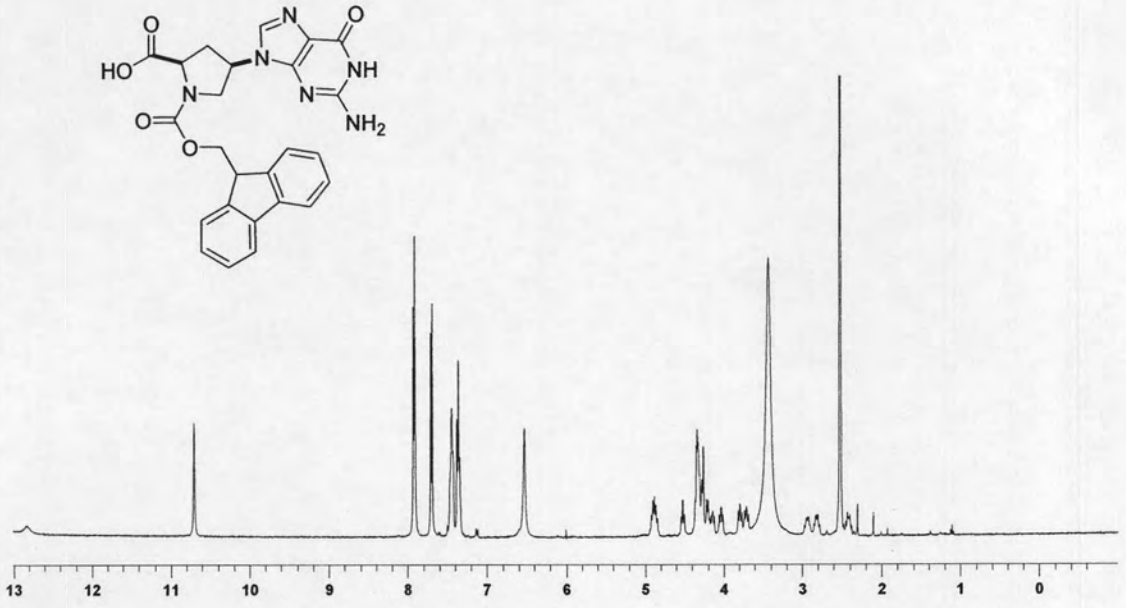

Figure A-67: ^{1}H NMR (400 MHz, DMSO-d_6) of (*N*-Fluoren-9-ylmethoxycarbonyl)-*cis*-4-(guanin-9-yl)-D-proline (**35**)

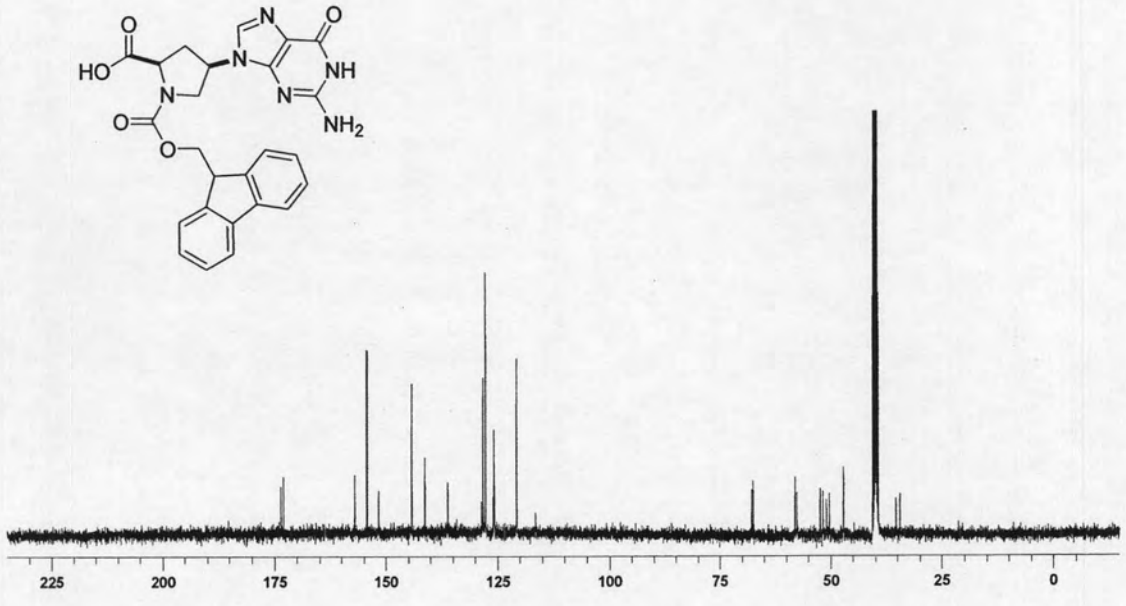

Figure A-68: ^{13}C NMR (100 MHz, DMSO-d_6) of (*N*-Fluoren-9-ylmethoxycarbonyl)-*cis*-4-(guanin-9-yl)-D-proline (**35**)

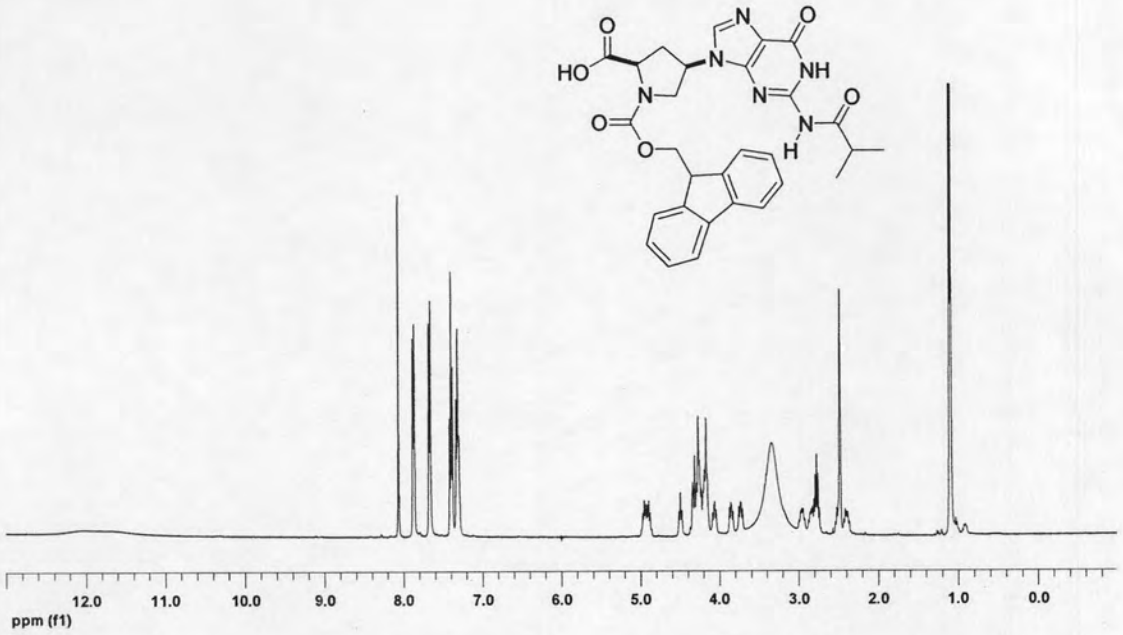

Figure A-69: ^{1}H NMR (400 MHz, DMSO-d_6) of (*N*-Fluoren-9-ylmethoxycarbonyl)-*cis*-4-(N^2-isobutyrylguanin-9-yl)-D-proline (**36**)

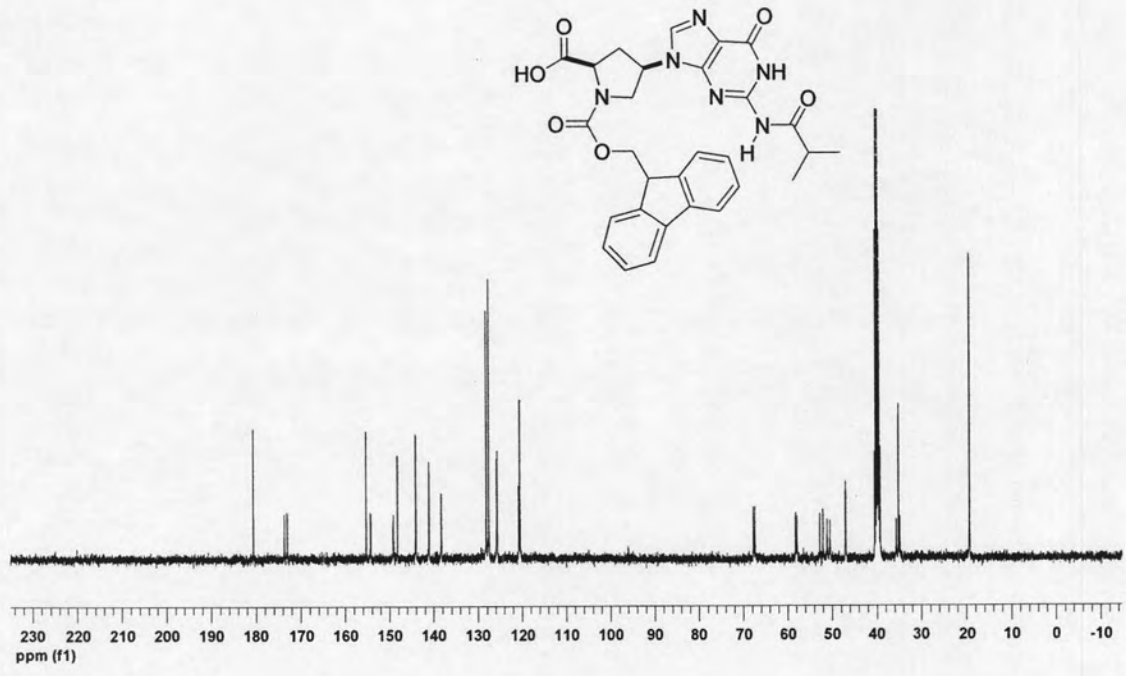

Figure A-70: ^{13}C NMR (100 MHz, DMSO-d_6) of (*N*-Fluoren-9-ylmethoxycarbonyl)-*cis*-4-(N^2-isobutyrylguanin-9-yl)-D-proline (**36**)

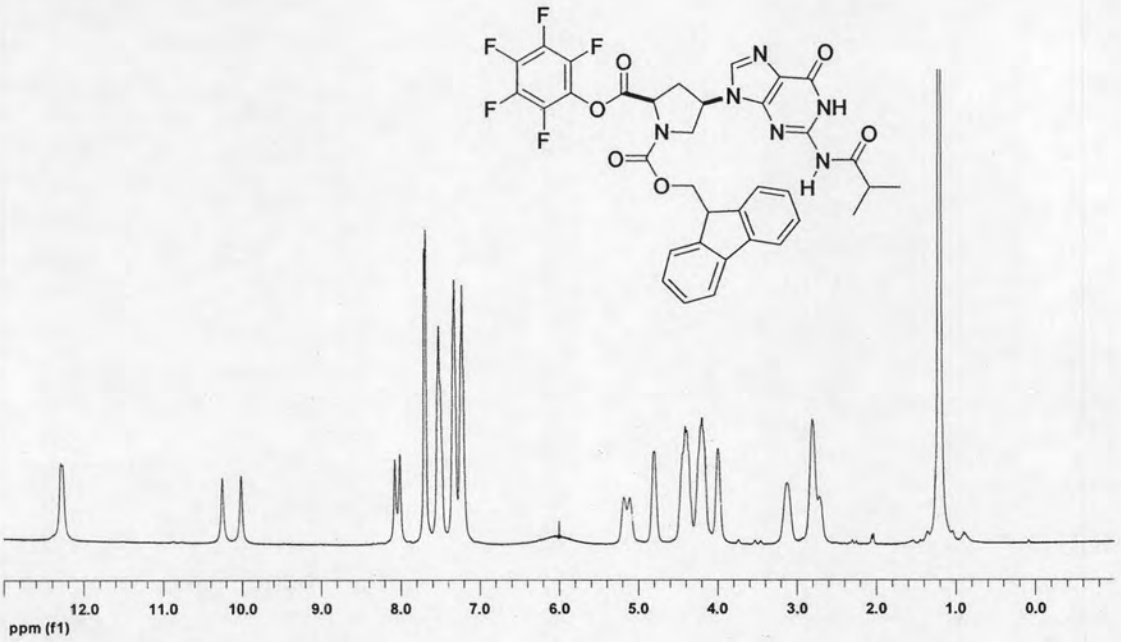

Figure A-71: ^{1}H NMR (400 MHz, $CDCl_3$) of (*N*-Fluoren-9-ylmethoxycarbonyl amino)-*cis*-4-(N^2-isobutyrylguanin-9-yl)-D-proline pentafluorophenyl ester (**37**)

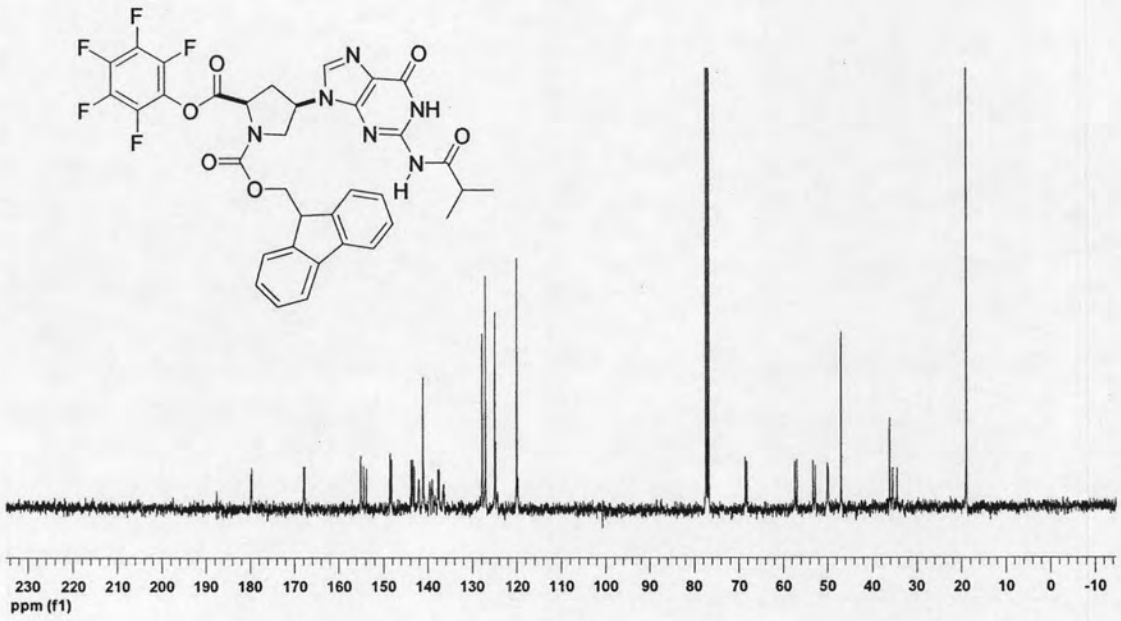

Figure A-72: ^{13}C NMR (100 MHz, $CDCl_3$) of (*N*-Fluoren-9-ylmethoxycarbonyl amino)-*cis*-4-(N^2-isobutyrylguanin-9-yl)-D-proline pentafluorophenyl ester (**37**)

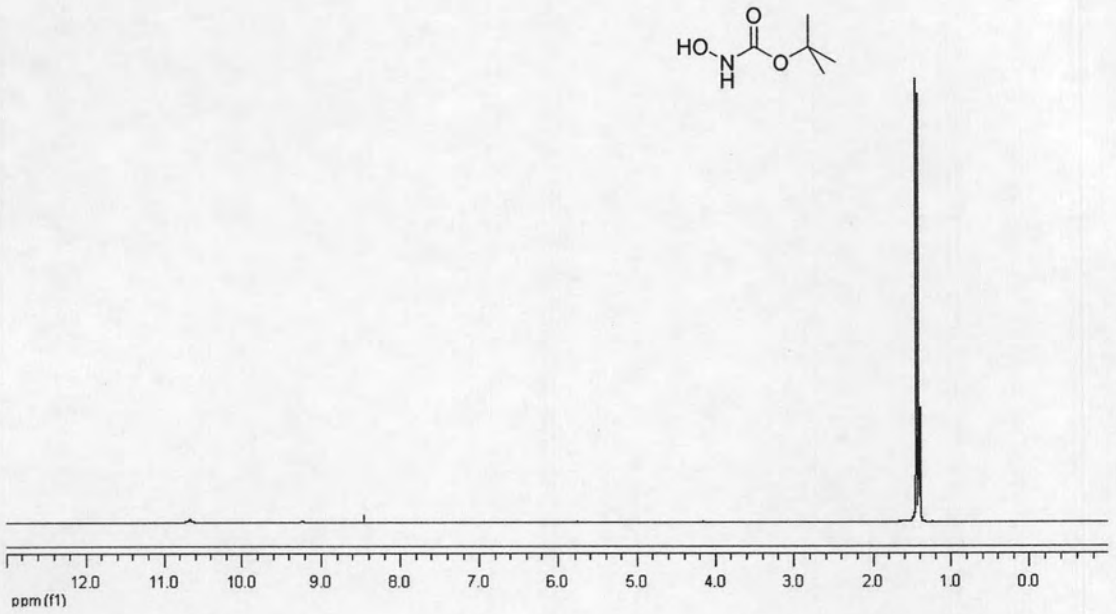

Figure A-73: ^{1}H NMR (200 MHz, $CDCl_3$) of *N-tert*-Butoxycarbonyl hydroxylamine (**38**)

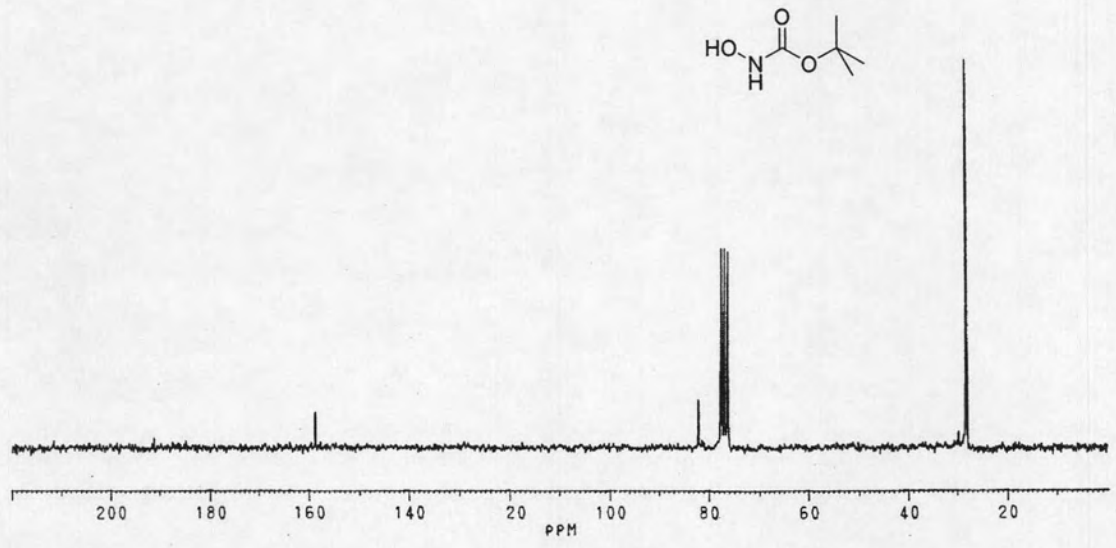

Figure A-74: ^{13}C NMR (50 MHz, $CDCl_3$) of *N-tert*-Butoxycarbonyl hydroxylamine (**38**)

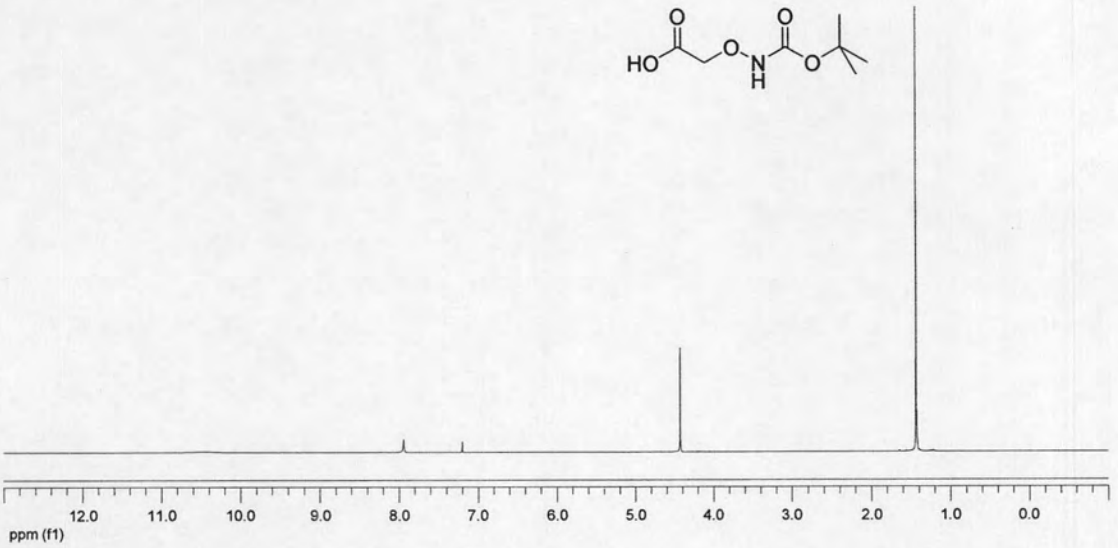

Figure A-75: ^{1}H NMR (300 MHz, DMSO-d_6) of *N-tert*-Butoxycarbonyl aminooxy-acetic acid (**39**)

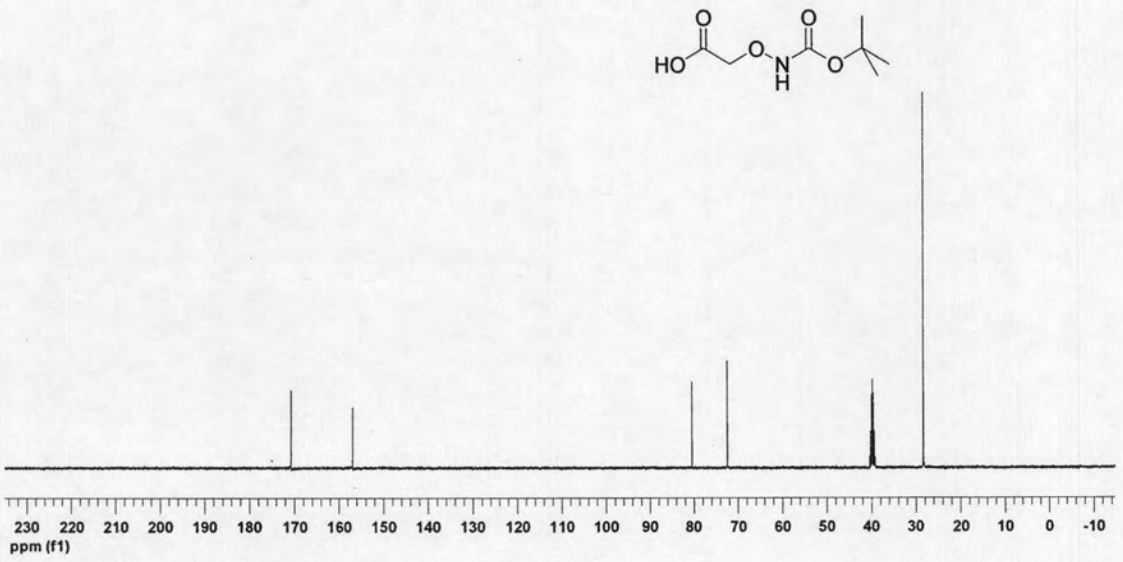

Figure A-76: ^{13}C NMR (75 MHz, DMSO-d_6) of *N-tert*-Butoxycarbonyl aminooxy-acetic acid (**39**)

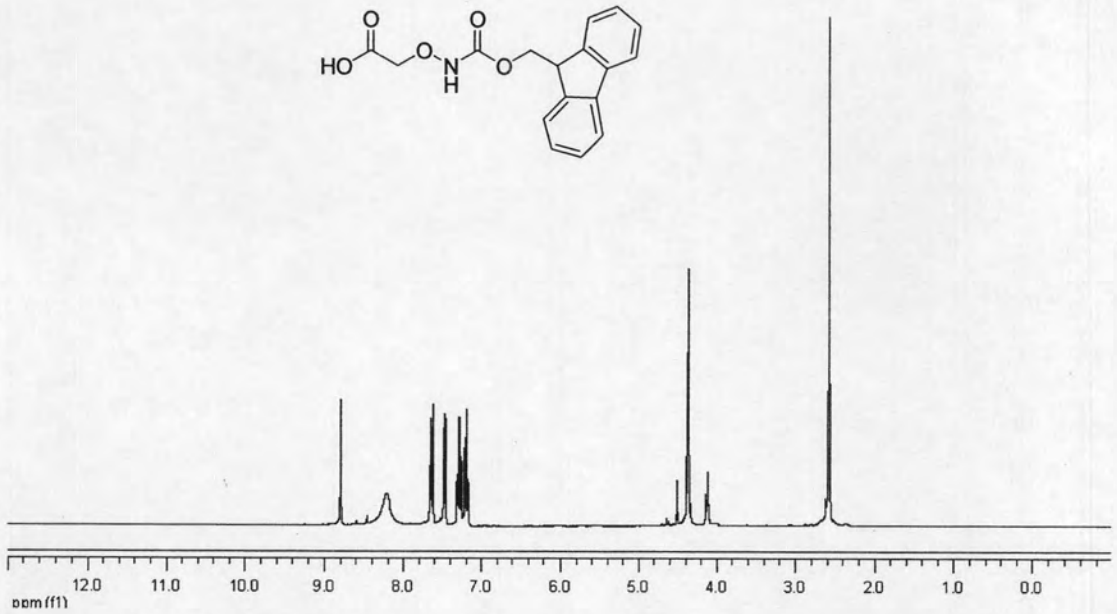

Figure A-77: ^{1}H NMR (300 MHz, $CDCl_3$) of (*N'*-Fluoren-9-ylmethoxycarbonyl)-aminooxy acetic acid (**41**)

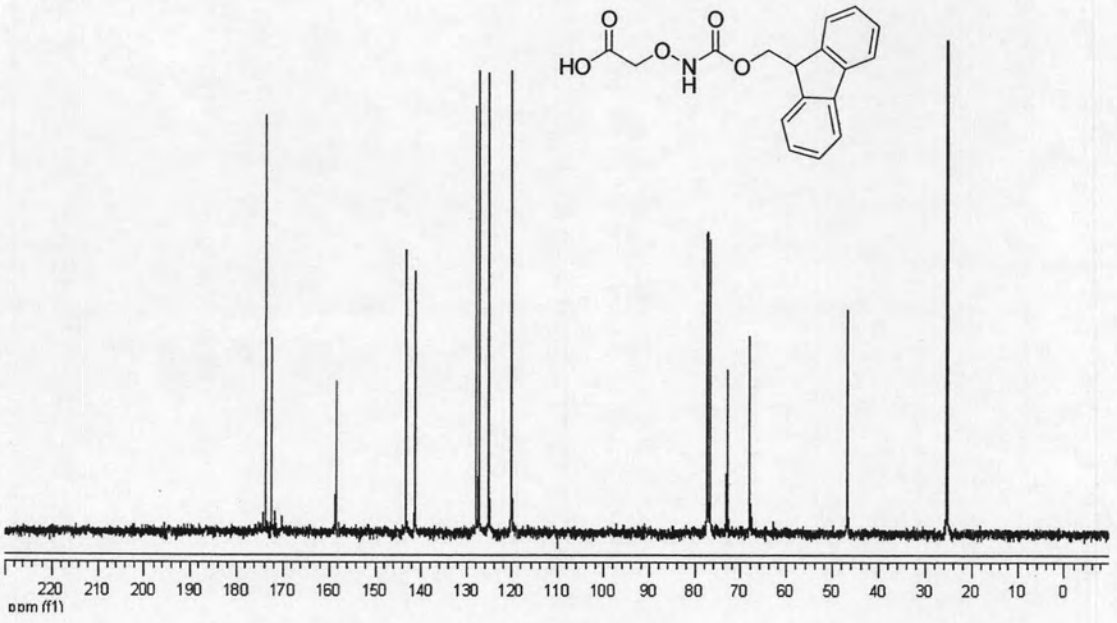

Figure A-78: ^{13}C NMR (67 MHz, $CDCl_3$) of (*N'*-Fluoren-9-ylmethoxycarbonyl)-aminooxy acetic acid (**41**)

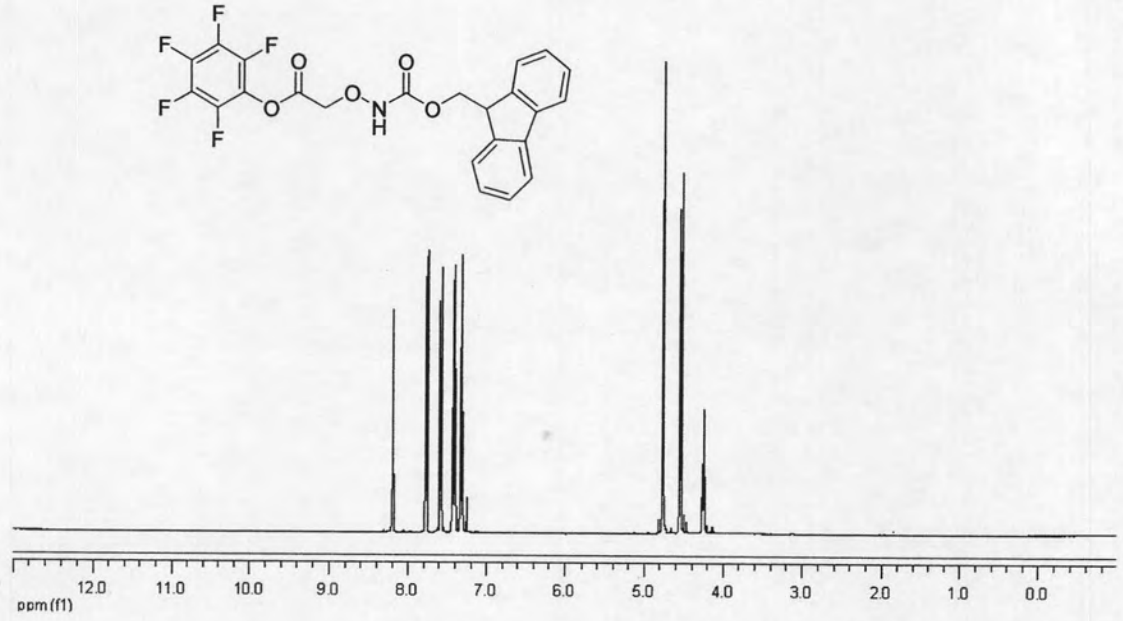

Figure A-79: ^{1}H NMR (400 MHz, $CDCl_3$) of (*N'*-Fluoren-9-ylmethoxycarbonyl)-aminooxy acetic acid pentafluorophenyl ester (**42**)

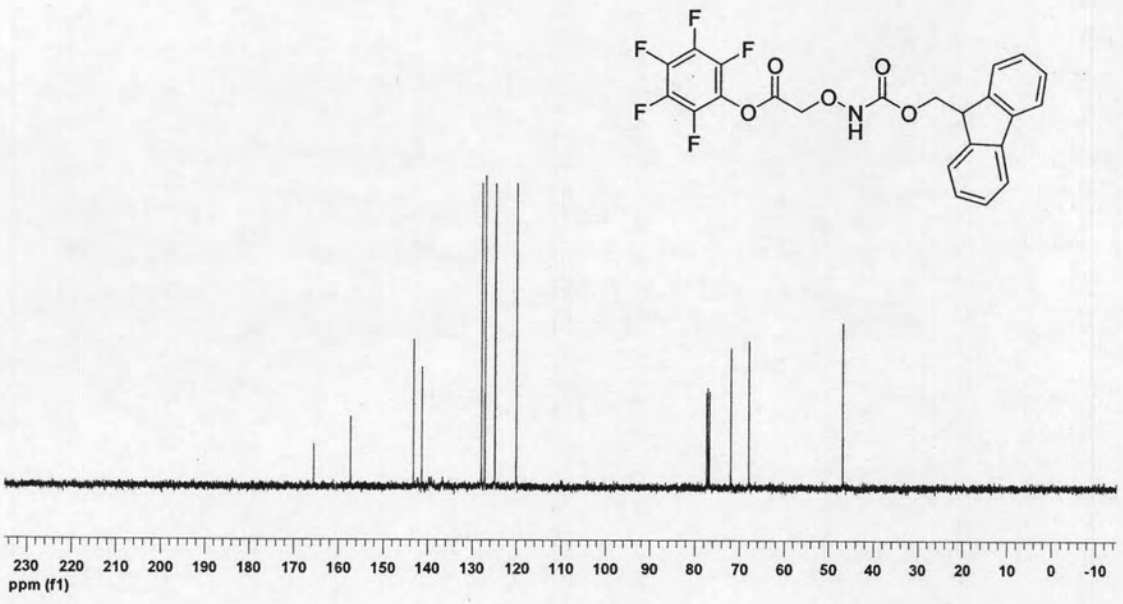

Figure A-80: ^{13}C NMR (100 MHz, $CDCl_3$) of (*N'*-Fluoren-9-ylmethoxycarbonyl)-aminooxy acetic acid pentafluorophenyl ester (**42**)

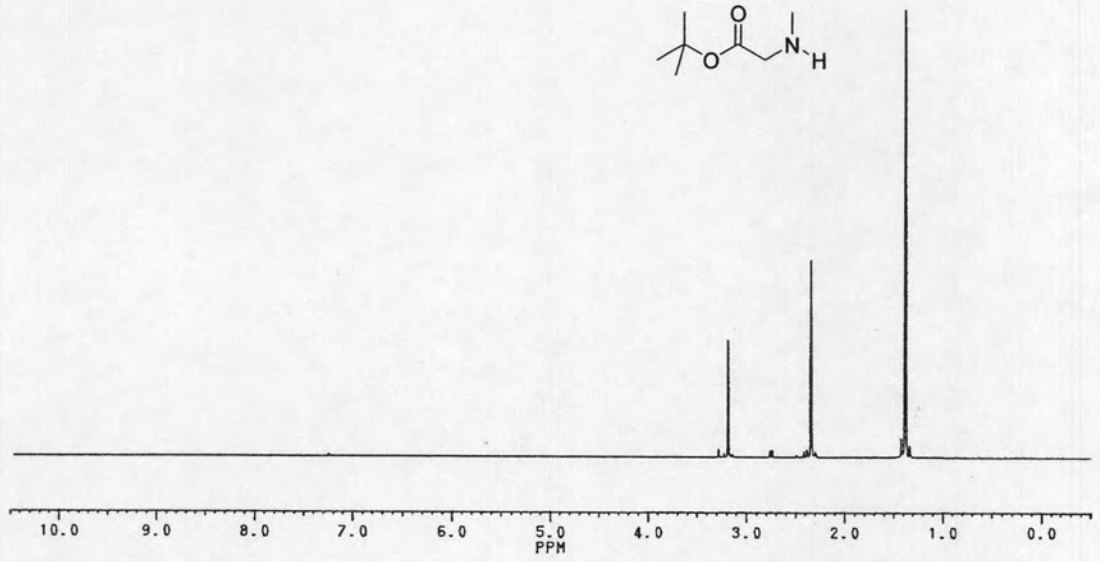

Figure A-81: ^{1}H NMR (200 MHz, $CDCl_3$) of *N*-methyl glycine *tert*-butyl ester (**43**)

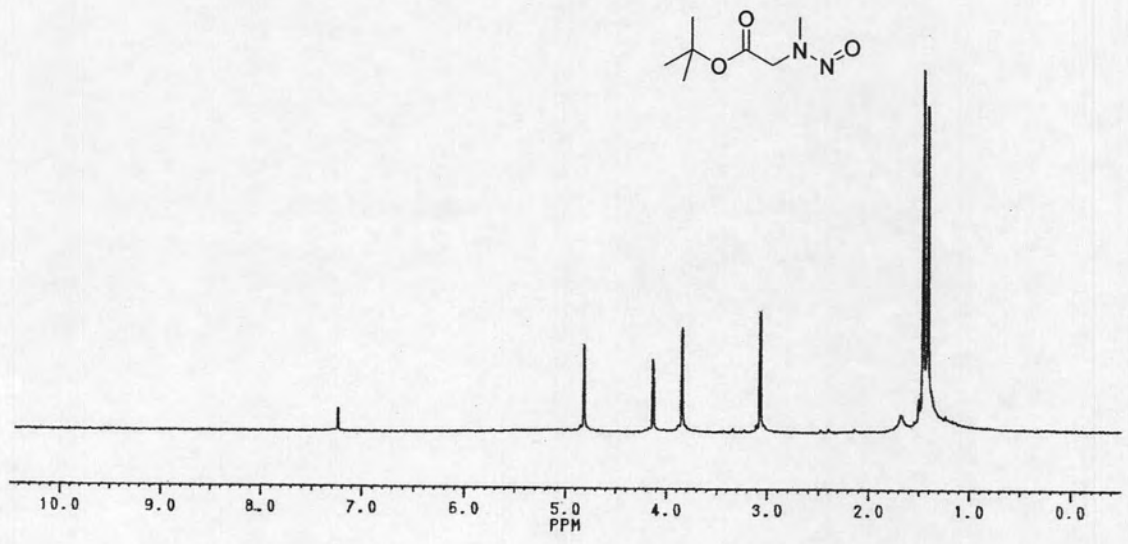

Figure A-82: ^{1}H NMR (200 MHz, $CDCl_3$) of (*N*-Nitroso)-*N*-methyl glycine *tert*-butyl ester (**44**)

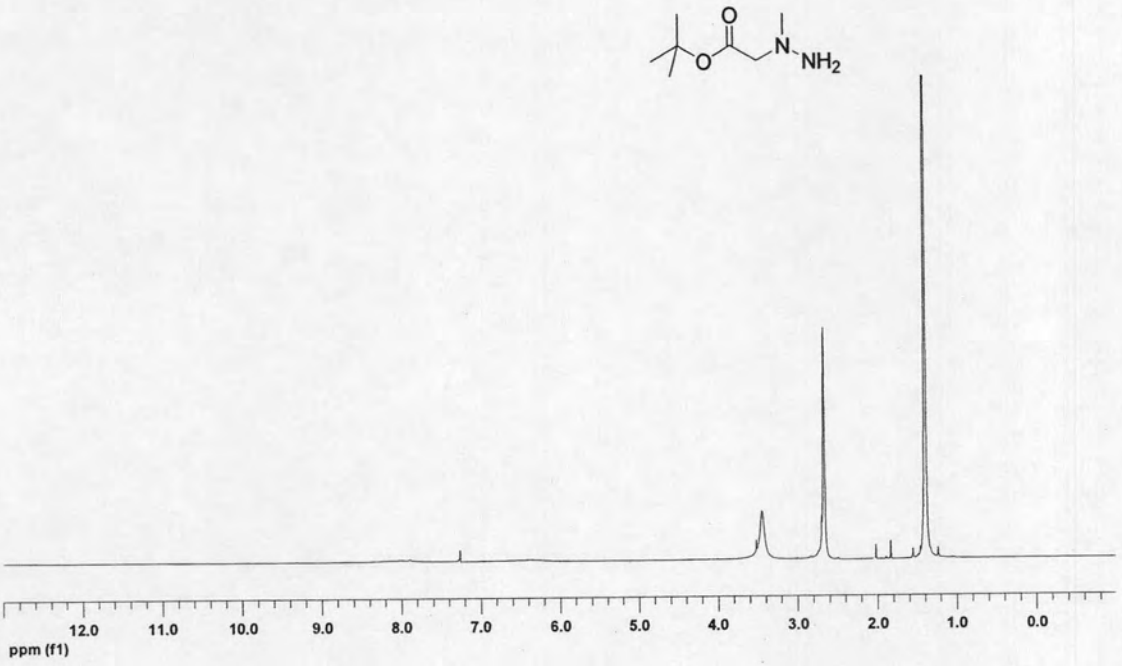

Figure A-83: ^{1}H NMR (400 MHz, $CDCl_3$) of (*N*-Amino)-*N*-methyl glycine *tert*-butyl ester (**45**)

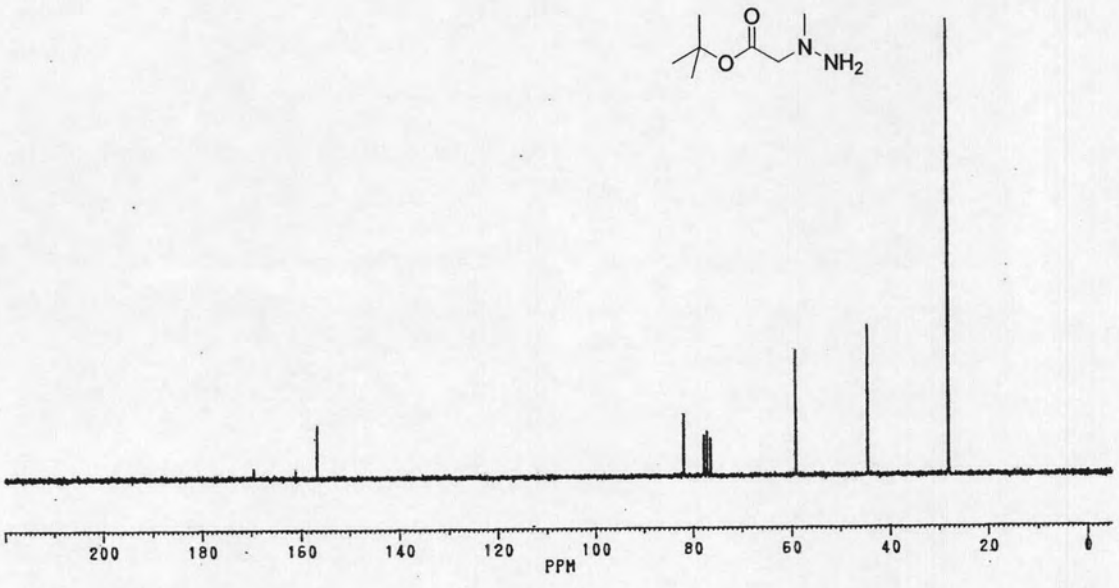

Figure A-84: ^{13}C NMR (50 MHz, $CDCl_3$) of (*N*-Amino)-*N*-methyl glycine *tert*-butyl ester (**45**)

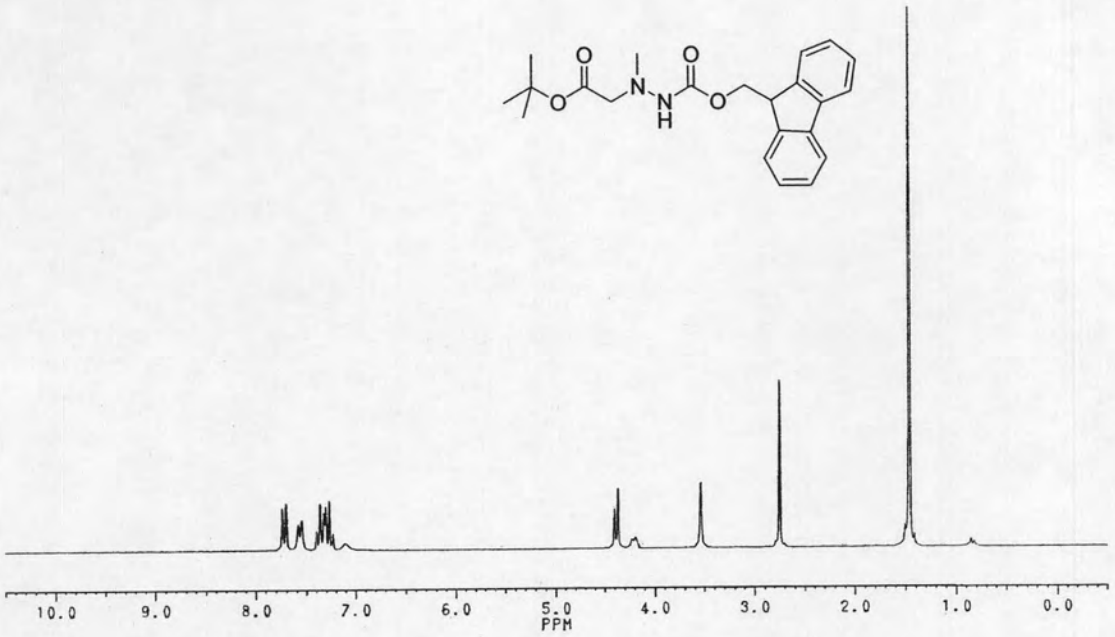

Figure A-85: ^{1}H NMR (200 MHz, $CDCl_3$) of (*N'*-Fluoren-9-ylmethoxycarbonyl)-(*N*-amino)-*N*-methyl glycine *tert*-butyl ester (**46**)

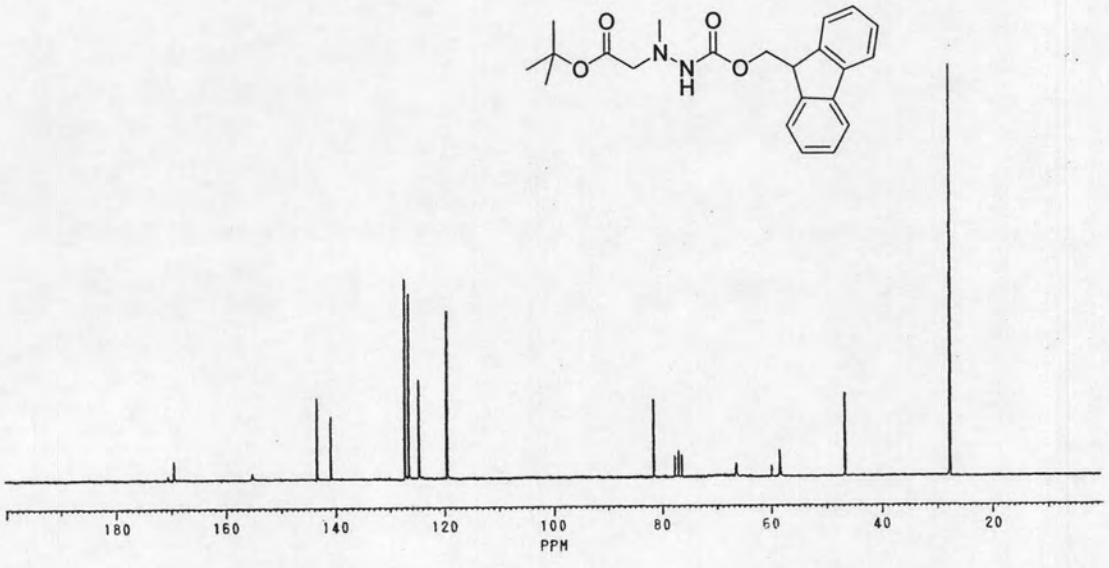

Figure A-86: ^{13}C NMR (50 MHz, $CDCl_3$) of (*N'*-Fluoren-9-ylmethoxycarbonyl)-(*N*-amino)-*N*-methyl glycine *tert*-butyl ester (**46**)

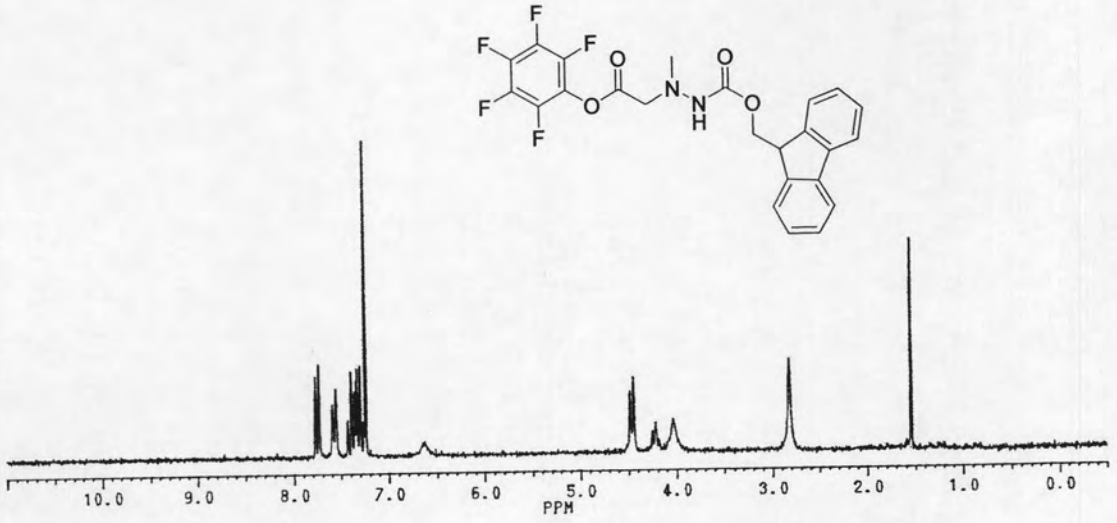

Figure A-87: ^{1}H NMR (200 MHz, $CDCl_3$) of (*N'*-Fluoren-9-ylmethoxycarbonyl)-(*N*-amino)-*N*-methyl glycine pentafluorophenyl ester (**47**)

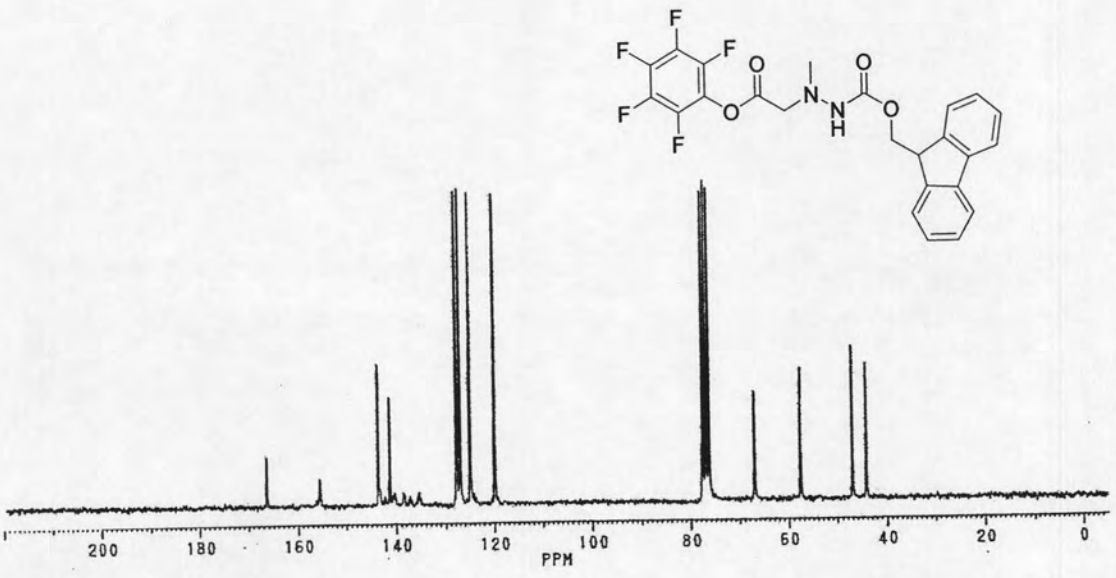

Figure A-88: ^{13}C NMR (50 MHz, $CDCl_3$) of (*N'*-Fluoren-9-ylmethoxycarbonyl)-(*N*-amino)-*N*-methyl glycine pentafluorophenyl ester (**47**)

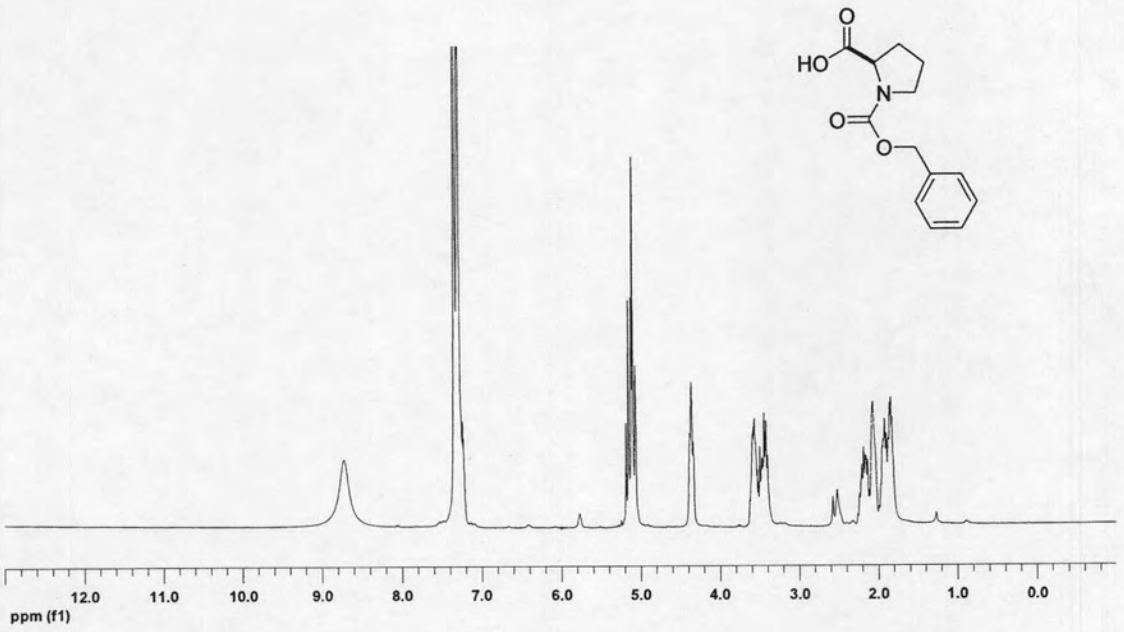

Figure A-89: ^{1}H NMR (400 MHz, $CDCl_3$) of *N*-Benzyloxycarbonyl-D-proline (**48**)

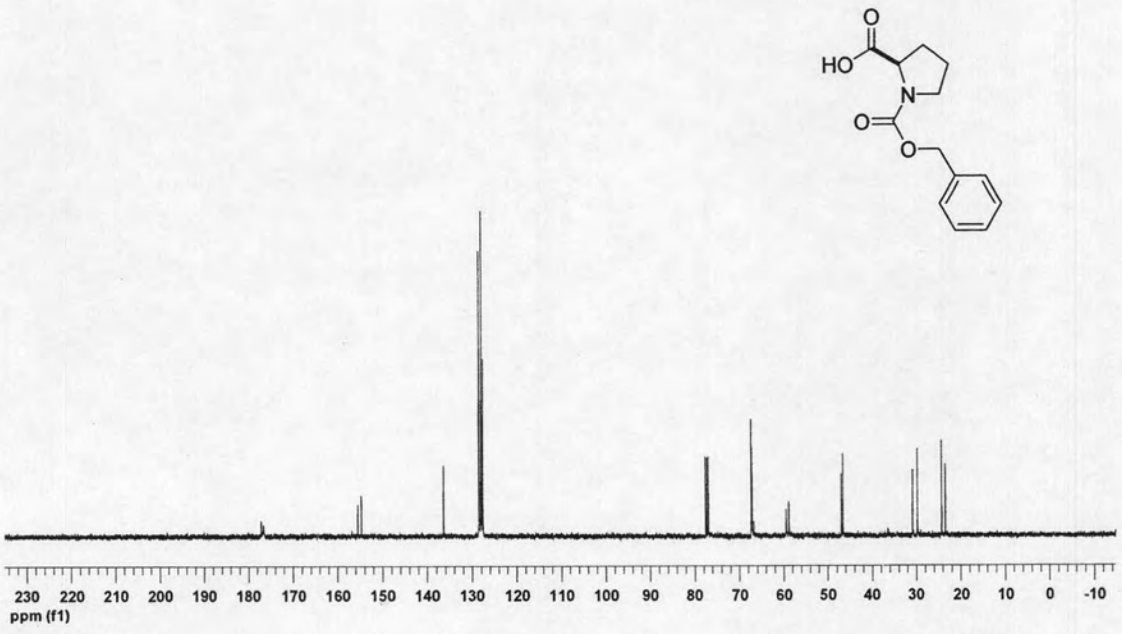

Figure A-90: ^{13}C NMR (100 MHz, $CDCl_3$) of *N*-Benzyloxycarbonyl-D-proline (**48**)

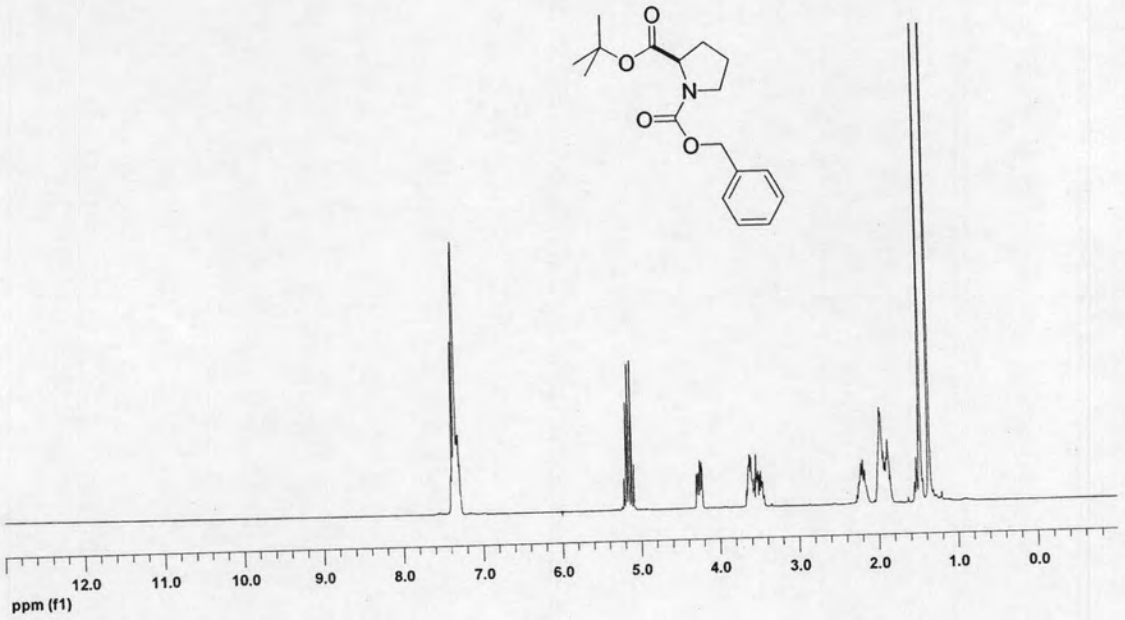

Figure A-91: ^{1}H NMR (300 MHz, $CDCl_3$) of *N*-Benzyloxycarbonyl-D-proline *tert*-butyl ester (**49**)

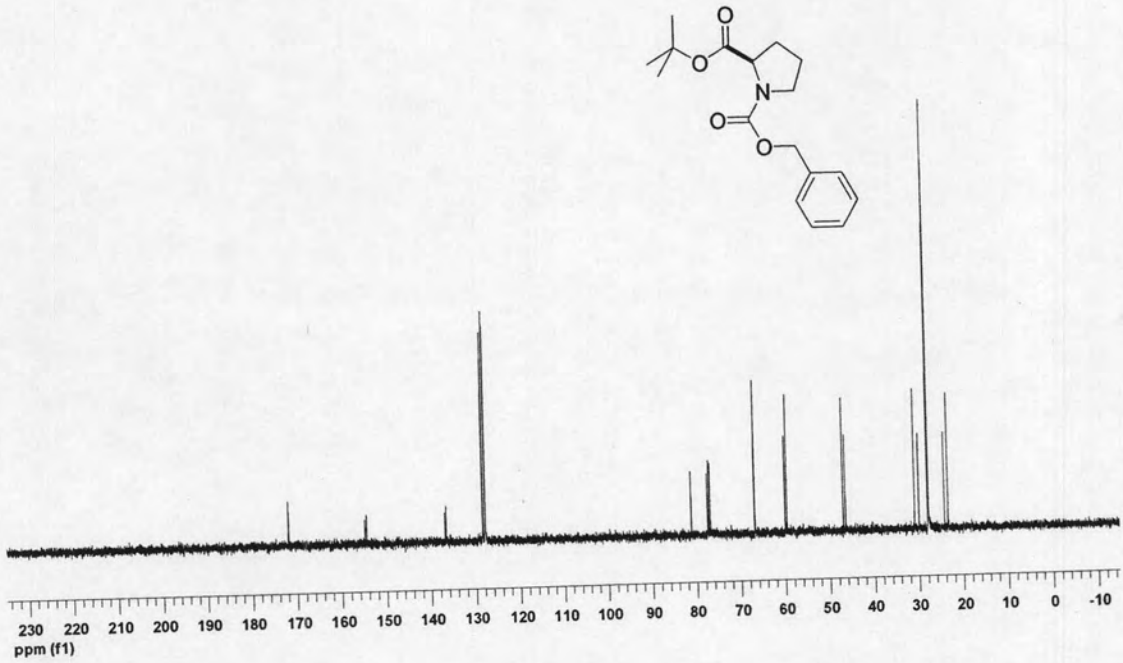

Figure A-92: ^{13}C NMR (75 MHz, $CDCl_3$) of *N*-Benzyloxycarbonyl-D-proline *tert*-butyl ester (**49**)

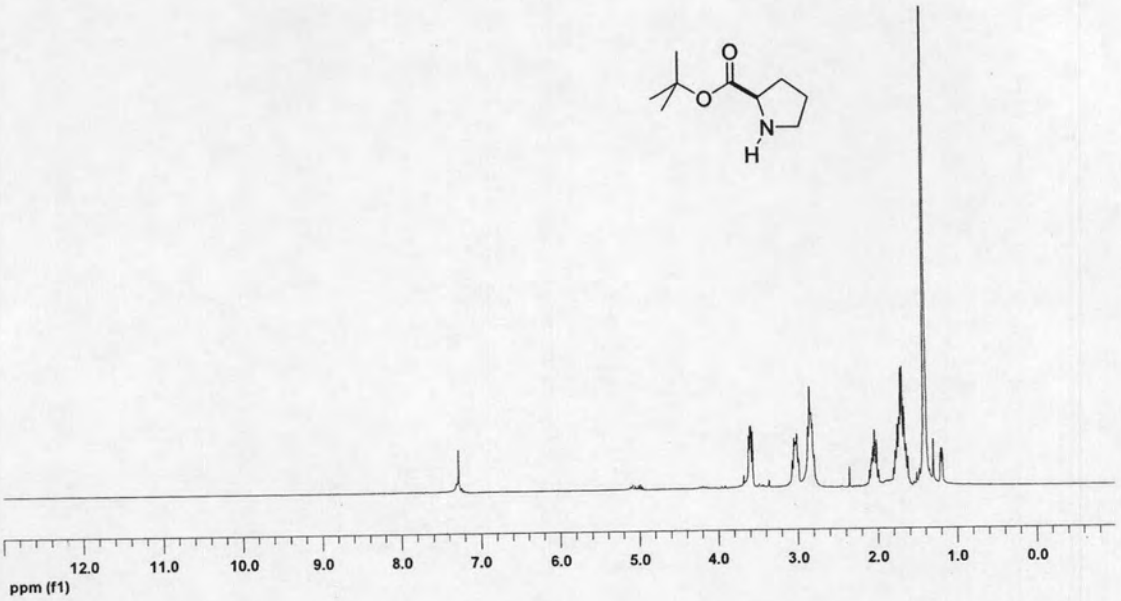

Figure A-93: ^{1}H NMR (300 MHz, $CDCl_3$) of D-Proline *tert*-butyl ester (**50**)

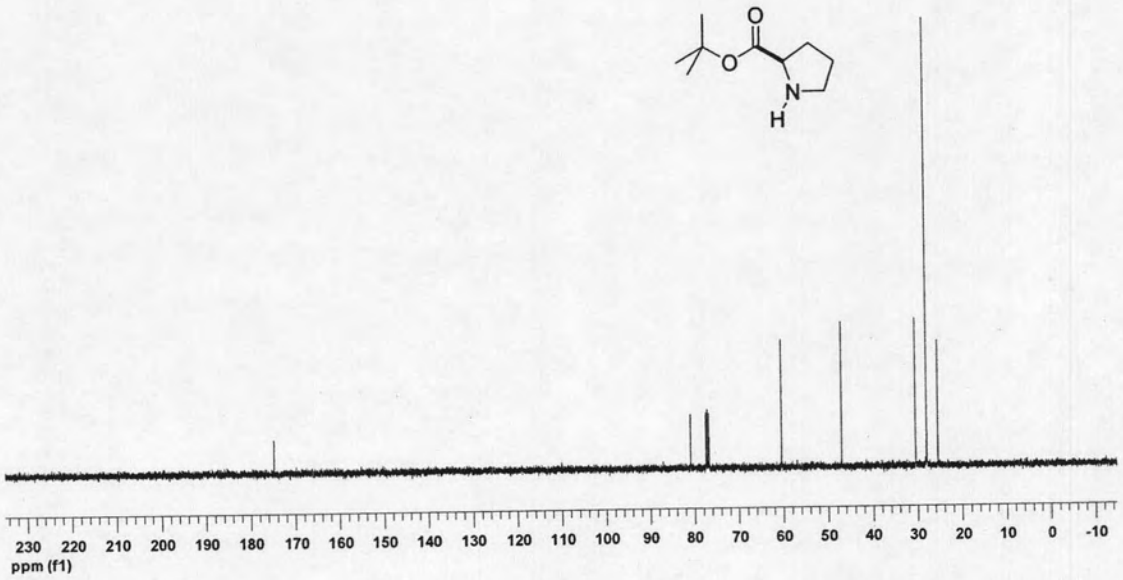

Figure A-94: ^{13}C NMR (75 MHz, $CDCl_3$) of D-Proline *tert*-butyl ester (**50**)

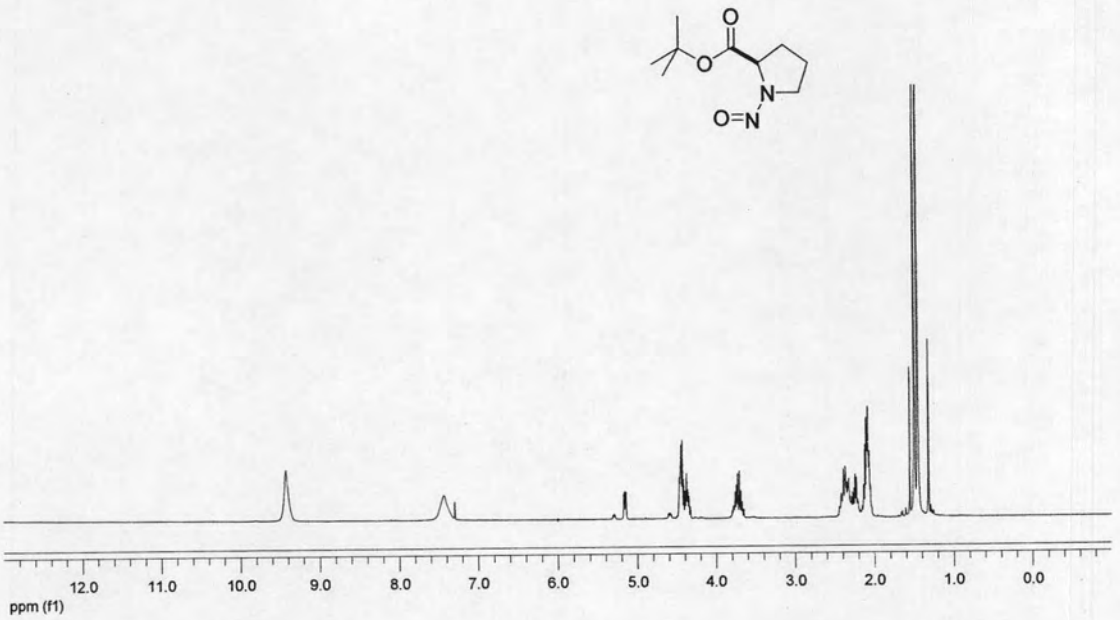

Figure A-95: ^{1}H NMR (300 MHz, $CDCl_3$) of *N*-Nitroso-D-proline tert-butyl ester **(51)**

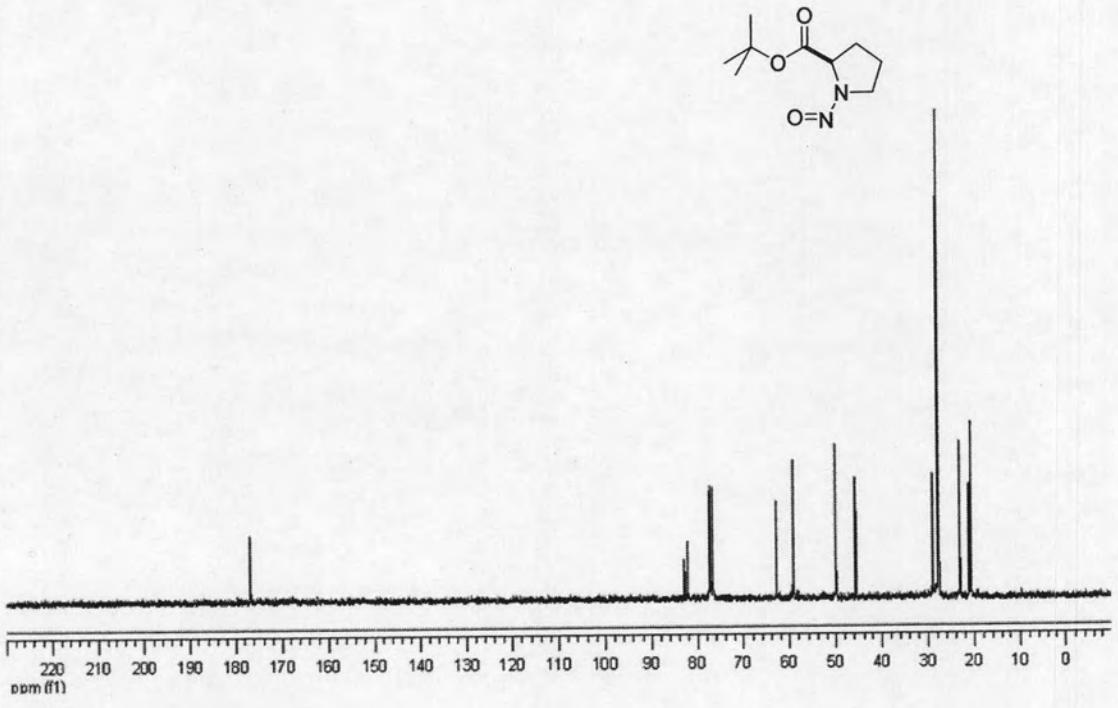

Figure A-96: ^{13}C NMR (75 MHz, $CDCl_3$) of *N*-Nitroso-D-proline *tert*-butyl ester **(51)**

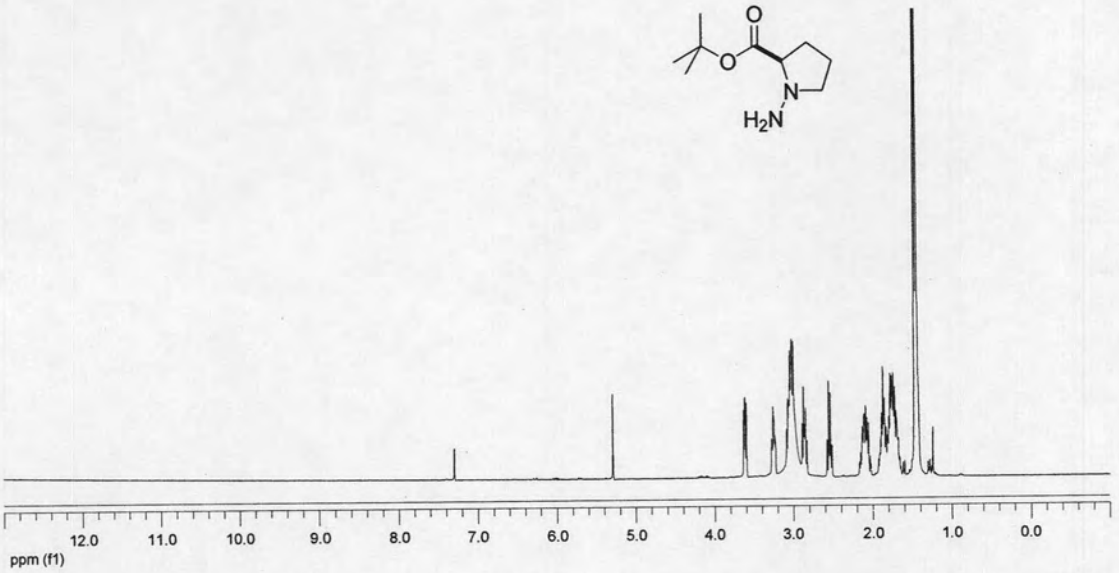

Figure A-97: ^{1}H NMR (400 MHz, $CDCl_3$) of *N*-Amino-D-proline *tert*-butyl ester (**52**)

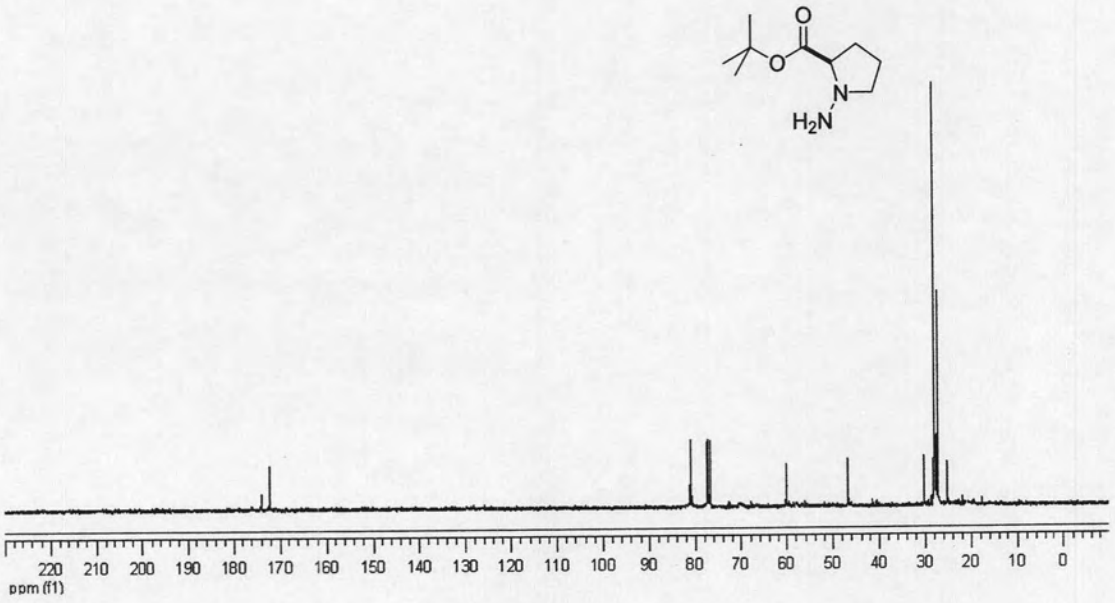

Figure A-98: ^{13}C NMR (100 MHz, $CDCl_3$) of *N*-Amino-D-proline *tert*-butyl ester (**52**)

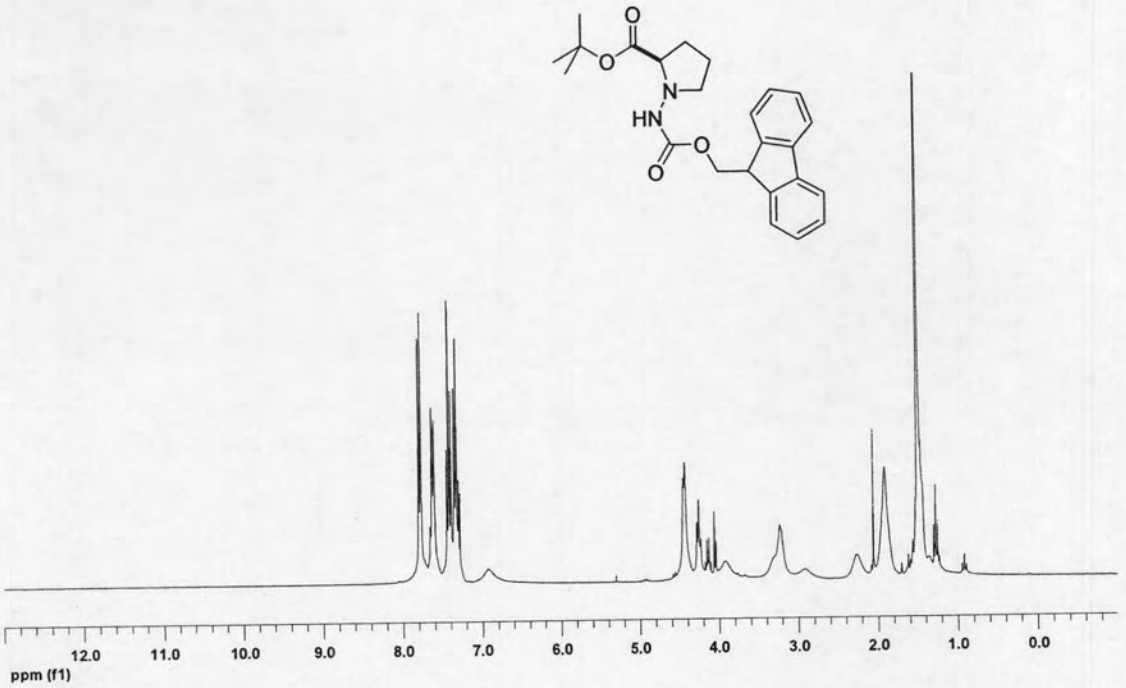

Figure A-99: ^{1}H NMR (300 MHz, $CDCl_3$) of (*N'*-Fluoren-9-ylmethoxycarbonyl)-*N*-Amino-D-proline *tert*-butyl ester (**53**)

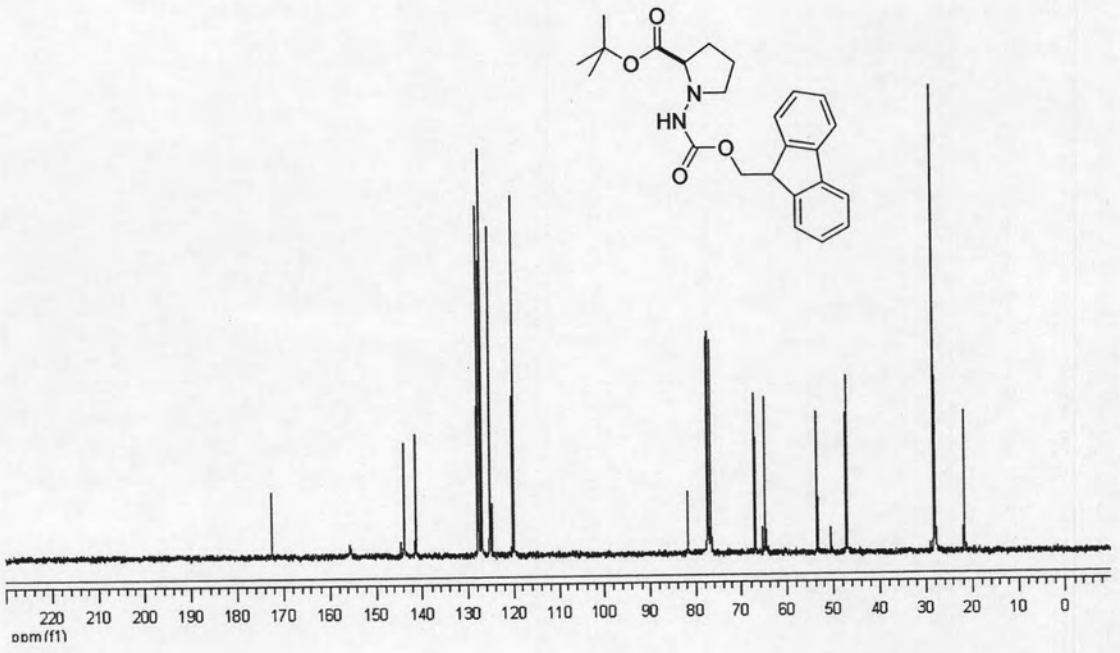

Figure A-100: ^{13}C NMR (75 MHz, $CDCl_3$) of (*N'*-Fluoren-9-ylmethoxycarbonyl)-*N*-Amino-D-proline *tert*-butyl ester (**53**)

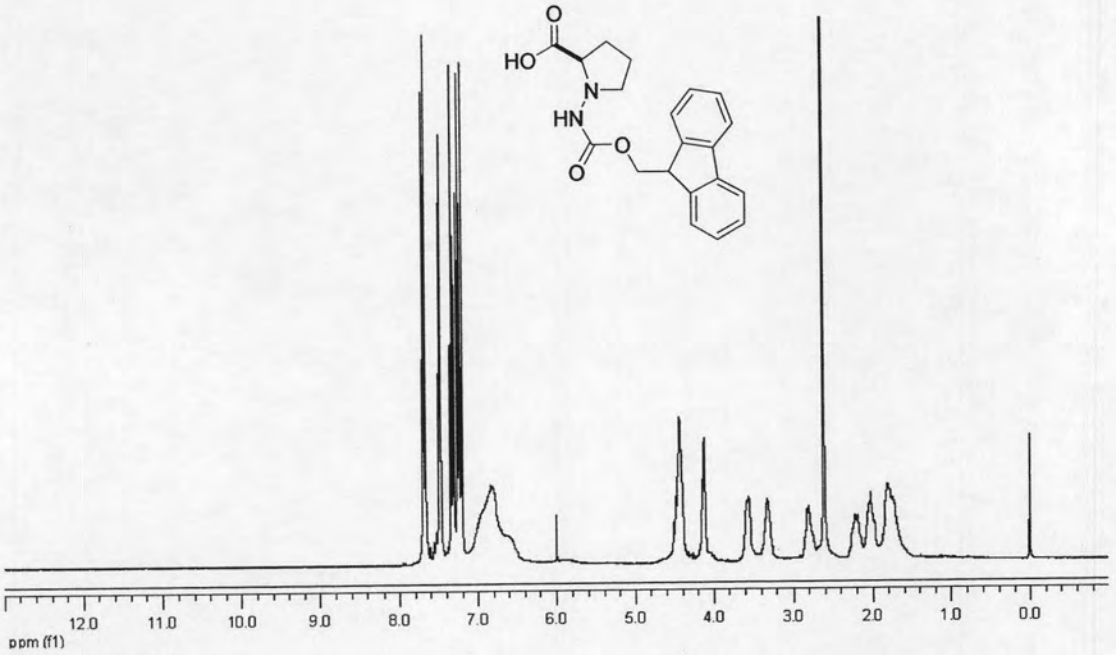

Figure A-101: ^{1}H NMR (300 MHz, $CDCl_3$) of (*N'*-Fluoren-9-ylmethoxycarbonyl)-*N*-Amino-D-proline (**54**)

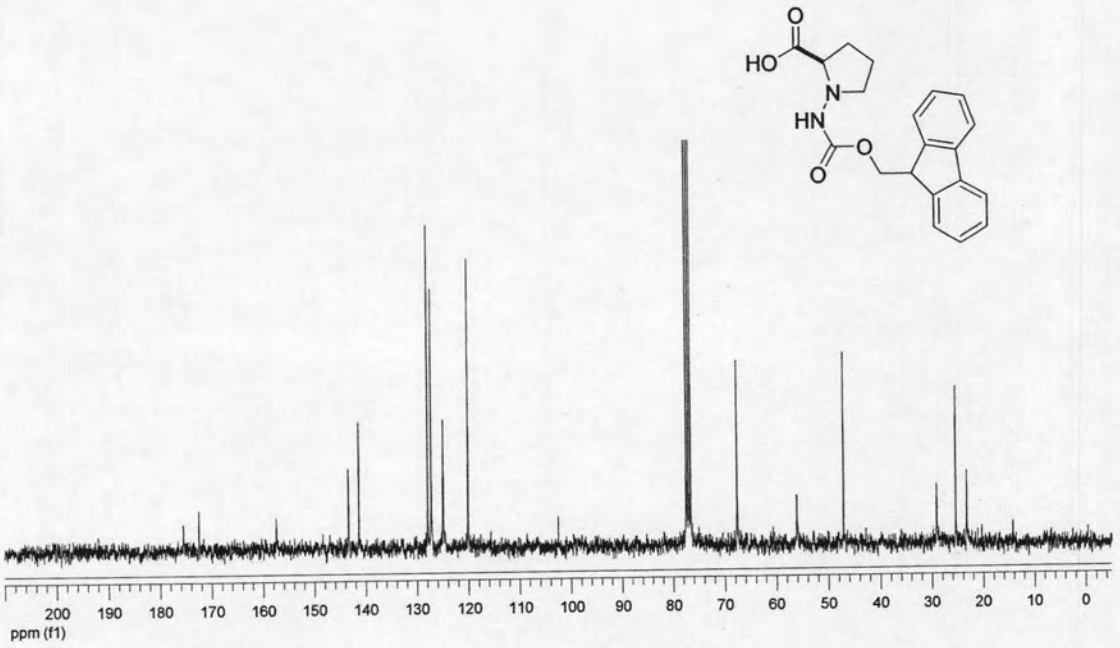

Figure A-102: ^{13}C NMR (75 MHz, $CDCl_3$) of (*N'*-Fluoren-9-ylmethoxycarbonyl)-*N*-Amino-D-proline (**54**)

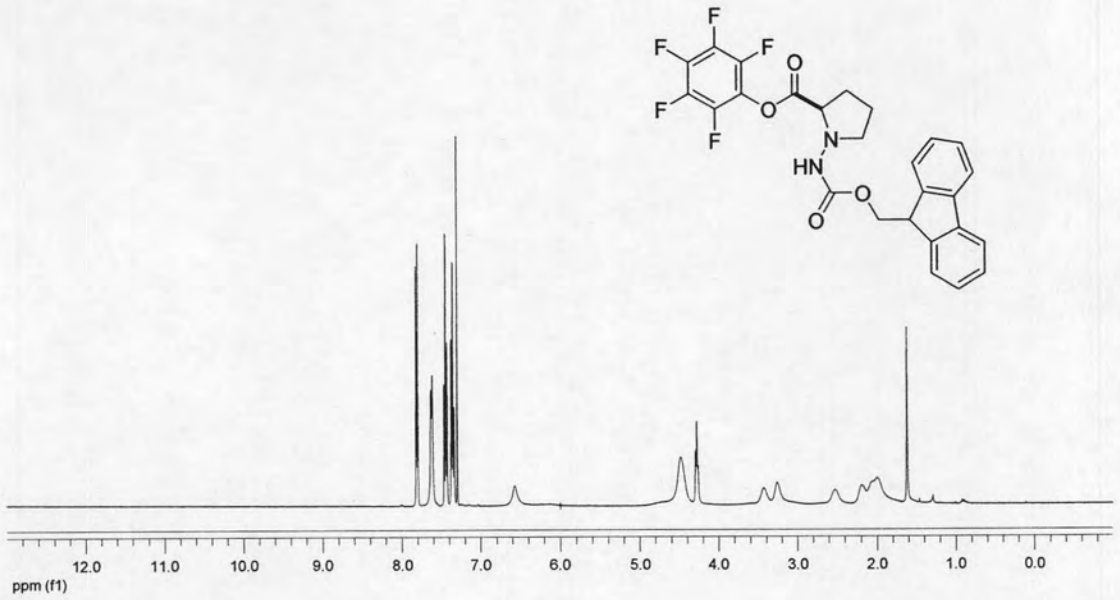

Figure A-103: ^{1}H NMR (400 MHz, $CDCl_3$) of (*N'*-Fluoren-9-ylmethoxycarbonyl)-*N*-Amino-D-proline pentafluorophenyl ester (**55**)

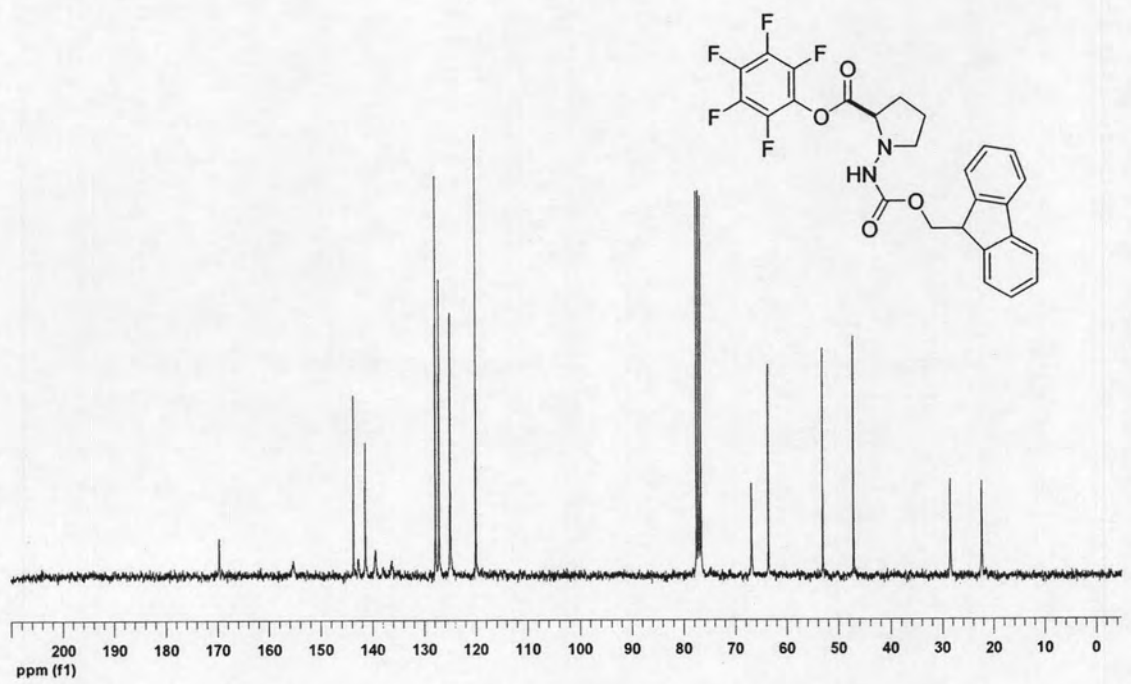

Figure A-104: ^{13}C NMR (100 MHz, $CDCl_3$) of (*N'*-Fluoren-9-ylmethoxycarbonyl)-*N*-Amino-D-proline pentafluorophenyl ester (**55**)

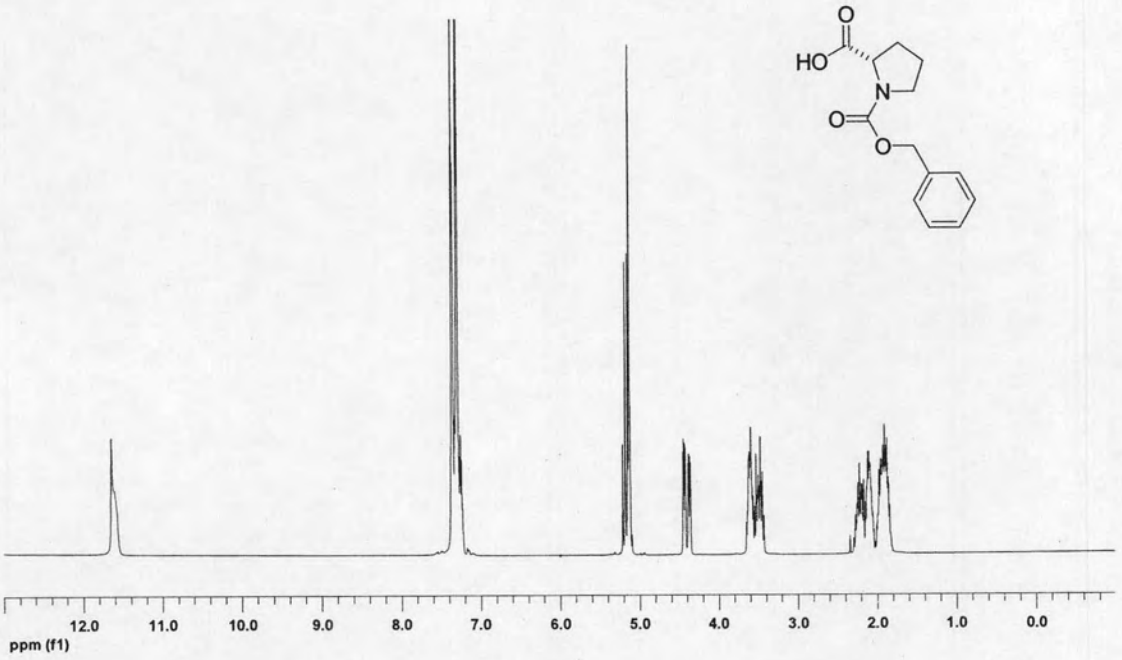

Figure A-105: ^{1}H NMR (400 MHz, $CDCl_3$) of *N*-Benzyloxycarbonyl-L-proline (**56**)

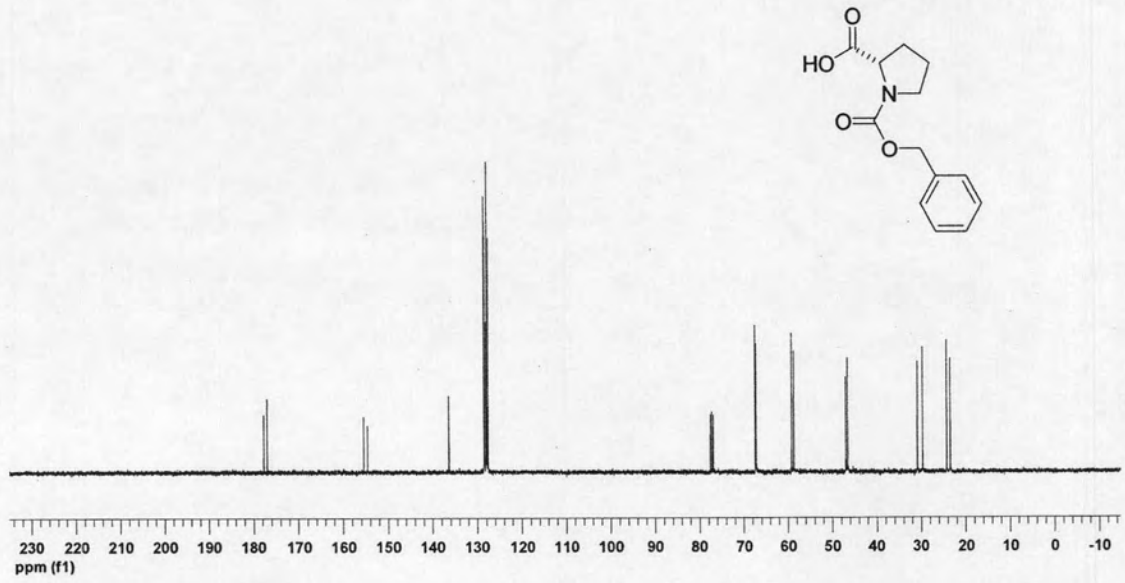

Figure A-106: ^{13}C NMR (100 MHz, $CDCl_3$) of *N*-Benzyloxycarbonyl-L-proline (**56**)

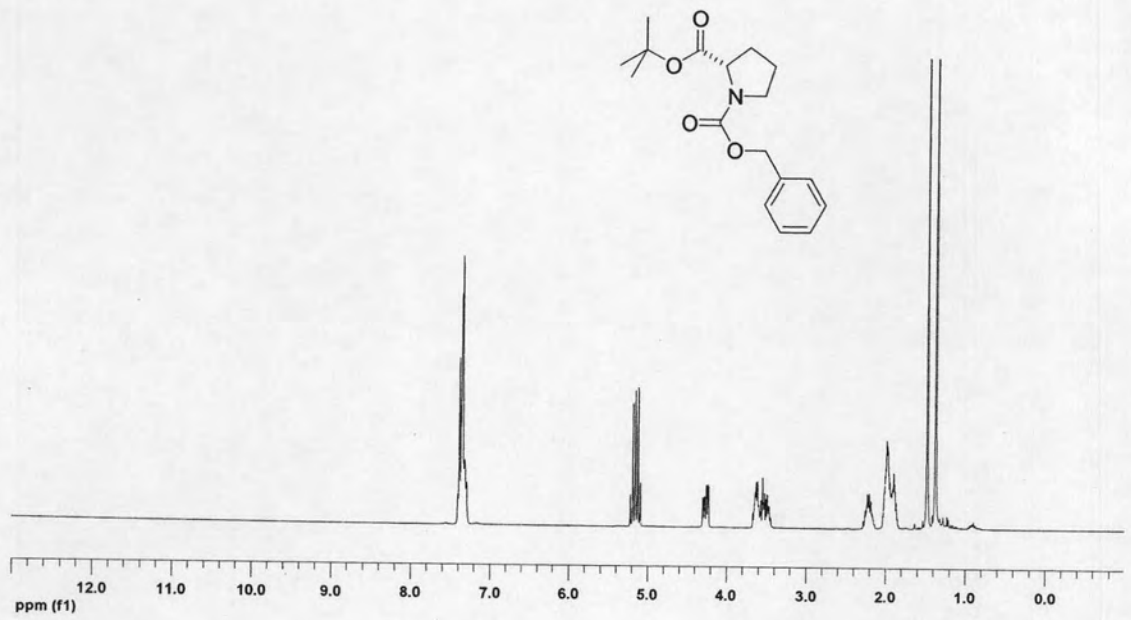

Figure A-107: ^{1}H NMR (400 MHz, $CDCl_3$) of *N*-Benzyloxycarbonyl-L-proline *tert*-butyl ester (**57**)

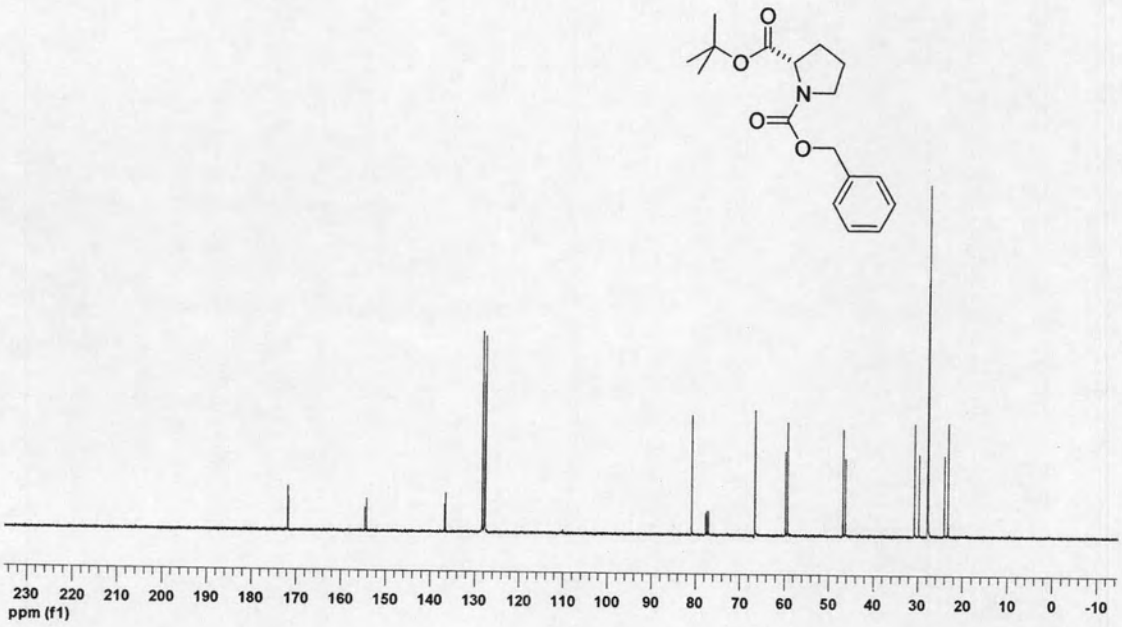

Figure A-108: ^{13}C NMR (100 MHz, $CDCl_3$) of *N*-Benzyloxycarbonyl-L-proline *tert*-butyl ester (**57**)

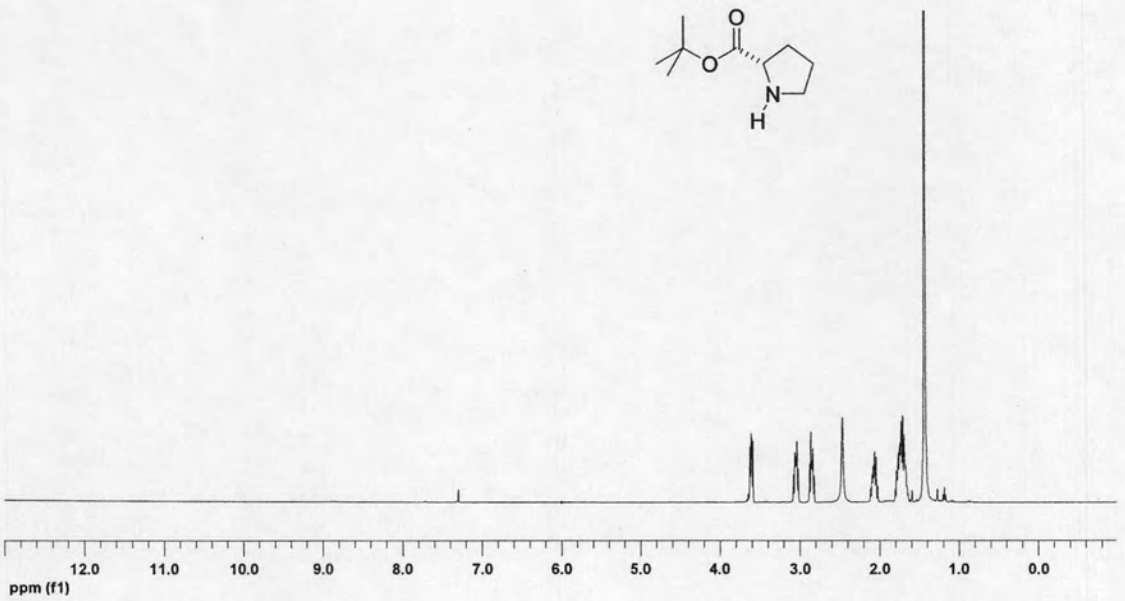

Figure A-109: ^{1}H NMR (400 MHz, $CDCl_3$) of L-Proline *tert*-butyl ester (**58**)

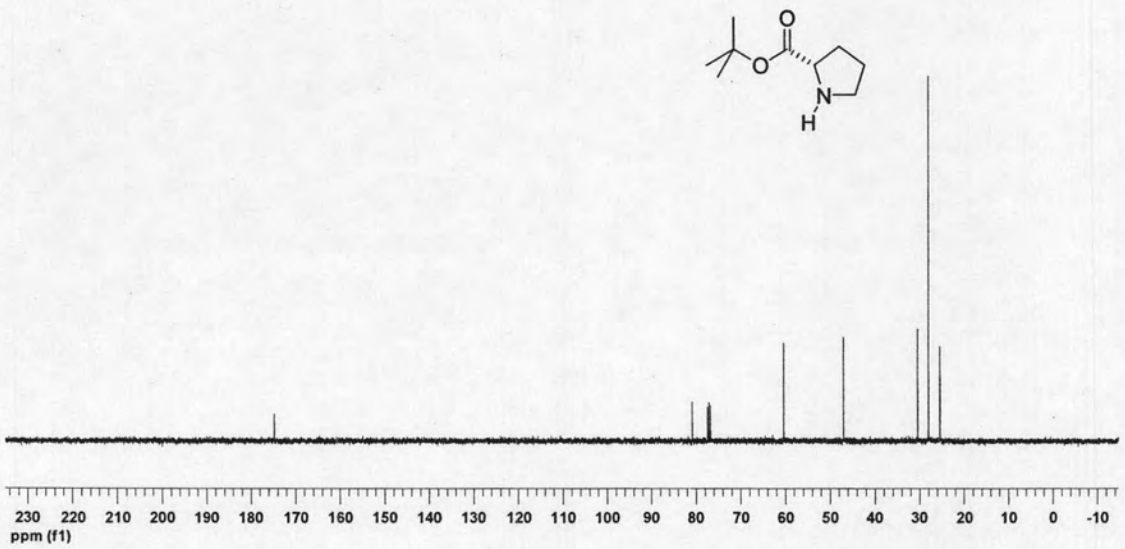

Figure A-110: ^{13}C NMR (100 MHz, $CDCl_3$) of L-Proline *tert*-butyl ester (**58**)

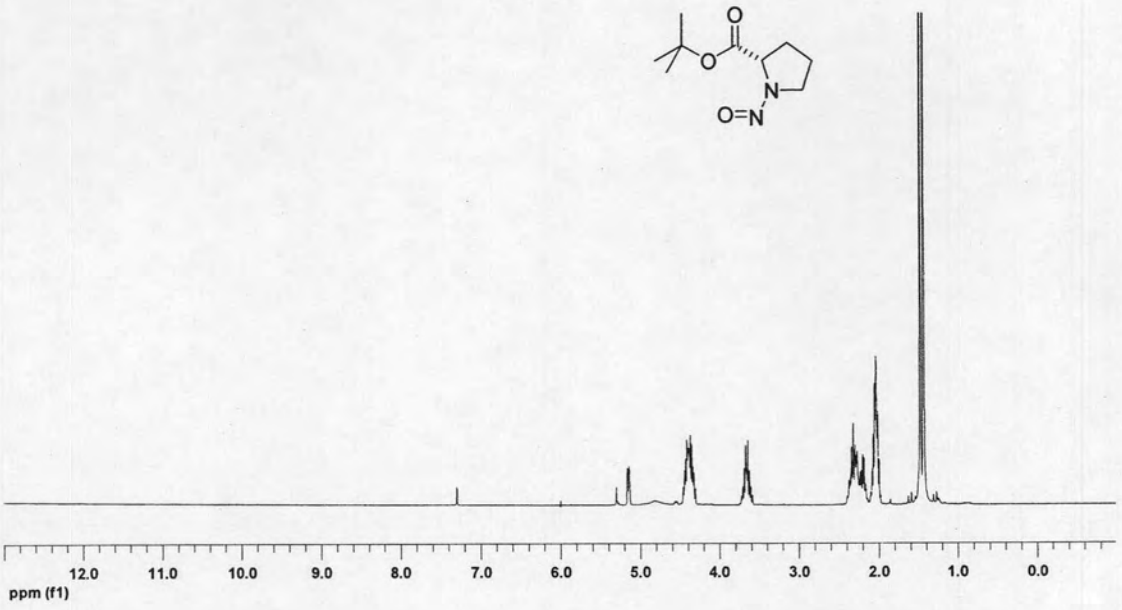

Figure A-111: ^{1}H NMR (400 MHz, $CDCl_3$) of *N*-Nitroso-L-proline *tert*-butyl ester **(59)**

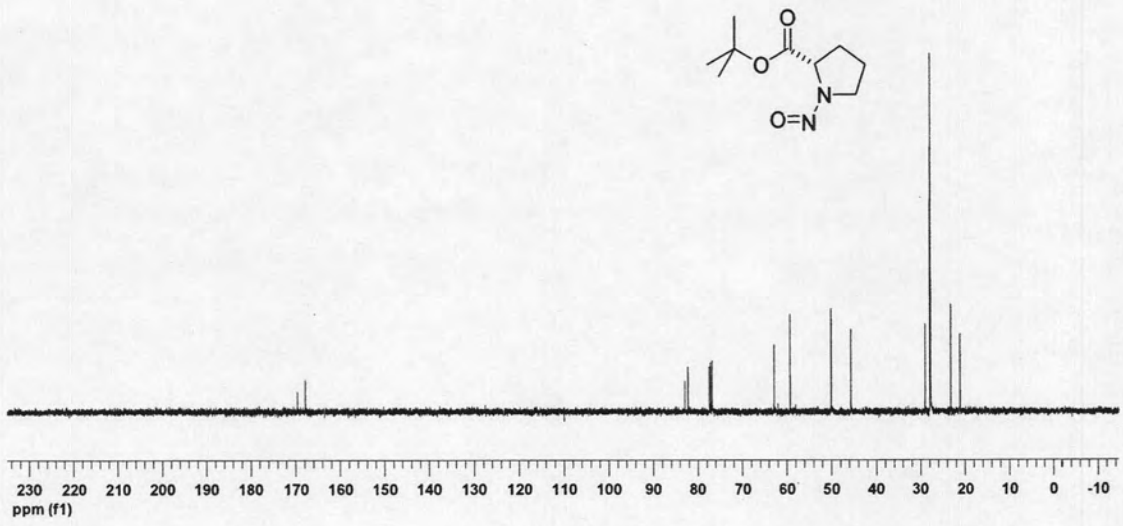

Figure A-112: ^{13}C NMR (100 MHz, $CDCl_3$) of *N*-Nitroso-L-proline *tert*-butyl ester **(59)**

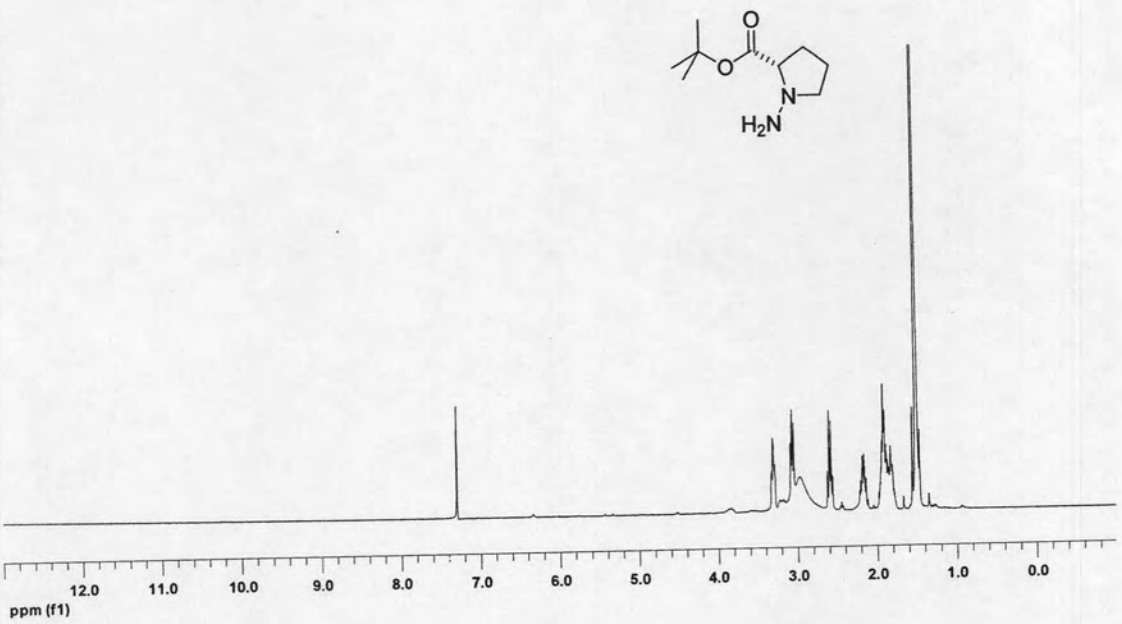

Figure A-113: ^{1}H NMR (400 MHz, $CDCl_3$) of *N*-Amino-L-proline *tert*-butyl ester (**60**)

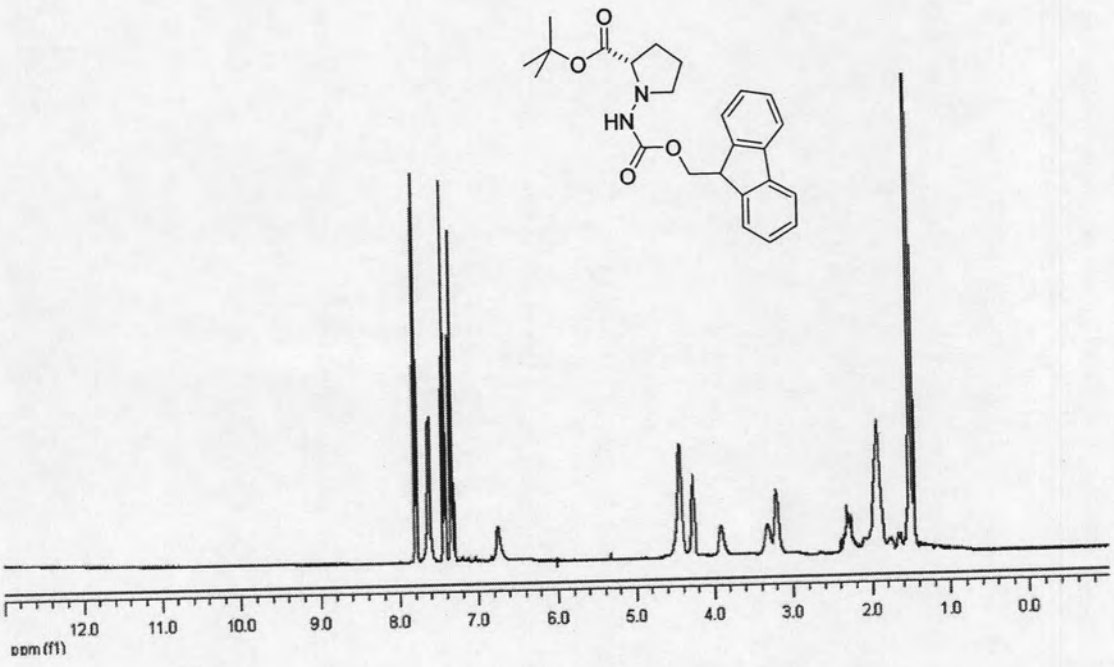

Figure A-114: ^{1}H NMR (400 MHz, $CDCl_3$) of (*N'*-Fluoren-9-ylmethoxycarbonyl)-*N*-Amino-L-proline *tert*-butyl ester (**61**)

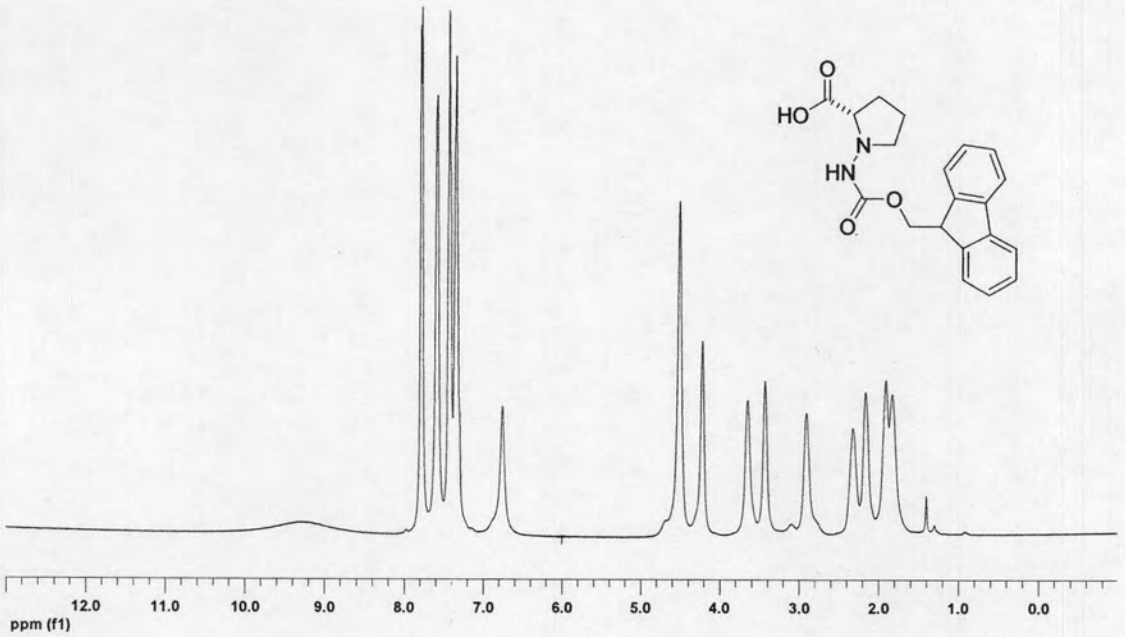

Figure A-115: ^{1}H NMR (400 MHz, $CDCl_3$) of (N'-Fluoren-9-ylmethoxycarbonyl)-N-Amino-L-proline (**62**)

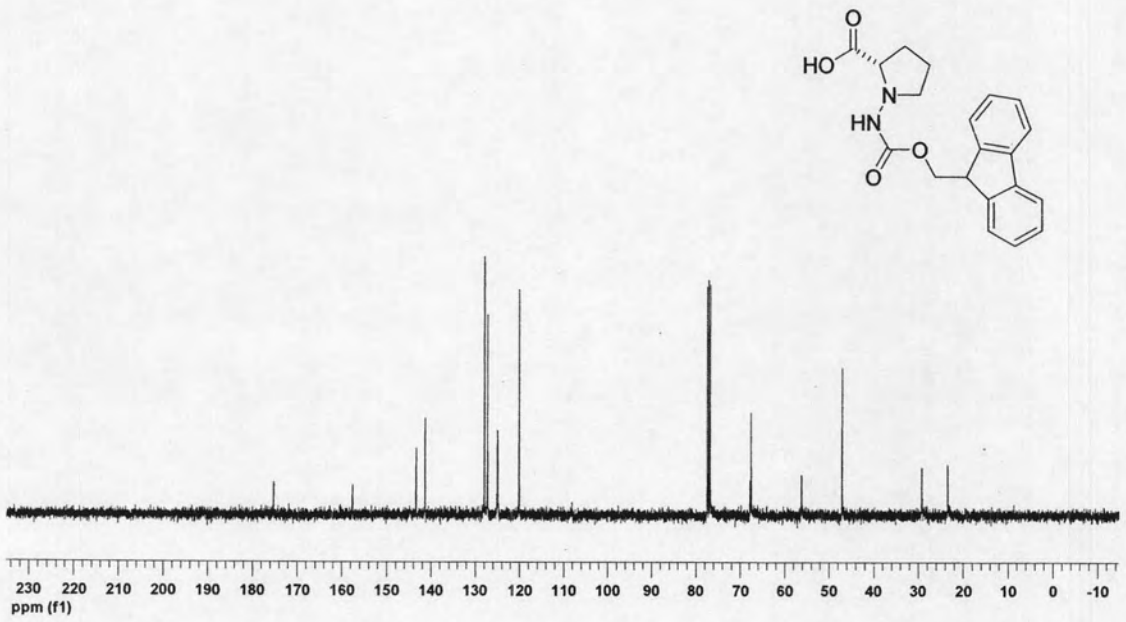

Figure A-116: ^{13}C NMR (100 MHz, $CDCl_3$) of (*N*'-Fluoren-9-ylmethoxycarbonyl)-*N*-Amino-L-proline (**62**)

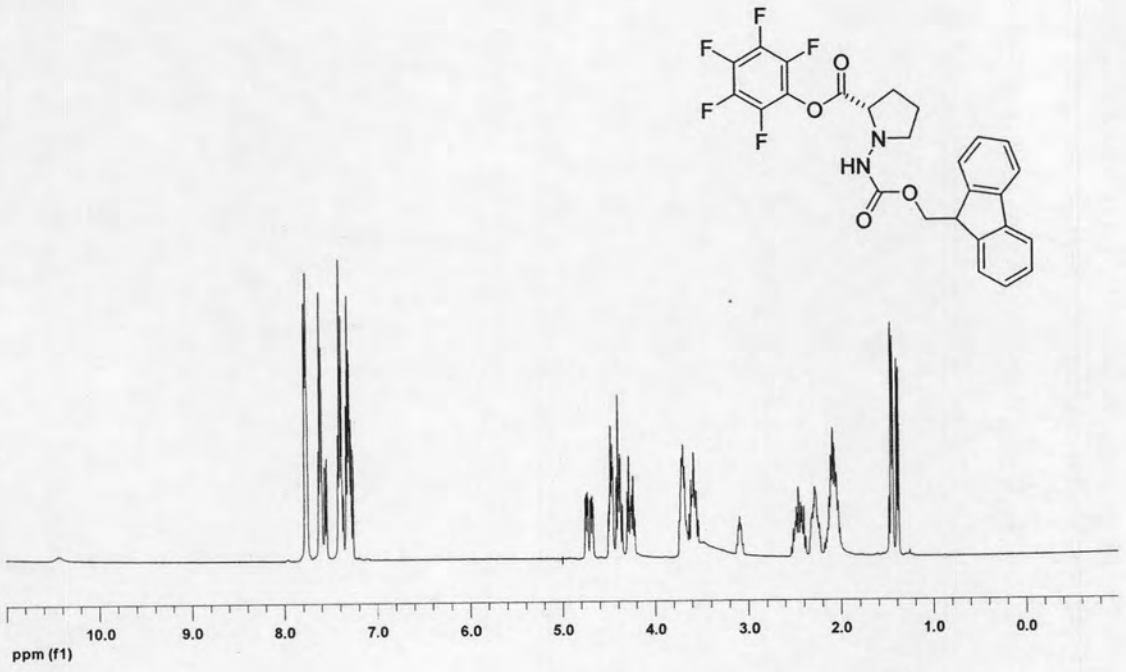

Figure A-117: ^{1}H NMR (400 MHz, $CDCl_3$) of (*N'*-Fluoren-9-ylmethoxycarbonyl)-*N*-Amino-L-proline pentafluorophenyl ester (**63**)

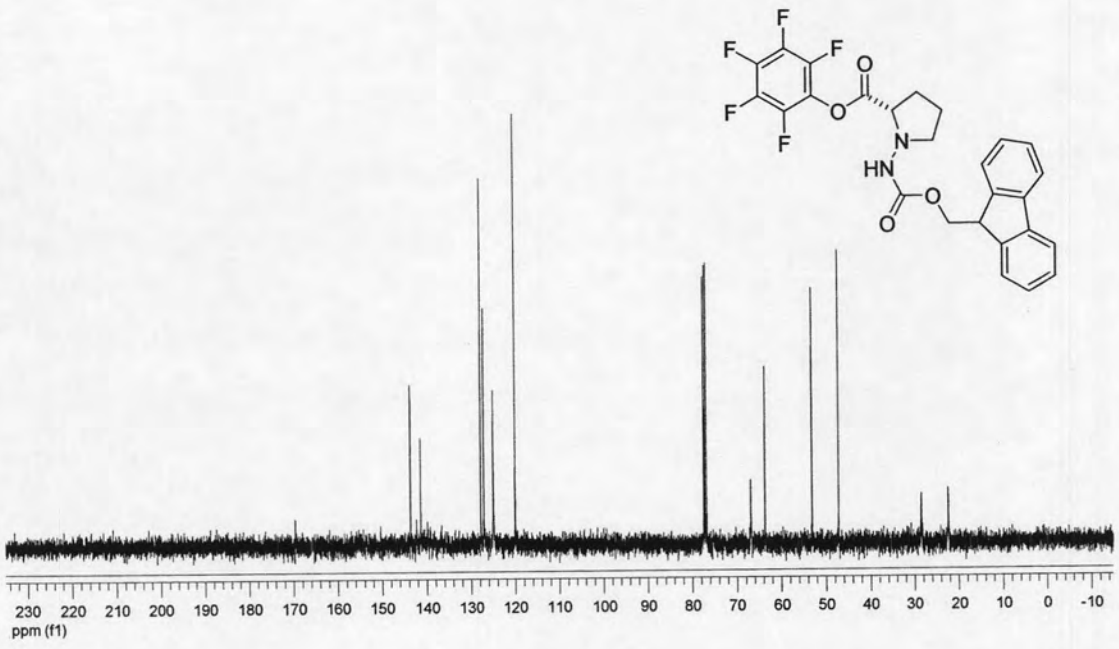

Figure A-118: ^{13}C NMR (100 MHz, $CDCl_3$) of (*N'*-Fluoren-9-ylmethoxycarbonyl)-*N*-Amino-L-proline pentafluorophenyl ester (**63**)

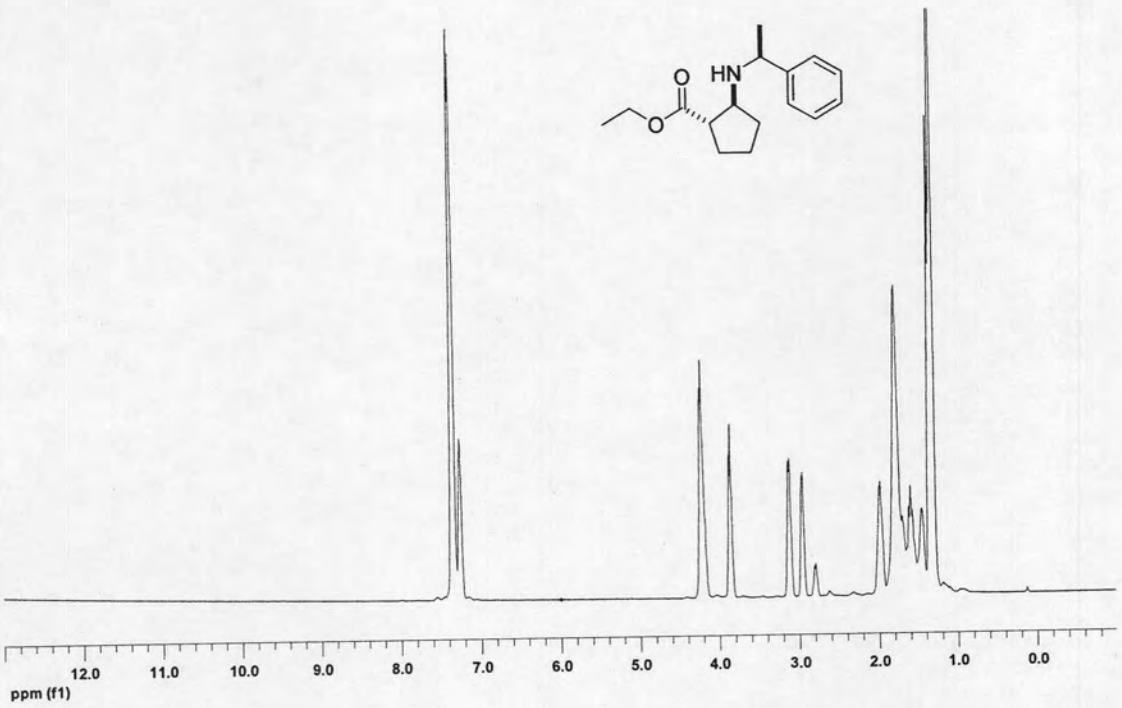

Figure A-119: ^{1}H NMR (400 MHz, $CDCl_3$) of ethyl (1*S*,2*S*)-2-[(1′*S*)-phenylethyl]-aminocyclopentane carboxylate (**64**)

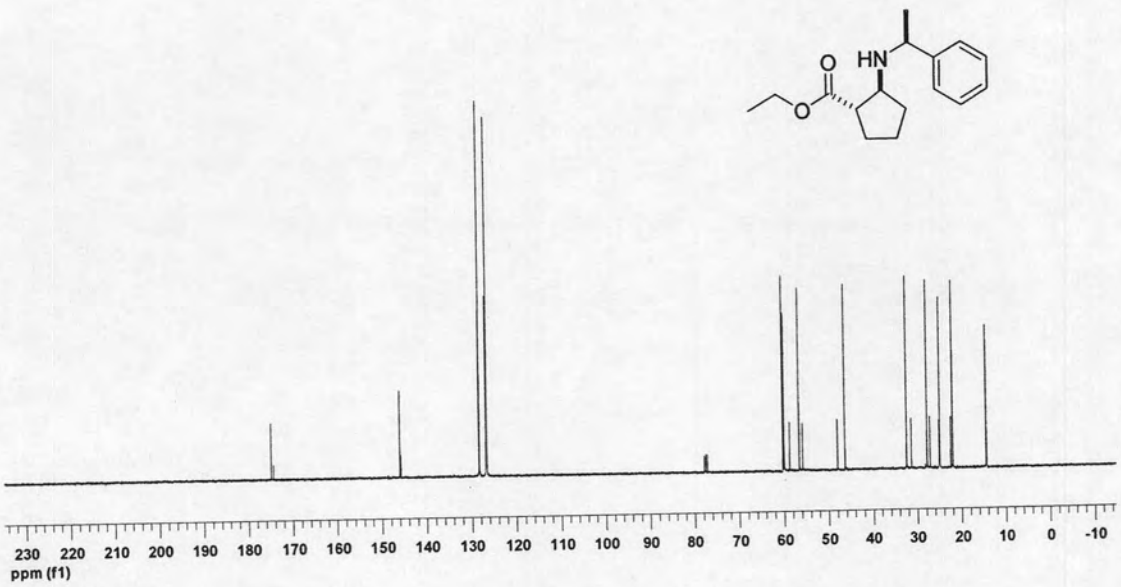

Figure A-120: ^{13}C NMR (100 MHz, $CDCl_3$) of ethyl (1*S*,2*S*)-2-[(1′*S*)-phenylethyl]-aminocyclopentane carboxylate (**64**)

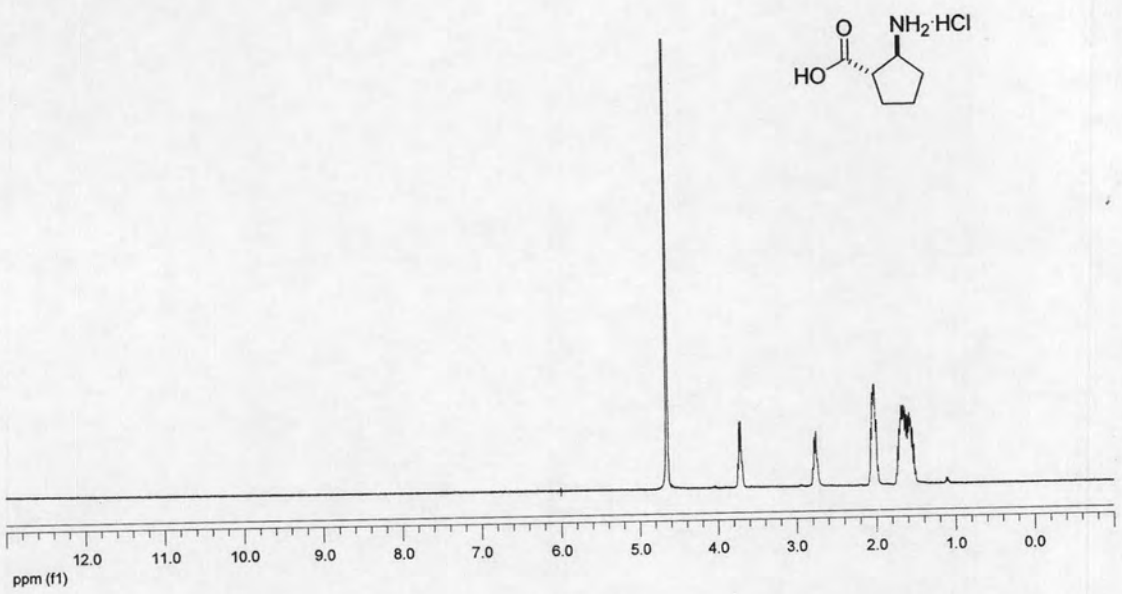

Figure A-121: ^{1}H NMR (400 MHz, D_2O) of (1*S*,2*S*)-2-Aminocyclopentane carboxylic acid hydrochloride (**66**)

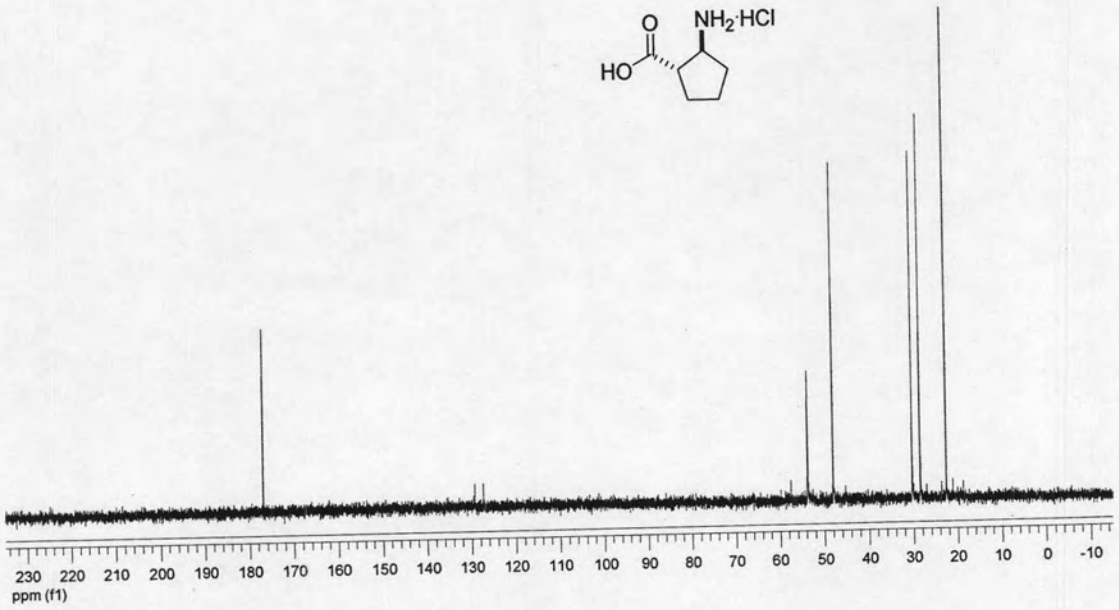

Figure A-122: ^{13}C NMR (100 MHz, D_2O) of (1*S*,2*S*)-2-Aminocyclopentane carboxylic acid hydrochloride (**66**)

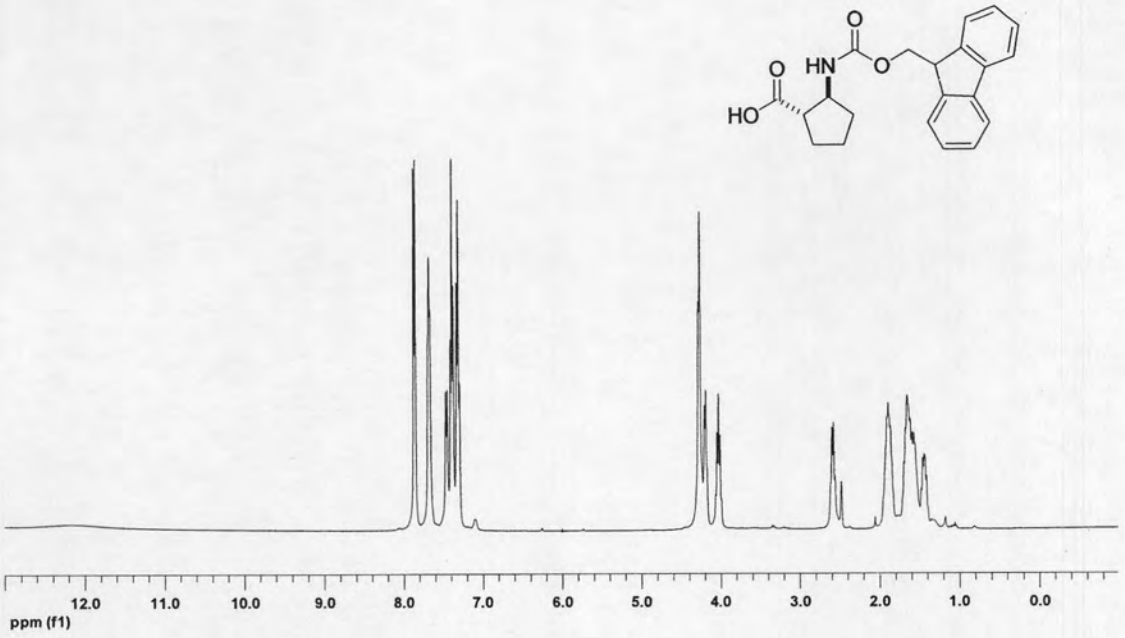

Figure A-123: ^{1}H NMR (400 MHz, DMSO-d_6) of (1*S*,2*S*)-2-(*N*-Fluoren-9-ylmethoxy carbonyl)-aminocyclopentanecarboxylic acid (**67**)

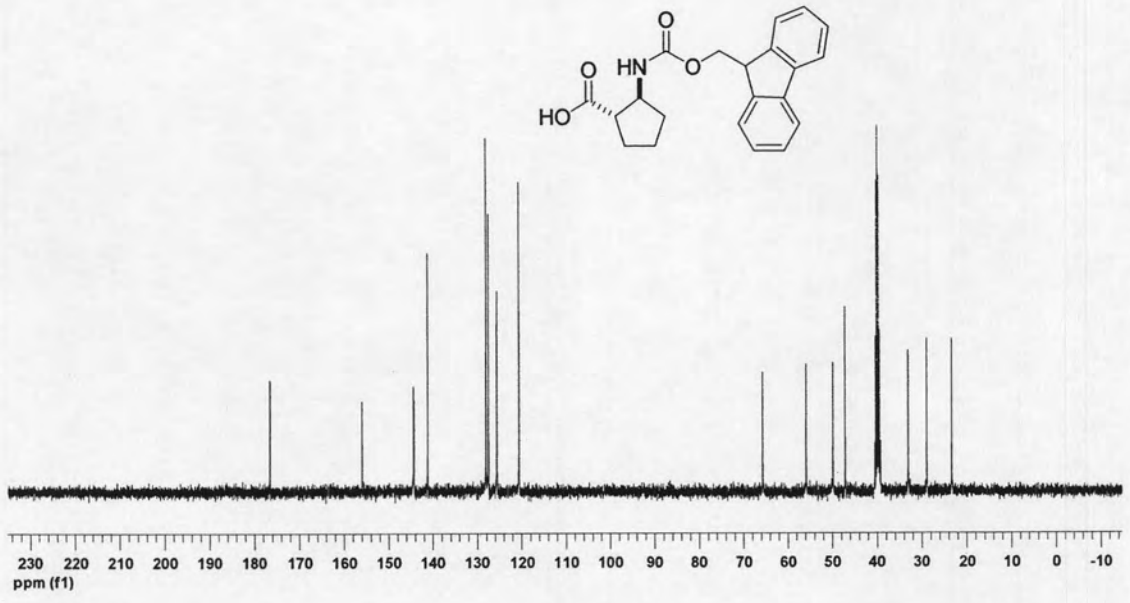

Figure A-124: ^{13}C NMR (100 MHz, DMSO-d_6) of (1*S*,2*S*)-2-(*N*-Fluoren-9-ylmethoxy carbonyl)-aminocyclopentanecarboxylic acid (**67**)

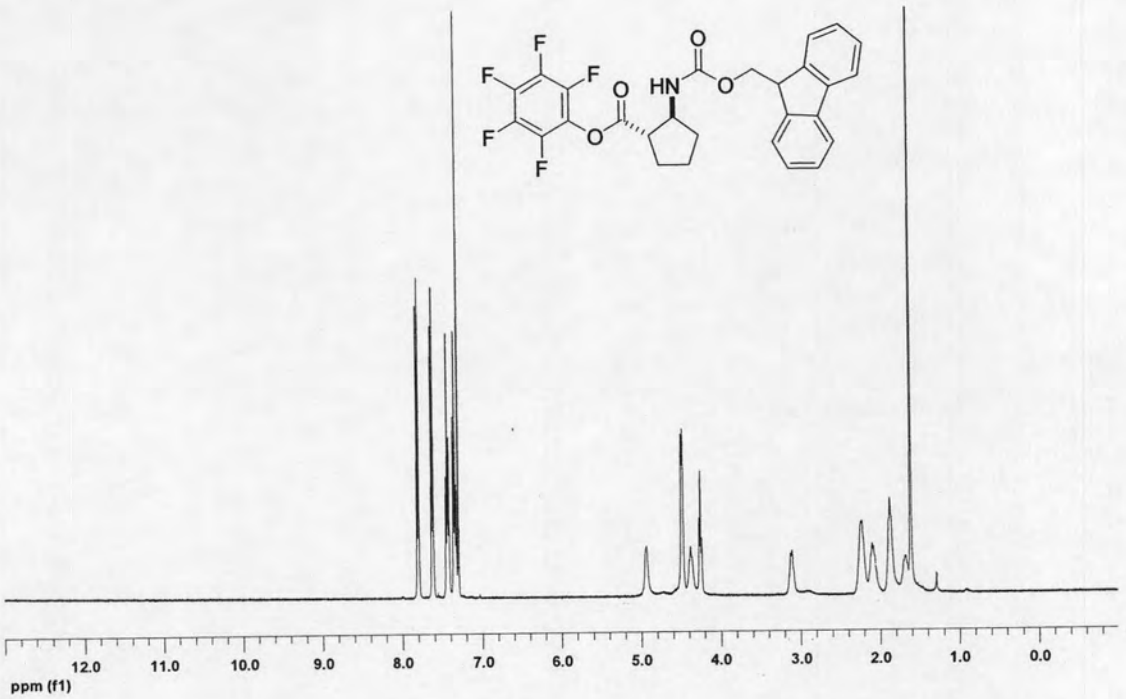

Figure A-125: ^{1}H NMR (400 MHz, $CDCl_3$) of (1*S*,2*S*)-2-(*N*-fluoren-9-ylmethoxy carbonyl)-aminocyclopentane pentafluorophenyl ester (**68**)

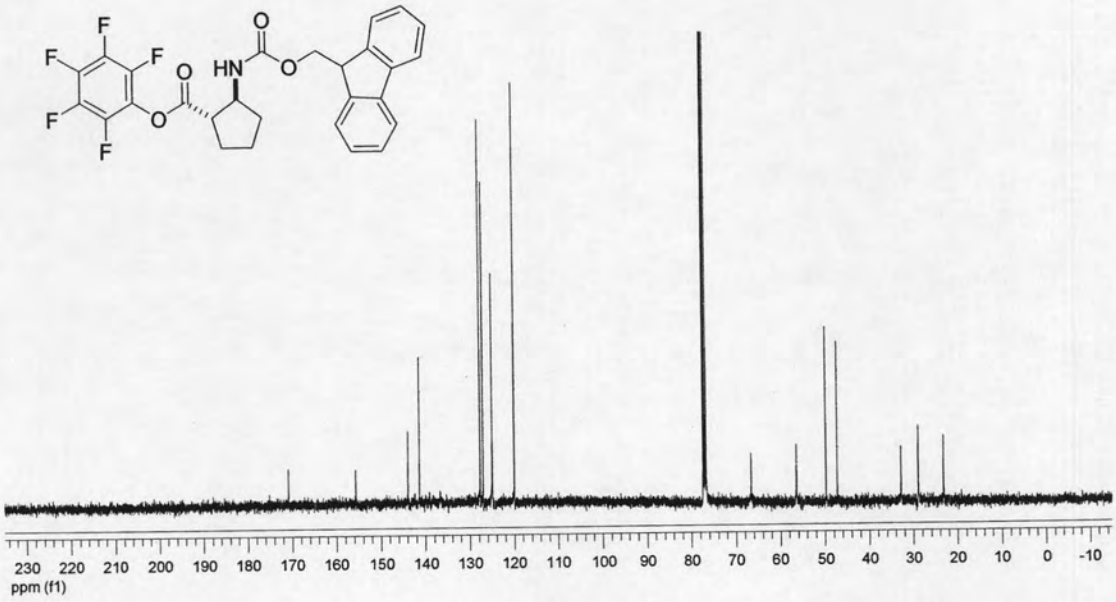

Figure A-126: ^{13}C NMR (100 MHz, $CDCl_3$) of (1*S*,2*S*)-2-(*N*-fluoren-9-ylmethoxy carbonyl)-aminocyclopentane pentafluorophenyl ester (**68**)

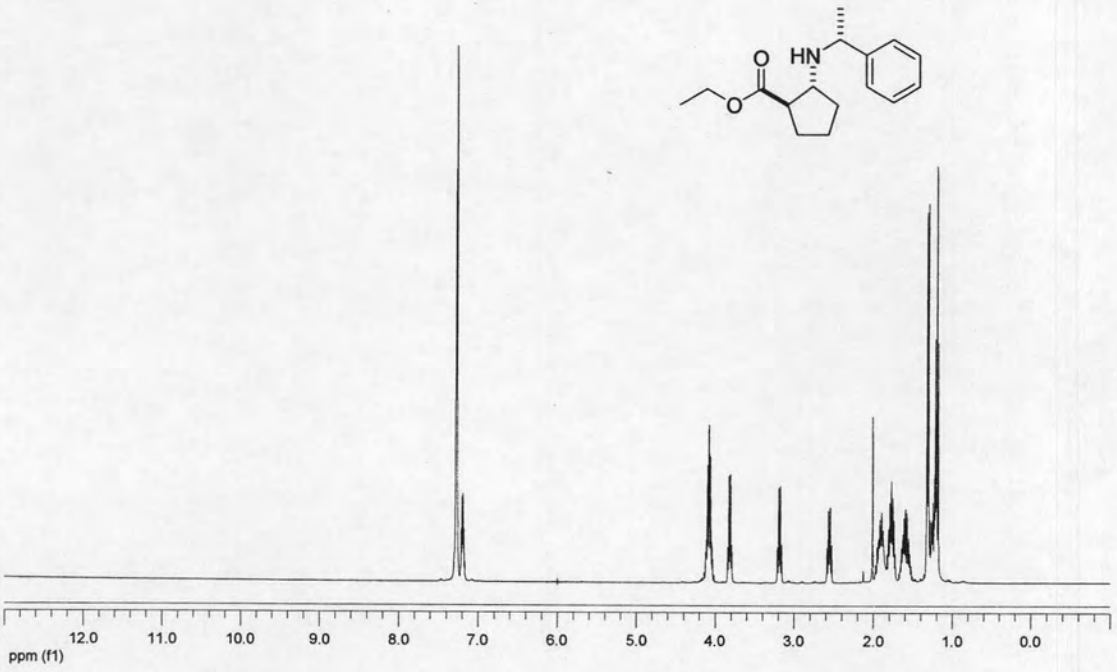

Figure A-127: ^{1}H NMR (400 MHz, $CDCl_3$) of Ethyl (1*R*,2*R*)-2-[(1′*R*)-phenylethyl]-aminocyclopentane carboxylate (**69**)

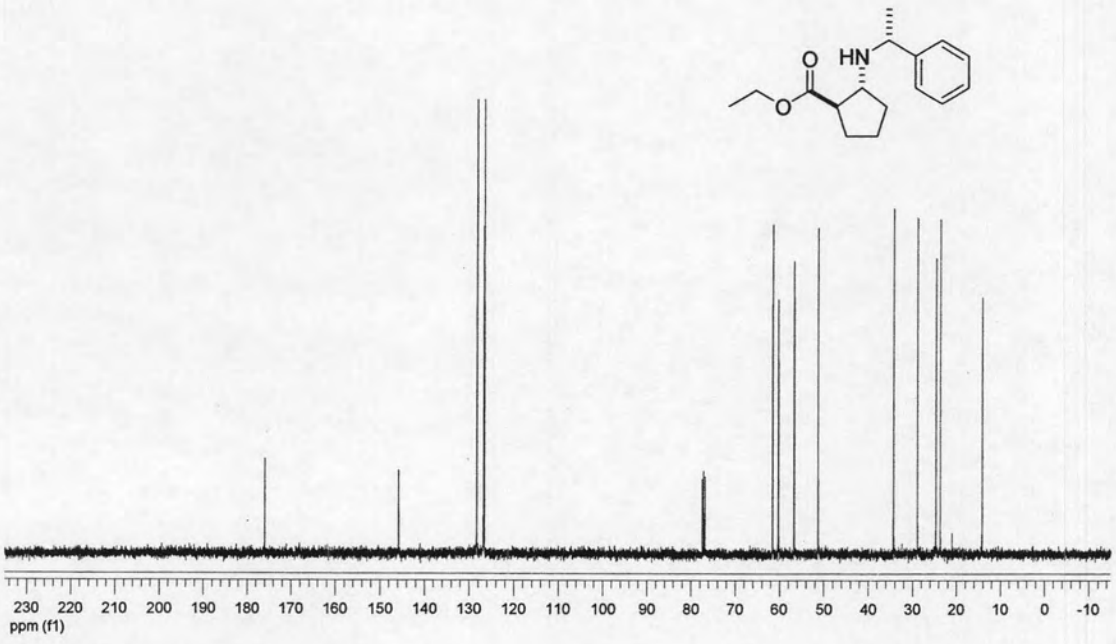

Figure A-128: ^{13}C NMR (100 MHz, $CDCl_3$) of Ethyl (1*R*,2*R*)-2-[(1′*R*)-phenylethyl]-aminocyclopentane carboxylate (**69**)

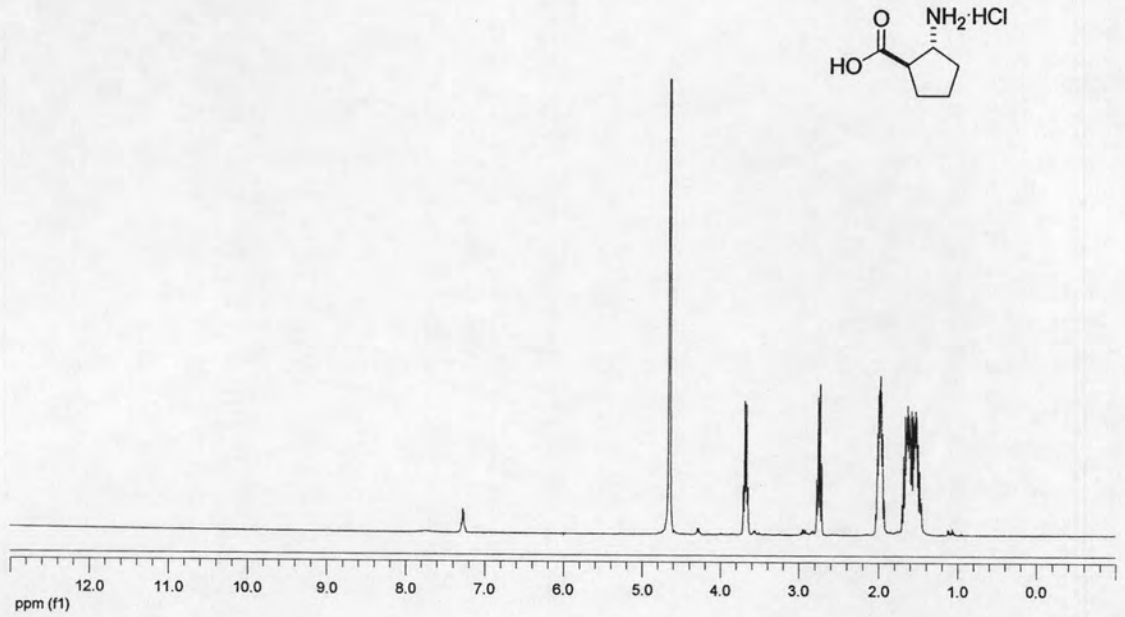

Figure A-129: ^{1}H NMR (400 MHz, D_2O) of (1*R*,2*R*)-2-Aminocyclopentane carboxylic acid hydrochloride (**71**)

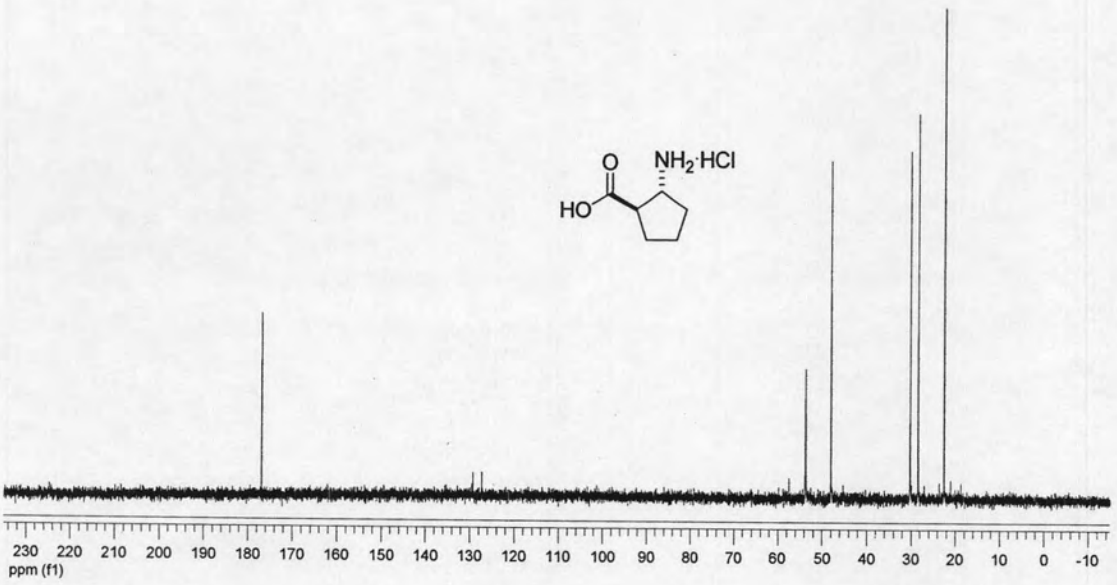

Figure A-130: ^{13}C NMR (100 MHz, D_2O) of (1*R*,2*R*)-2-Aminocyclopentane carboxylic acid hydrochloride (**71**)

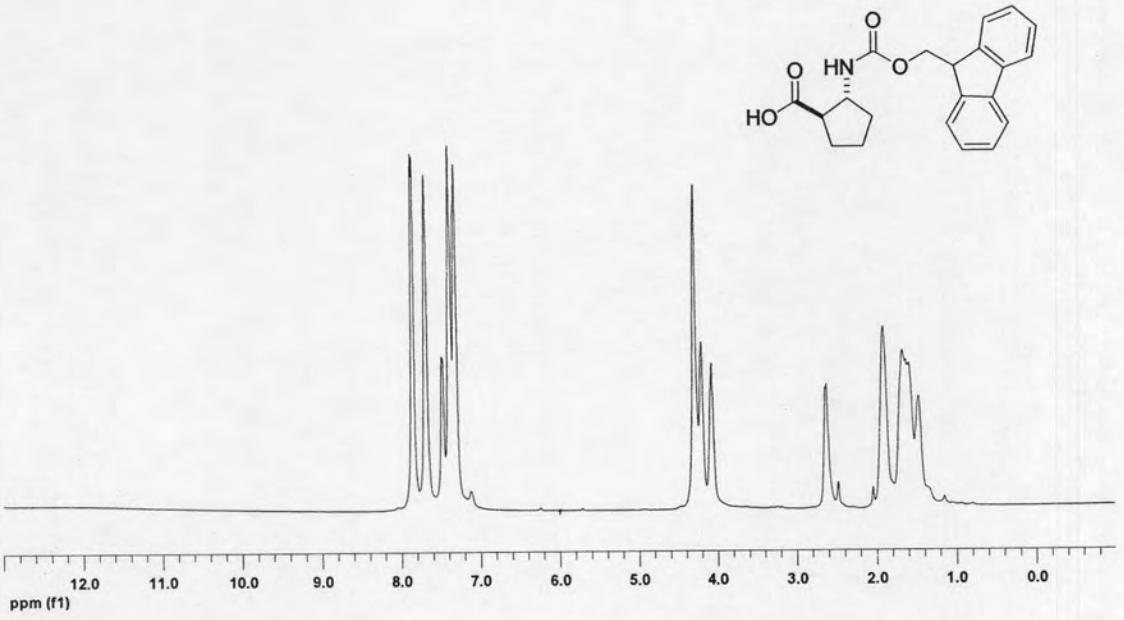

Figure A-131: ^{1}H NMR (400 MHz, DMSO-d_6) of (1*R*,2*R*)-2-(*N*-Fluoren-9-ylmethoxy carbonyl)-aminocyclopentanecarboxylic acid (**72**)

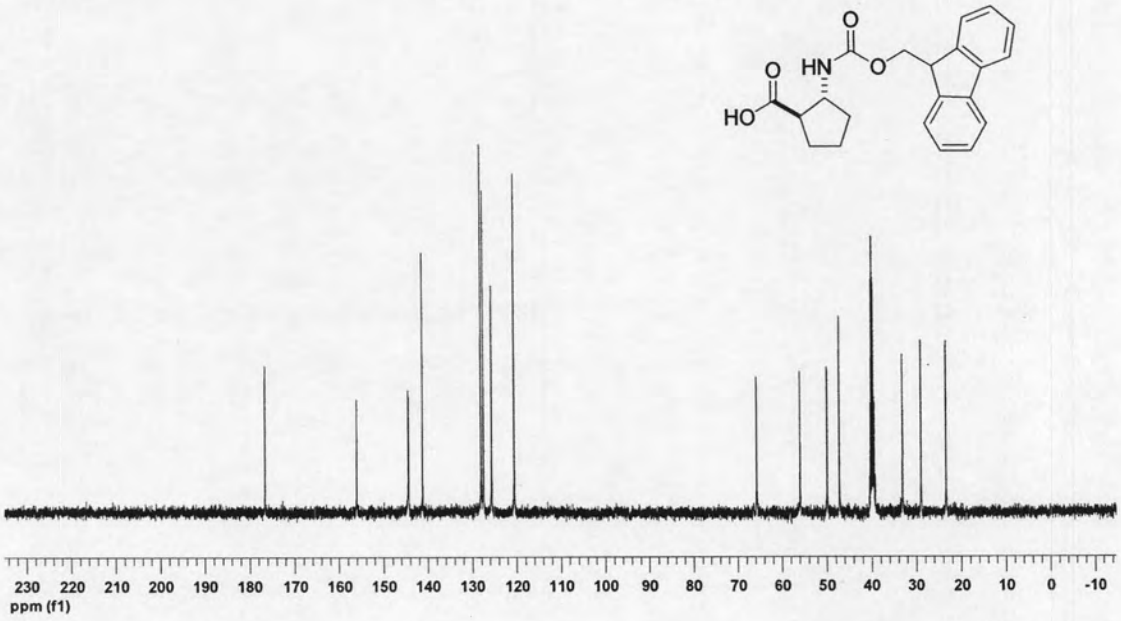

Figure A-132: ^{13}C NMR (100 MHz, DMSO-d_6) of (1*R*,2*R*)-2-(*N*-Fluoren-9-ylmethoxycarbonyl)-aminocyclopentanecarboxylic acid (**72**)

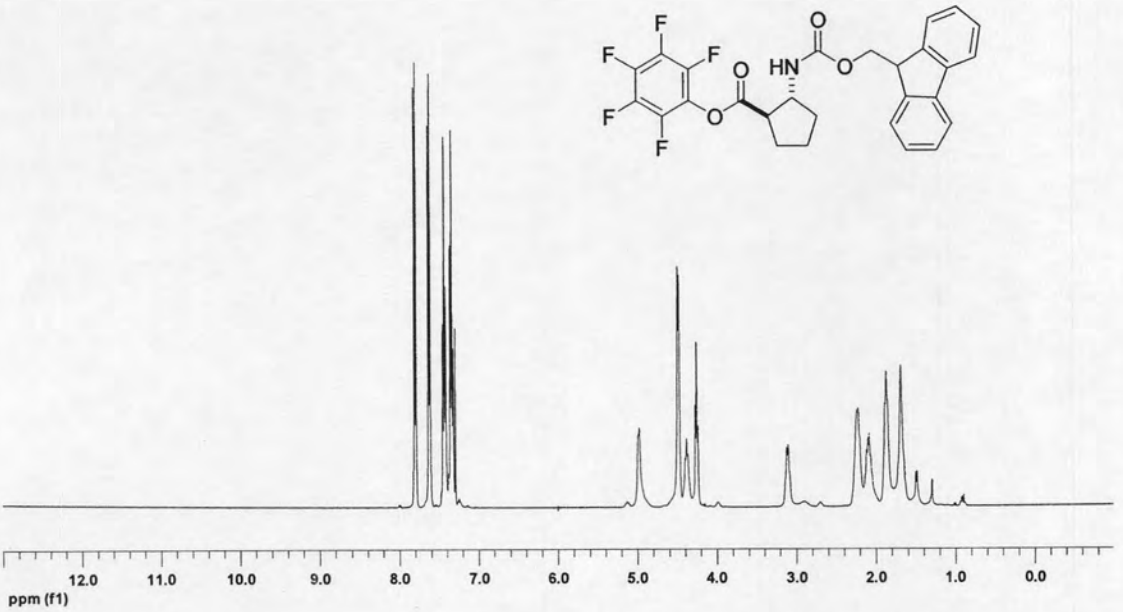

Figure A-133: ^{1}H NMR (400 MHz, $CDCl_3$) of (1*R*,2*R*)-2-(*N*-fluoren-9-ylmethoxy carbonyl)-aminocyclopentane pentafluorophenyl ester (**73**)

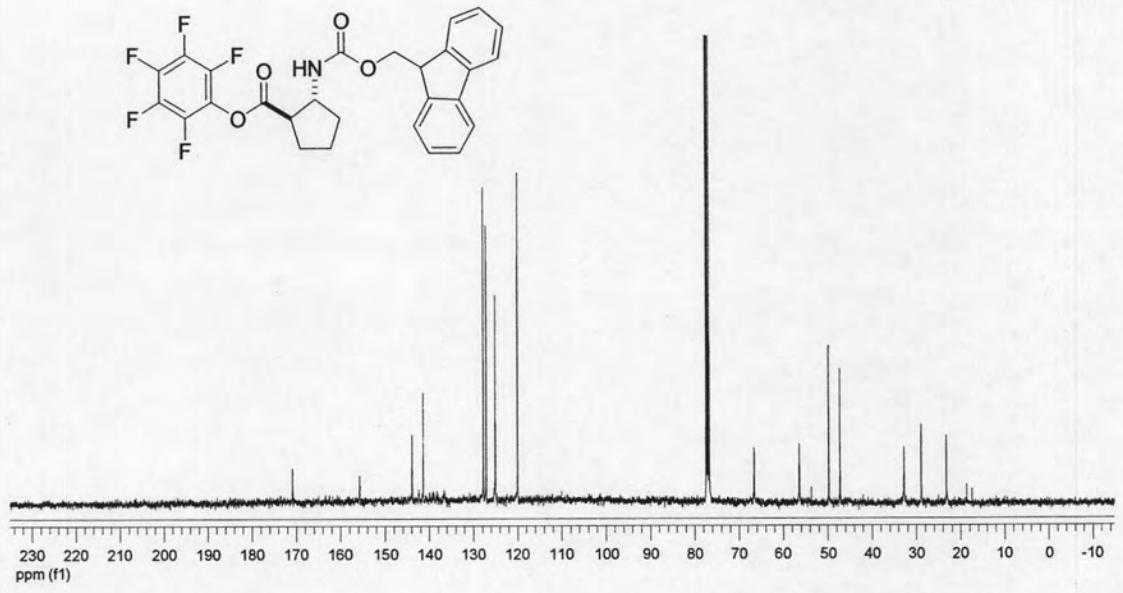

Figure A-134: ^{13}C NMR (100 MHz, $CDCl_3$) of (1*R*,2*R*)-2-(*N*-fluoren-9-ylmethoxy carbonyl)-aminocyclopentane pentafluorophenyl ester (**73**)

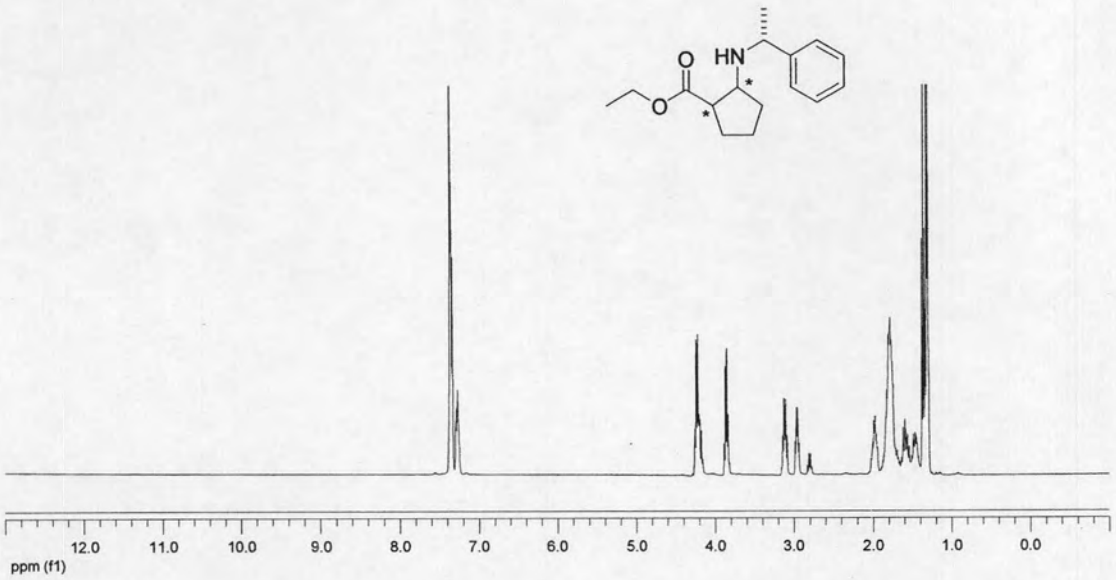

Figure A-135: ^{1}H NMR (400 MHz, $CDCl_3$) of Ethyl *cis*-(±)-2-[(1′*R*)-phenylethyl]-aminocyclopentane carboxylate (**74**)

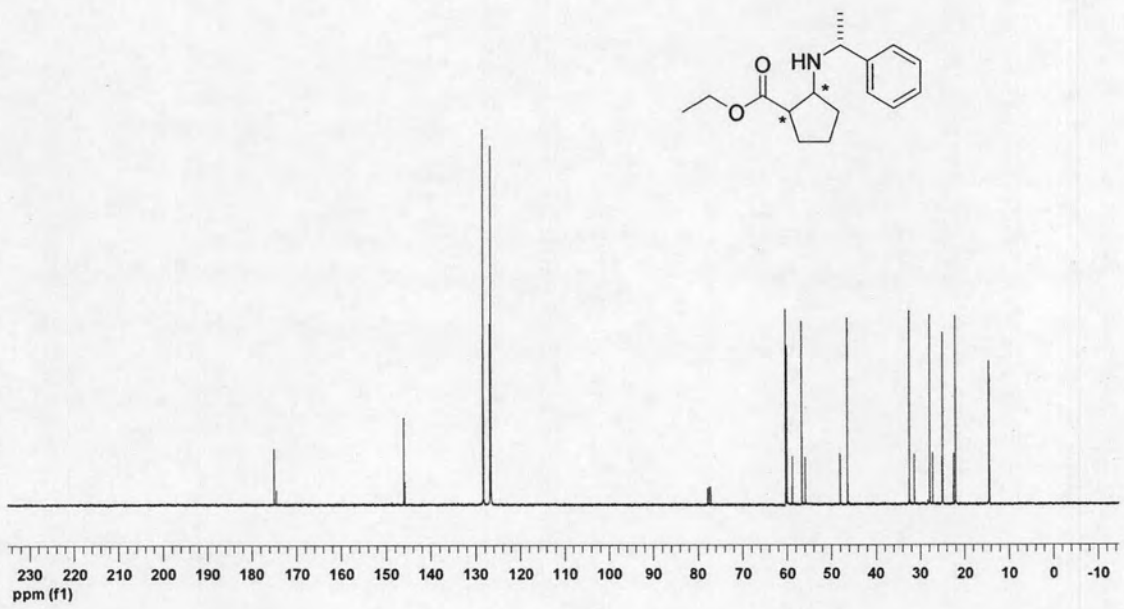

Figure A-136: ^{13}C NMR (100 MHz, $CDCl_3$) of Ethyl *cis*-(±)-2-[(1′*R*)-phenylethyl]-aminocyclopentane carboxylate (**74**)

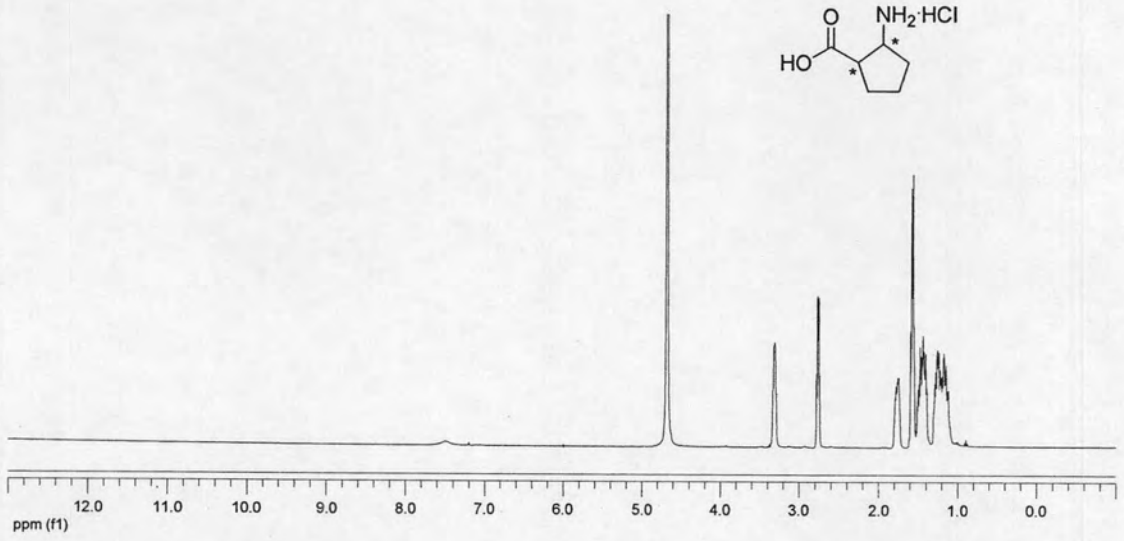

Figure A-137: ^{1}H NMR (400 MHz, D_2O) of *cis*-(±)-2-Aminocyclopentane carboxylic acid hydrochloride (**75**)

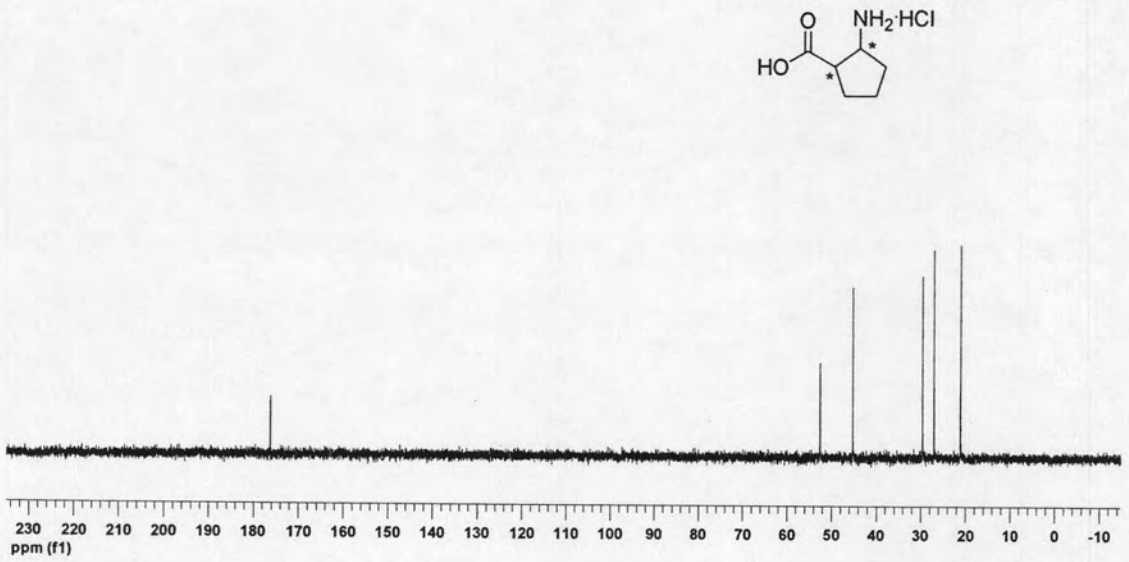

Figure A-138: ^{13}C NMR (100 MHz, D_2O) of *cis*-(±)-2-Aminocyclopentane carboxylic acid hydrochloride (**75**)

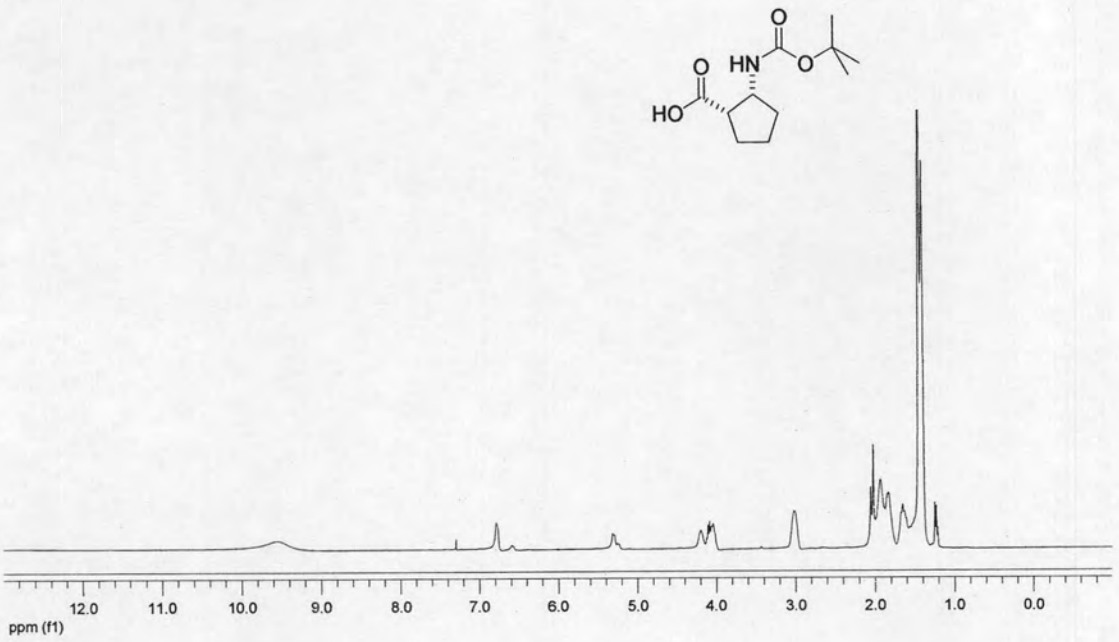

Figure A-139: ^{1}H NMR (400 MHz, $CDCl_3$) of (1*S*,2*R*)-2-(*N-tert*-Butoxycarbonyl)-amino cyclopentane carboxylic acid (**76**)

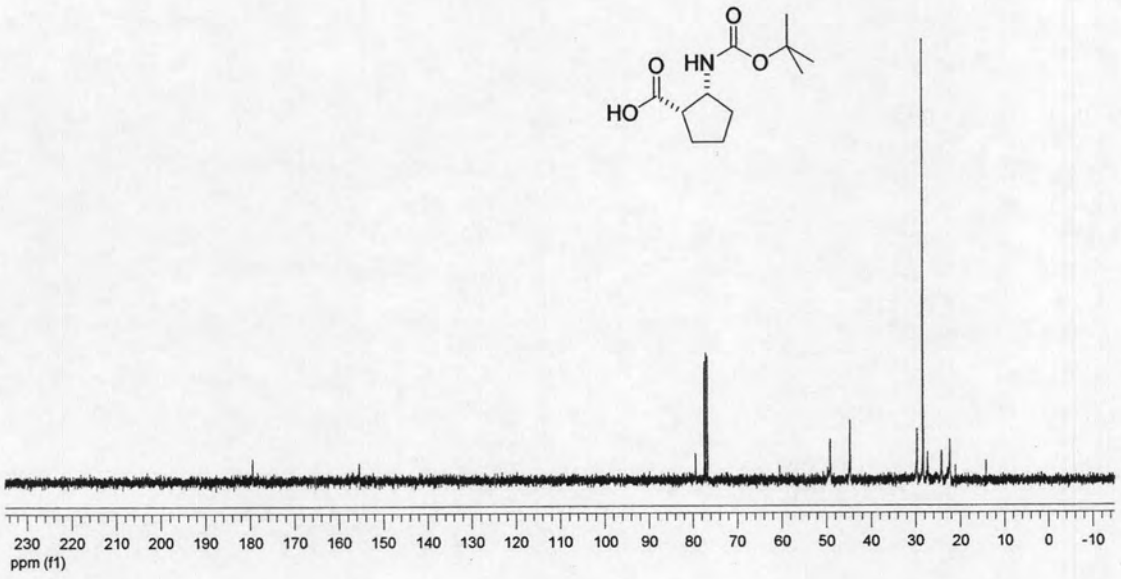

Figure A-140: ^{13}C NMR (100 MHz, $CDCl_3$) of (1*S*,2*R*)-2-(*N-tert*-Butoxycarbonyl)-amino cyclopentane carboxylic acid (**76**)

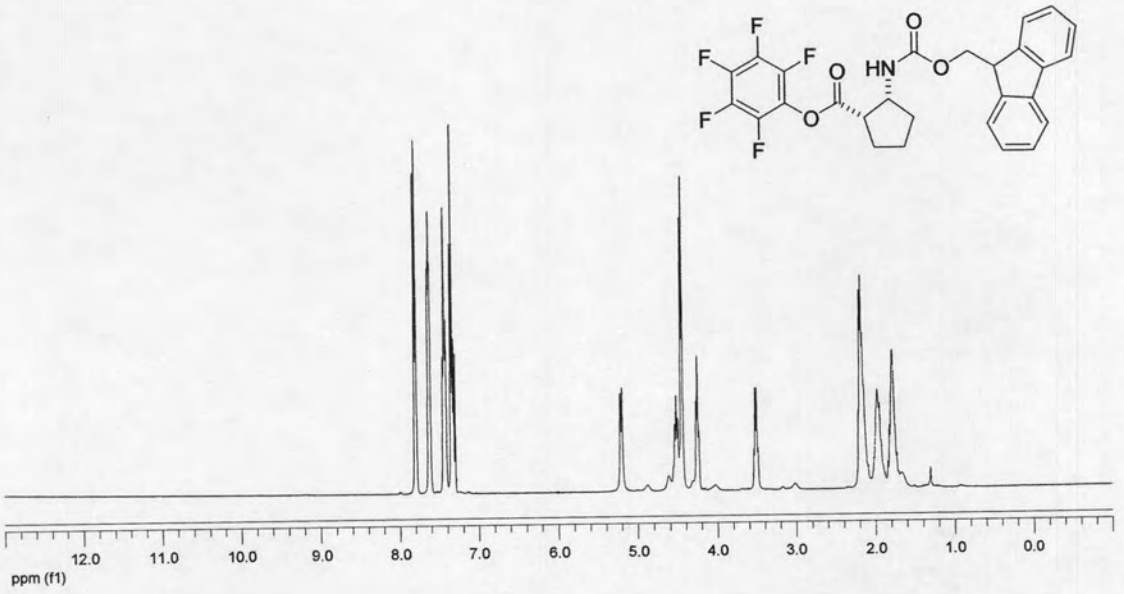

Figure A-141: ^{1}H NMR (400 MHz, $CDCl_3$) of (1*S*,2*R*)-2-(*N*-fluoren-9-ylmethoxy carbonyl)-aminocyclopentane pentafluorophenyl ester (**77**)

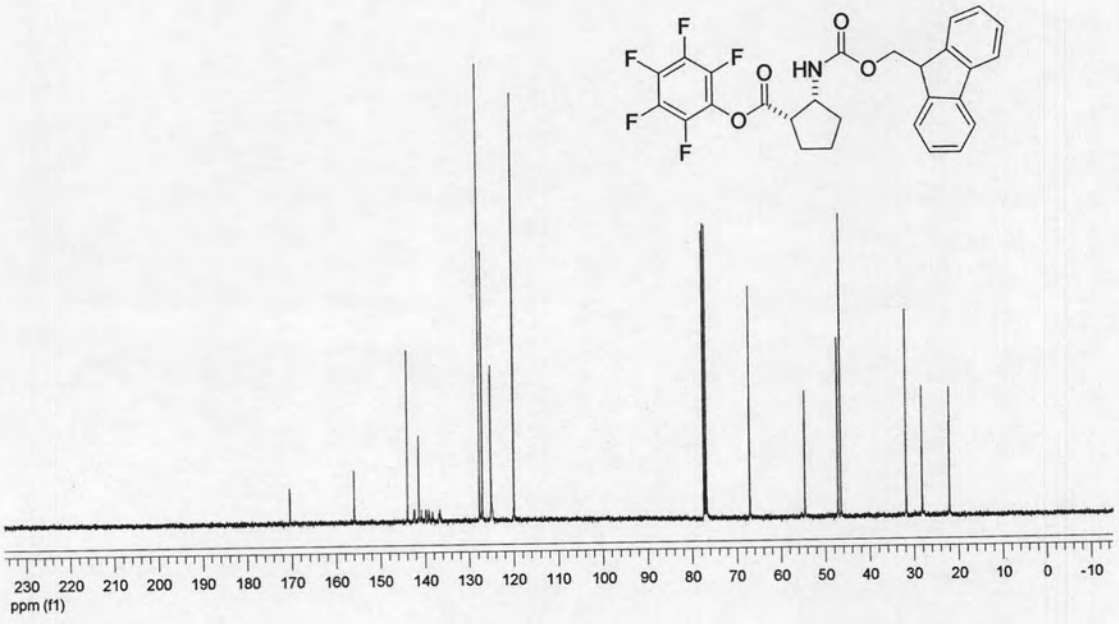

Figure A-142: ^{13}C NMR (100 MHz, $CDCl_3$) of (1*S*,2*R*)-2-(*N*-fluoren-9-ylmethoxy carbonyl)-aminocyclopentane pentafluorophenyl ester (**77**)

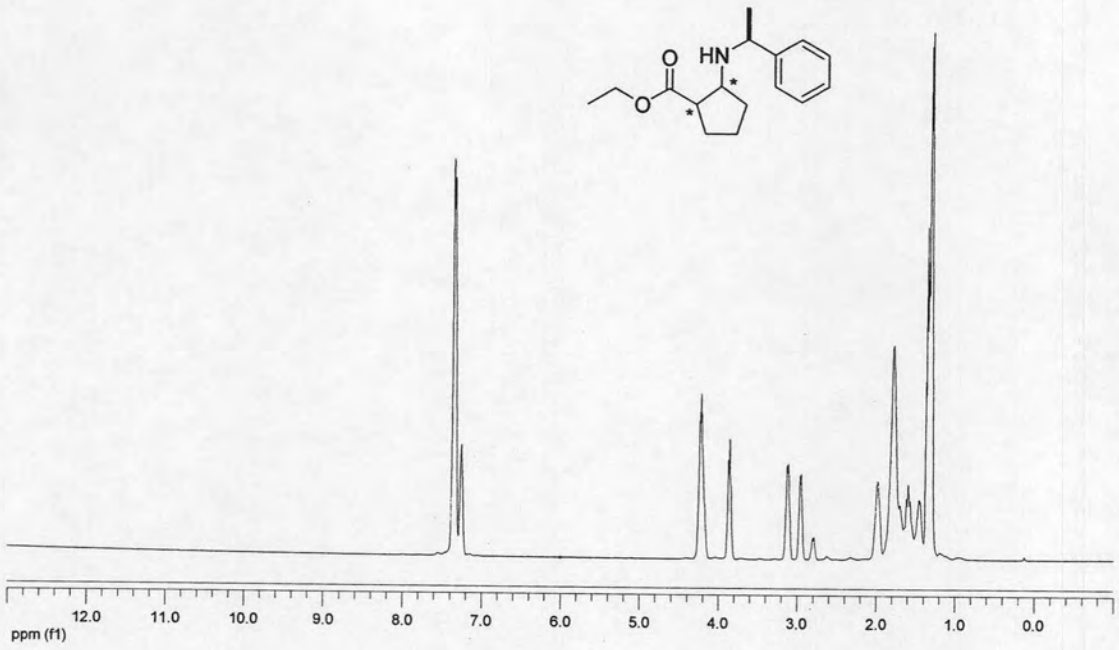

Figure A-143: ^{1}H NMR (400 MHz, $CDCl_3$) of Ethyl *cis*-(±)-2-[(1′*S*)-phenylethyl]-aminocyclopentane carboxylate (**78**)

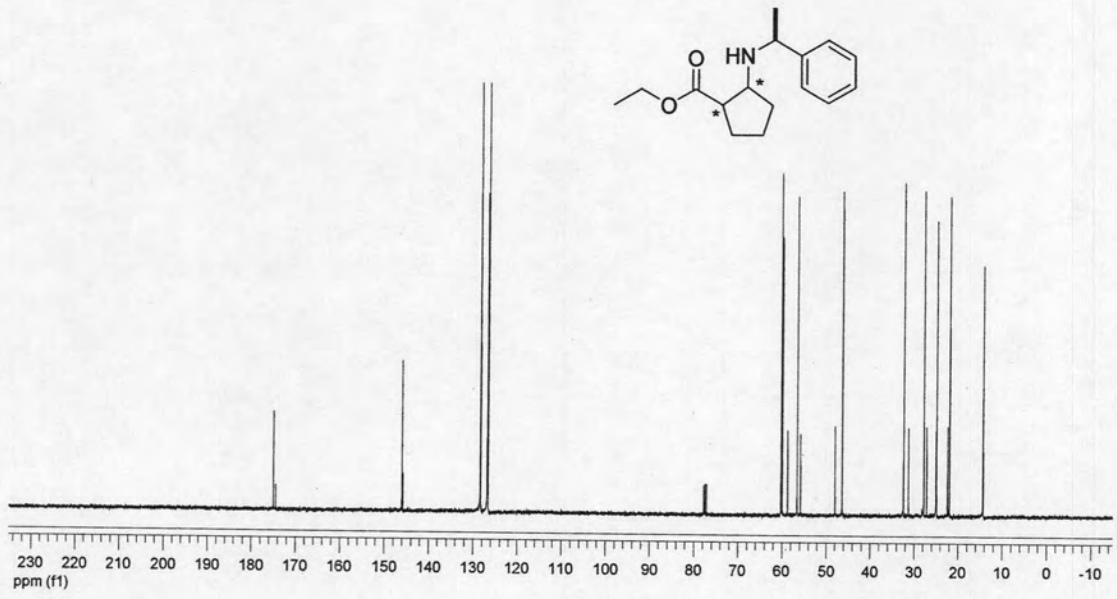

Figure A-144: ^{13}C NMR (100 MHz, $CDCl_3$) of Ethyl *cis*-(±)-2-[(1′*S*)-phenylethyl]-aminocyclopentane carboxylate (**78**)

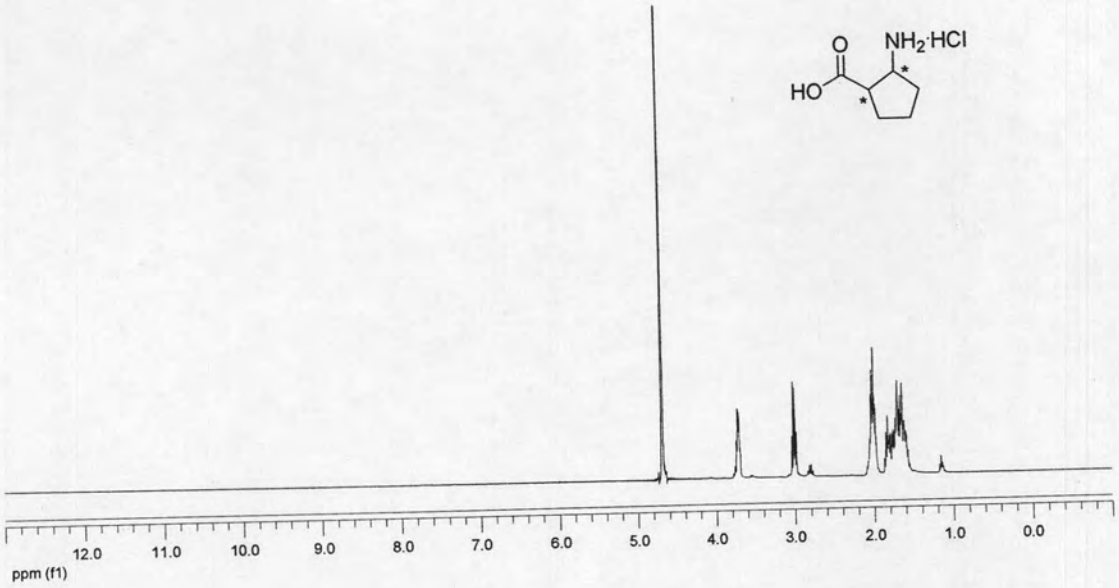

Figure A-145: ^{1}H NMR (400 MHz, D_2O) of *cis*-(±)-2-Aminocyclopentane carboxylic acid hydrochloride (**79**)

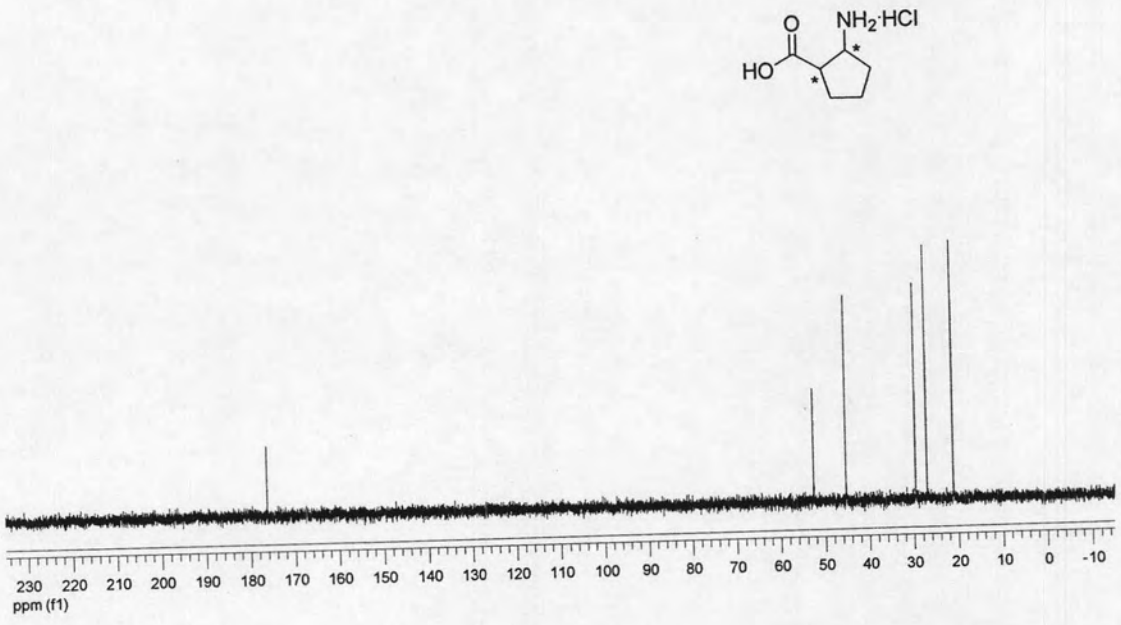

Figure A-146: ^{13}C NMR (100 MHz, D_2O) of *cis*-(±)-2-Aminocyclopentane carboxylic acid hydrochloride (**79**)

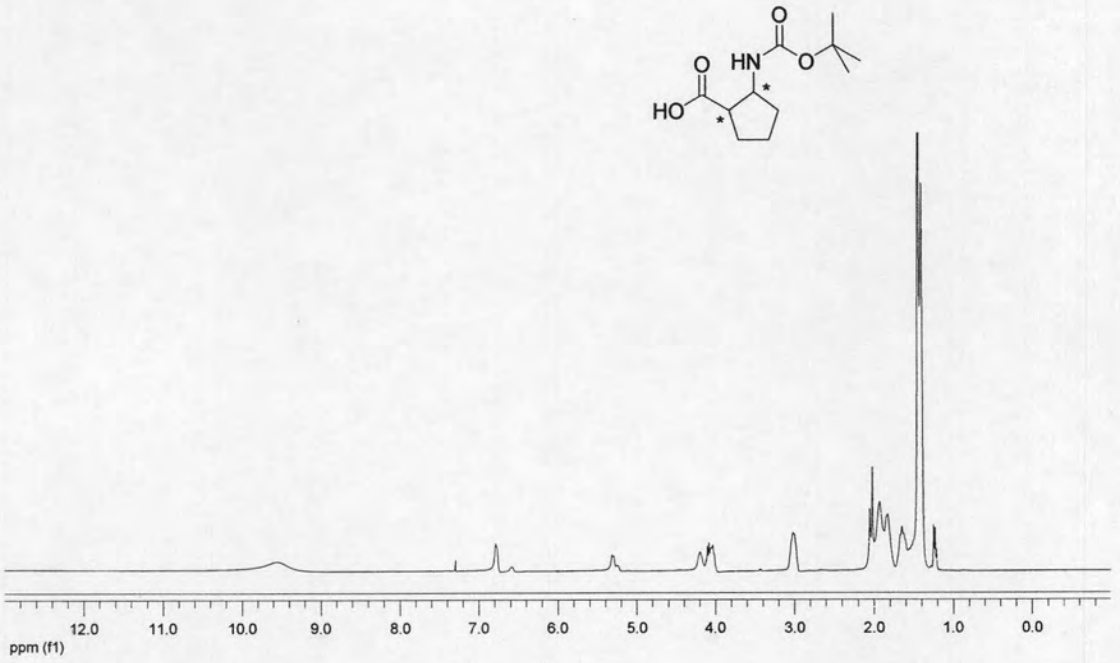

Figure A-147: ^{1}H NMR (400 MHz, $CDCl_3$) of *cis*-(±)-2-(*N-tert*-Butoxycarbonyl)-Aminocyclopentane carboxylic acid (**80**)

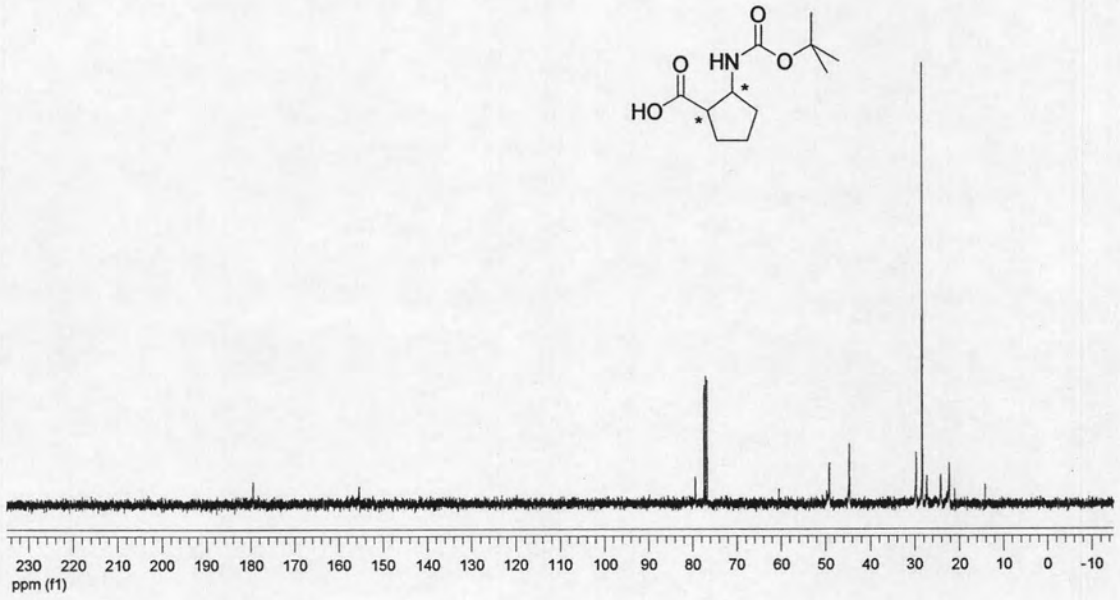

Figure A-148: ^{13}C NMR (100 MHz, $CDCl_3$) of *cis*-(±)-2-(*N-tert*-Butoxycarbonyl)-Aminocyclopentane carboxylic acid (**80**)

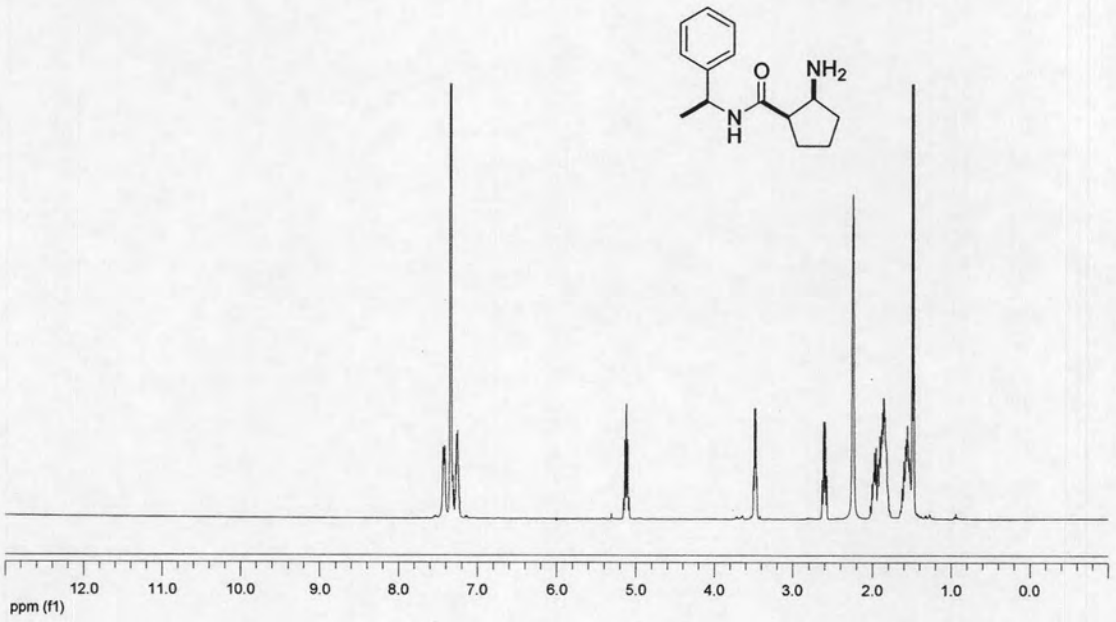

Figure A-149: ^{1}H NMR (400 MHz, $CDCl_3$) of (1*R*,2*S*)-2-Aminocyclopentane carboxylic acid hydrochloride (**81**)

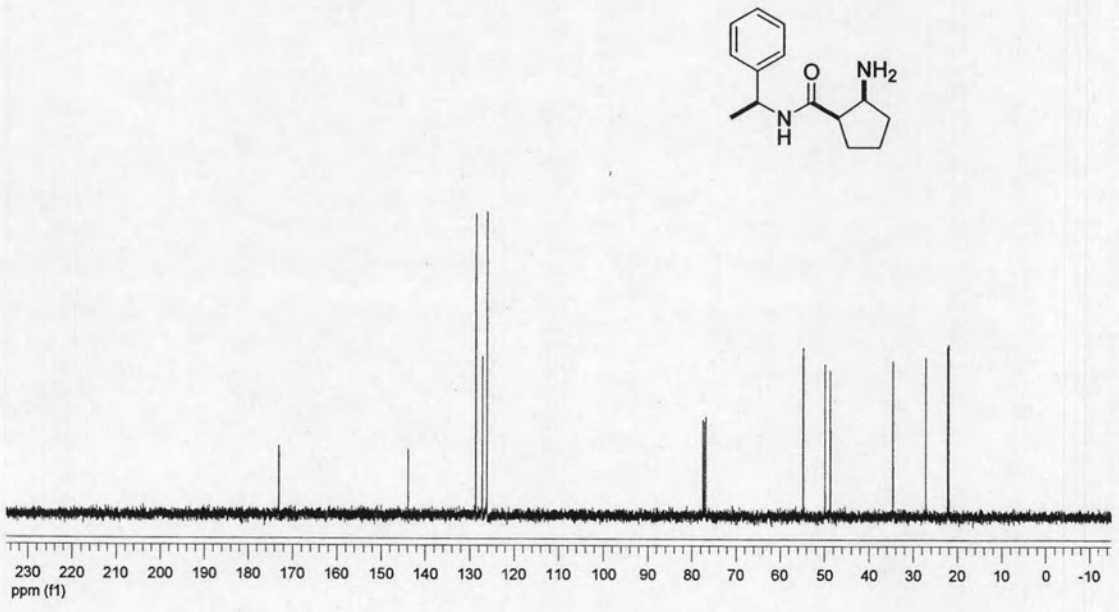

Figure A-150: ^{13}C NMR (100 MHz, $CDCl_3$) of (1*R*,2*S*)-2-Aminocyclopentane carboxylic acid hydrochloride (**81**)

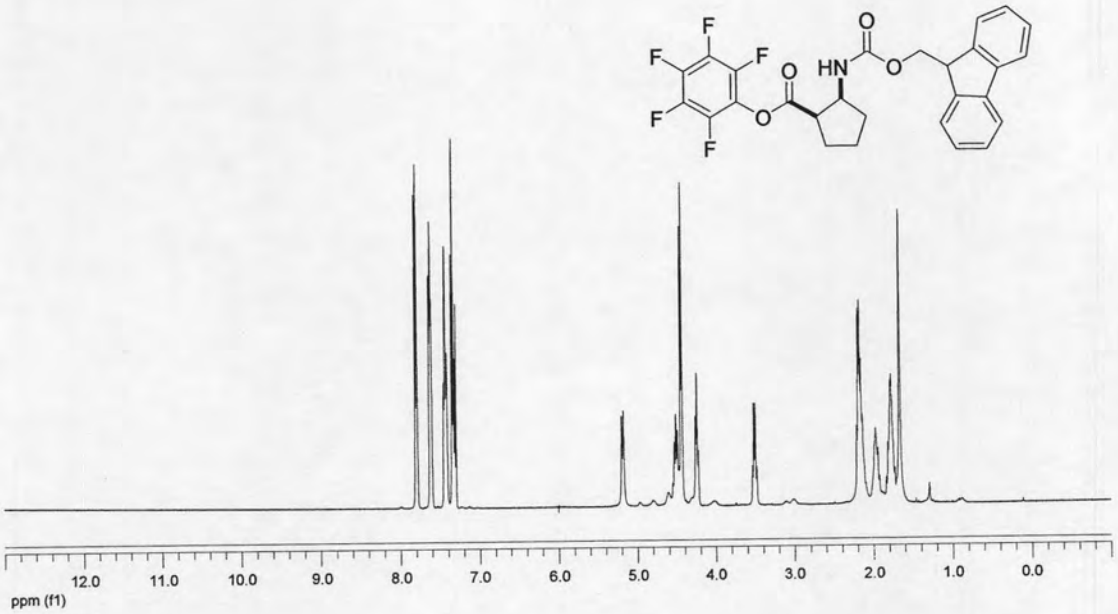

Figure A-151: ^{1}H NMR (400 MHz, $CDCl_3$) of (1*R*,2*S*)-2-(*N*-fluoren-9-ylmethoxy carbonyl)-aminocyclopentane pentafluorophenyl ester (**82**)

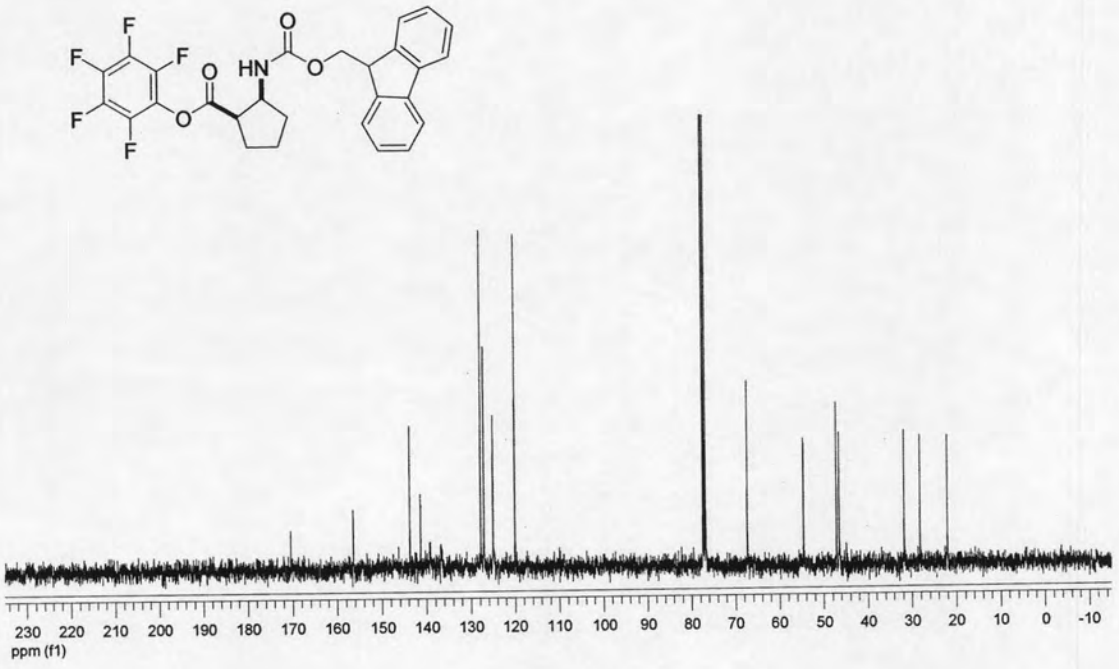

Figure A-152: ^{13}C NMR (100 MHz, $CDCl_3$) of (1*R*,2*S*)-2-(*N*-fluoren-9-ylmethoxy carbonyl)-aminocyclopentane pentafluorophenyl ester (**82**)

APPENDIX B

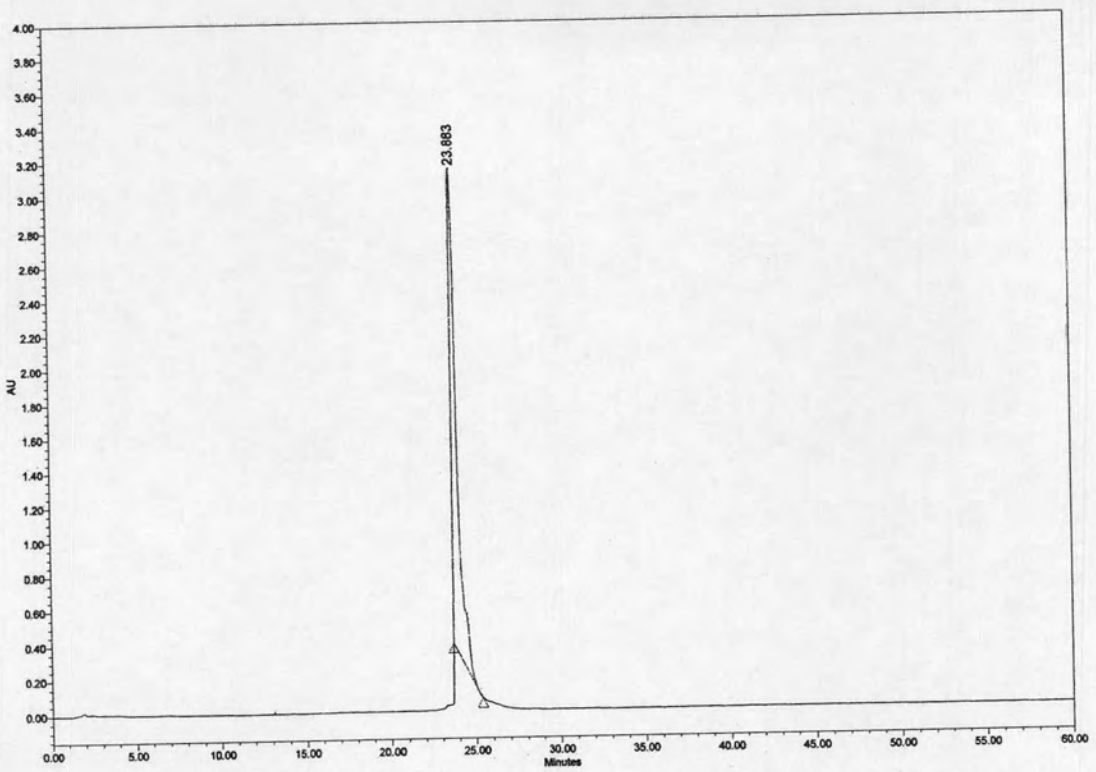

Figure B-1 : HPLC chromatogram of *cis*-D/D-APC Fmoc-T_5-LysNH_2 **(P1)**

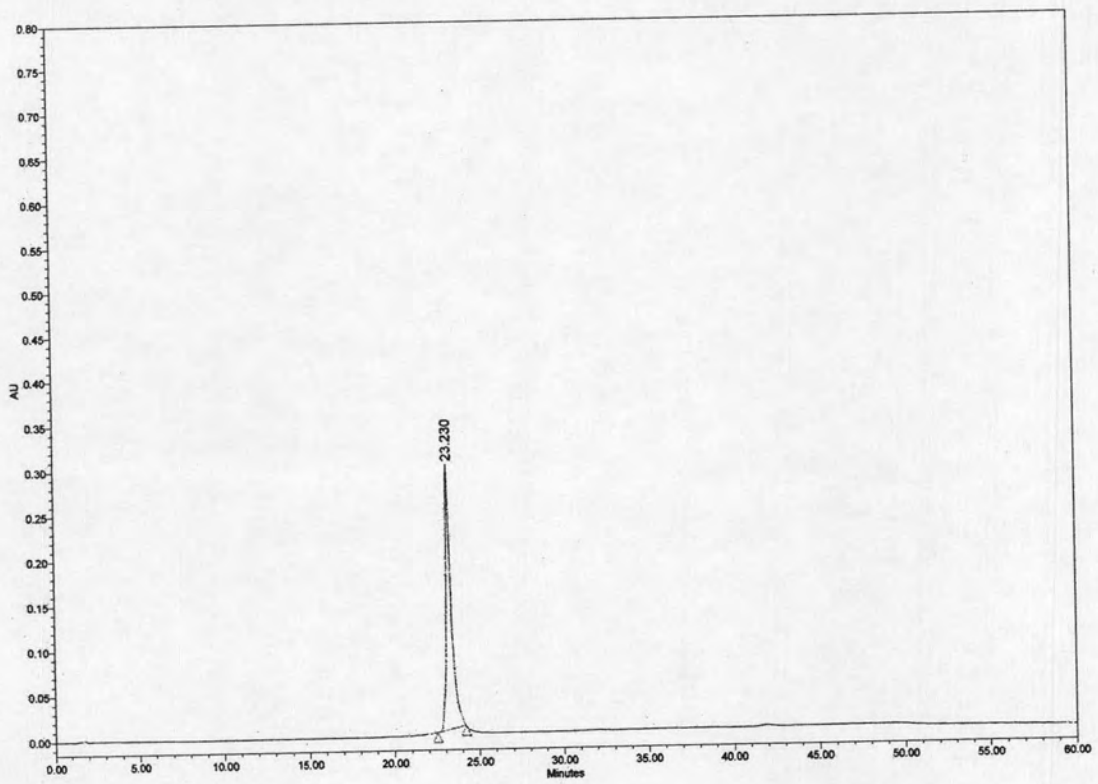

Figure B-2 : HPLC chromatogram of *trans*-D/D-APC Fmoc-T_5-LysNH_2 **(P2)**

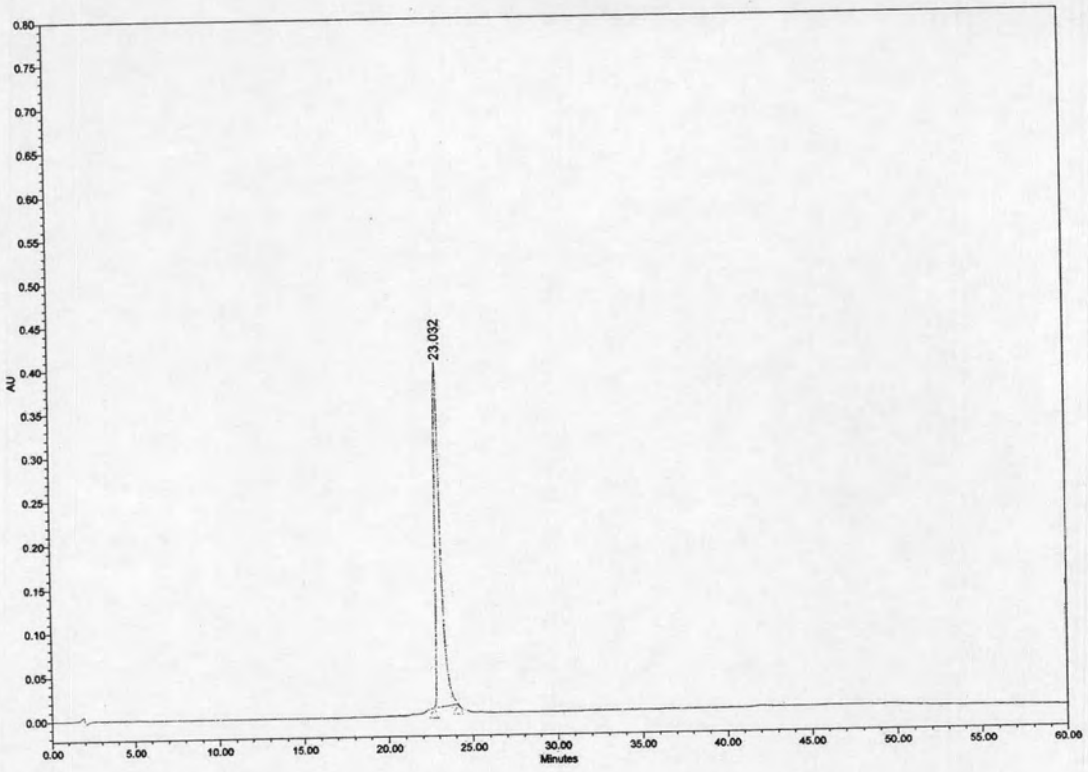

Figure B-3 : HPLC chromatogram of *cis*-L/D-APC Fmoc-T_5-LysNH_2 **(P3)**

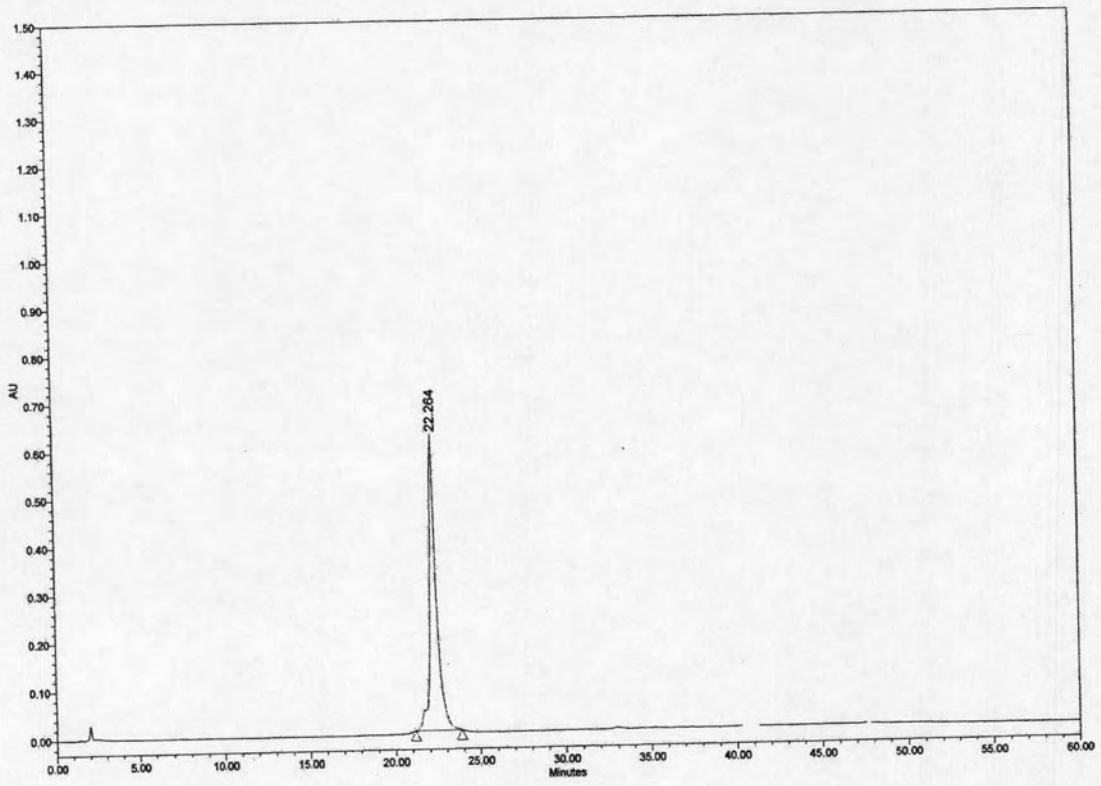

Figure B-4 : HPLC chromatogram of *trans*-L/D-APC Fmoc-T_5-LysNH_2 **(P4)**

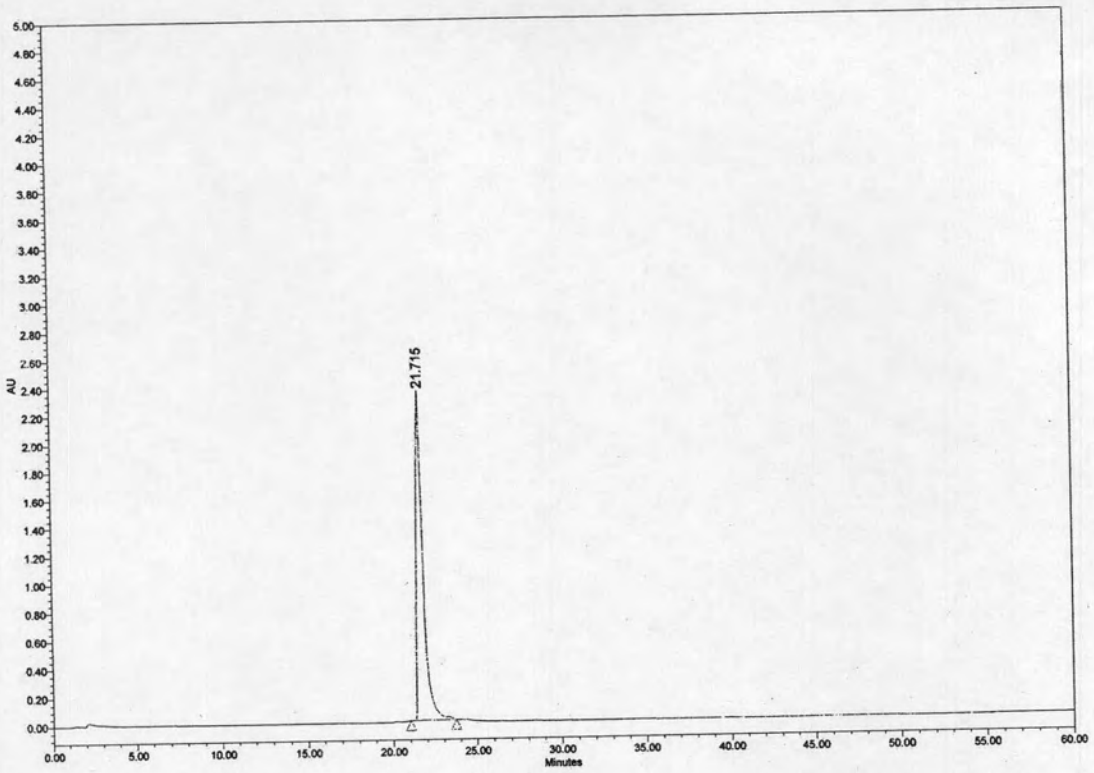

Figure B-5 : HPLC chromatogram of *cis*-D/L-APC Fmoc-T_5-LysNH_2 **(P5)**

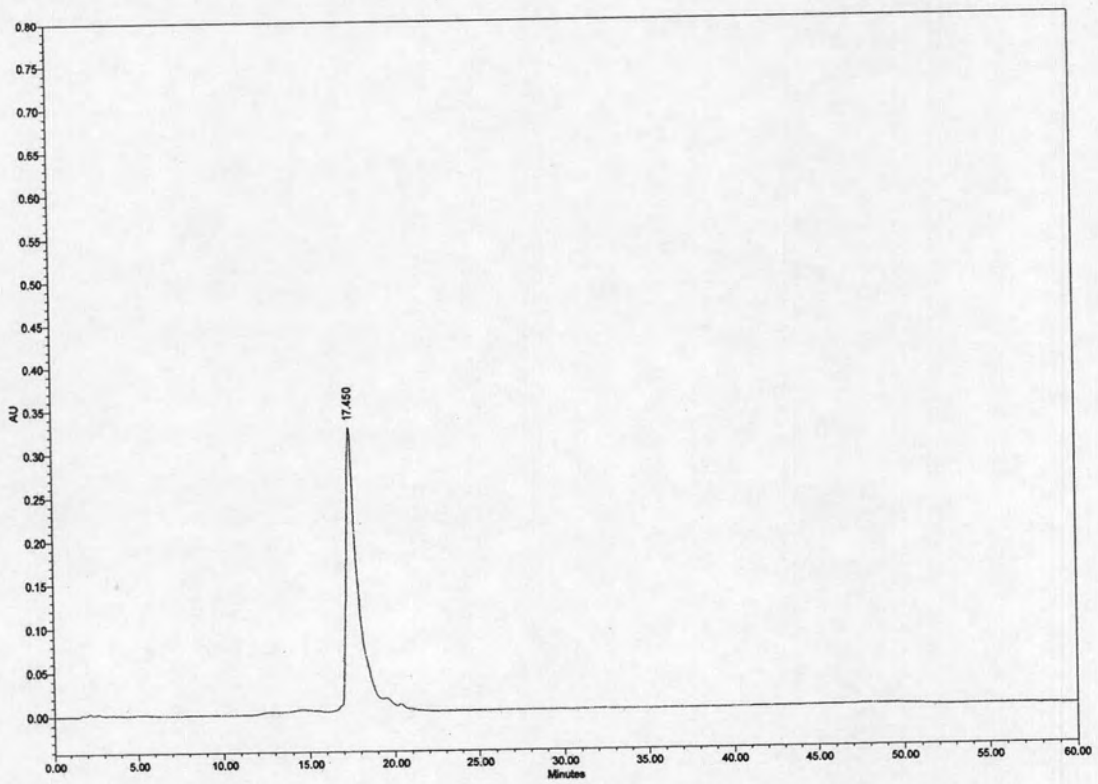

Figure B-6 : HPLC chromatogram of *cis*-D/(1*S*,2*S*)-ACPC H-T_5-LysNH_2 **(P6)**

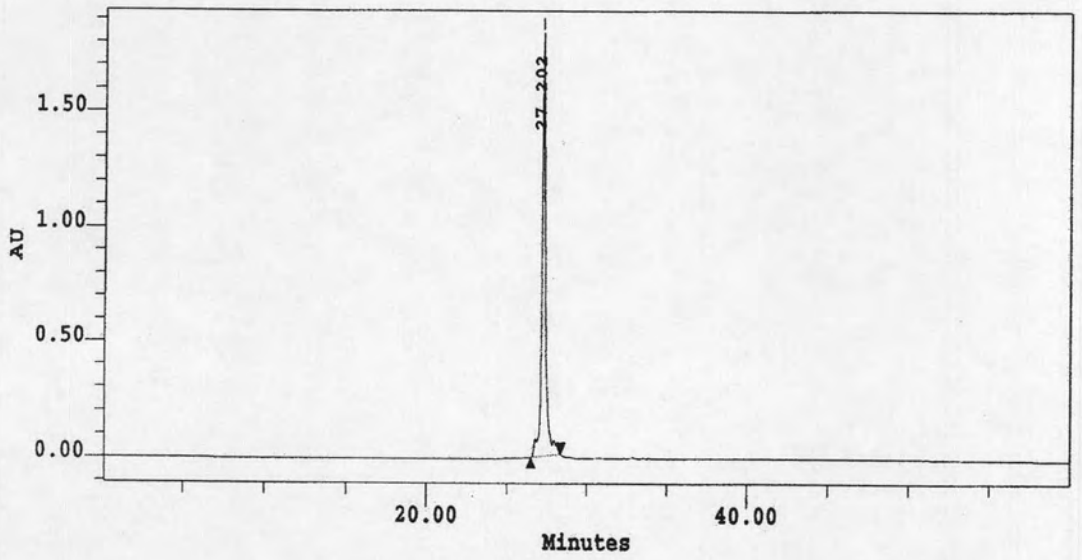

Figure B-7 : HPLC chromatogram of *cis*-D/(1*R*,2*R*)-ACPC H-T_5-LysNH_2 **(P7)**

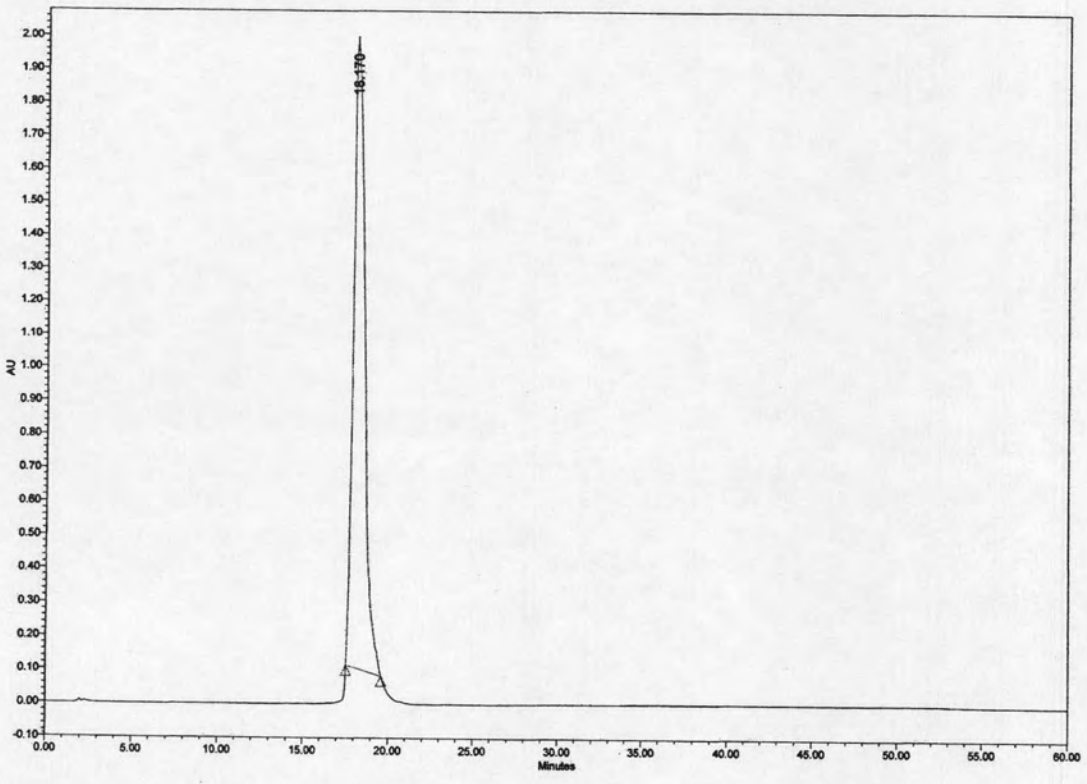

Figure B-8 : HPLC chromatogram of *cis*-D/(1*S*,2*R*)-ACPC H-T_5-LysNH_2 **(P8)**

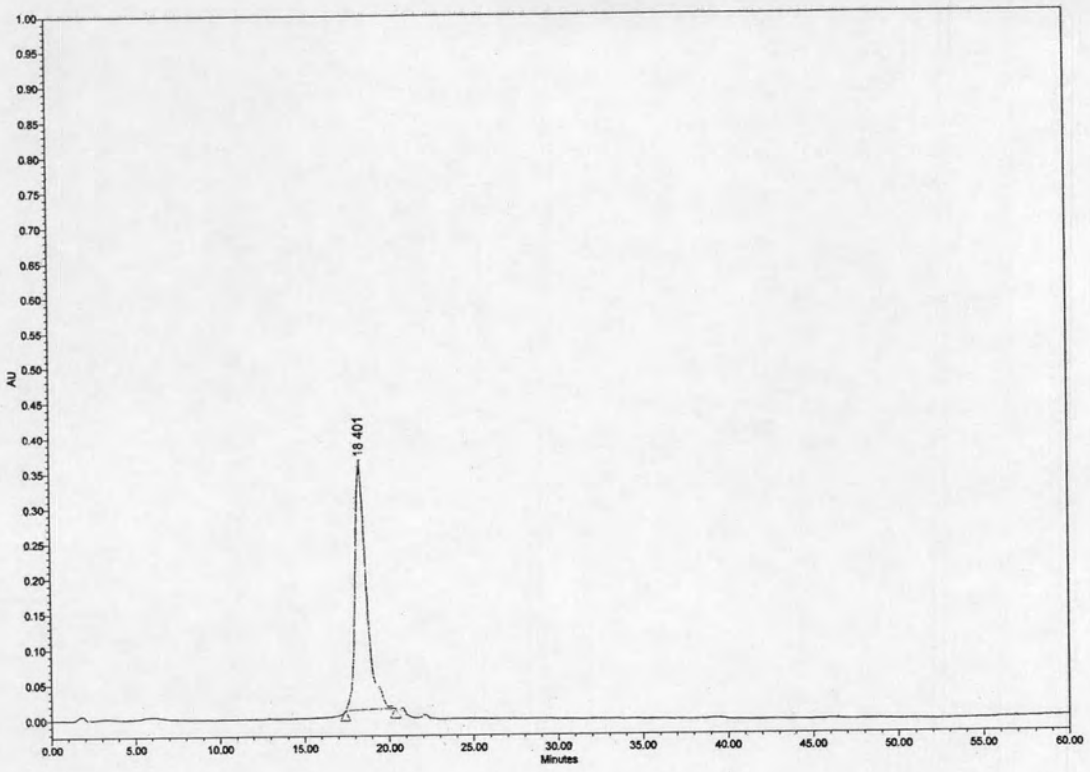

Figure B-9 : HPLC chromatogram of *cis*-D/(1*R*,2*S*)-ACPC H-T_5-LysNH_2 **(P9)**

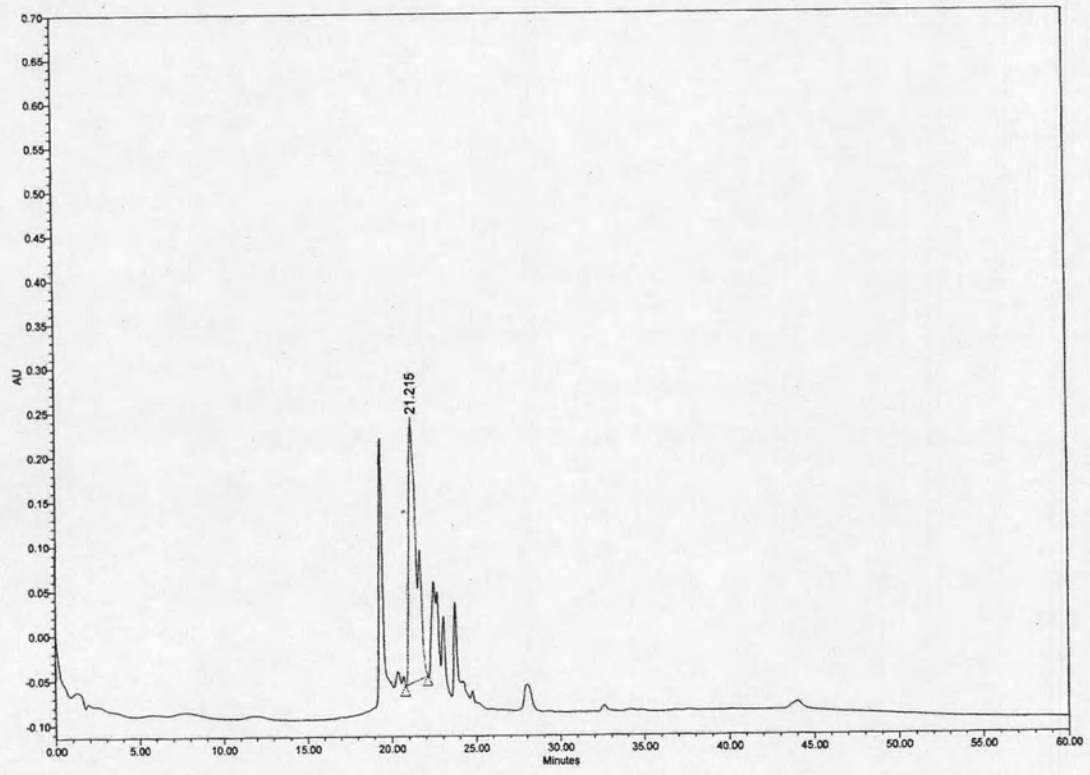

Figure B-10 : HPLC chromatogram of *cis*-D/N-Spacer Ac-T_5-LysNH_2 **(P10)**

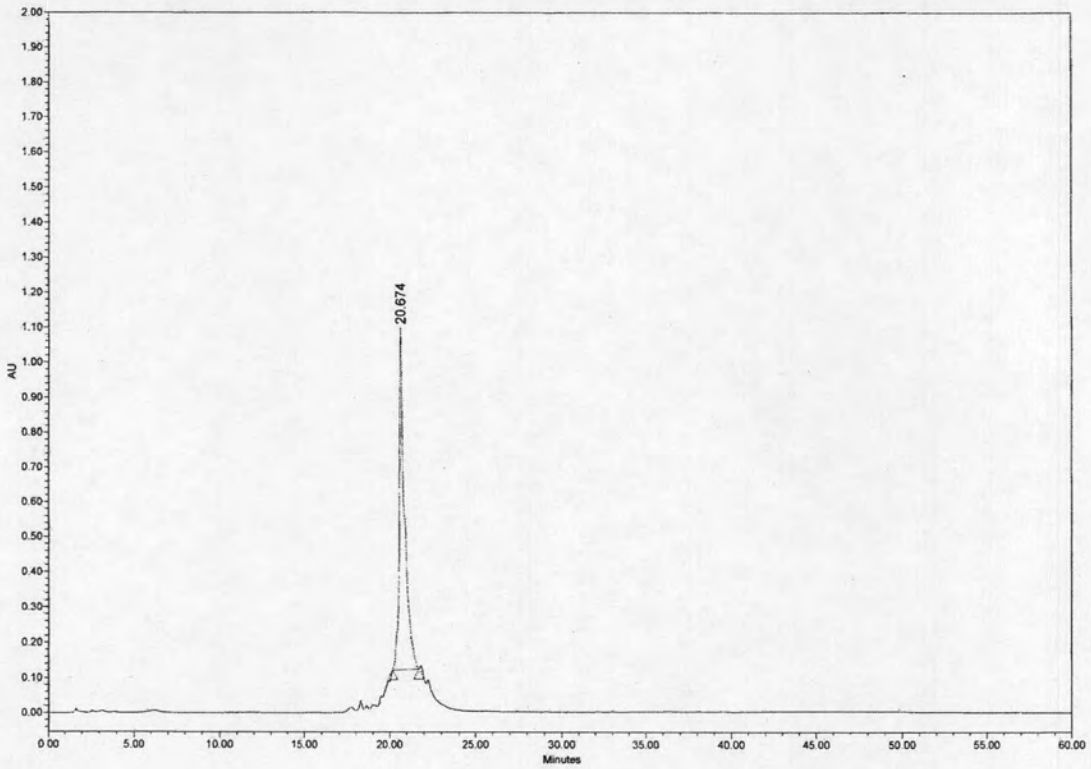

Figure B-11 : HPLC chromatogram of *cis*-D/D-APC Ac-A_5-LysNH_2 **(P12)**

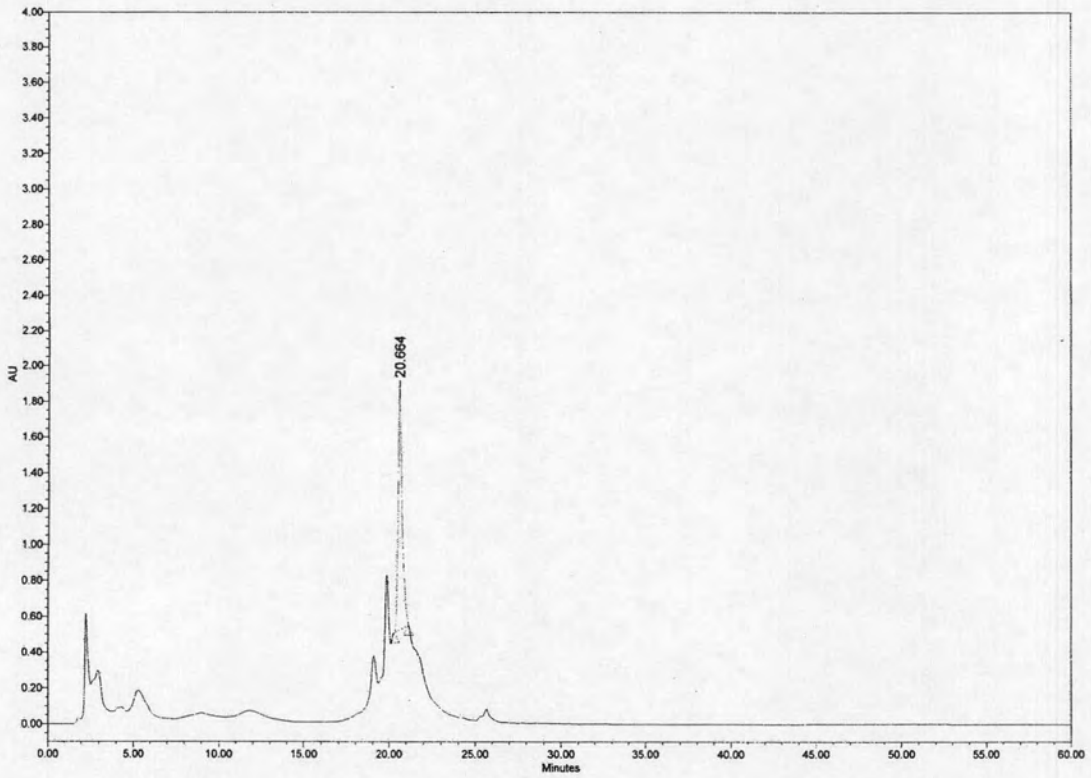

Figure B-12 : HPLC chromatogram of *cis*-D/D-APC Ac-T_7-LysNH_2 **(P13)**

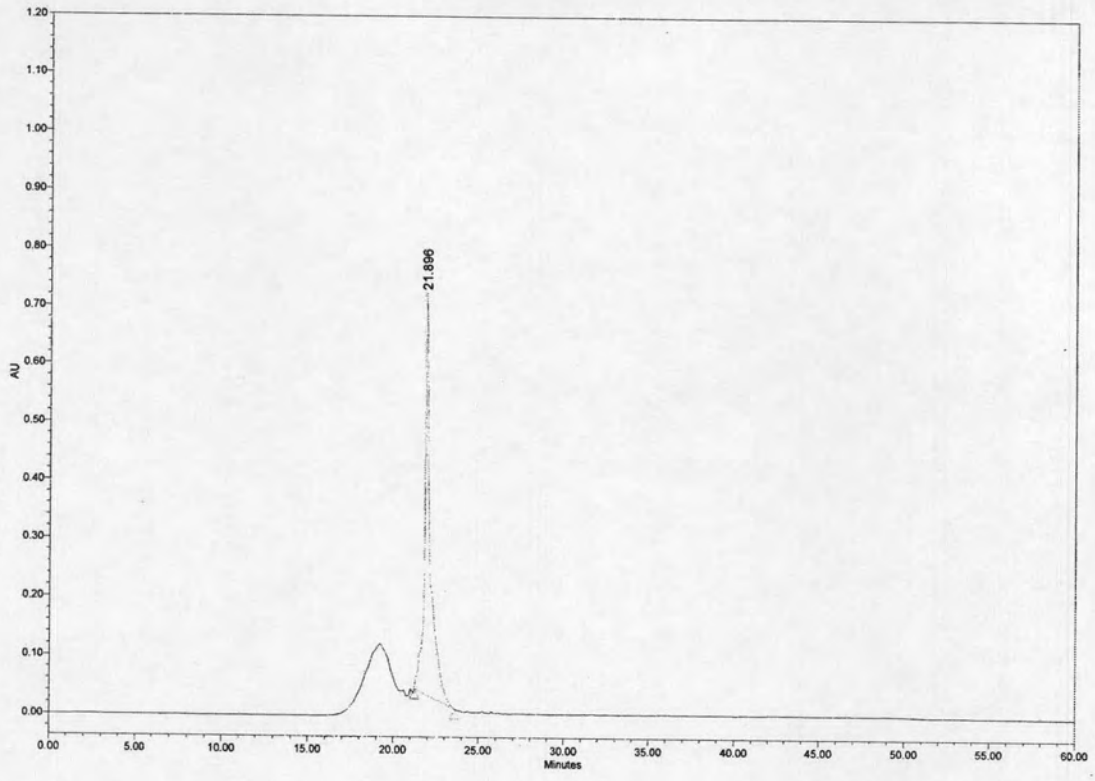

Figure B-13 : HPLC chromatogram of *cis*-D/D-APC Ac-T_3AT_3-$LysNH_2$ **(P14)**

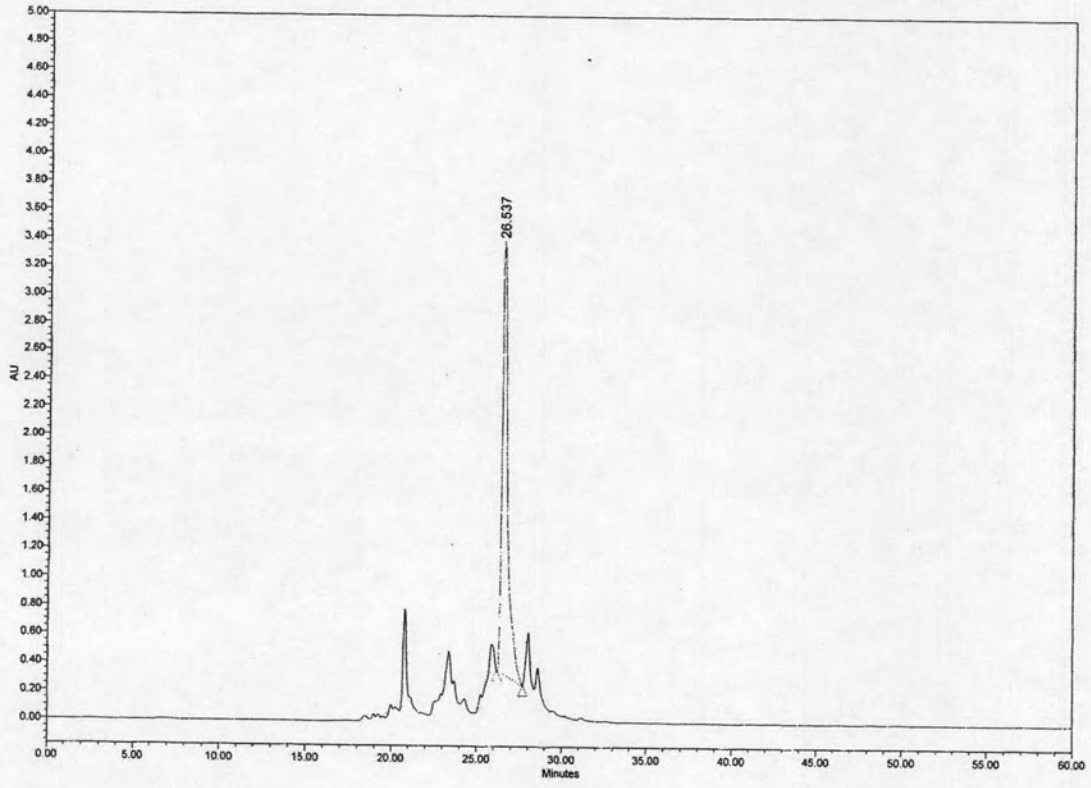

Figure B-14 : HPLC chromatogram of *cis*-D/D-APC Ac-T_3CT_3-$LysNH_2$ **(P15)**

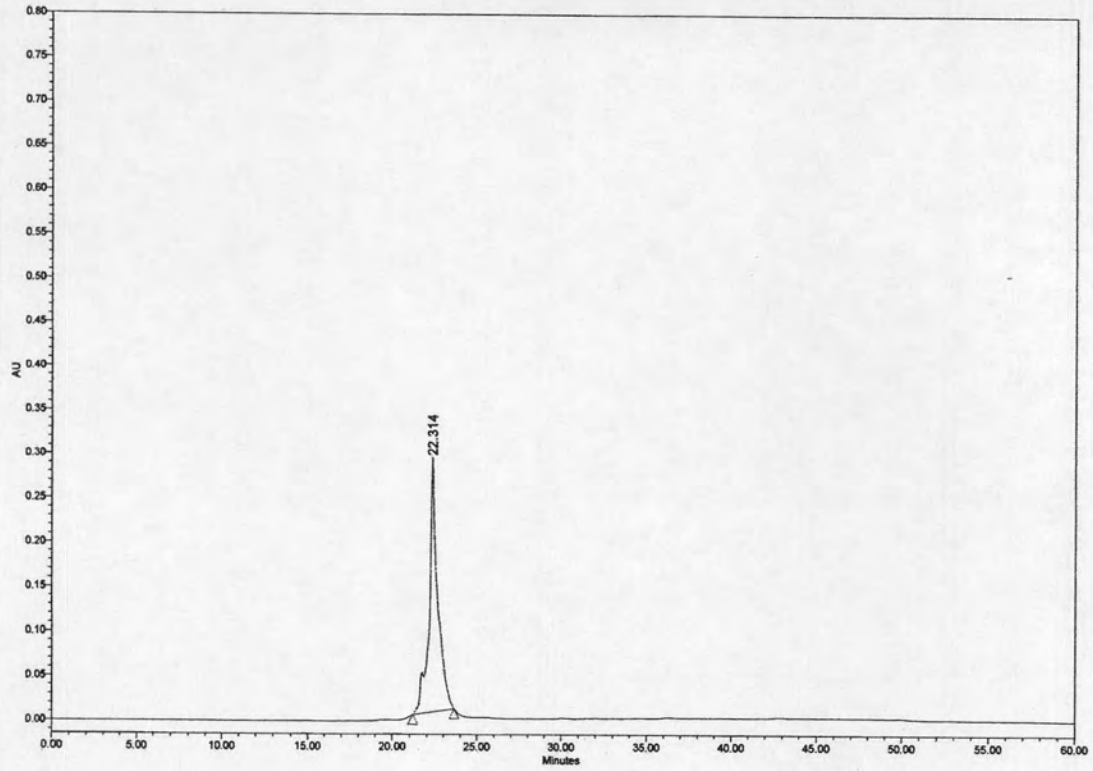

Figure B-15 : HPLC chromatogram of *cis*-D/D-APC Ac-T_3GT_3-LysNH_2 **(P16)**

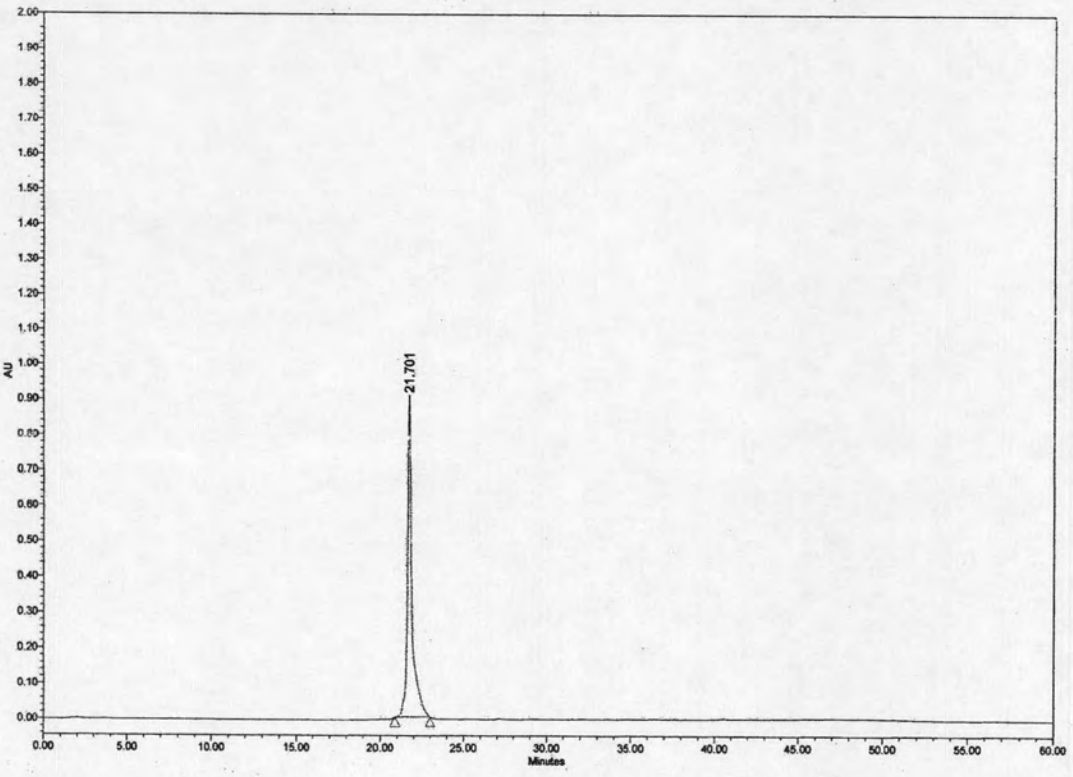

Figure B-16 : HPLC chromatogram of *cis*-D/D-APC Ac-T_9-LysNH_2 **(P17)**

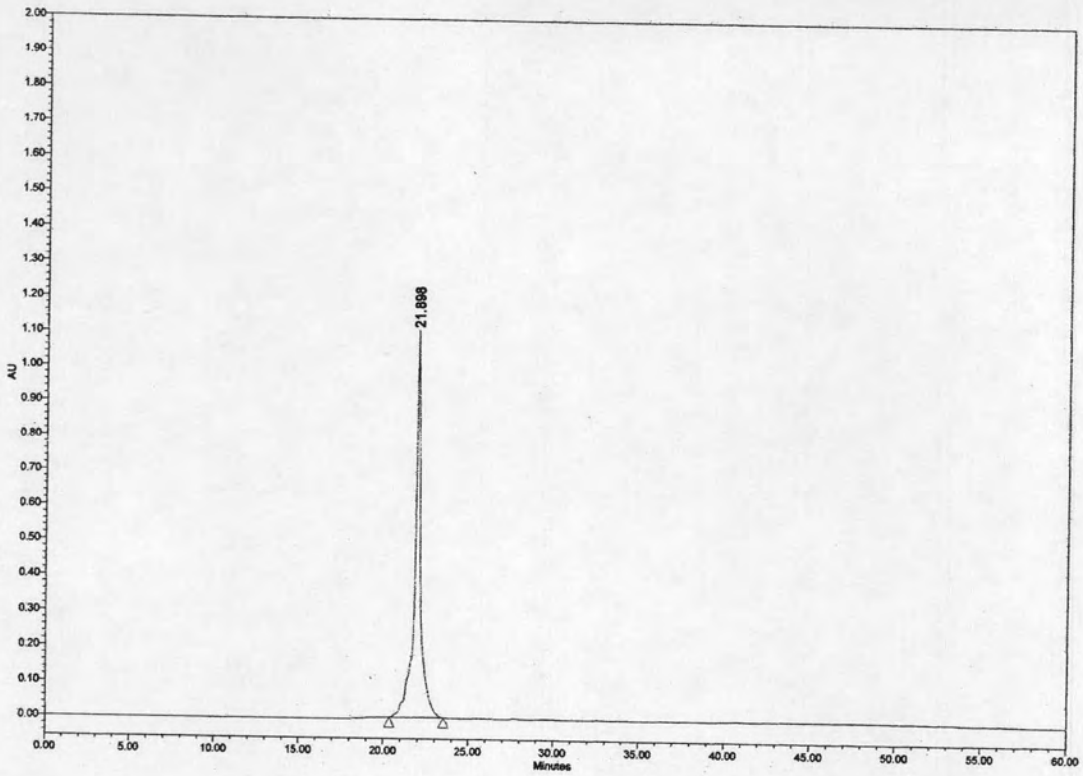

Figure B-17 : HPLC chromatogram of *cis*-D/D-APC Ac-T_4AT_4-LysNH_2 **(P18)**

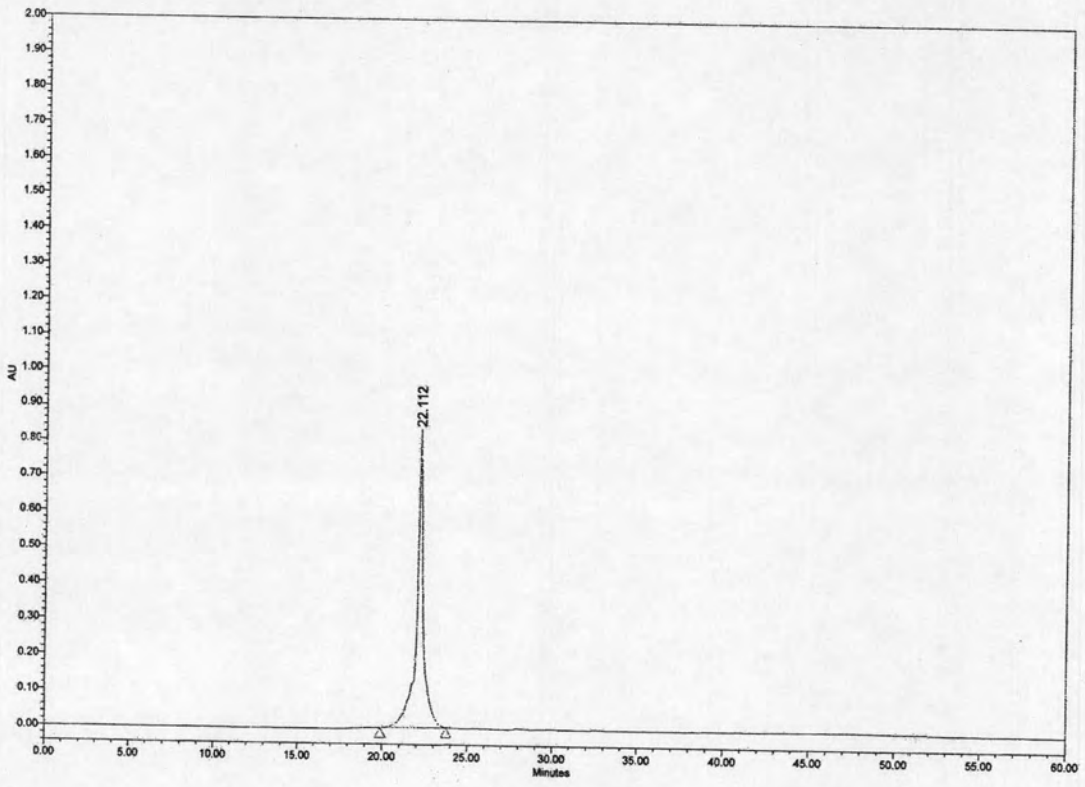

Figure B-18 : HPLC chromatogram of *cis*-D/D-APC Ac-T_4CT_4-LysNH_2 **(P19)**

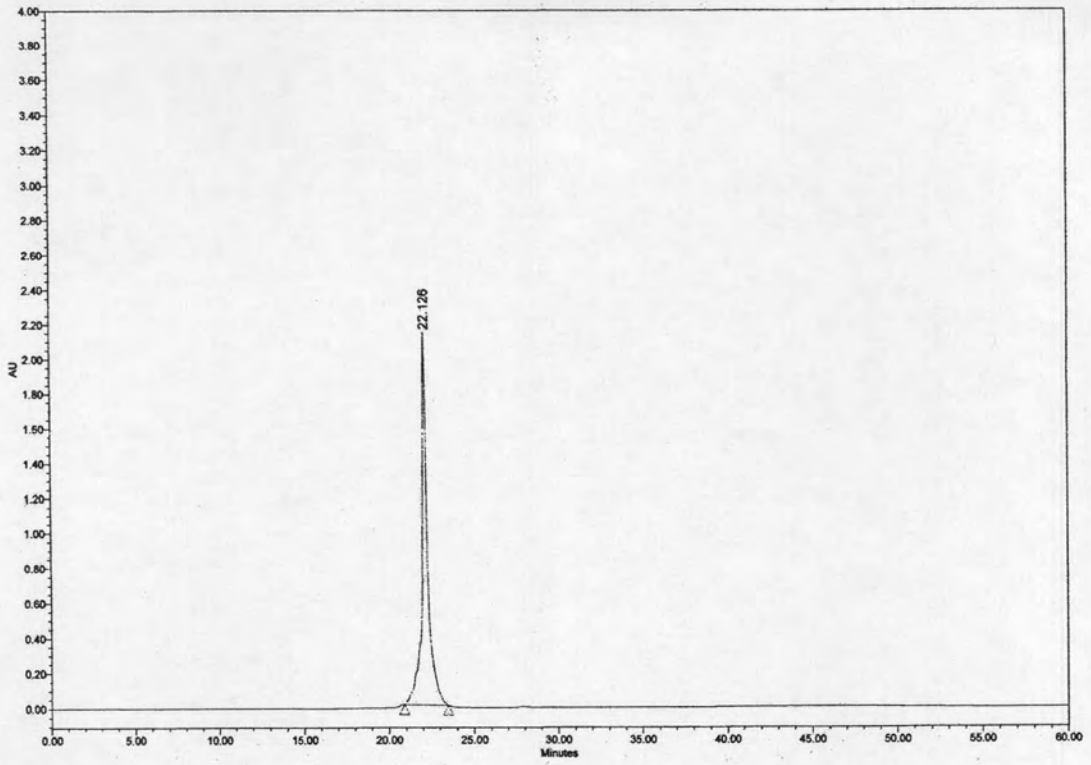

Figure B-19 : HPLC chromatogram of *cis*-D/D-APC Ac-T_4GT_4-LysNH_2 **(P20)**

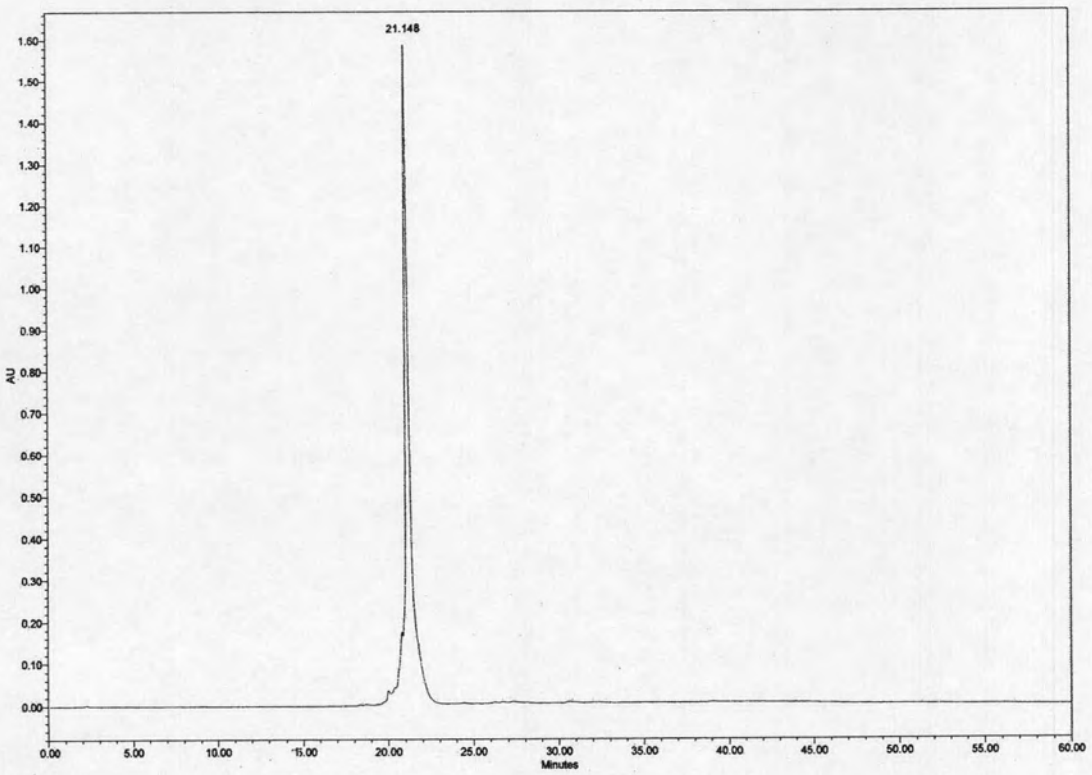

Figure B-20 : HPLC chromatogram of *cis*-D/D-APC Ac-T_4ATAT-LysNH_2 **(P21)**

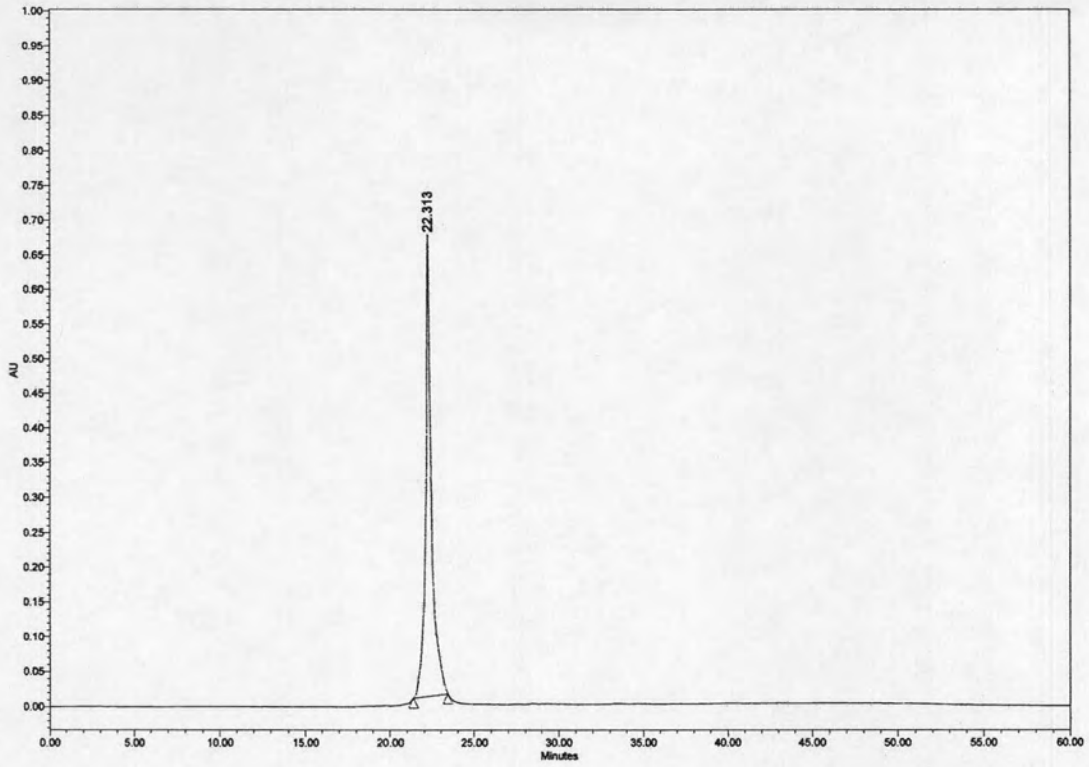

Figure B-21 : HPLC chromatogram of *cis*-D/D-APC Ac-TATAT$_4$-LysNH$_2$ **(P22)**

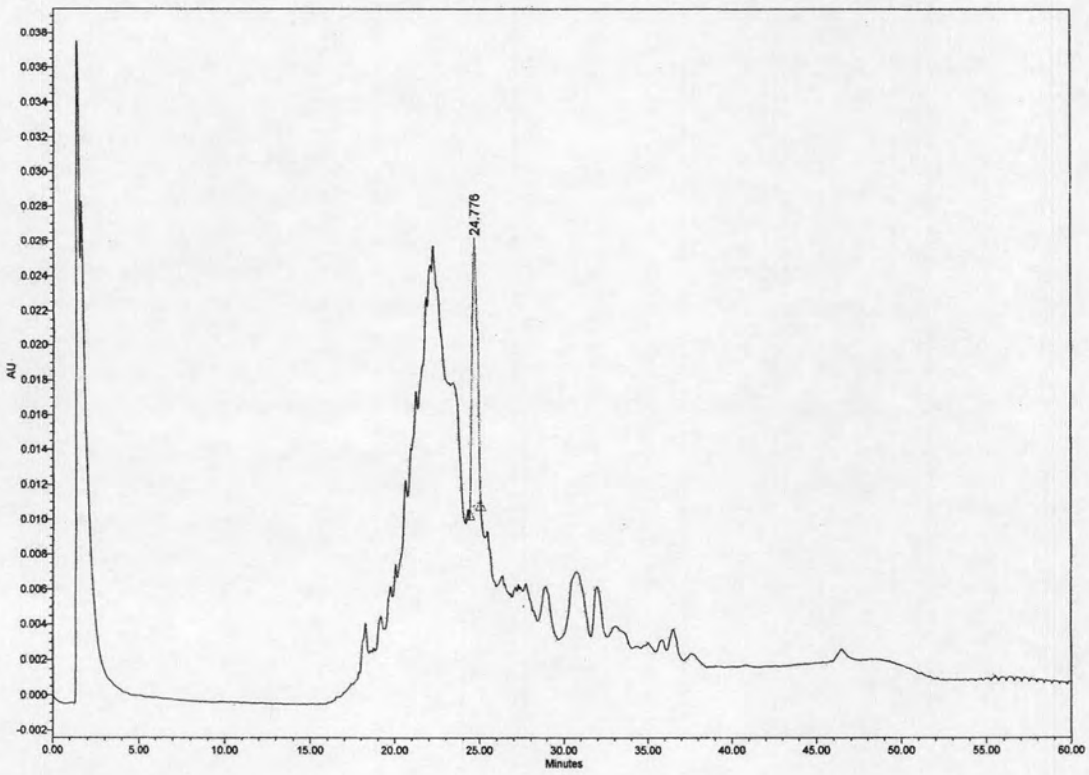

Figure B-22 : HPLC chromatogram of *cis*-D/D-APC Ac-Ser- Lys(F)-T$_9$- Ser-NH$_2$ **(P25)** detected at 260 nm

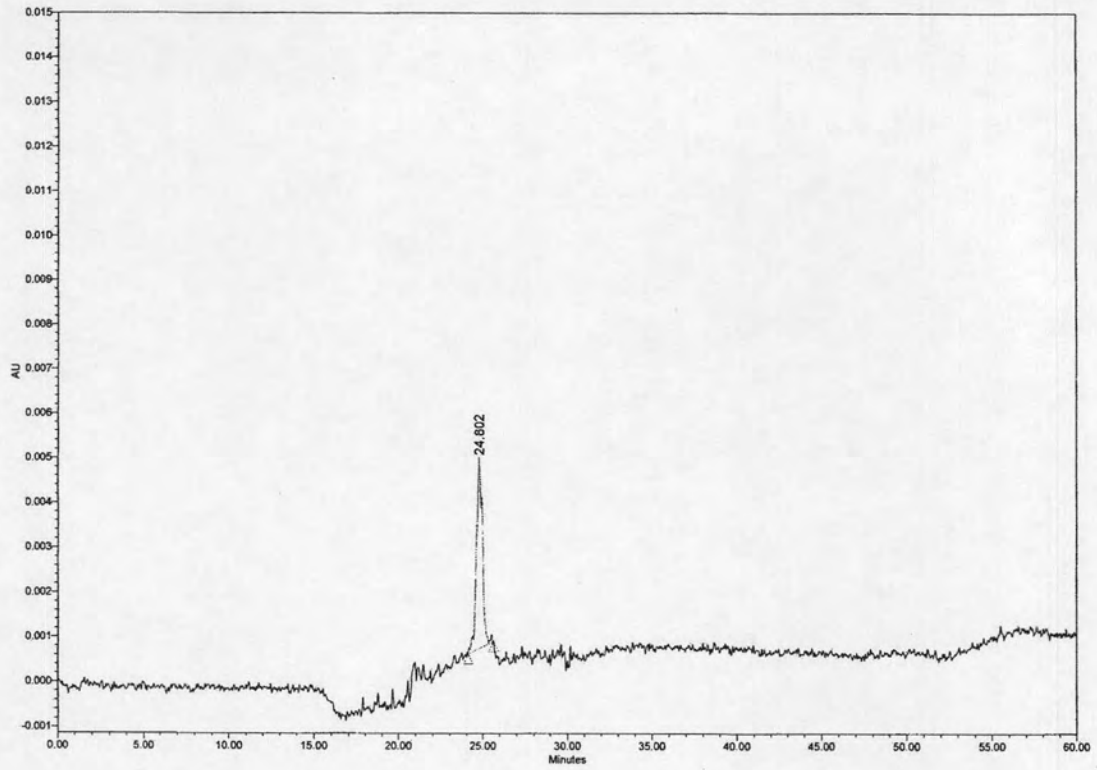

Figure B-23 : HPLC chromatogram of *cis*-D/D-APC Ac-Ser- Lys(F)-T_9- Ser-NH_2 **(P25)** detected at 440 nm

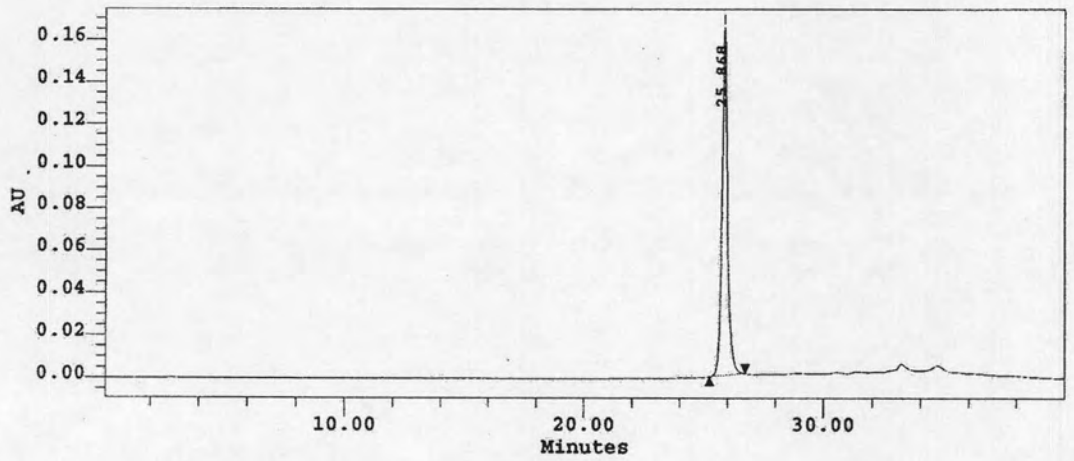

Figure B-24 : HPLC chromatogram of *cis*-D/(1*S*,2*S*)-ACPC H-T_{10}-LysNH_2 **(P26)**

APPENDIX C

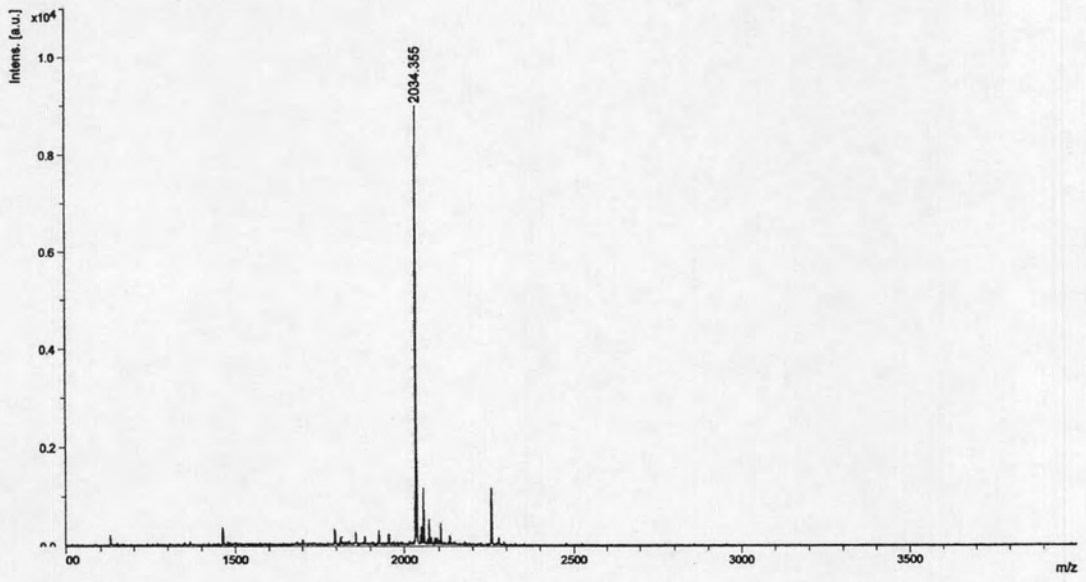

Figure C-1 : MALDI-TOF mass spectrum of *cis*-D/D-APC Fmoc-T_5-LysNH_2 (**P1**)

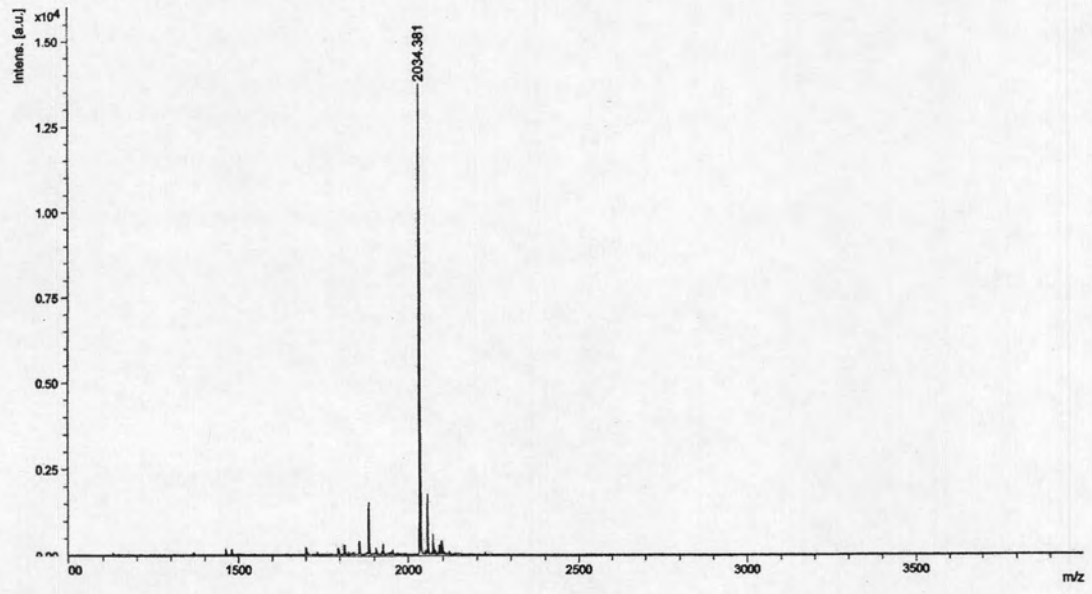

Figure C-2 : MALDI-TOF mass spectrum of *trans*-D/D-APC Fmoc-T_5-LysNH_2 (**P2**)

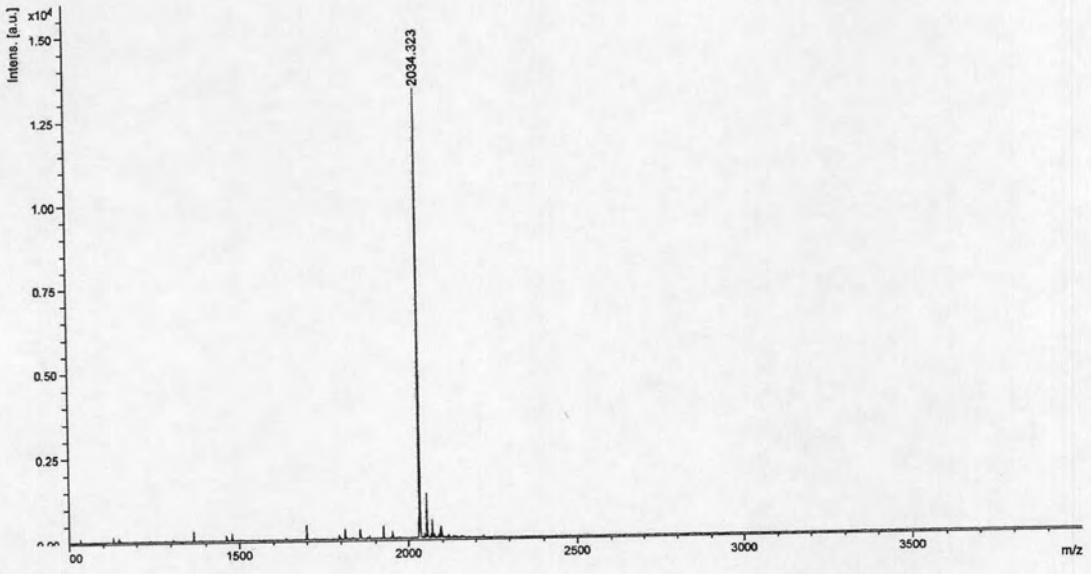

Figure C-3 : MALDI-TOF mass spectrum of *cis*-L/D-APC Fmoc-T_5-LysNH_2 (**P3**)

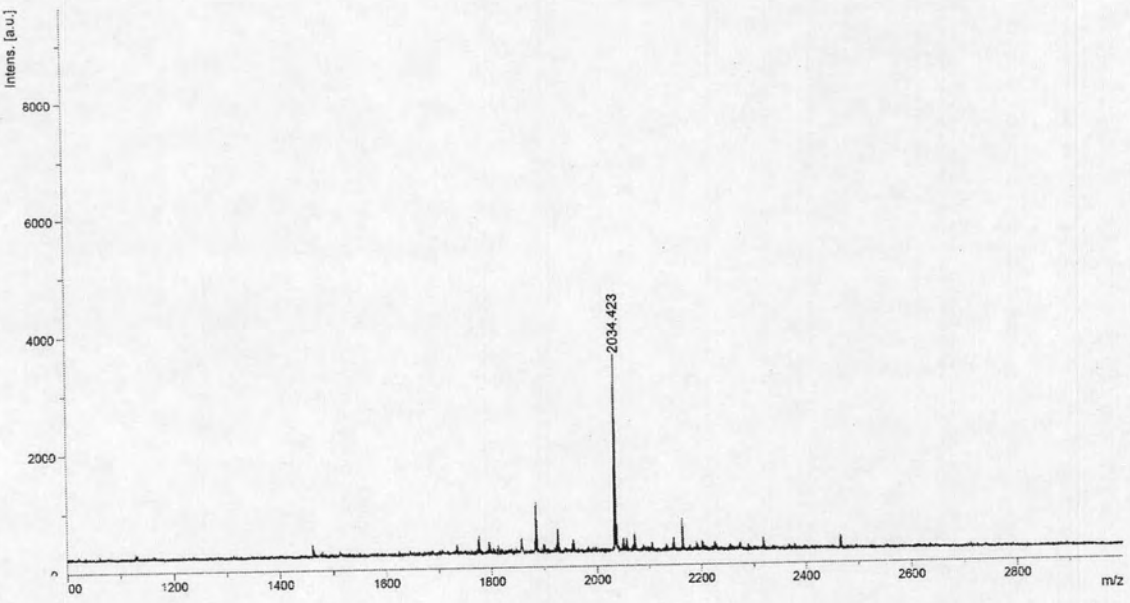

Figure C-4 : MALDI-TOF mass spectrum of *trans*-L/D-APC Fmoc-T_5-LysNH_2 (**P4**)

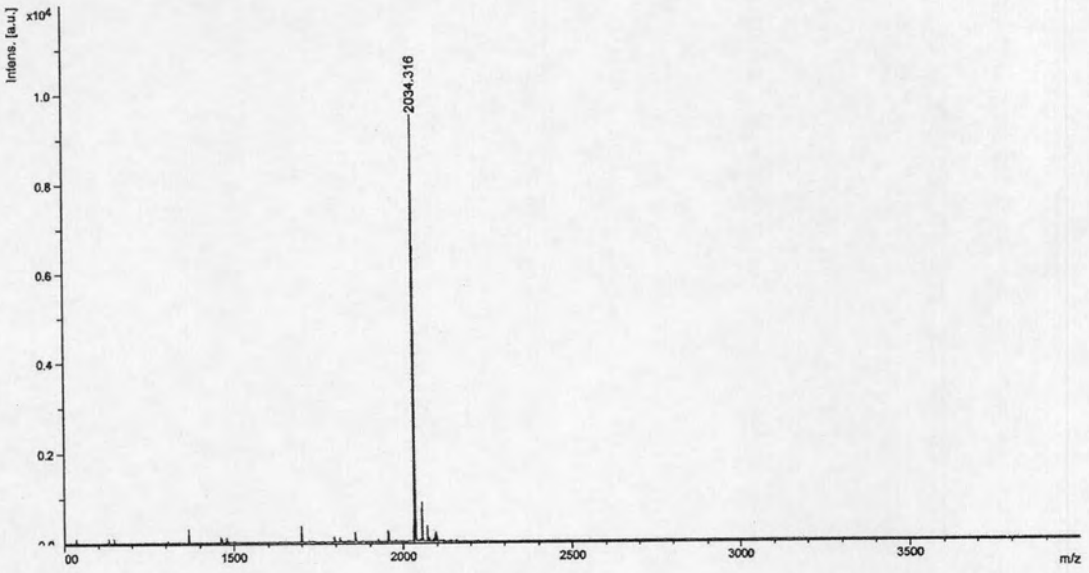

Figure C-5 : MALDI-TOF mass spectrum of *cis*-D/L-APC Fmoc-T_5-LysNH_2 (**P5**)

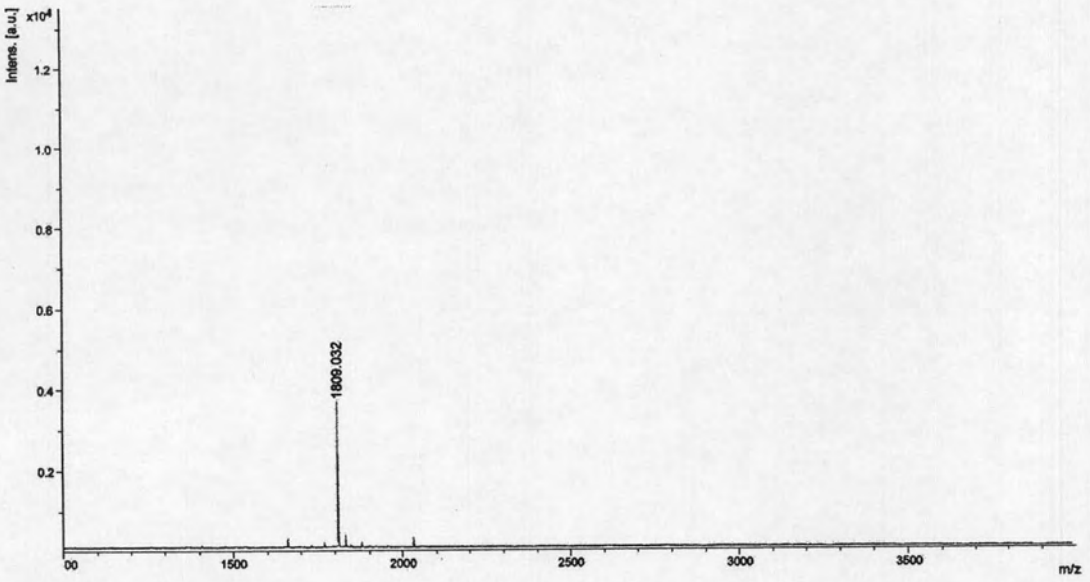

Figure C-6 : MALDI-TOF mass spectrum of *cis*-D/(1*S*,2*S*)-ACPC H-T_5-LysNH_2 (**P6**)

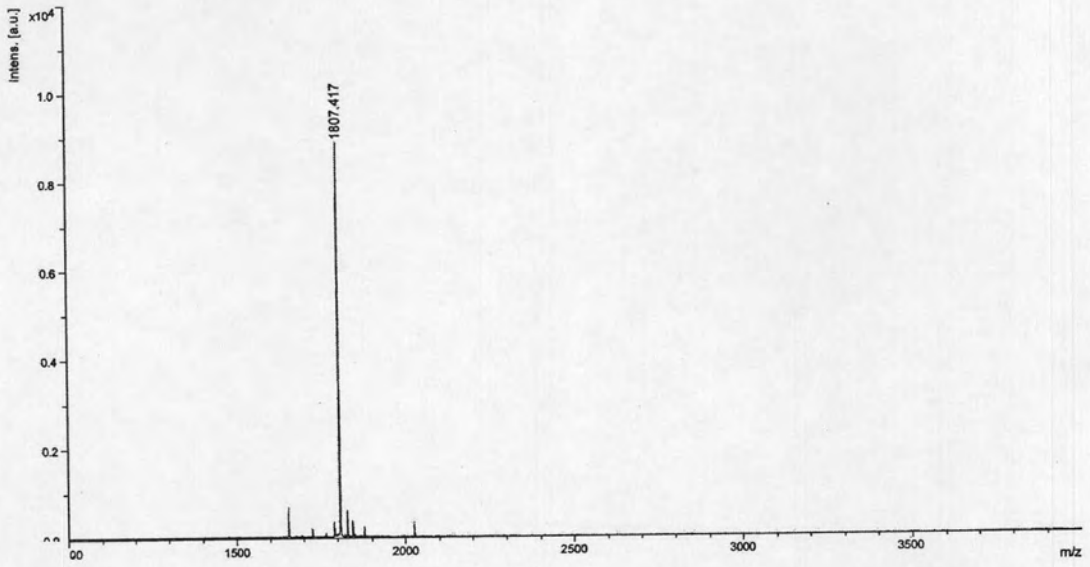

Figure C-7 : MALDI-TOF mass spectrum of *cis*-D/(1*R*,2*R*)-ACPC H-T_5-LysNH_2(**P7**)

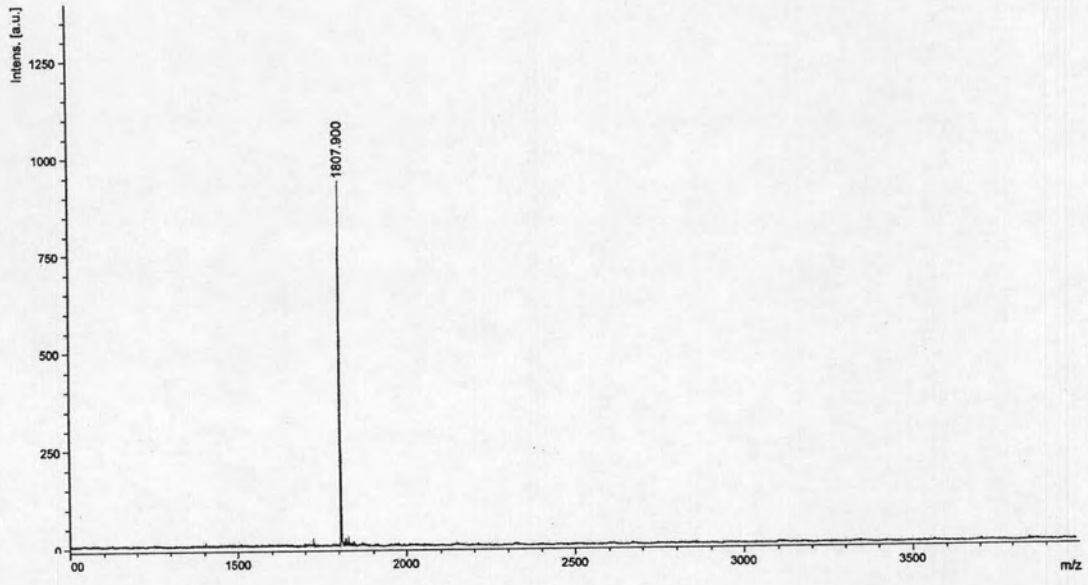

Figure C-8 : MALDI-TOF mass spectrum of *cis*-D/(1*S*,2*R*)-ACPC H-T_5-LysNH_2 (**P8**)

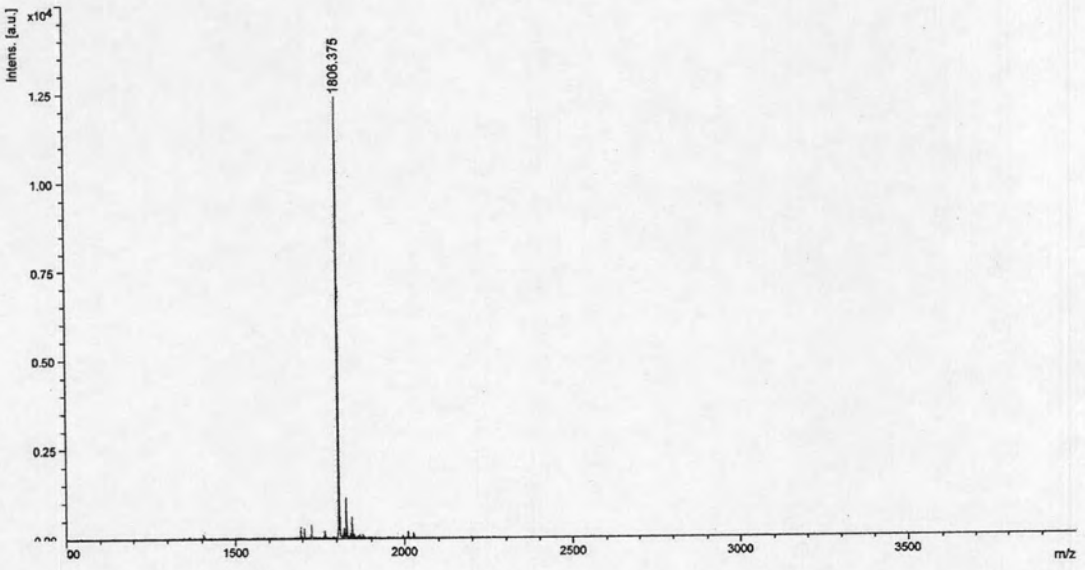

Figure C-9 : MALDI-TOF mass spectrum of *cis*-D/(1*R*,2*S*)-ACPC H-T_5-LysNH_2 (**P9**)

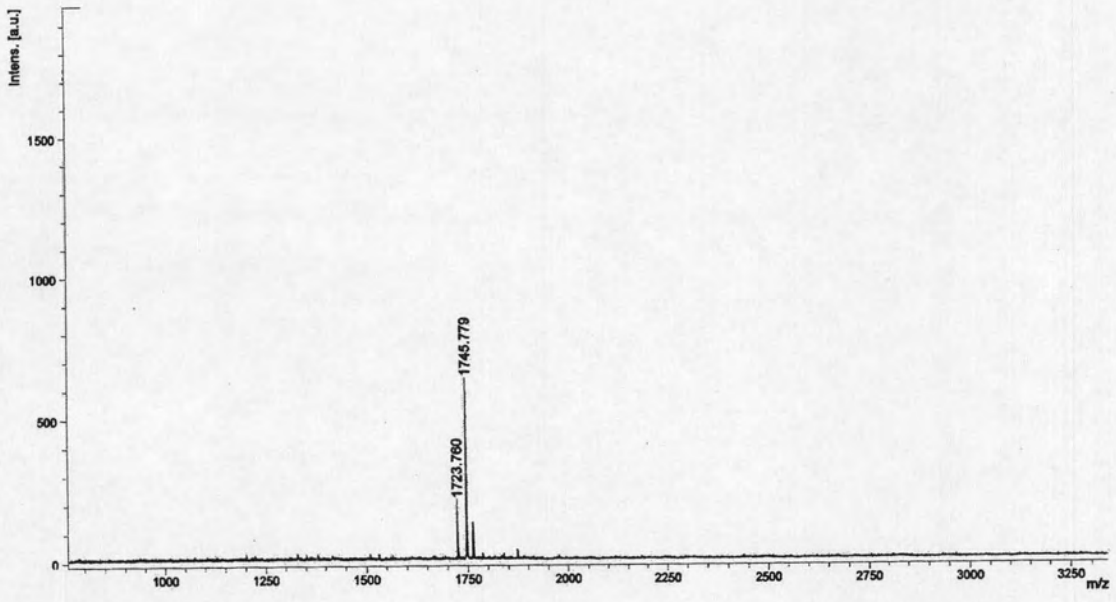

Figure C-10 : MALDI-TOF mass spectrum of *cis*-D/N-Spacer Ac-T_5-LysNH_2 (**P10**)

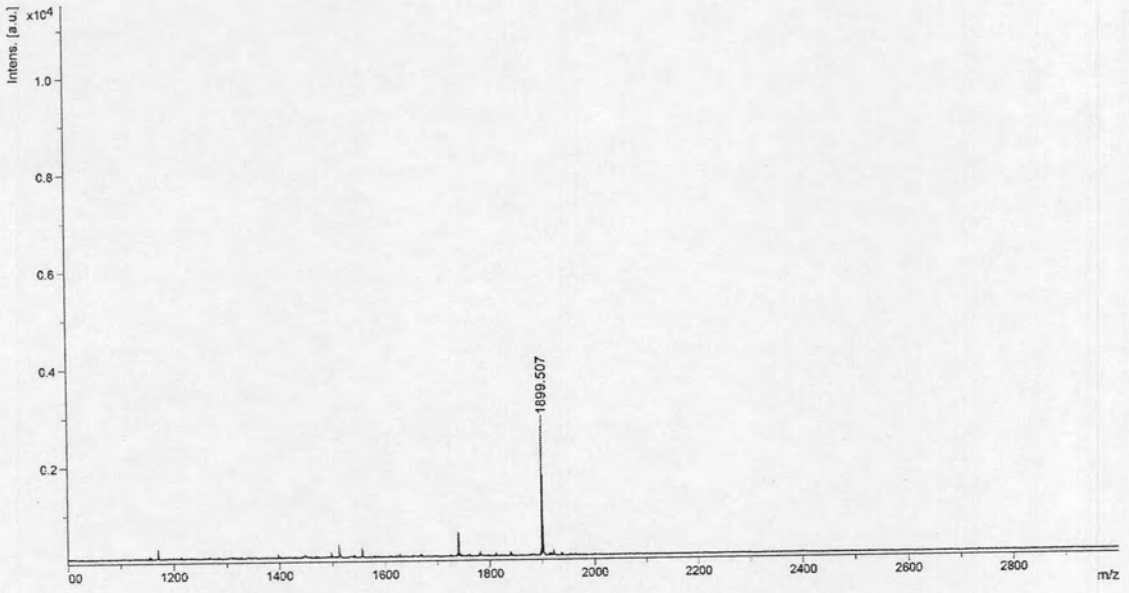

Figure C-11 : MALDI-TOF mass spectrum of *cis*-D/D-APC Ac-A_5-LysNH_2 (**P12**)

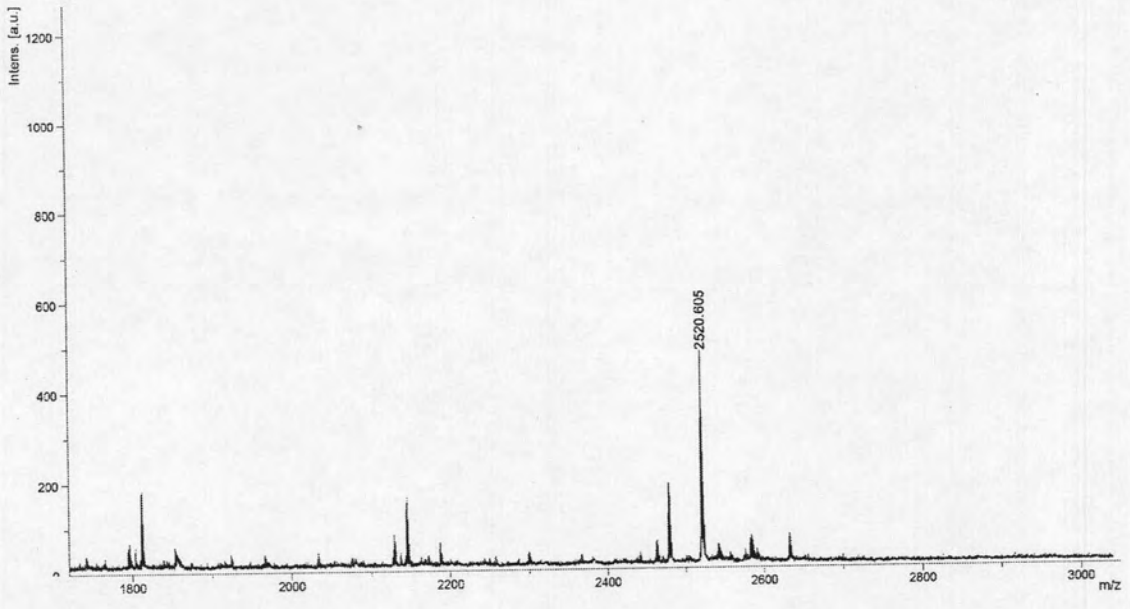

Figure C-12 : MALDI-TOF mass spectrum of *cis*-D/D-APC Ac-T_7-LysNH_2 (**P13**)

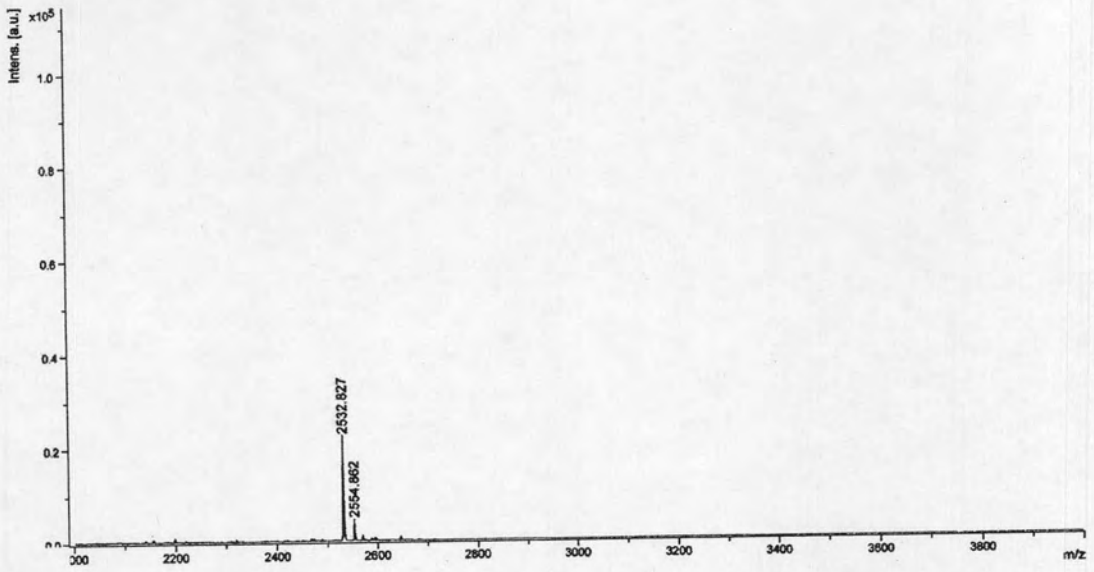

Figure C-13 : MALDI-TOF mass spectrum of *cis*-D/D-APC Ac-T_3AT_3-LysNH_2(**P14**)

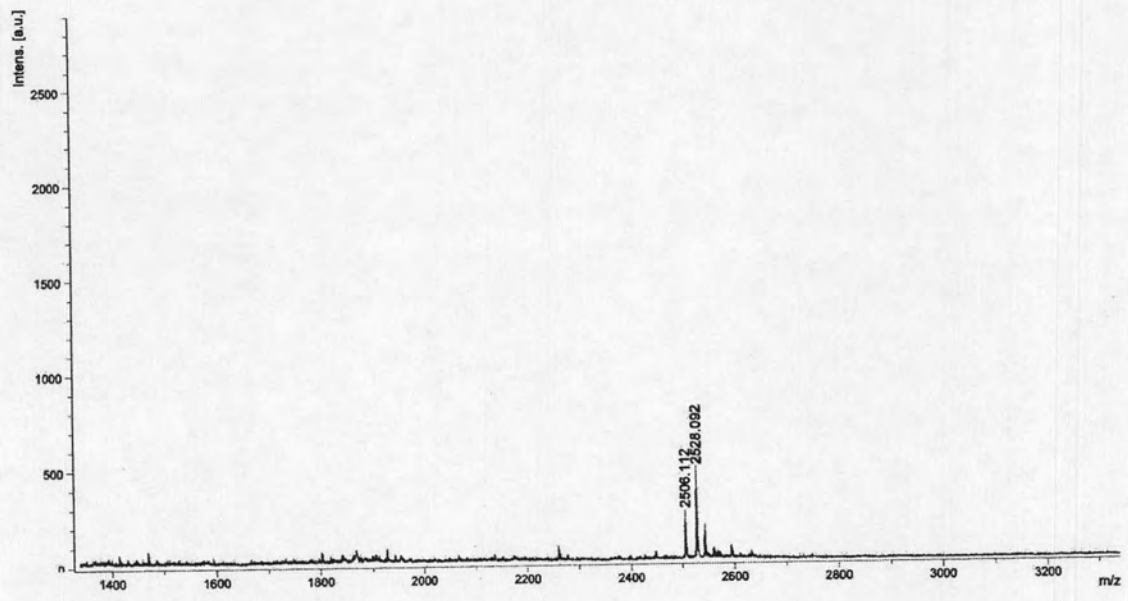

Figure C-14 : MALDI-TOF mass spectrum of *cis*-D/D-APC Ac-T_3CT_3-LysNH_2 (**P15**)

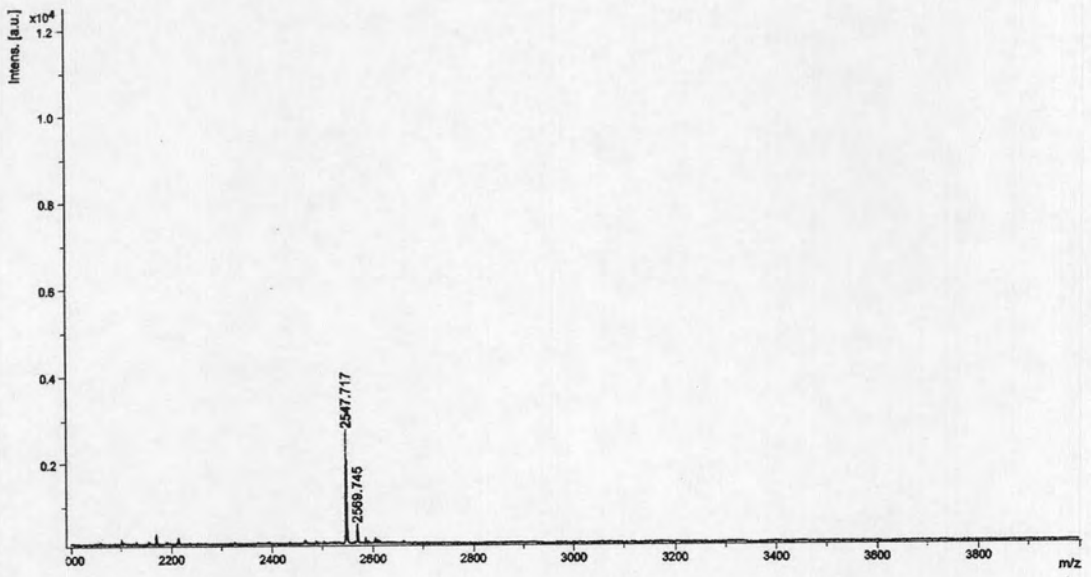

Figure C-15 : MALDI-TOF mass spectrum of *cis*-D/D-APC Ac-T_3GT_3-LysNH_2(**P16**)

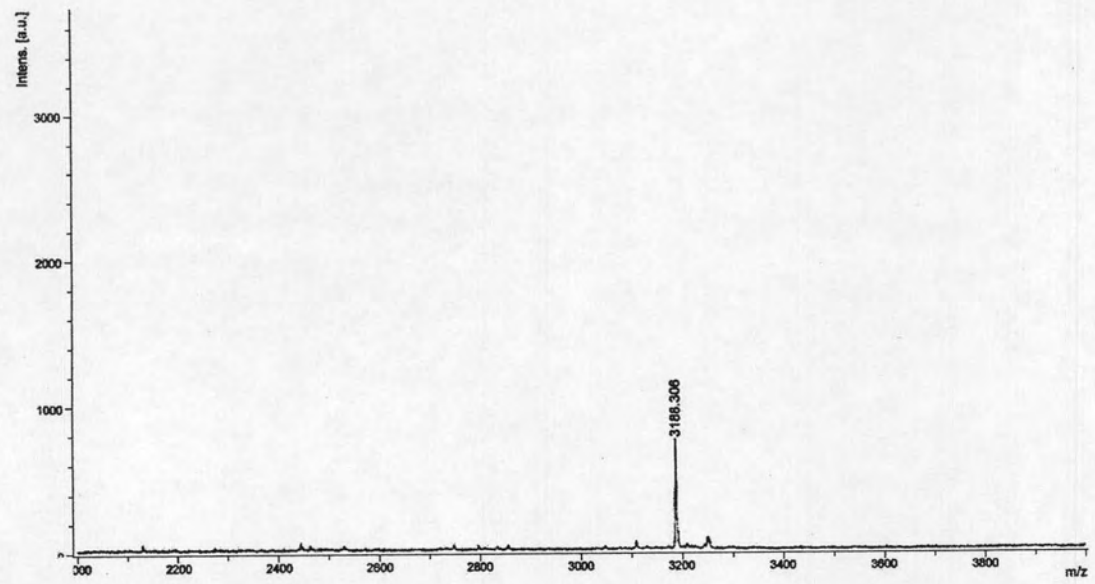

Figure C-16 : MALDI-TOF mass spectrum of *cis*-D/D-APC Ac-T_9-LysNH_2 (**P17**)

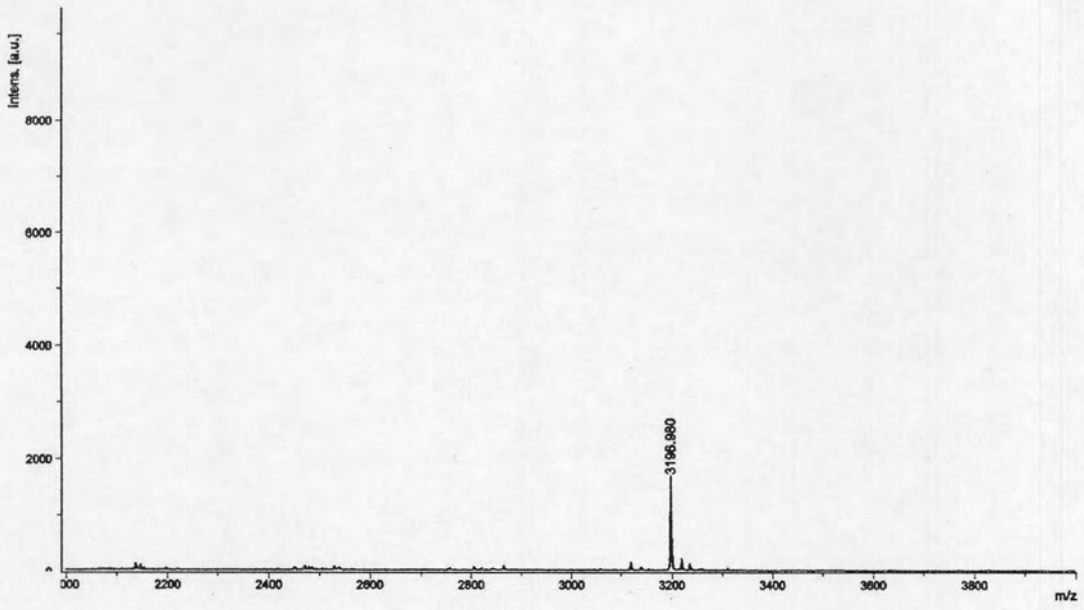

Figure C-17 : MALDI-TOF mass spectrum of *cis*-D/D-APC Ac-T_4AT_4-LysNH_2(**P18**)

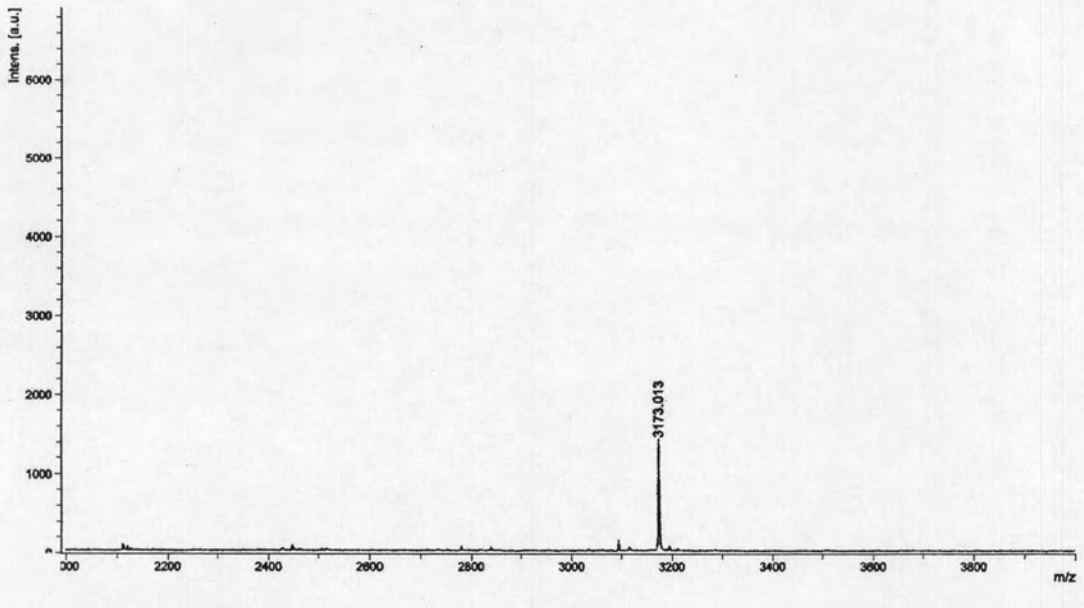

Figure C-18 : MALDI-TOF mass spectrum of *cis*-D/D-APC Ac-T_4CT_4-LysNH_2 (**P19**)

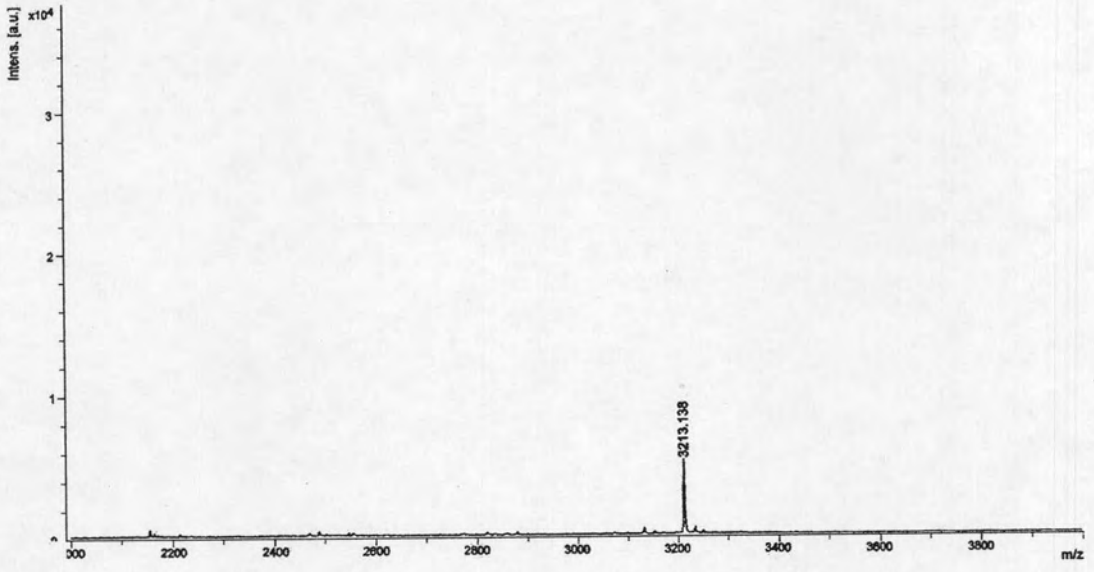

Figure C-19 : MALDI-TOF mass spectrum of *cis*-D/D-APC Ac-T_4GT_4-LysNH_2(**P20**)

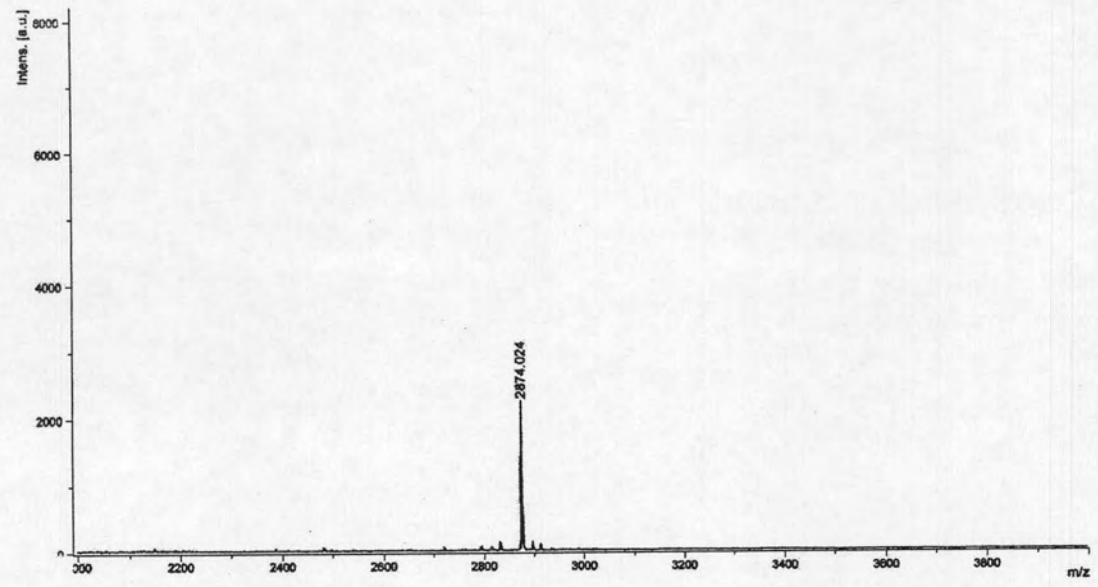

Figure C-20 : MALDI-TOF mass spectrum of *cis*-D/D-APC Ac-T_4ATAT-LysNH_2 (**P21**)

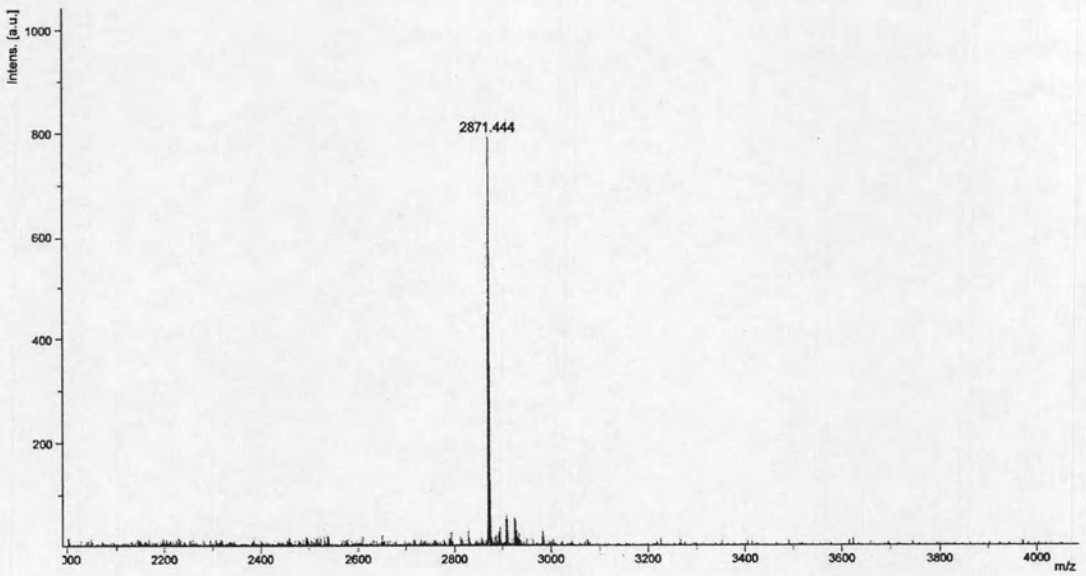

Figure C-21 : MALDI-TOF mass spectrum of *cis*-D/D-APC Ac-TATAT$_4$-LysNH$_2$ (**P22**)

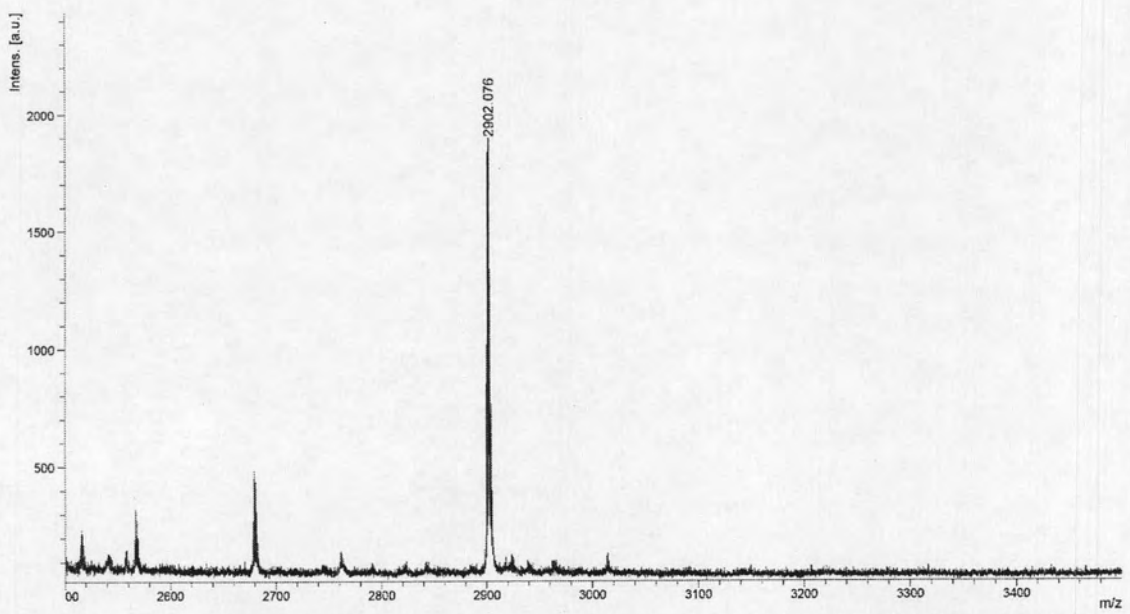

Figure C-22 : MALDI-TOF mass spectrum of *cis*-D/D-APC Ac-T$_4$ATA-Lys(FAM) NH$_2$ (**P23**)

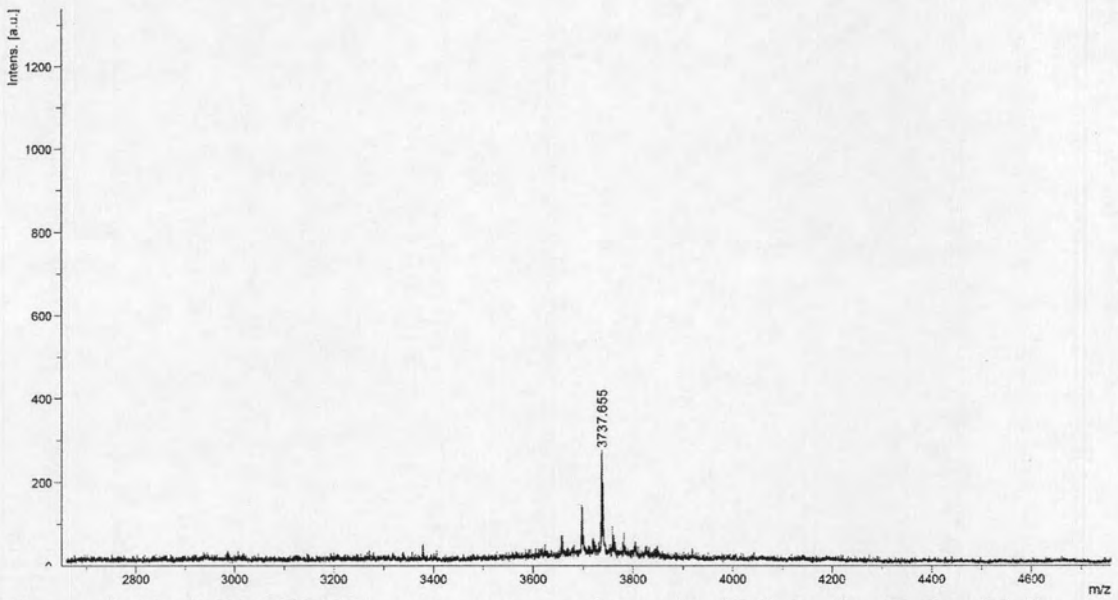

Figure C-23 : MALDI-TOF mass spectrum of *cis*-D/D-APC Ac-Ser-T_9-Lys(F)-Ser-NH_2 (**P24**)

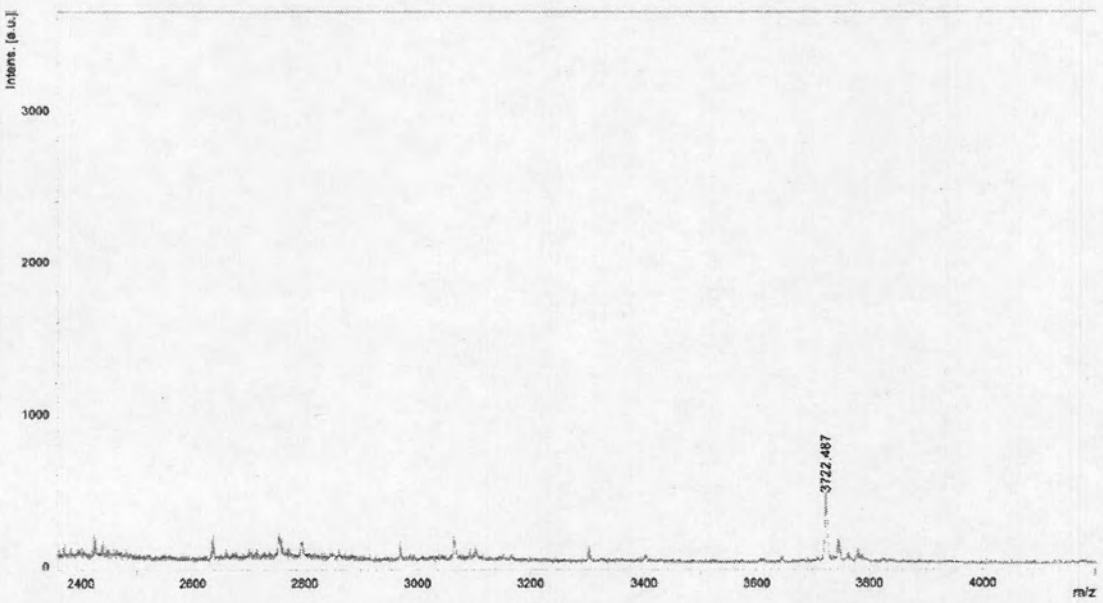

Figure C-24 : MALDI-TOF mass spectrum of *cis*-D/D-APC Ac-Ser- Lys(F)-T_9- Ser-NH_2 (**P25**)

APPENDIX D

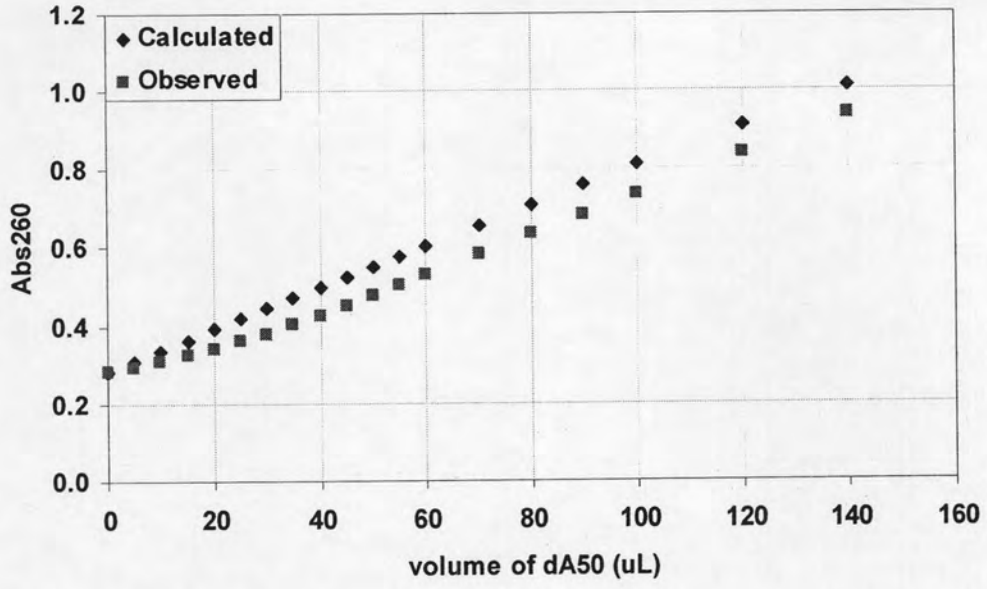

(a)

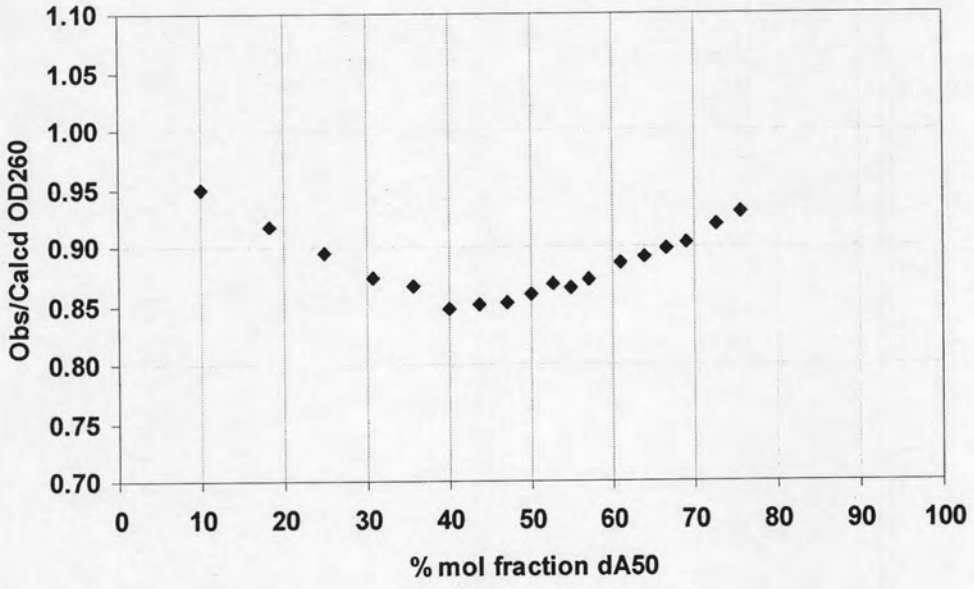

(b)

Figure D-1 UV titration plot of dA_{50} and *cis*-D/D-APC Fmoc-T_5-LysNH_2 (**P1**). (a) a plot between Abs_{260} and volume of dA_{50}. (b) a plot between the ratio of observed Abs_{260}/calculated Abs_{260} and % mole of dA_{50}.

Concentration of PNA: 765.5 μM (constant)

Concentration of DNA: 85.1 μM

Conditions: 10 mM sodium phosphate buffer, pH 7.0, 25 °C.

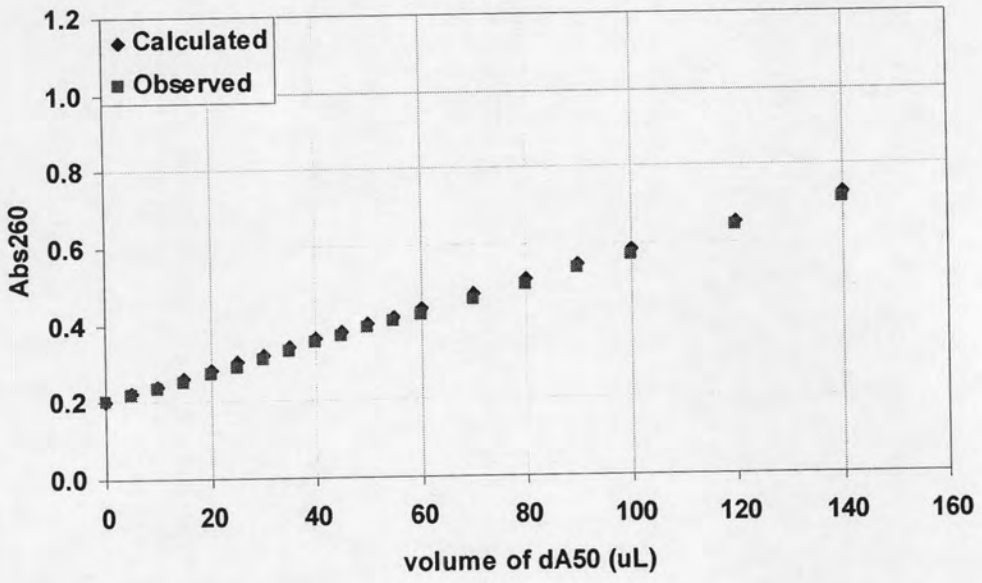

(a)

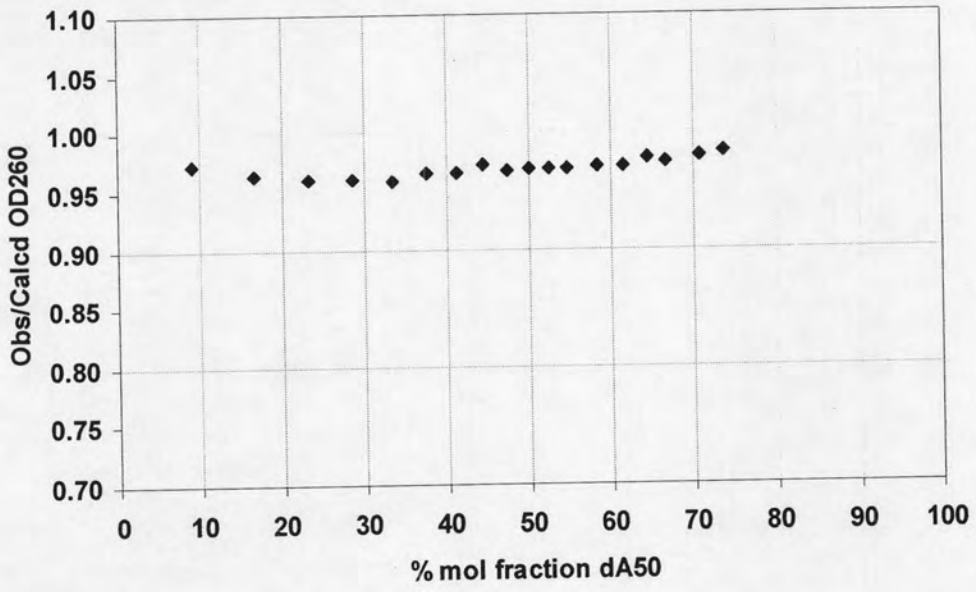

(b)

Figure D-2 UV titration plot of dA_{50} and *cis*-D/L-APC Fmoc-T_5-LysNH_2 (**P5**). (a) a plot between Abs_{260} and volume of dA_{50}. (b) a plot between the ratio of observed Abs_{260}/calculated Abs_{260} and % mole of dA_{50}.

Concentration of PNA: 1.02 mM (constant)

Concentration of DNA: 85.1 μM

Conditions: 10 mM sodium phosphate buffer, pH 7.0, 25 °C.

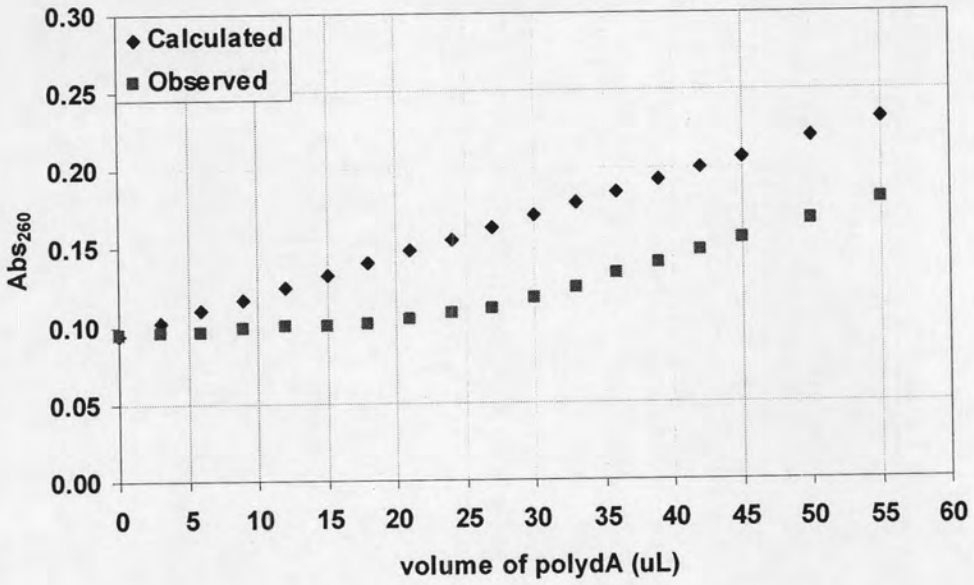

(a)

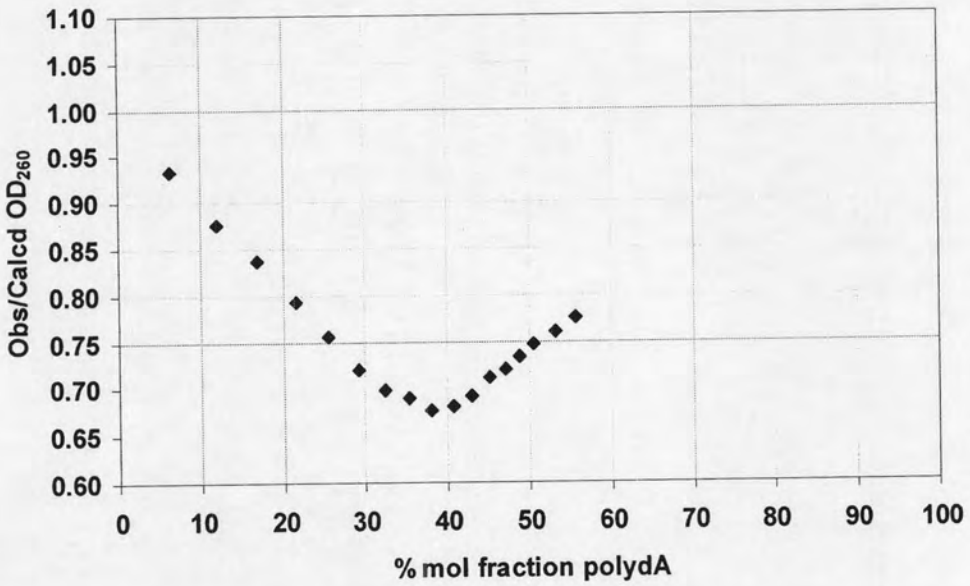

(b)

Figure D-3 UV titration plot of polydA and *cis*-D/(1*S*,2*S*)-ACPC H-T_{10}-LysNH_2 (**P26**). (a) a plot between Abs_{260} and volume of polydA. (b) a plot between the ratio of observed Abs_{260}/calculated Abs_{260} and % mole of polydA.

Concentration of PNA: 2.41 mM (constant)

Concentration of DNA: 85.1 μM

Conditions: 10 mM sodium phosphate buffer, pH 7.0, 25 °C.

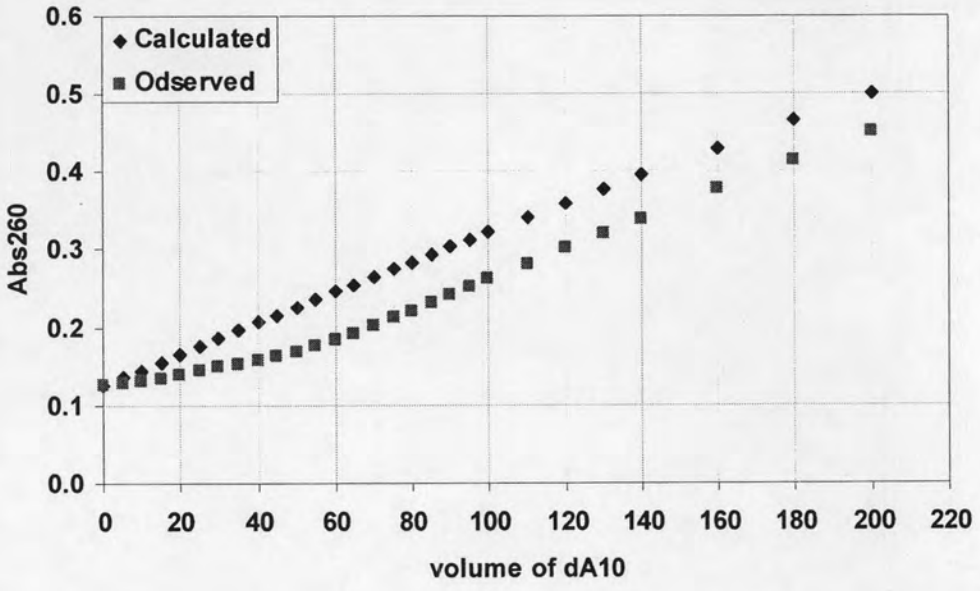

(a)

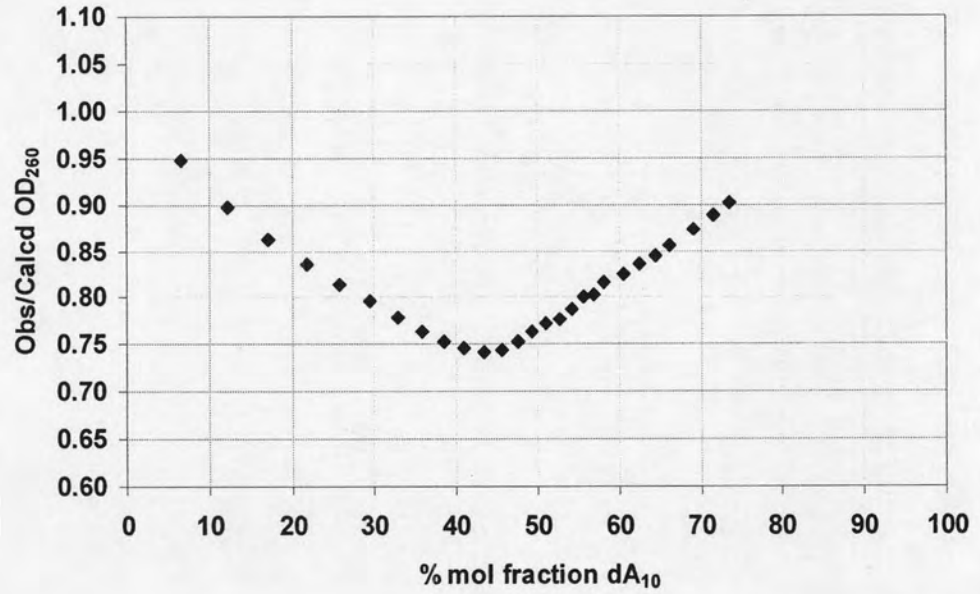

(b)

Figure D-4 UV titration plot of dA_{10} and *cis*-D/(1*S*,2*S*)-ACPC H-T_{10}-LysNH_2 (**P26**). (a) a plot between Abs_{260} and volume of dA_{10}. (b) a plot between the ratio of observed Abs_{260}/calculated Abs_{260} and % mole of dA_{10}.

Concentration of PNA: 2.41 mM (constant)

Concentration of DNA: 85.1 μM

Conditions: 10 mM sodium phosphate buffer, pH 7.0, 25 °C.

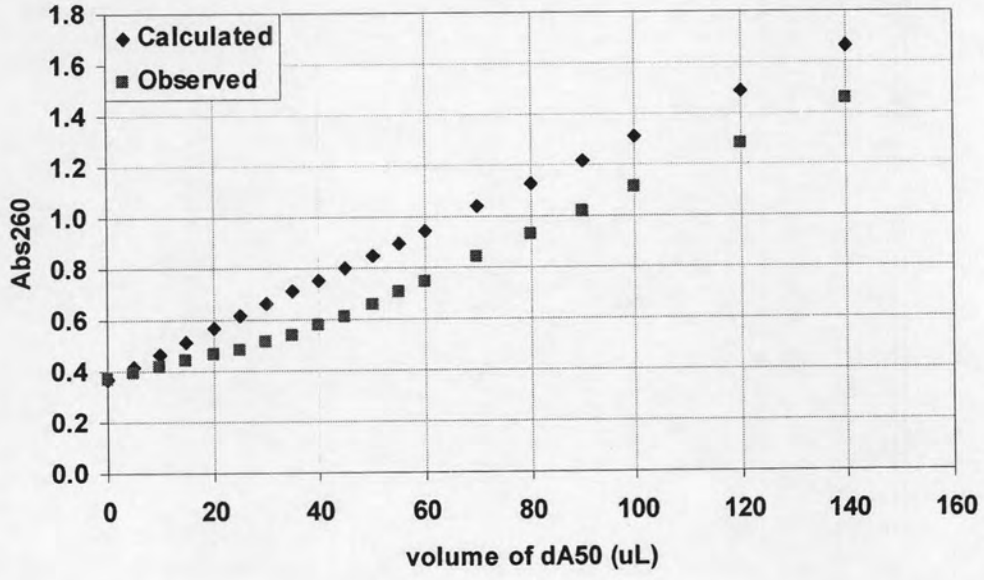

(a)

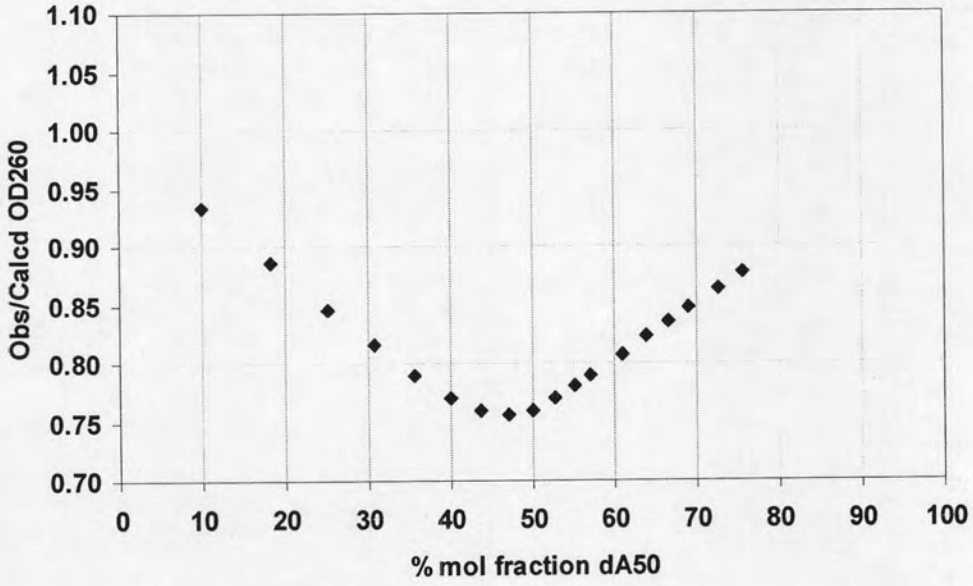

(b)

Figure D-5 UV titration plot of dA_{50} and *cis*-D/(1*S*,2*S*)-ACPC H-T_5-LysNH_2 (**P7**). (a) a plot between Abs_{260} and volume of dA_{50}. (b) a plot between the ratio of observed Abs_{260}/calculated Abs_{260} and % mole of dA_{50}.

Concentration of PNA: 2.41 mM (constant)

Concentration of DNA: 85.1 μM

Conditions: 10 mM sodium phosphate buffer, pH 7.0, 25 °C.

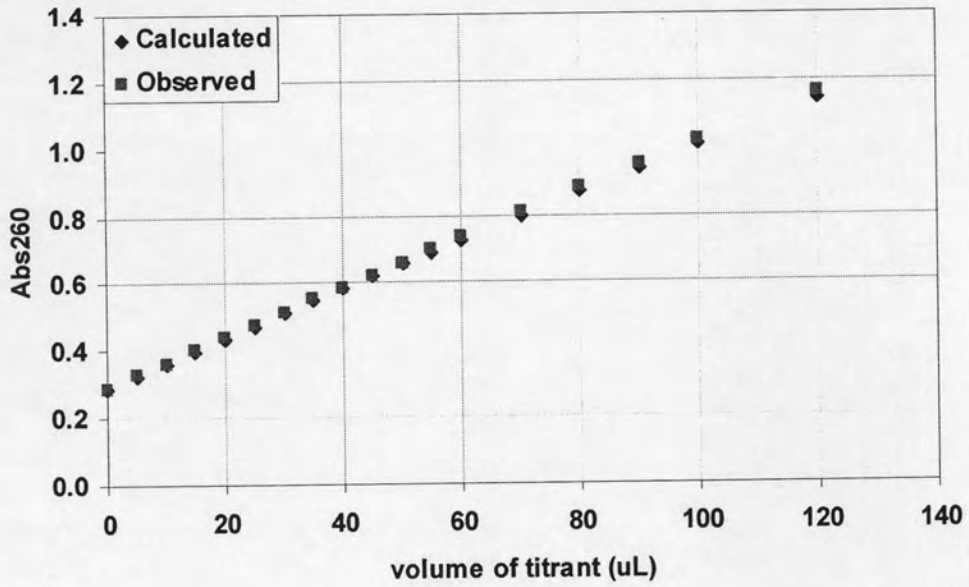

(a)

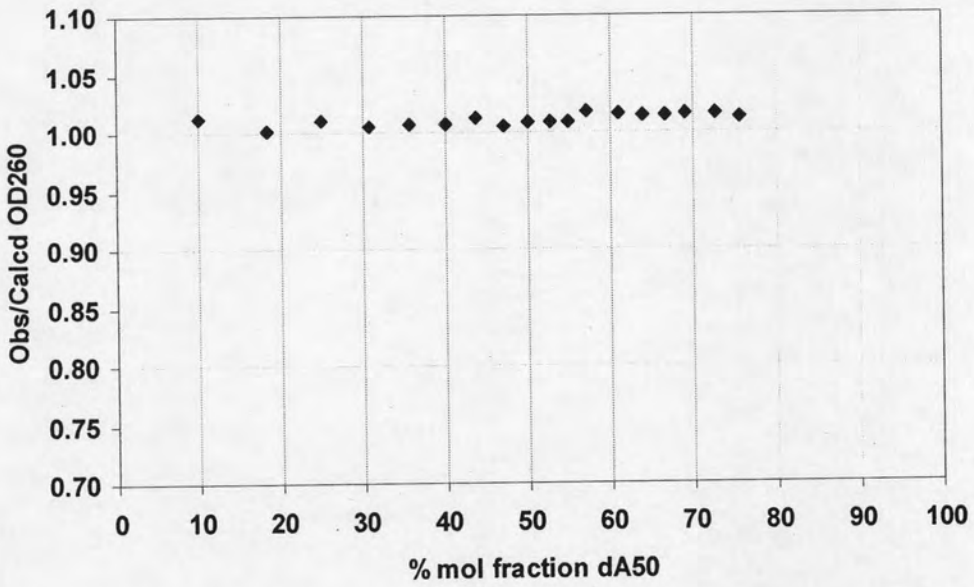

(b)

Figure D-6 UV titration plot of dA_{50} and *cis*-D/(1*R*,2*R*)-ACPC H-T_5-LysNH_2 (**P8**). (a) a plot between Abs_{260} and volume of dA_{50}. (b) a plot between the ratio of observed Abs_{260}/calculated Abs_{260} and % mole of dA_{50}.

Concentration of PNA: 1.53 mM (constant)

Concentration of DNA: 85.1 μM

Conditions: 10 mM sodium phosphate buffer, pH 7.0, 25 °C.

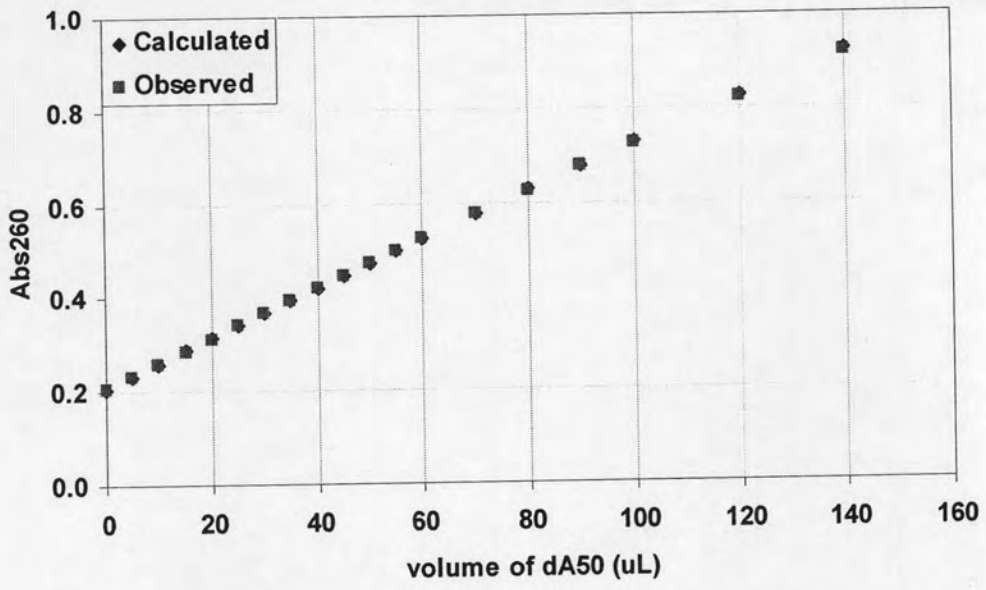

(a)

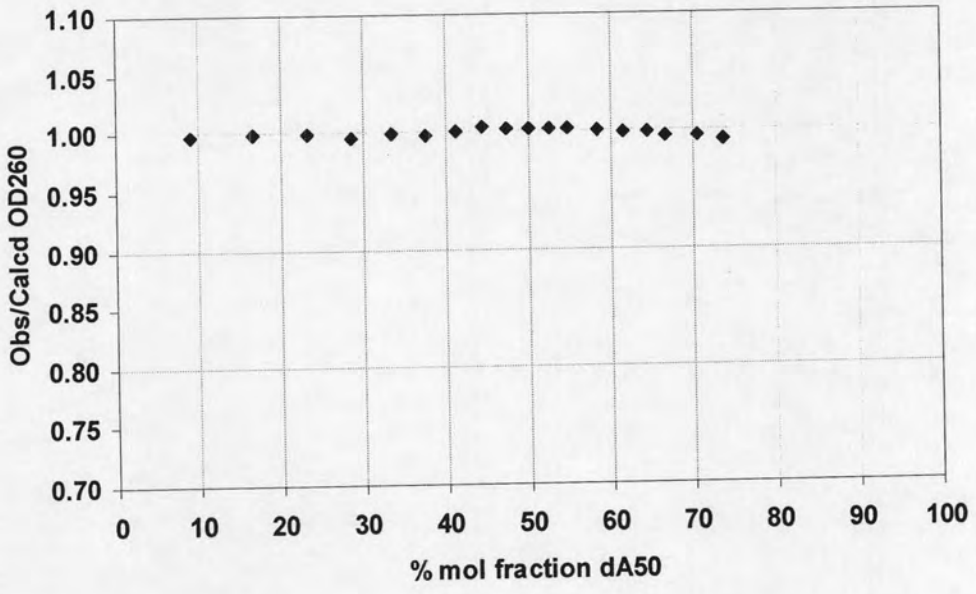

(b)

Figure D-7 UV titration plot of dA_{50} and *cis*-D/(1*S*,2*R*)-ACPC H-T_5-LysNH_2 (**P9**). (a) a plot between Abs_{260} and volume of dA_{50}. (b) a plot between the ratio of observed Abs_{260}/calculated Abs_{260} and % mole of dA_{50}.

Concentration of PNA: 1.34 mM (constant)

Concentration of DNA: 85.1 μM

Conditions: 10 mM sodium phosphate buffer, pH 7.0, 25 °C.

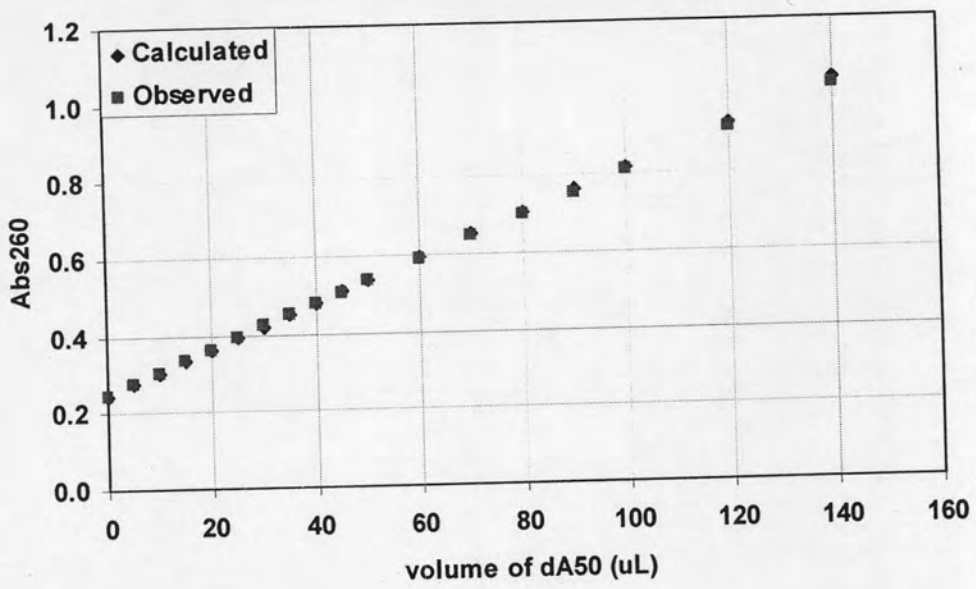

(a)

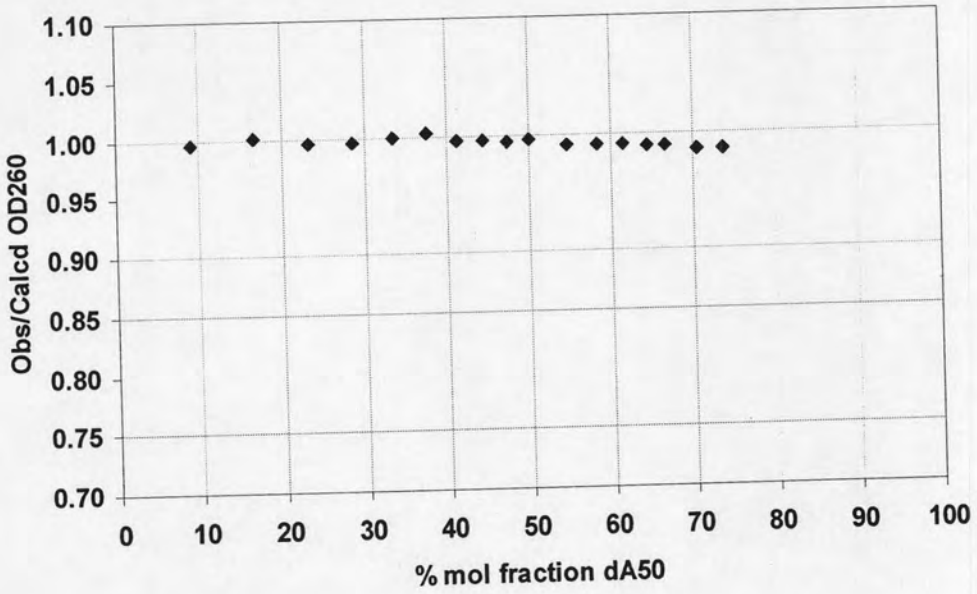

(b)

Figure D-8 UV titration plot of dA_{50} and *cis*-D/(1*R*,2*S*)-ACPC H-T_5-LysNH_2 (**P10**). (a) a plot between Abs_{260} and volume of dA_{50}. (b) a plot between the ratio of observed Abs_{260}/calculated Abs_{260} and % mole of dA_{50}.

Concentration of PNA: 3.61 mM (constant)

Concentration of DNA: 85.1 μM

Conditions: 10 mM sodium phosphate buffer, pH 7.0, 25 °C.

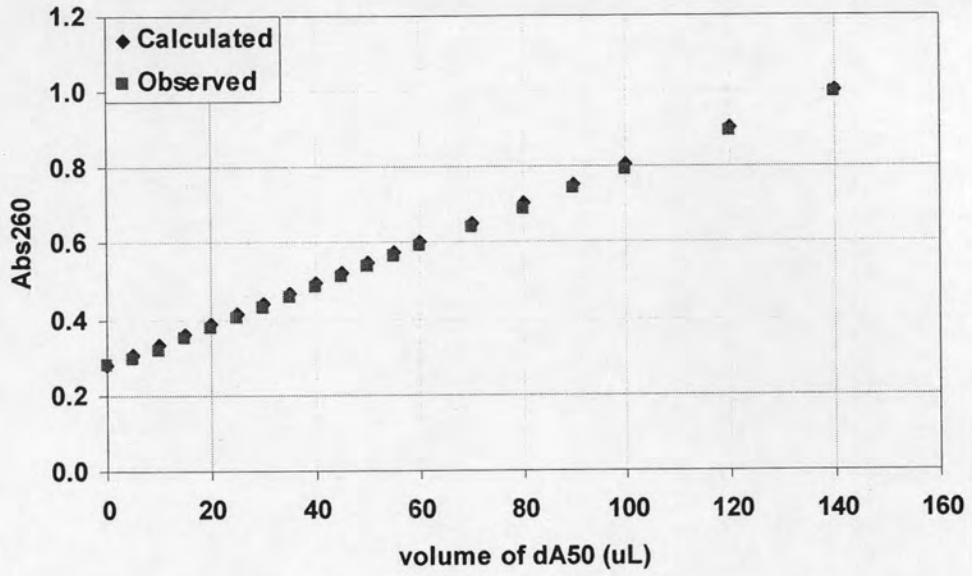

(a)

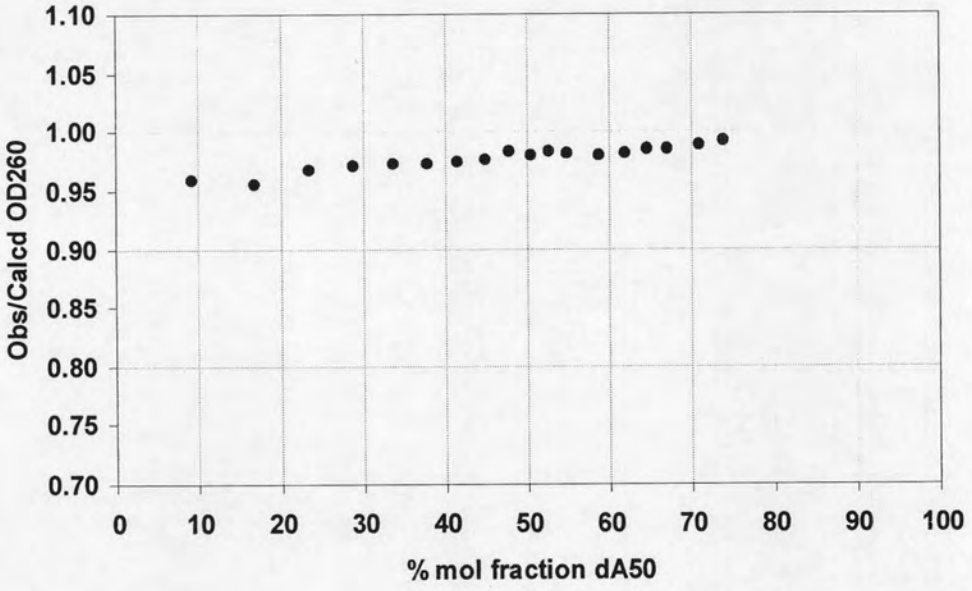

(b)

Figure D-9 UV titration plot of dA_{50} and *trans*-D/D-APC Fmoc-T_5-LysNH_2 (**P2**). (a) a plot between Abs_{260} and volume of dA_{50}. (b) a plot between the ratio of observed Abs_{260}/calculated Abs_{260} and % mole of dA_{50}.

Concentration of PNA: 893.4 μM (constant)

Concentration of DNA: 85.1 μM

Conditions: 10 mM sodium phosphate buffer, pH 7.0, 25 °C.

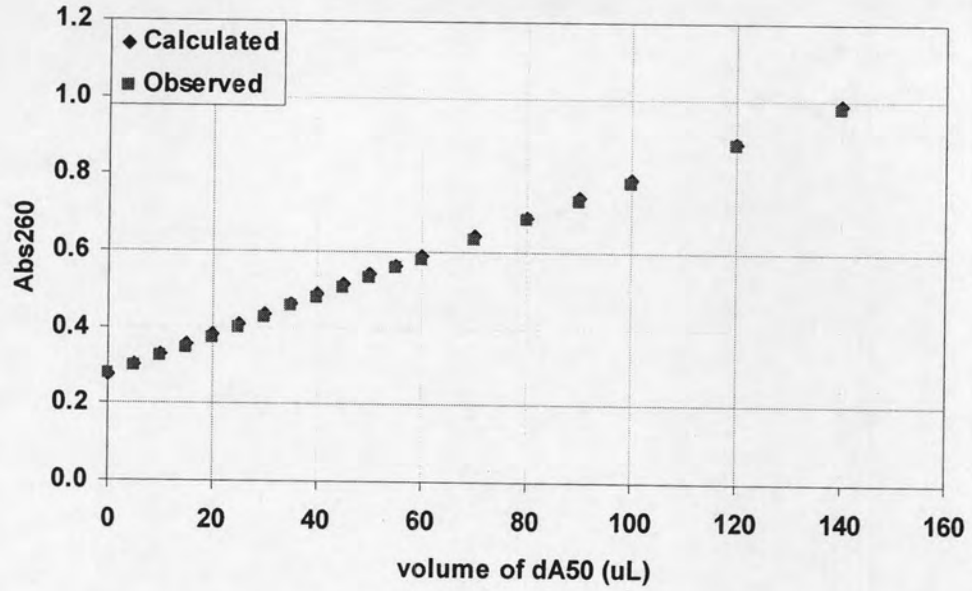

(a)

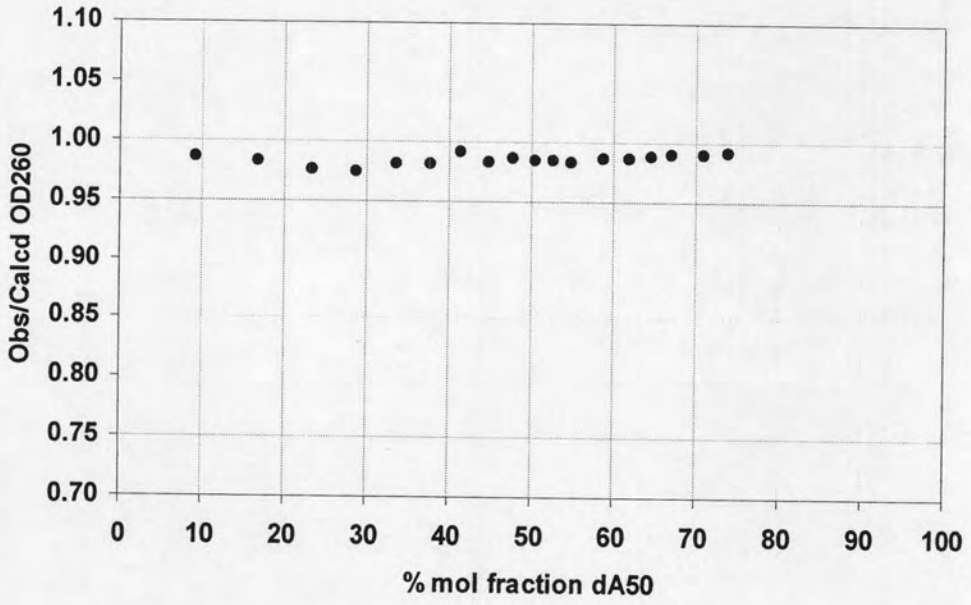

(b)

Figure D-10 UV titration plot of dA_{50} and *trans*-L/D-APC Fmoc-T_5-LysNH_2 (**P3**). (a) a plot between Abs_{260} and volume of dA_{50}. (b) a plot between the ratio of observed Abs_{260}/calculated Abs_{260} and % mole of dA_{50}.

Concentration of PNA: 862.7 μM (constant)

Concentration of DNA: 85.1 μM

Conditions: 10 mM sodium phosphate buffer, pH 7.0, 25 °C.

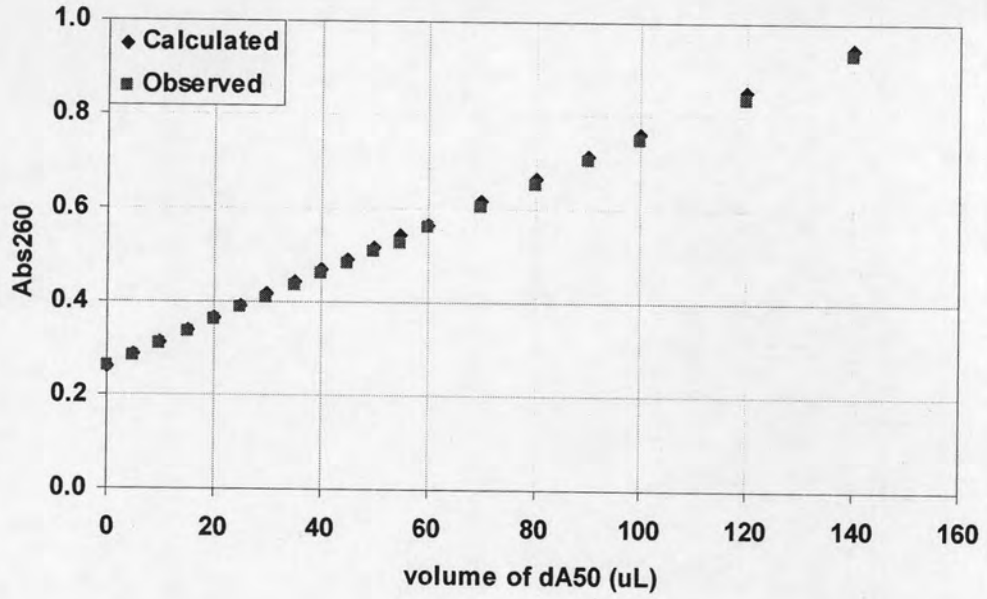

(a)

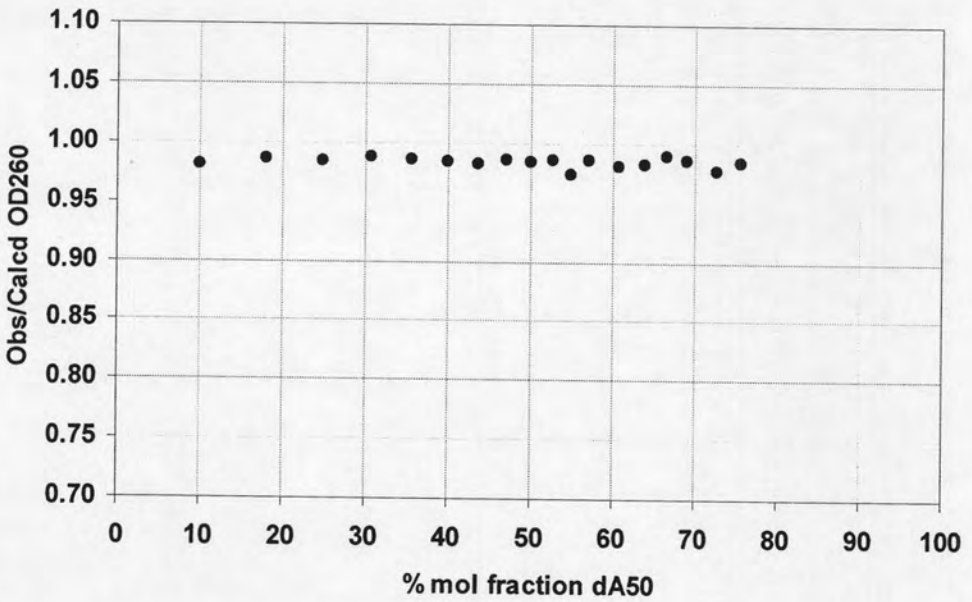

(b)

Figure D-11 UV titration plot of dA_{50} and *cis*-L/D-APC Fmoc-T_5-LysNH_2 (**P4**). (a) a plot between Abs_{260} and volume of dA_{50}. (b) a plot between the ratio of observed Abs_{260}/calculated Abs_{260} and % mole of dA_{50}.

Concentration of PNA: 2.08 mM (constant)

Concentration of DNA: 85.1 μM

Conditions: 10 mM sodium phosphate buffer, pH 7.0, 25 °C.

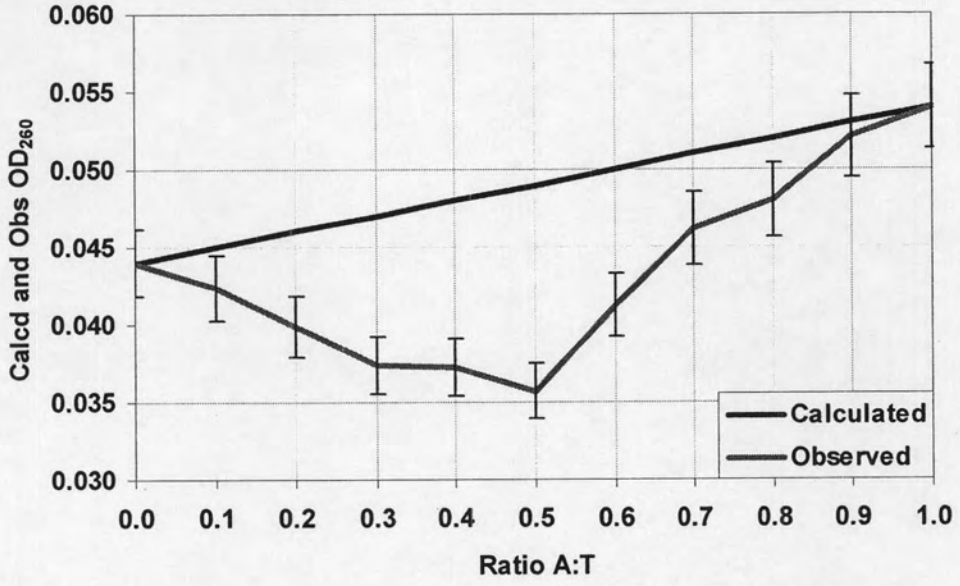

Figure D-12 Job plot of dA_{50} and *cis*-D/(1*S*,2*S*)-ACPC H-T_{10}-LysNH_2 (**P26**). [PNA+DNA] = 1.1 μM of each ratio, Conditions: 10 mM sodium phosphate buffer, pH 7.0, 25 °C.

APPENDIX E

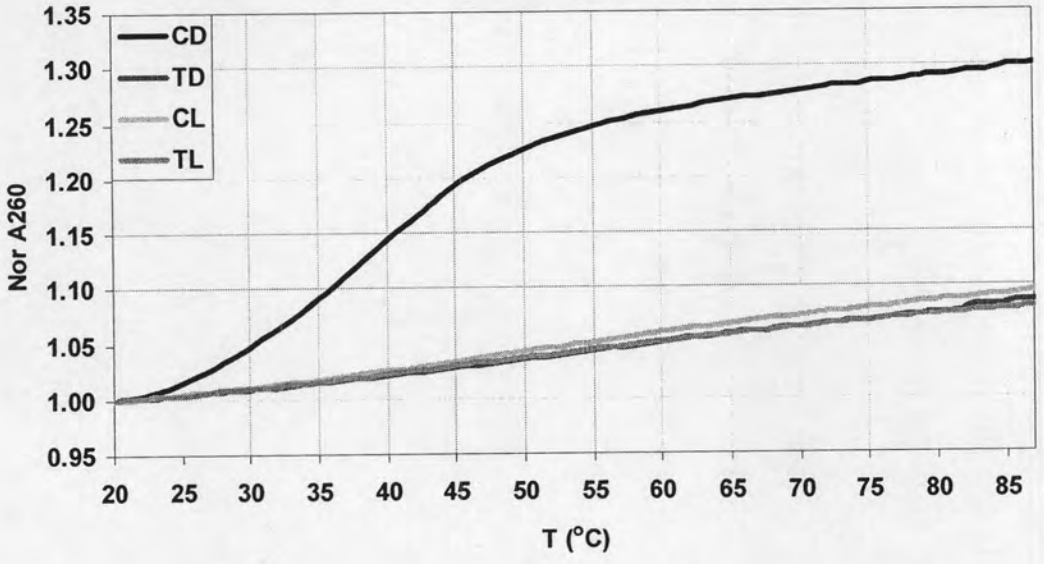

Figure E-1 T_m curves of PNA *cis*-D,*trans*-D,*trans*-L,*cis*-L/D-APC Fmoc-TTTTT-$LysNH_2$ with dA_{50}: Condition PNA:DNA = 1:1, [PNA] = 1 μM, 10 mM sodium phosphate buffer, pH 7.0, heating rate 1.0 °C/min.

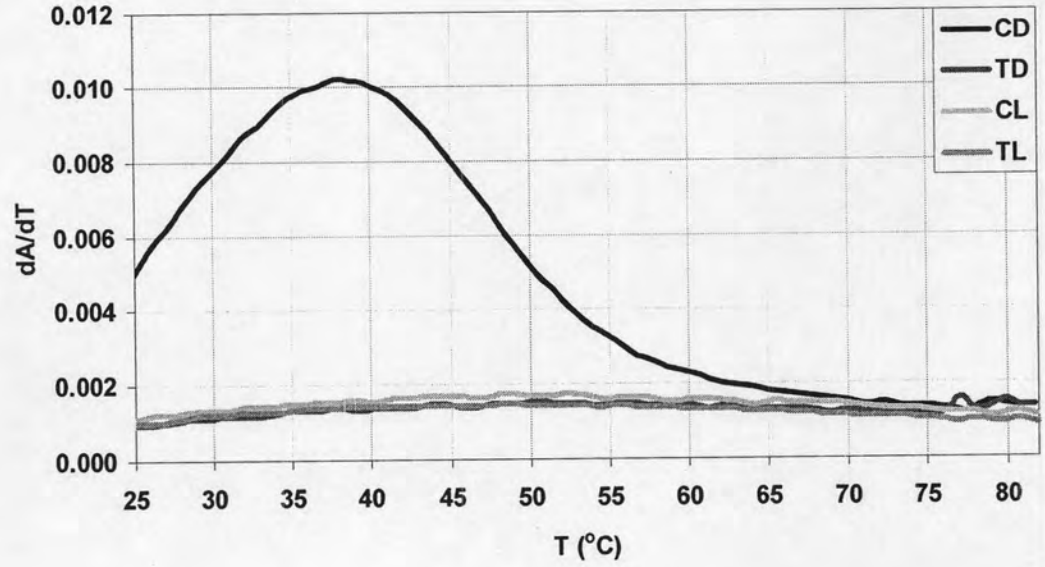

Figure E-2 First-derivative normalized UV-T_m plots between PNA *cis*-D,*trans*-D,*trans*-L,*cis*-L/D-APC Fmoc-TTTTT-$LysNH_2$ with dA_{50}: Condition PNA:DNA = 1:1, [PNA] = 1 μM, 10 mM sodium phosphate buffer, pH 7.0, heating rate 1.0 °C/min.

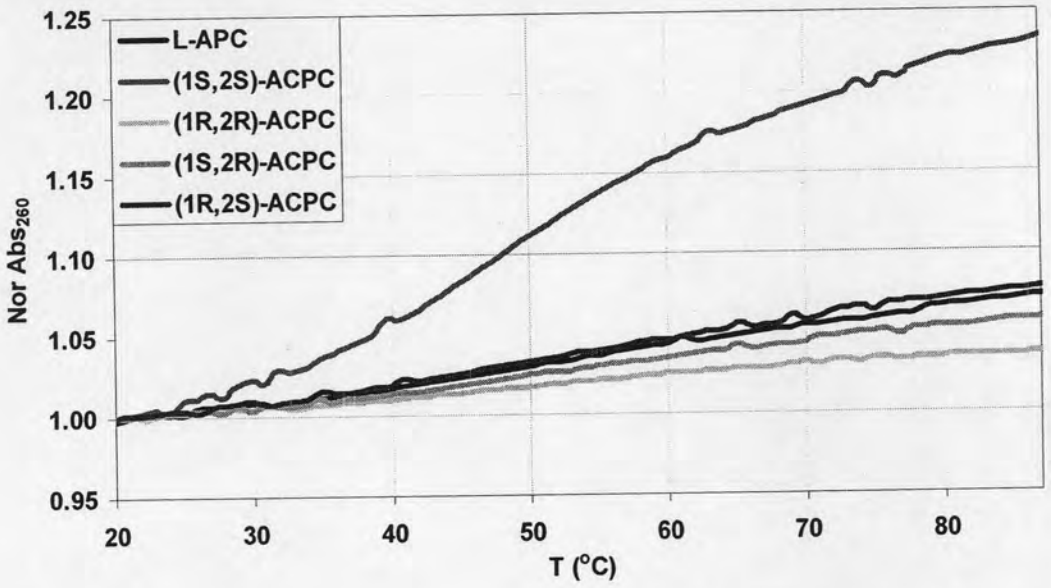

Figure E-3 T_m curves of PNA *cis*-D/L-APC Fmoc-T_5-LysNH_2 and *cis*-D/(1*S*,2*S*), (1*R*,2*R*), (1*S*,2*R*), (1*R*,2*S*)-ACPC H-T_5-LysNH_2 with dA_{50}: Condition PNA:DNA = 1:1, [PNA] = 1 μM, 10 mM sodium phosphate buffer, pH 7.0, heating rate 1.0 °C/min.

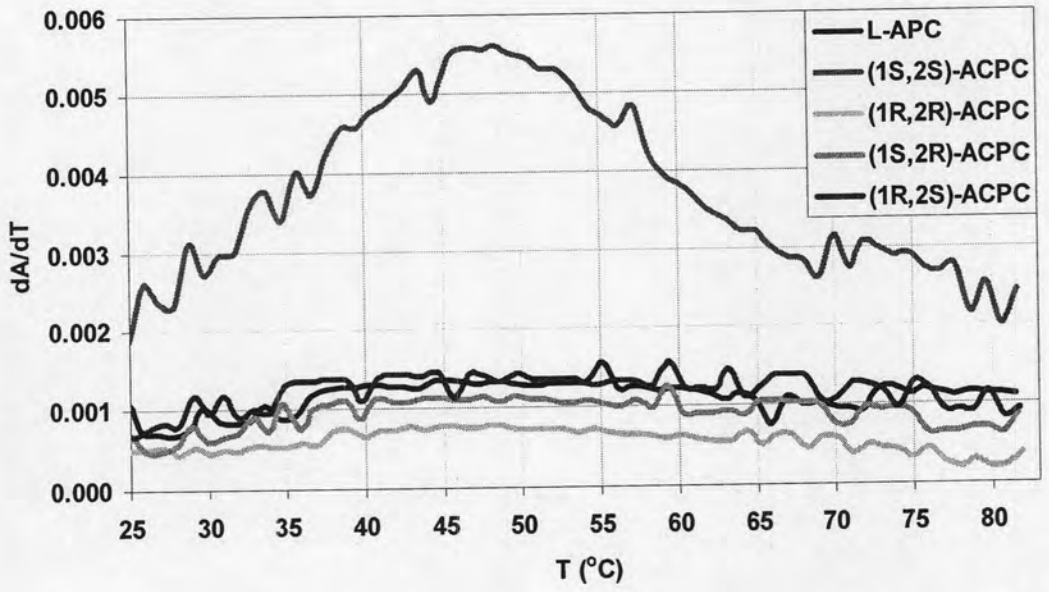

Figure E-4 First-derivative normalized UV-T_m plots between PNA *cis*-D/L-APC Fmoc-T_5-LysNH_2 and *cis*-D/(1*S*,2*S*), (1*R*,2*R*), (1*S*,2*R*), (1*R*,2*S*)-ACPC H-T_5-LysNH_2 with dA_{50}: Condition PNA:DNA = 1:1, [PNA] = 1 μM, 10 mM sodium phosphate buffer, pH 7.0, heating rate 1.0 °C/min.

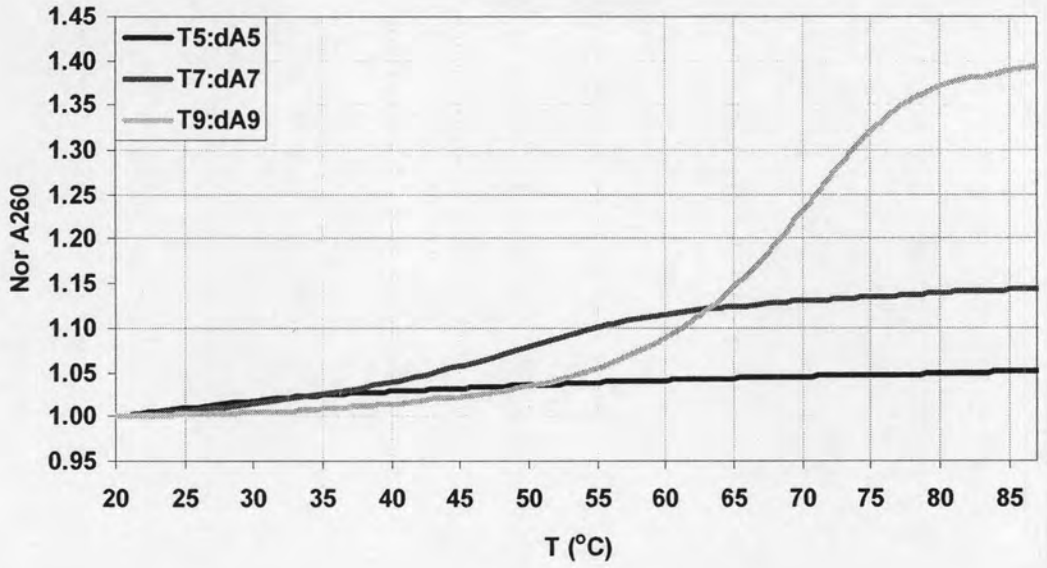

Figure E-5 T_m curves of PNA *cis*-D/D-APC Ac-T5-LysNH$_2$, Ac-T$_7$-LysNH$_2$ and Ac-T$_9$-LysNH$_2$ with dA$_5$, dA$_7$ and dA$_9$: Condition PNA:DNA = 1:1, [PNA] = 1 μM, 10 mM sodium phosphate buffer, pH 7.0, heating rate 1.0 °C/min.

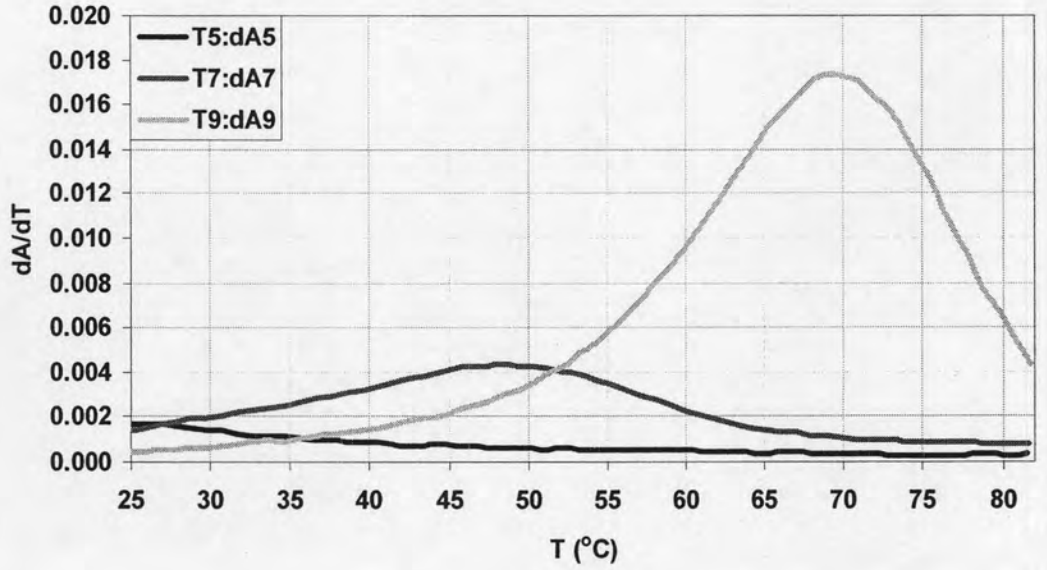

Figure E-6 First-derivative normalized UV-T_m plots between PNA *cis*-D/D-APC Ac-T$_5$-LysNH$_2$, Ac-T$_7$-LysNH$_2$ and Ac-T$_9$-LysNH$_2$ with dA$_5$, dA$_7$ and dA$_9$: Condition PNA:DNA = 1:1, [PNA] = 1 μM, 10 mM sodium phosphate buffer, pH 7.0, heating rate 1.0 °C/min.

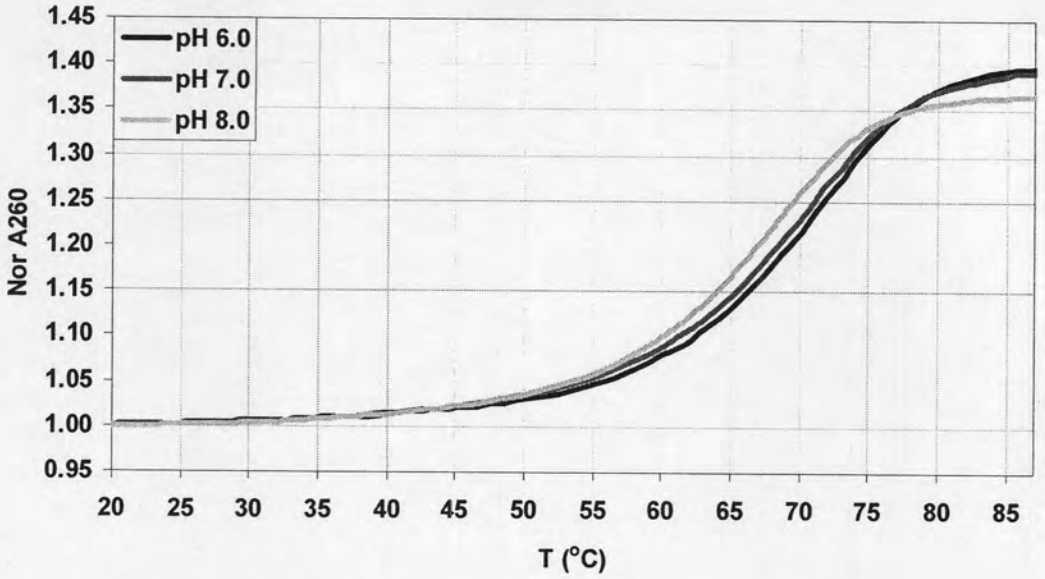

Figure E-7 T_m curves of PNA *cis*-D/D-APC Ac-T_9-LysNH_2 with dA_9 at pH 6.0, 7.0 and 8.0: Condition PNA:DNA = 1:1, [PNA] = 1 μM, 10 mM sodium phosphate buffer, heating rate 1.0 °C/min.

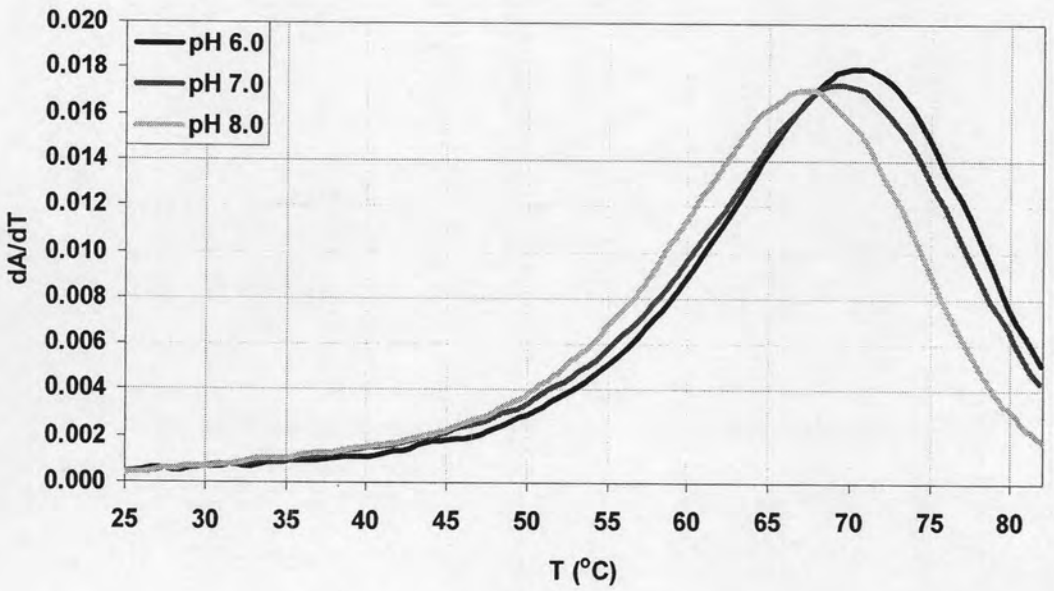

Figure E-8 First-derivative normalized UV-T_m plots between PNA *cis*-D/D-APC Ac-T_9-LysNH_2 with dA_9 at pH 6.0, 7.0 and 8.0: Condition PNA:DNA = 1:1, [PNA] = 1 μM, 10 mM sodium phosphate buffer, heating rate 1.0 °C/min.

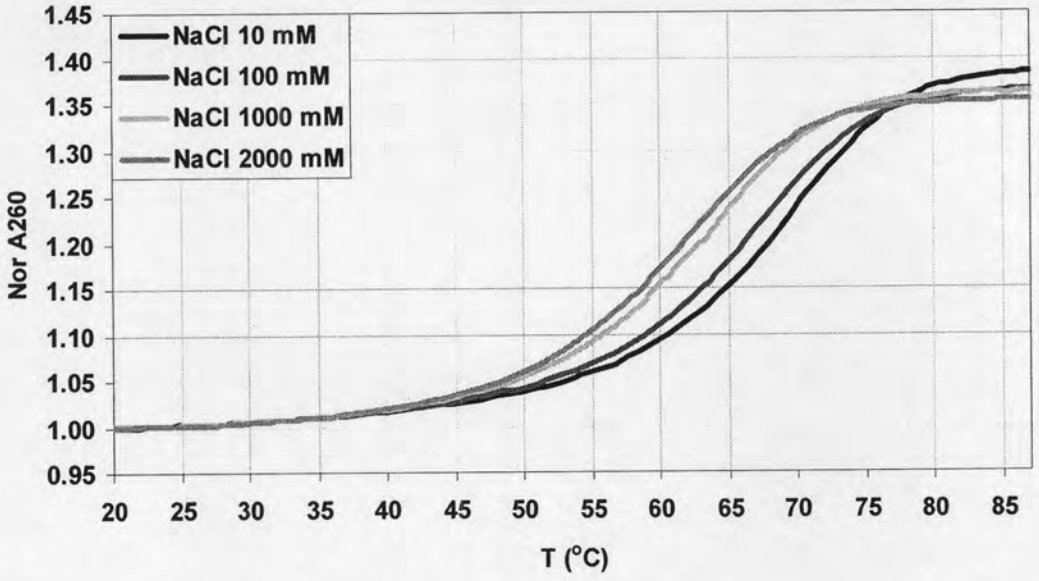

Figure E-9 T_m curves of PNA *cis*-D/D-APC Ac-T_9-LysNH_2 with dA_9 at various salt concentration: Condition PNA:DNA = 1:1, [PNA] = 1 μM, 10 mM sodium phosphate buffer, heating rate 1.0 °C/min.

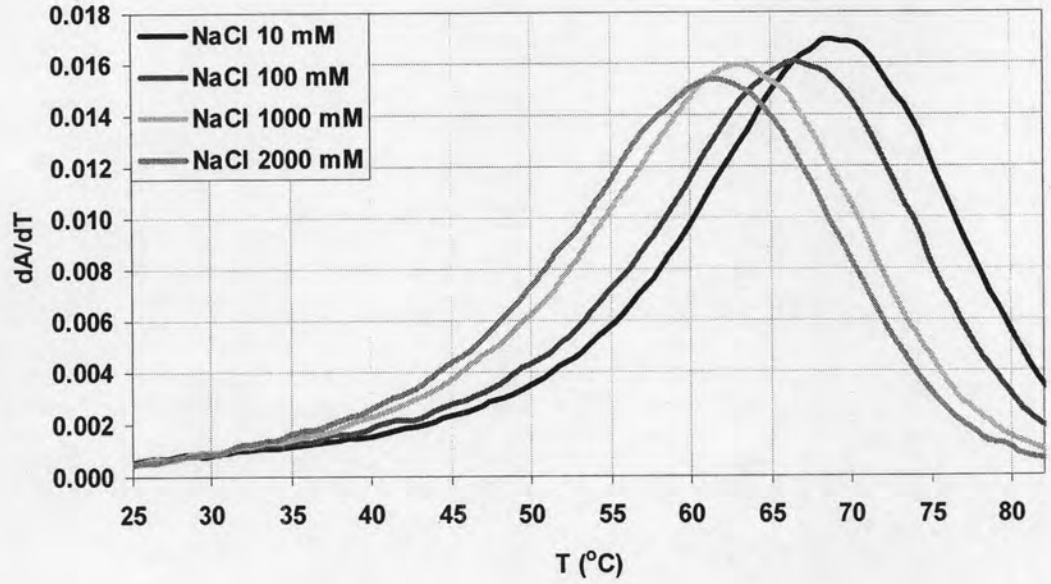

Figure E-10 First-derivative normalized UV-T_m plots between PNA *cis*-D/D-APC Ac-T_9-LysNH_2 with dA_9 at various salt concentration: Condition PNA:DNA = 1:1, [PNA] = 1 μM, 10 mM sodium phosphate buffer, pH 7.0, heating rate 1.0 °C/min.

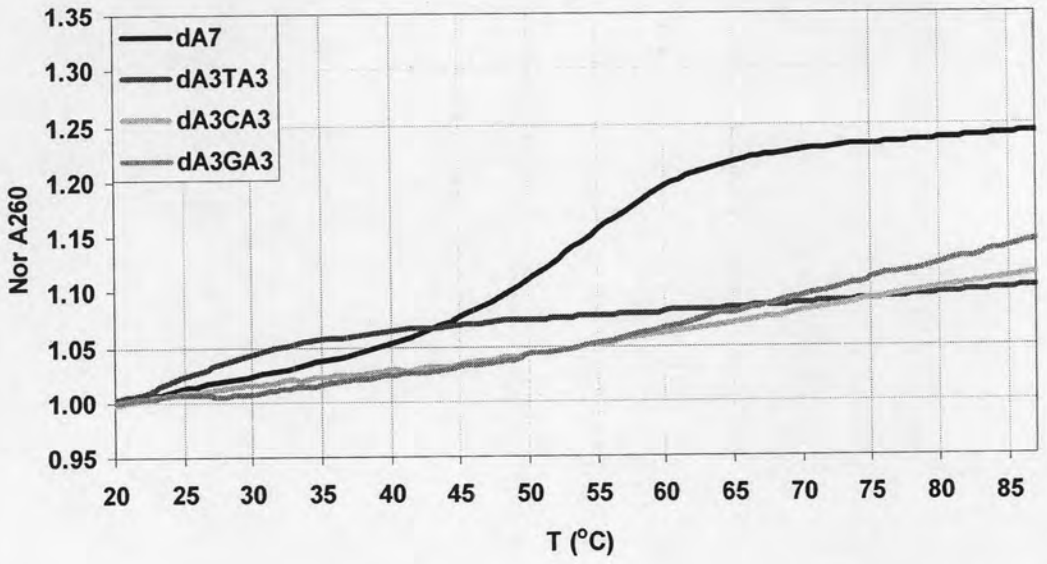

Figure E-11 T_m curves of PNA *cis*-D/D-APC Ac-TTTTTTT-LysNH$_2$ with DNA 5′-AAAXAAA-3′ (when X = T, A, C and G): Condition PNA:DNA = 1:1, [PNA] = 1 μM, 10 mM sodium phosphate buffer, pH 7.0, heating rate 1.0 °C/min.

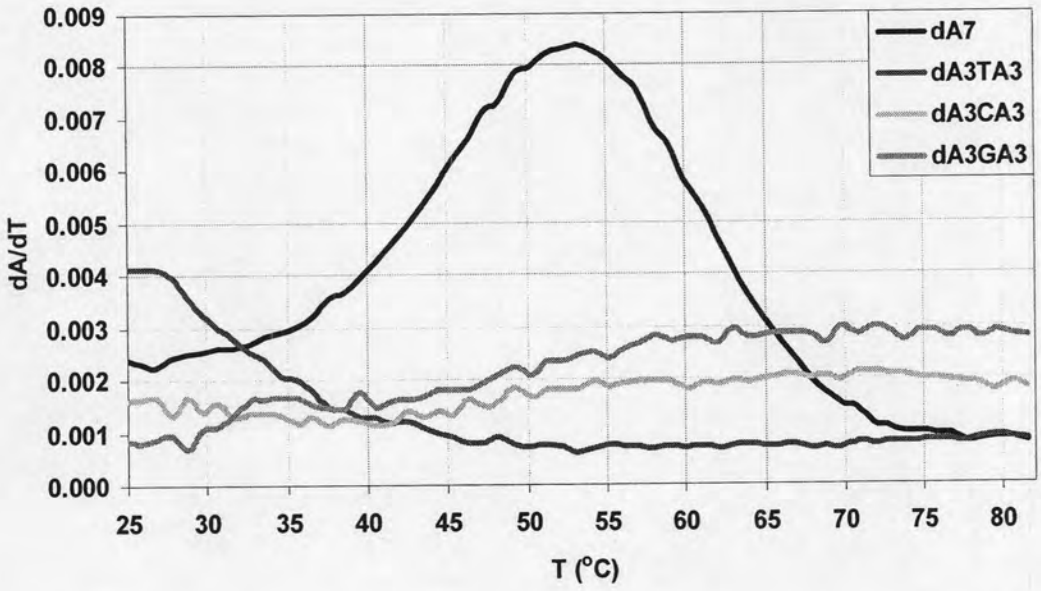

Figure E-12 First-derivative normalized UV-T_m plots between PNA *cis*-D/D-APC Ac-TTTTTTT-LysNH$_2$ with DNA 5′-AAAXAAA-3′ (when X = T, A, C and G): Condition PNA:DNA = 1:1, [PNA] = 1 μM, 10 mM sodium phosphate buffer, pH 7.0, heating rate 1.0 °C/min.

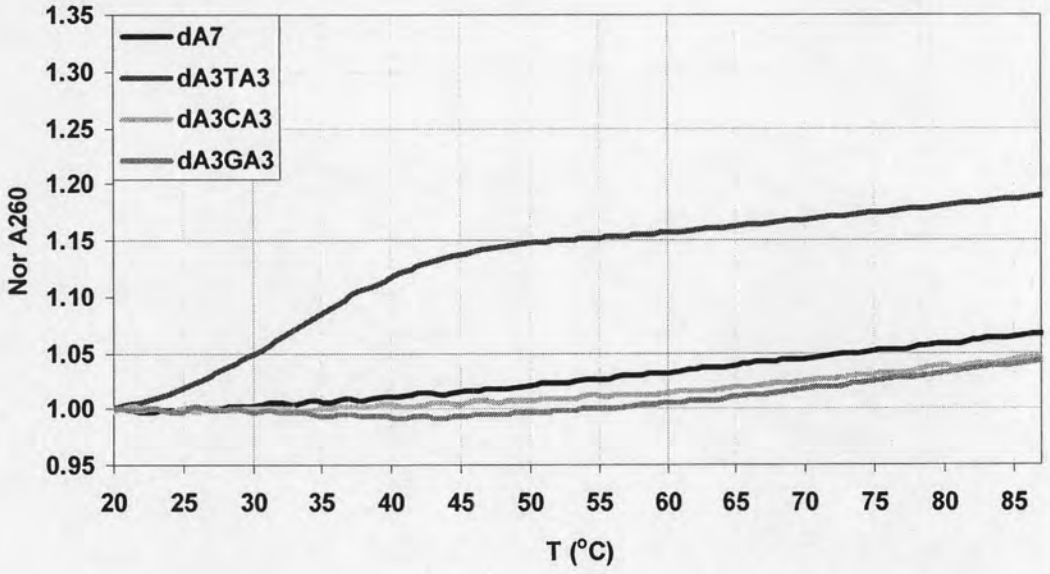

Figure E-13 T_m curves of PNA *cis*-D/D-APC Ac-TTTATTT-LysNH$_2$ with DNA 5′-AAAXAAA-3′ (when X = T, A, C and G): Condition PNA:DNA = 1:1, [PNA] = 1 μM, 10 mM sodium phosphate buffer, pH 7.0, heating rate 1.0 °C/min.

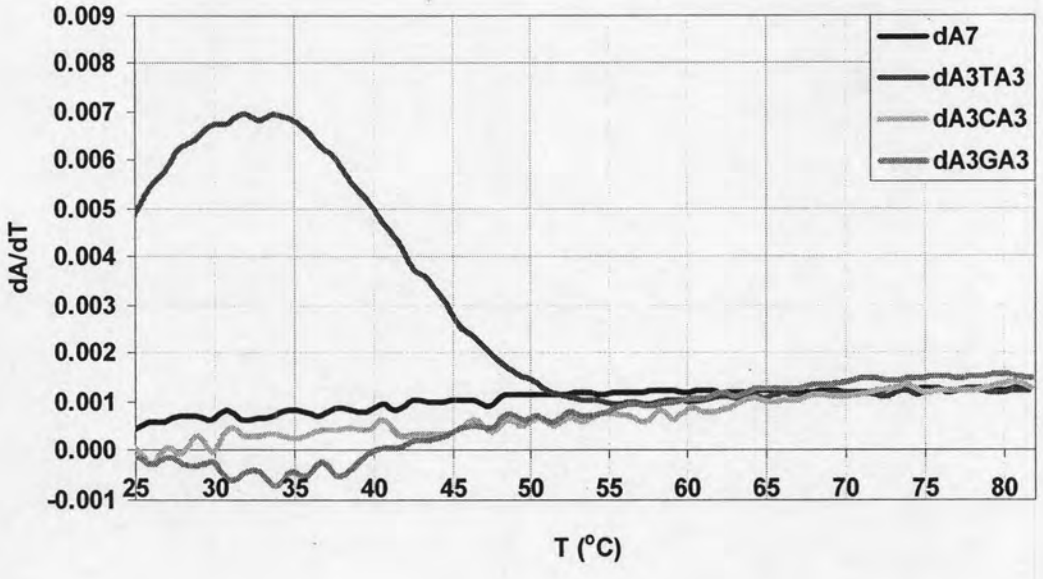

Figure E-14 First-derivative normalized UV-T_m plots between PNA *cis*-D/D-APC Ac-TTTATTT-LysNH$_2$ with DNA 5′-AAAXAAA-3′ (when X = T, A, C and G): Condition PNA:DNA = 1:1, [PNA] = 1 μM, 10 mM sodium phosphate buffer, pH 7.0, heating rate 1.0 °C/min.

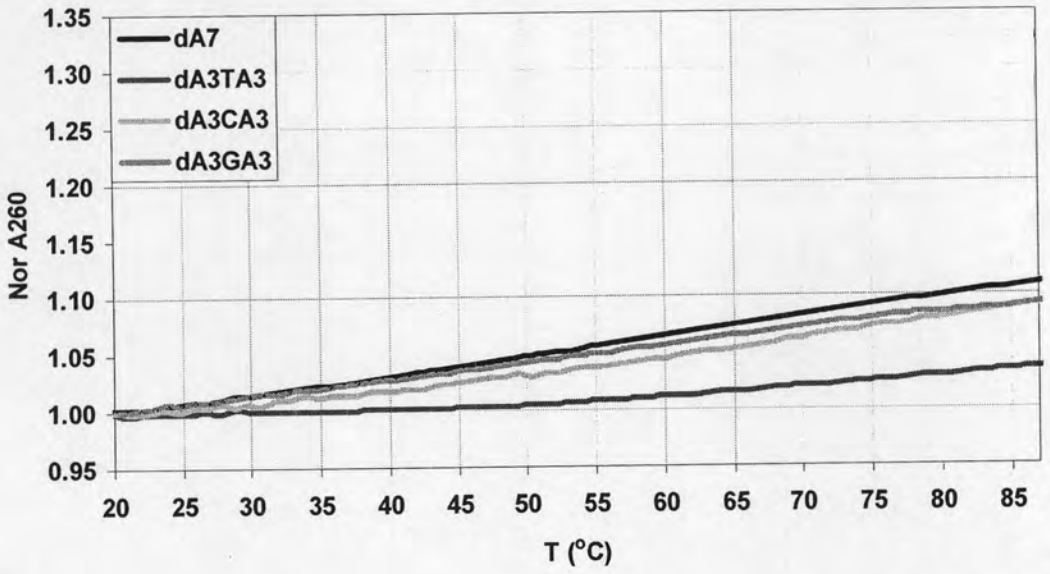

Figure E-15 T_m curves of PNA *cis*-D/D-APC Ac-TTTCTTT-LysNH$_2$ with DNA 5′-AAAXAAA-3′ (when X = T, A, C and G): Condition PNA:DNA = 1:1, [PNA] = 1 μM, 10 mM sodium phosphate buffer, pH 7.0, heating rate 1.0 °C/min.

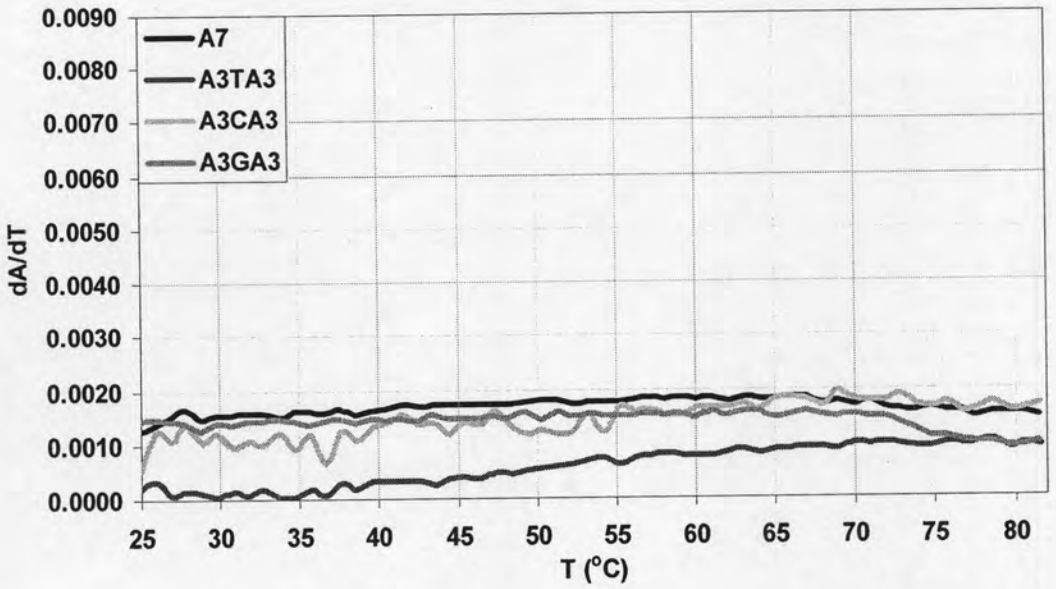

Figure E-16 First-derivative normalized UV-T_m plots between PNA *cis*-D/D-APC Ac-TTTCTTT-LysNH$_2$ with DNA 5′-AAAXAAA-3′ (when X = T, A, C and G): Condition PNA:DNA = 1:1, [PNA] = 1 μM, 10 mM sodium phosphate buffer, pH 7.0, heating rate 1.0 °C/min.

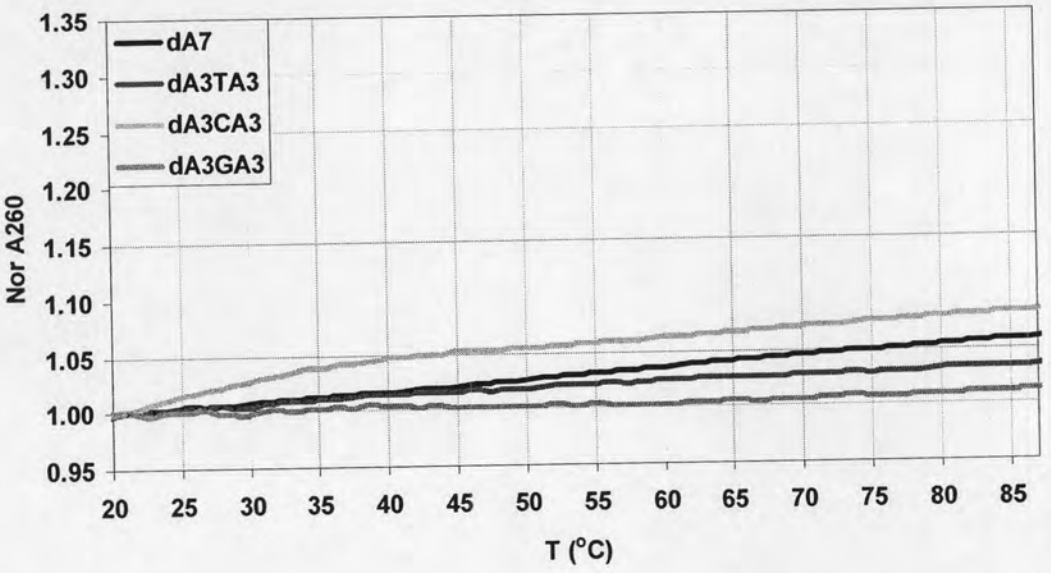

Figure E-17 T_m curves of PNA *cis*-D/D-APC Ac-TTTGTTT-LysNH$_2$ with DNA 5′-AAAXAAA-3′ (when X = T, A, C and G): Condition PNA:DNA = 1:1, [PNA] = 1 μM, 10 mM sodium phosphate buffer, pH 7.0, heating rate 1.0 °C/min.

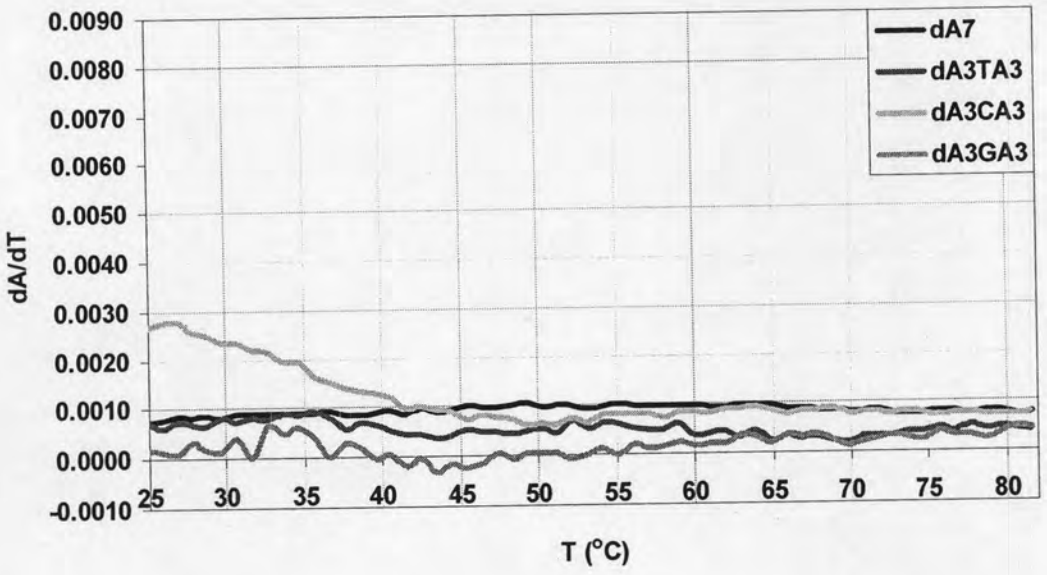

Figure E-18 First-derivative normalized UV-T_m plots between PNA *cis*-D/D-APC Ac-TTTGTTT-LysNH$_2$ with DNA 5′-AAAXAAA-3′ (when X = T, A, C and G): Condition PNA:DNA = 1:1, [PNA] = 1 μM, 10 mM sodium phosphate buffer, pH 7.0, heating rate 1.0 °C/min.

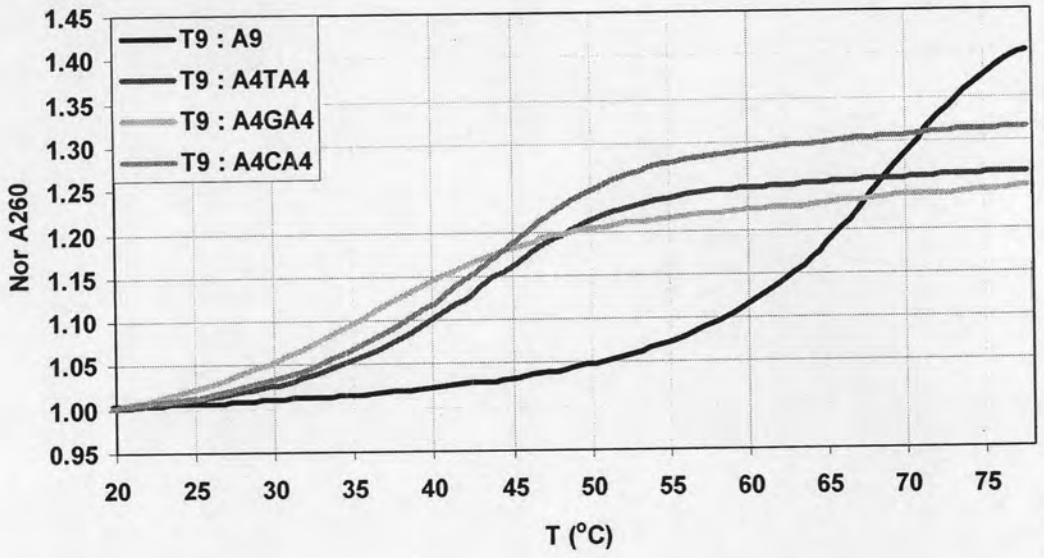

Figure E-19 T_m curves of PNA *cis*-D/D-APC Ac-TTTTTTTTT-LysNH$_2$ with DNA 5′-AAAAXAAAA-3′ (when X = T, A, C and G): Condition PNA:DNA = 1:1, [PNA] = 1 μM, 10 mM sodium phosphate buffer, pH 7.0, heating rate 1.0 °C/min.

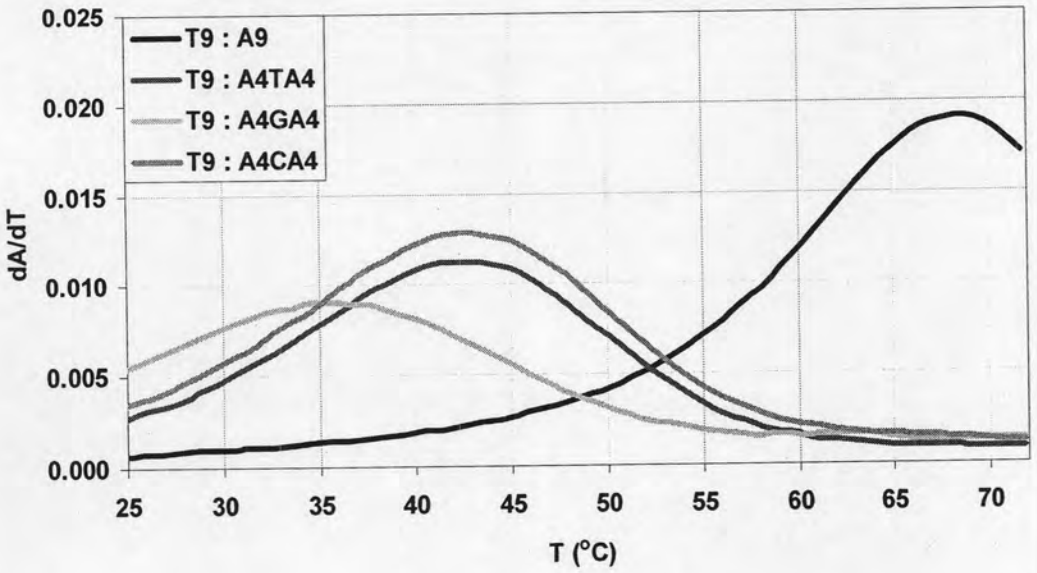

Figure E-20 First-derivative normalized UV-T_m plots between PNA *cis*-D/D-APC Ac-TTTTTTTTT-LysNH$_2$ with DNA 5′-AAAAXAAAA-3′ (when X = T, A, C and G): Condition PNA:DNA = 1:1, [PNA] = 1 μM, 10 mM sodium phosphate buffer, pH 7.0, heating rate 1.0 °C/min.

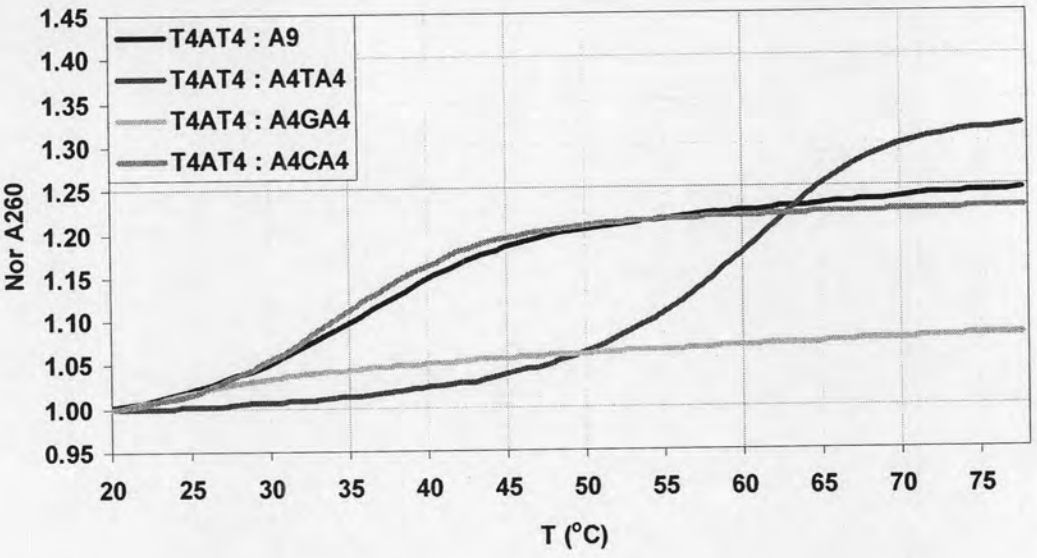

Figure E-21 T_m curves of PNA *cis*-D/D-APC Ac-TTTTATTTT-LysNH$_2$ with DNA 5′-AAAAXAAAA-3′ (when X = T, A, C and G): Condition PNA:DNA = 1:1, [PNA] = 1 μM, 10 mM sodium phosphate buffer, pH 7.0, heating rate 1.0 °C/min.

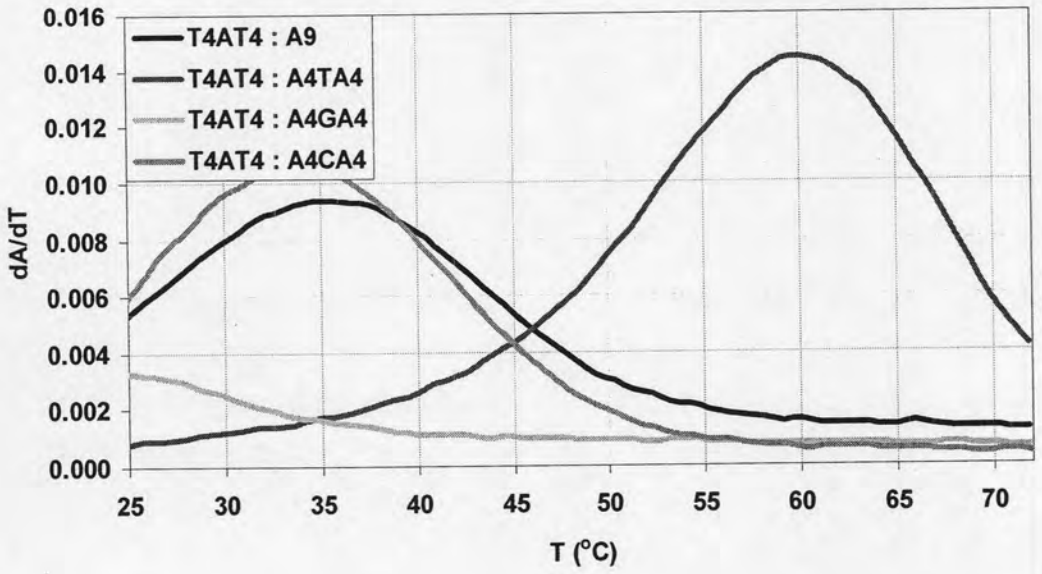

Figure E-22 First-derivative normalized UV-T_m plots between PNA *cis*-D/D-APC Ac-TTTTATTTT-LysNH$_2$ with DNA 5′-AAAAXAAAA-3′ (when X = T, A, C and G): Condition PNA:DNA = 1:1, [PNA] = 1 μM, 10 mM sodium phosphate buffer, pH 7.0, heating rate 1.0 °C/min.

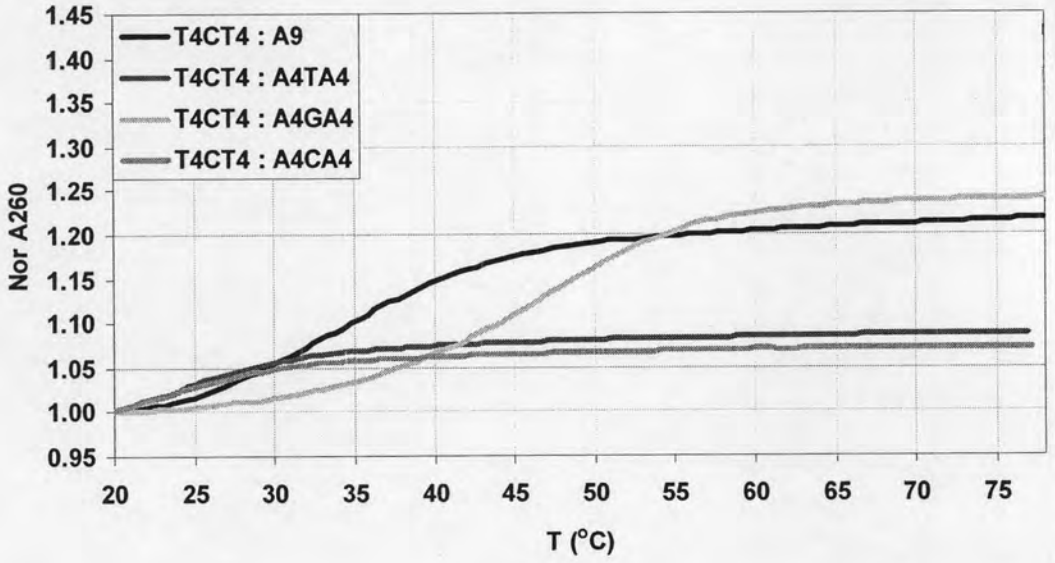

Figure E-23 T_m curves of PNA *cis*-D/D-APC Ac-TTTTCTTTT-LysNH$_2$ with DNA 5′-AAAAXAAAA-3′ (when X = T, A, C and G): Condition PNA:DNA = 1:1, [PNA] = 1 μM, 10 mM sodium phosphate buffer, pH 7.0, heating rate 1.0 °C/min.

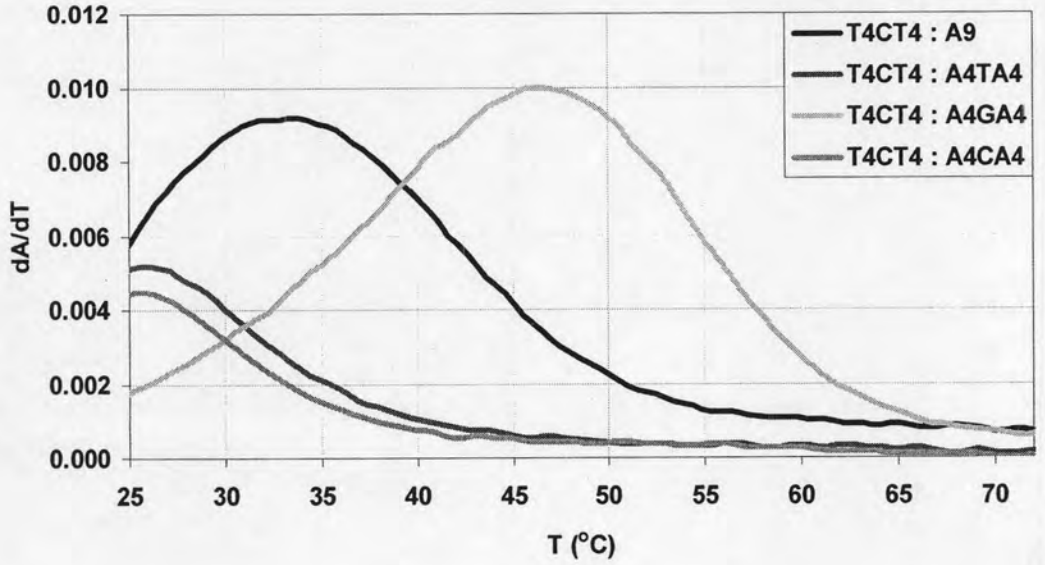

Figure E-24 First-derivative normalized UV-T_m plots between PNA *cis*-D/D-APC Ac-TTTTCTTTT-LysNH$_2$ with DNA 5′-AAAAXAAAA-3′ (when X = T, A, C and G): Condition PNA:DNA = 1:1, [PNA] = 1 μM, 10 mM sodium phosphate buffer, pH 7.0, heating rate 1.0 °C/min.

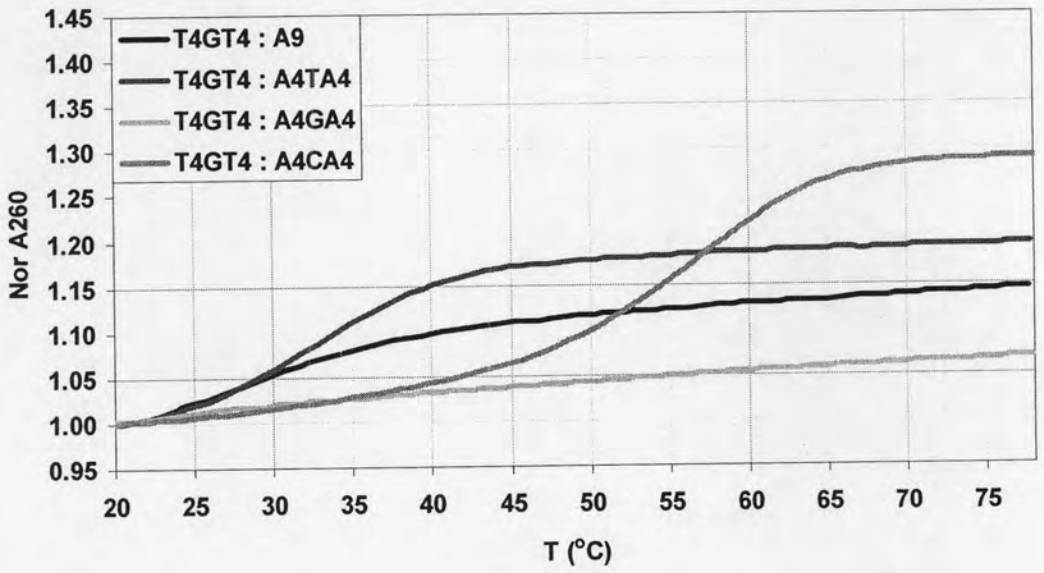

Figure E-25 T_m curves of PNA *cis*-D/D-APC Ac-TTTTGTTTT-LysNH$_2$ with DNA 5′-AAAAXAAAA-3′ (when X = T, A, C and G): Condition PNA:DNA = 1:1, [PNA] = 1 μM, 10 mM sodium phosphate buffer, pH 7.0, heating rate 1.0 °C/min.

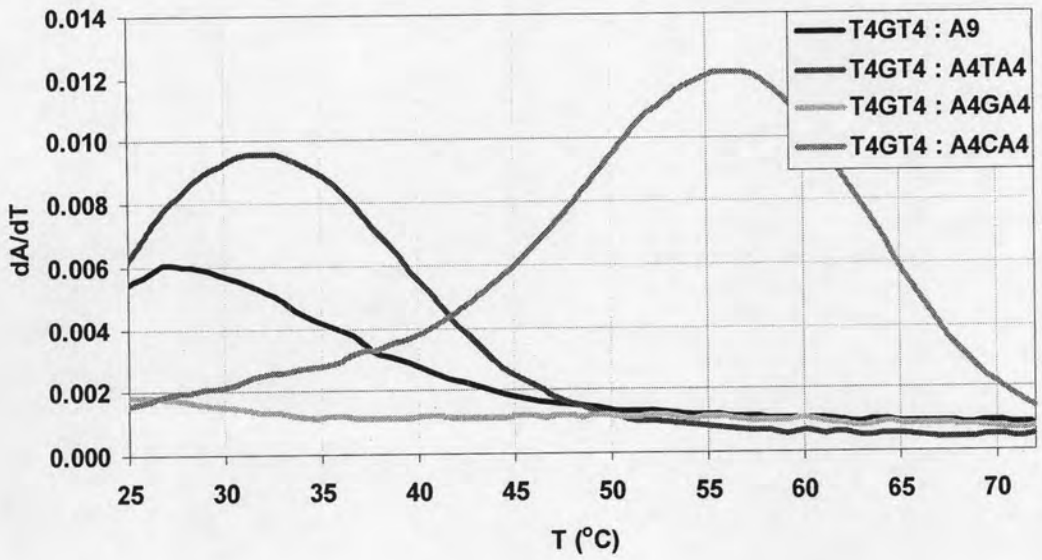

Figure E-26 First-derivative normalized UV-T_m plots between PNA *cis*-D/D-APC Ac-TTTTGTTTT-LysNH$_2$ with DNA 5′-AAAAXAAAA-3′ (when X = T, A, C and G): Condition PNA:DNA = 1:1, [PNA] = 1 μM, 10 mM sodium phosphate buffer, pH 7.0, heating rate 1.0 °C/min.

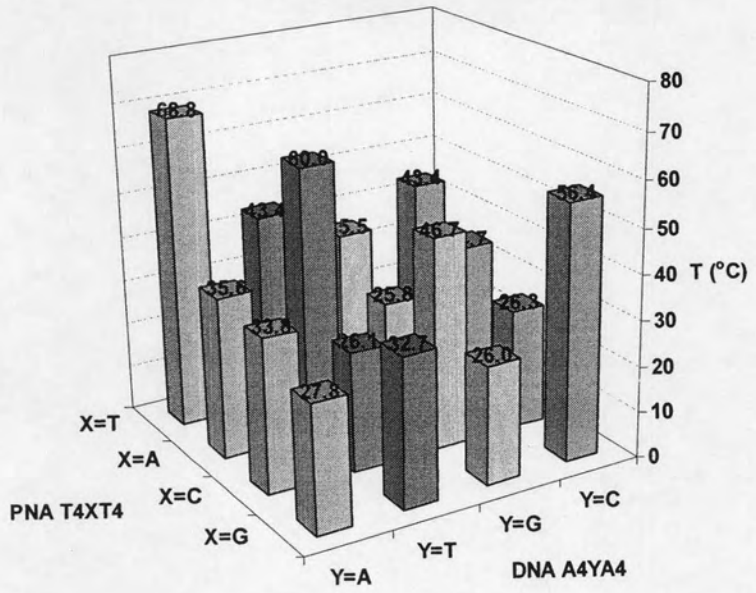

Figure E-27 3-D column graph of T_m values of *cis*-D/D-APC Ac-TTTTXTTTT-$LysNH_2$ (when X = T, A, C and G) with DNA 5′-AAAAYAAAA-3′ (when Y = T, A, C and G).

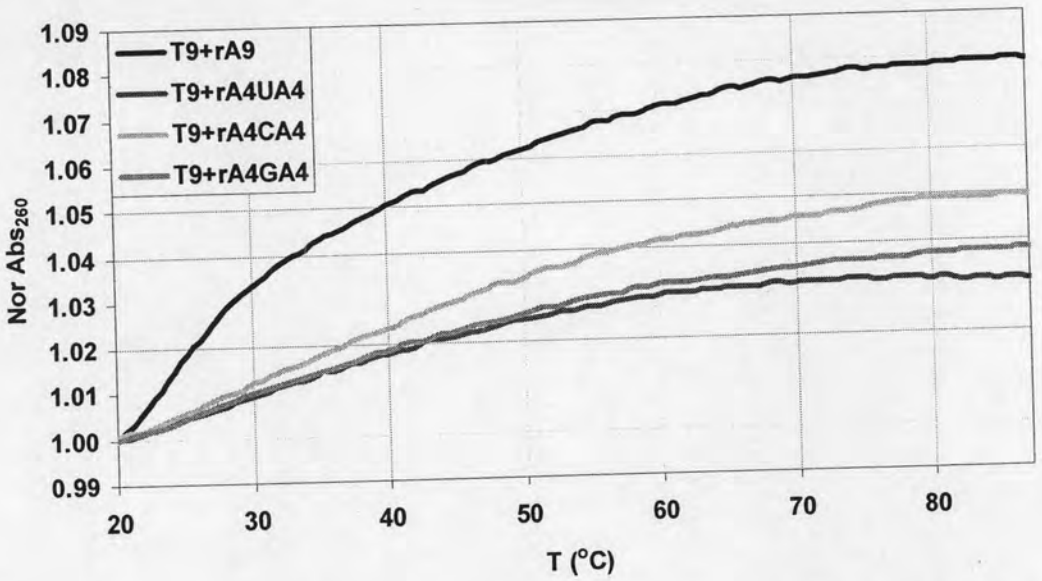

Figure E-28 T_m curves of PNA *cis*-D/D-APC Ac-TTTTTTTTT-LysNH$_2$ with RNA 5′-AAAAXAAAA-3′ (when X = A, U, C and G): Condition PNA:RNA = 1:1, [PNA] = 1 μM, 10 mM sodium phosphate buffer, pH 7.0, heating rate 1.0 °C/min.

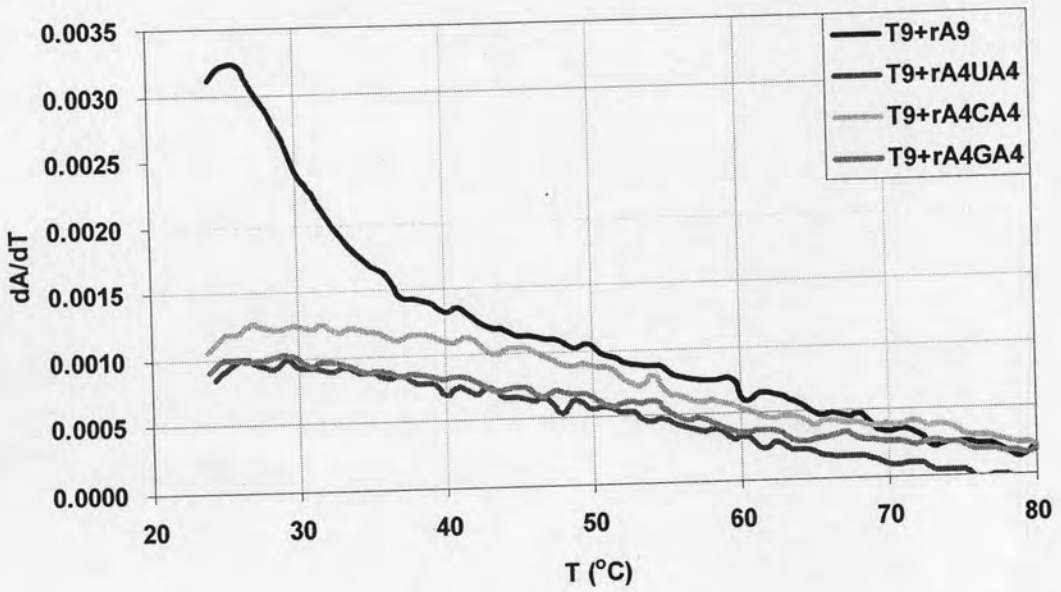

Figure E-29 First-derivative normalized UV-T_m plots between PNA *cis*-D/D-APC Ac-TTTTTTTTT-LysNH$_2$ with RNA 5′-AAAAXAAAA-3′ (when X = A, U, C and G): Condition PNA:RNA = 1:1, [PNA] = 1 μM, 10 mM sodium phosphate buffer, pH 7.0, heating rate 1.0 °C/min.

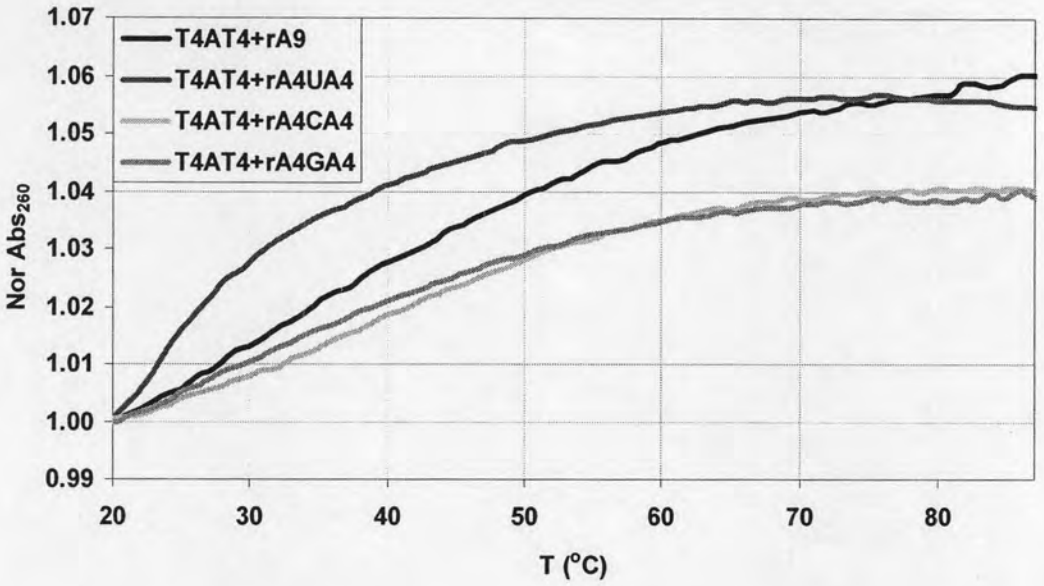

Figure E-30 T_m curves of PNA *cis*-D/D-APC Ac-TTTTATTTT-LysNH$_2$ with RNA 5′-AAAAXAAAA-3′ (when X = A, U, C and G): Condition PNA:RNA = 1:1, [PNA] = 1 μM, 10 mM sodium phosphate buffer, pH 7.0, heating rate 1.0 °C/min.

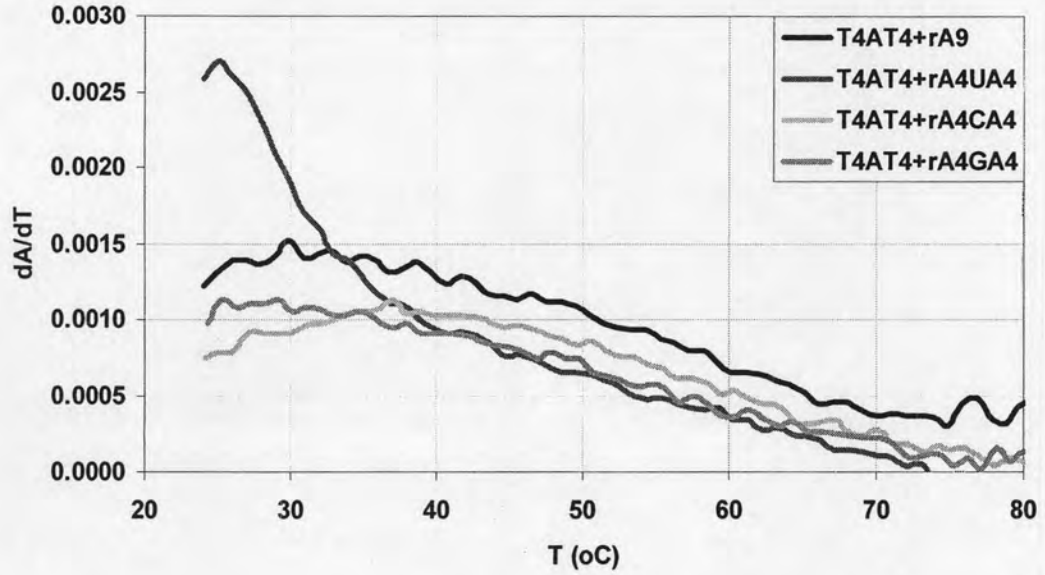

Figure E-31 First-derivative normalized UV-T_m plots between PNA *cis*-D/D-APC Ac-TTTTATTTT-LysNH$_2$ with RNA 5′-AAAAXAAAA-3′ (when X = A, U, C and G): Condition PNA:RNA = 1:1, [PNA] = 1 μM, 10 mM sodium phosphate buffer, pH 7.0, heating rate 1.0 °C/min.

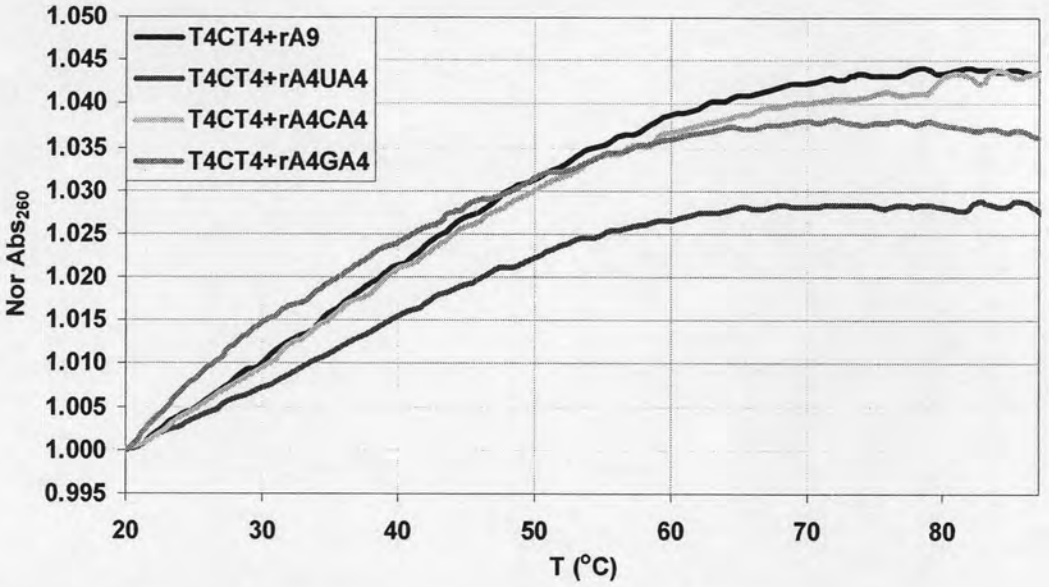

Figure E-32 T_m curves of PNA *cis*-D/D-APC Ac-TTTTCTTTT-LysNH$_2$ with RNA 5′-AAAAXAAAA-3′ (when X = A, U, C and G): Condition PNA:RNA = 1:1, [PNA] = 1 μM, 10 mM sodium phosphate buffer, pH 7.0, heating rate 1.0 °C/min.

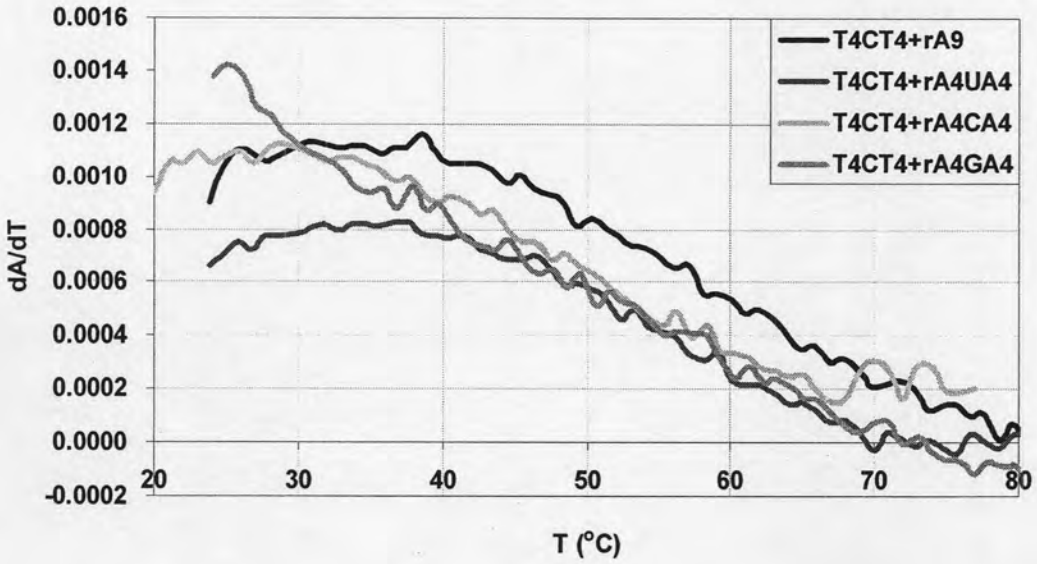

Figure E-33 First-derivative normalized UV-T_m plots between PNA *cis*-D/D-APC Ac-TTTTCTTTT-LysNH$_2$ with RNA 5′-AAAAXAAAA-3′ (when X = A, U, C and G): Condition PNA:RNA = 1:1, [PNA] = 1 μM, 10 mM sodium phosphate buffer, pH 7.0, heating rate 1.0 °C/min.

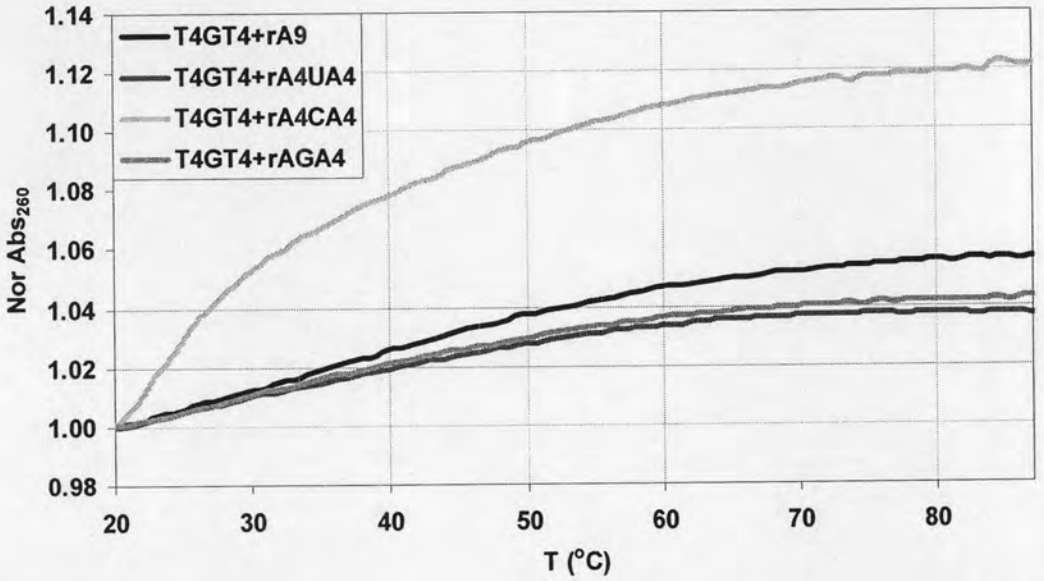

Figure E-34 T_m curves of PNA *cis*-D/D-APC Ac-TTTTGTTTT-LysNH$_2$ with RNA 5′-AAAAXAAAA-3′ (when X = A, U, C and G): Condition PNA:RNA = 1:1, [PNA] = 1 μM, 10 mM sodium phosphate buffer, pH 7.0, heating rate 1.0 °C/min.

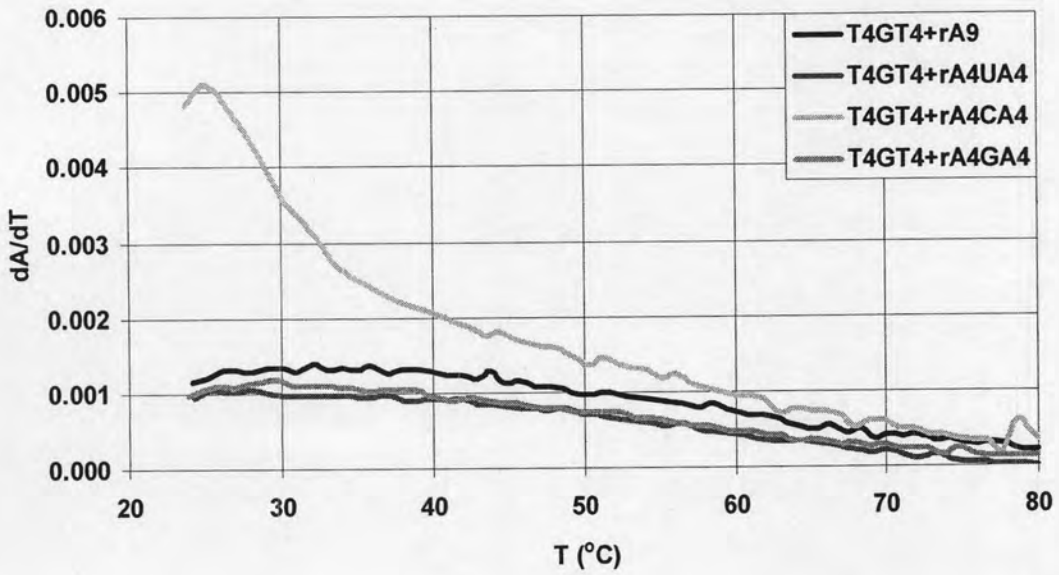

Figure E-35 First-derivative normalized UV-T_m plots between PNA *cis*-D/D-APC Ac-TTTTGTTTT-LysNH$_2$ with RNA 5′-AAAAXAAAA-3′ (when X = A, U, C and G): Condition PNA:RNA = 1:1, [PNA] = 1 μM, 10 mM sodium phosphate buffer, pH 7.0, heating rate 1.0 °C/min.

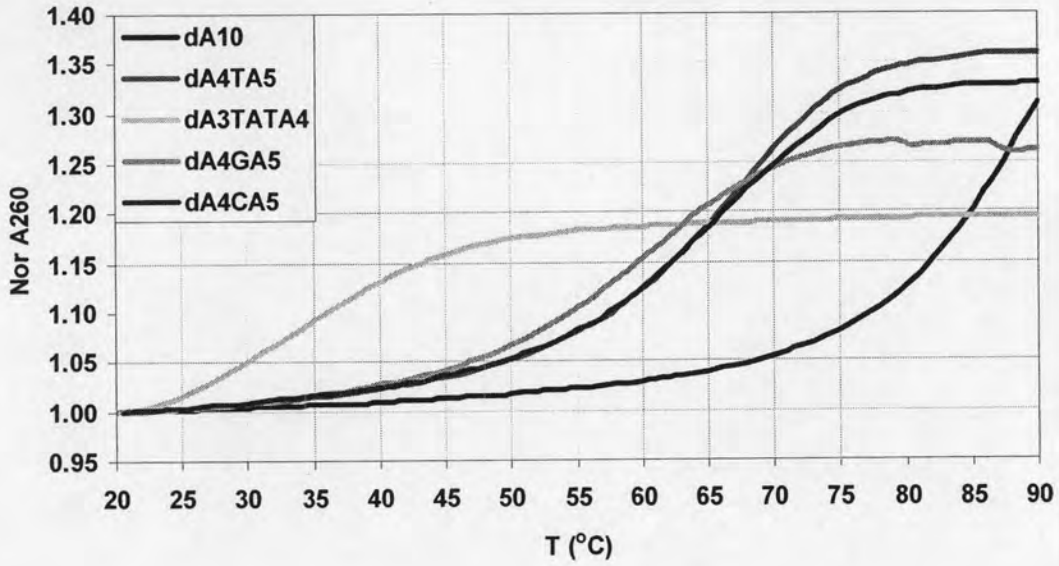

Figure E-36 T_m curves of PNA *cis*-D/(1*S*,2*S*)-ACPC H-TTTTTTTTTT-LysNH$_2$ with DNA 5′-AAAAXAAAAA-3′ (when X = T, A, C and G) and 5′-AAATATAAAA-3′: Condition PNA:DNA = 1:1, [PNA] = 1 μM, 10 mM sodium phosphate buffer, pH 7.0, heating rate 1.0 °C/min.

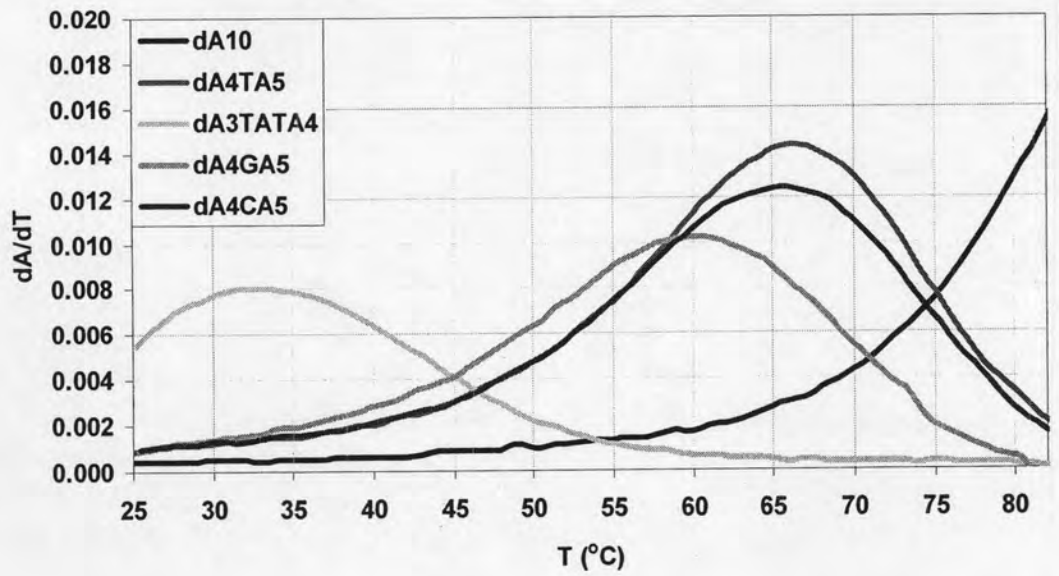

Figure E-37 First-derivative normalized UV-T_m plots between PNA *cis*-D/(1*S*,2*S*)-ACPC H-TTTTTTTTTT-LysNH$_2$ with DNA 5′-AAAAXAAAAA-3′ (when X = T, A, C and G) and 5′-AAATATAAAA-3′: Condition PNA:DNA = 1:1, [PNA] = 1 μM, 10 mM sodium phosphate buffer, pH 7.0, heating rate 1.0 °C/min.

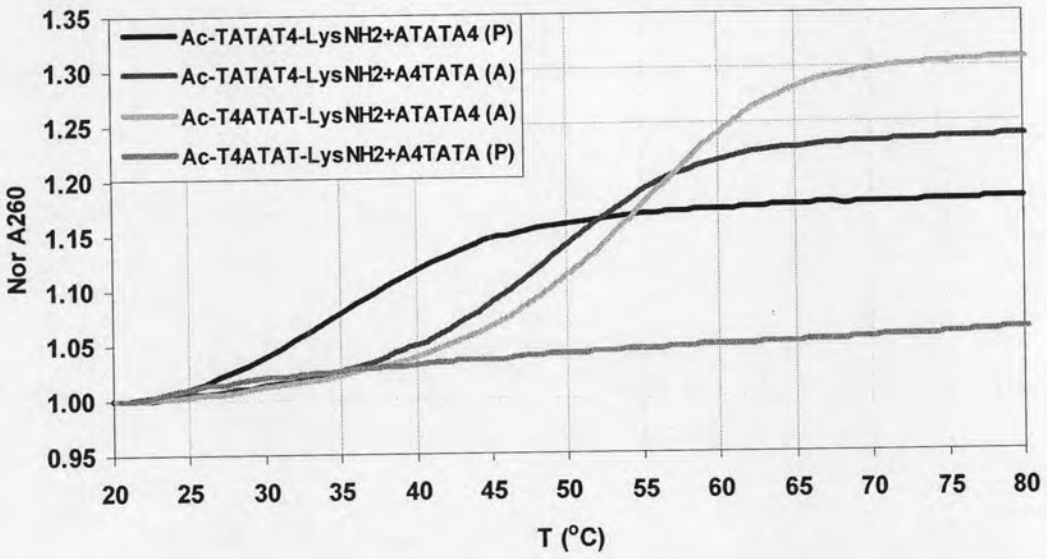

Figure E-38 T_m curves of PNA *cis*-D/D-APC Ac-TATATTTT-LysNH$_2$ and *cis*-D/D-APC Ac-TTTTATAT-LysNH$_2$ with DNA 5′-AAAATATA-3′ and 5′-ATATAAAA-3′ : Condition PNA:DNA = 1:1, [PNA] = 1 μM, 10 mM sodium phosphate buffer, pH 7.0, heating rate 1.0 °C/min.

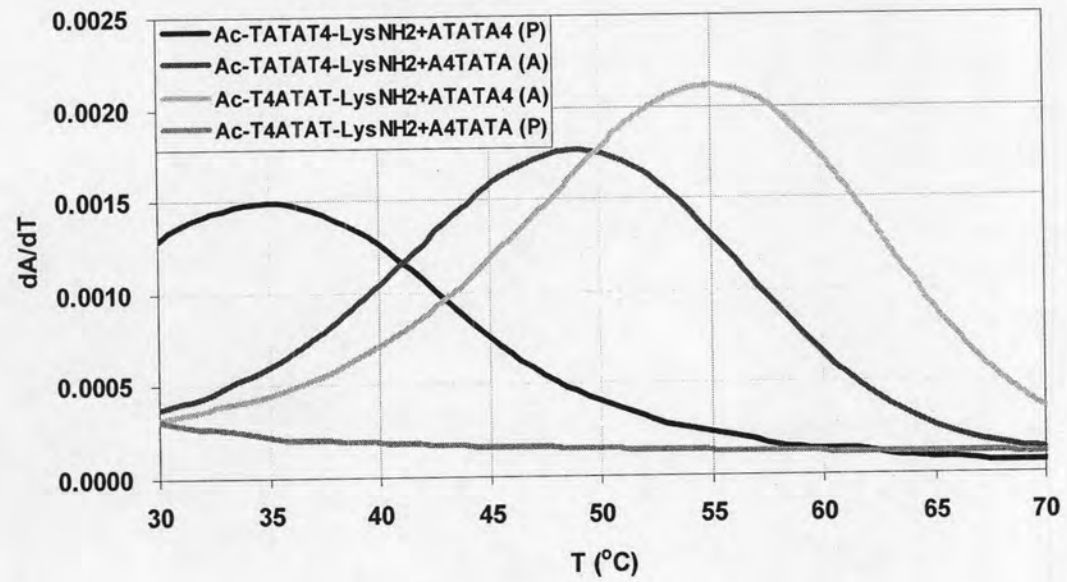

Figure E-39 First-derivative normalized UV-T_m plots between PNA *cis*-D/D-APC Ac-TATATTTT-LysNH$_2$ and *cis*-D/D-APC Ac-TTTTATAT-LysNH$_2$ with DNA 5′-AAAATATA-3′ and 5′-ATATAAAA-3′: Condition PNA:DNA = 1:1, [PNA] = 1 μM, 10 mM sodium phosphate buffer, pH 7.0, heating rate 1.0 °C/min.

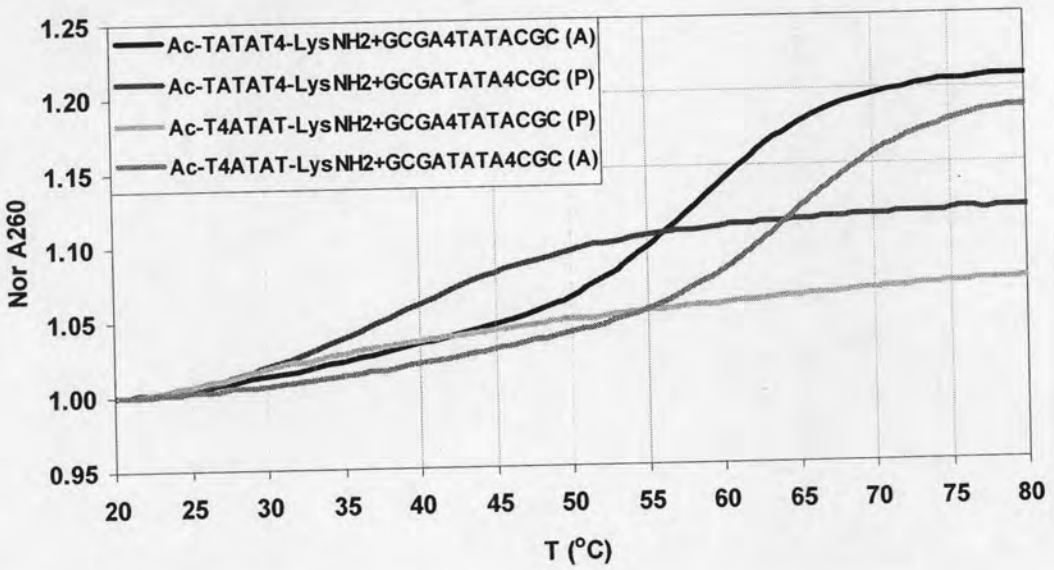

Figure E-40 T_m curves of PNA *cis*-D/D-APC Ac-TATATTTT-LysNH$_2$ and *cis*-D/D-APC Ac-TTTTATAT-LysNH$_2$ with DNA 5′-GCGAAAATATACGC-3′ and 5′-GCGATATAAAACGC-3′ : Condition PNA:DNA = 1:1, [PNA] = 1 μM, 10 mM sodium phosphate buffer, pH 7.0, heating rate 1.0 °C/min.

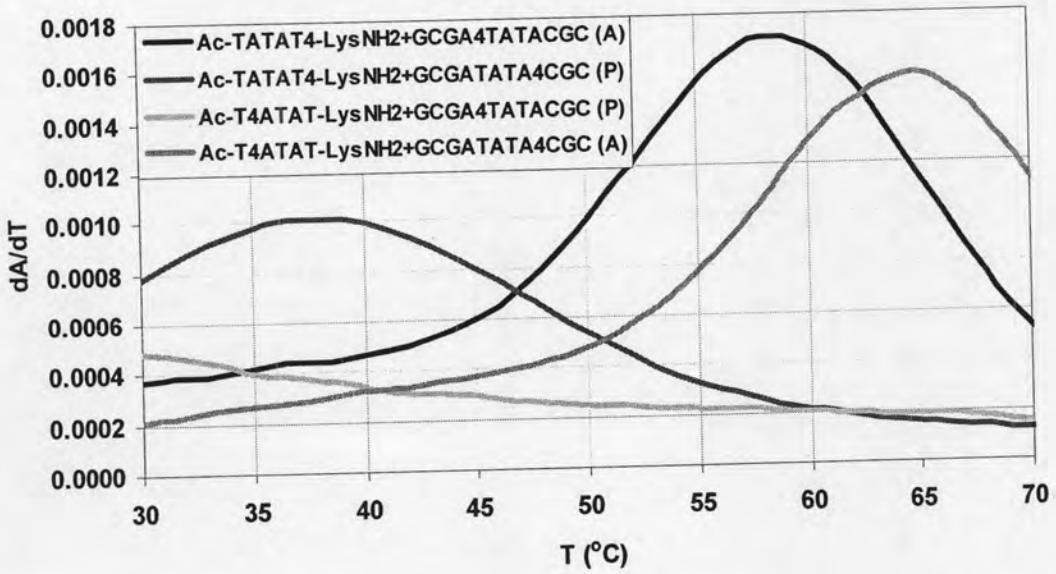

Figure E-41 First-derivative normalized UV-T_m plots between PNA *cis*-D/D-APC Ac-TATATTTT-LysNH$_2$ and *cis*-D/D-APC Ac-TTTTATAT-LysNH$_2$ with DNA 5′-GCGAAAATATACGC-3′ and 5′-GCGATATAAAACGC-3′: Condition PNA:DNA = 1:1, [PNA] = 1 μM, 10 mM sodium phosphate buffer, pH 7.0, heating rate 1.0 °C/min.

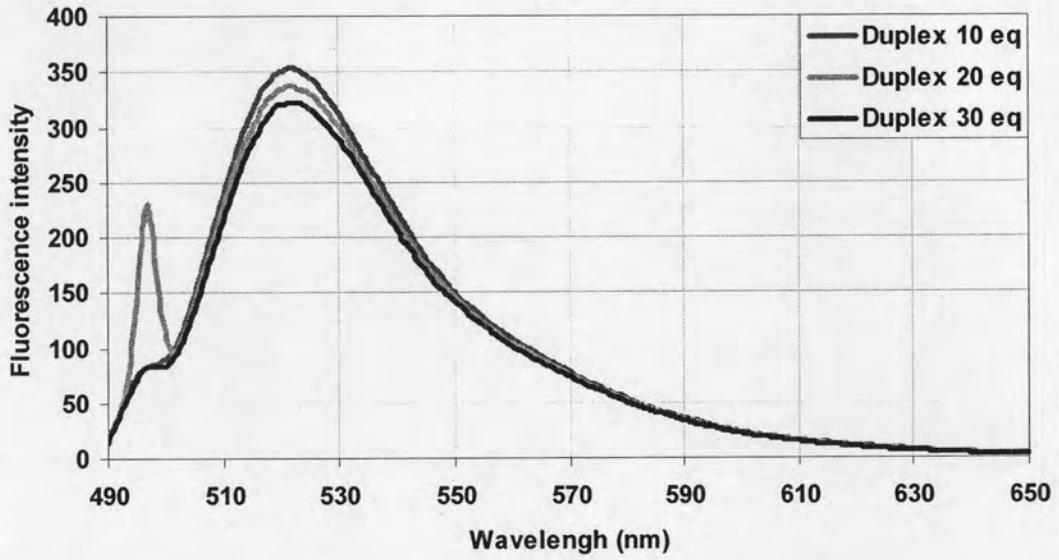

Figure E-42 The fluorescence measurement of PNA *cis*-D/D-APC Ac-TTTTATA-Lys(FAM)-NH_2 **(P23)** and DNA probes for parallel binding. Condition [PNA] = 1 μM, 10 mM sodium phosphate buffer, pH 7.0.

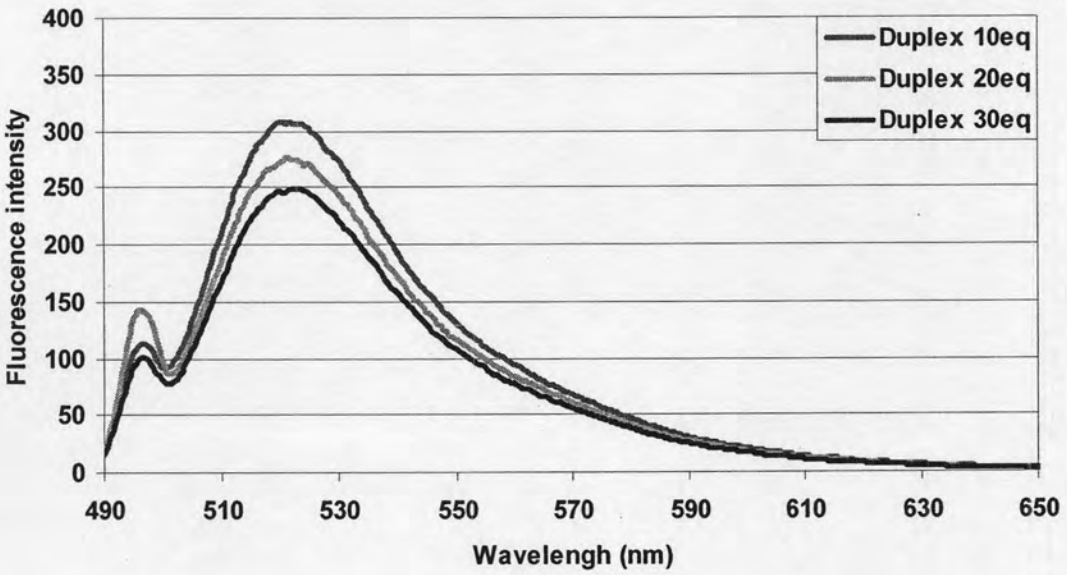

Figure E-43 The fluorescence measurement of PNA *cis*-D/D-APC Ac-TTTTATA-Lys(FAM)-NH_2 **(P23)** and DNA probes for antiparallel binding. Condition [PNA] = 1 μM, 10 mM sodium phosphate buffer, pH 7.0.

CURRICULUM VITAE

PERSONAL INFORMATION

Name Mr. Chaturong Suparpprom
Nationality Thai
Religion Buddhism
Birth Date Oct 17, 1978
Address 27/22 Soi 39, Rama II Rd. Bangmod, Chomthong, Bangkok, 10150

GRADUATE AND POSTGRADUATE STUDIES

2000-2006 Student in Doctor of Philosophy
Chulalongkorn University, Bangkok, Thailand
1996-1999 Bachelor of Science (B.Sc.) in Chemistry (Second Class Honors)
Chulalongkorn University, Bangkok, Thailand

SCHOLARSHIPS

2002-2006 Promotion 'Royal Golden Jubilee' Grant
1993-2001 The Development and Promotion of Science and Technology Talent Project (DPST)

PUBLICATIONS

1. **Suparpprom, C.**; Vilaivan, T., Synthesis of 2-[4'-(ethylearbamoyl)phenyl]-*N*-acetylglycine, the proposed structure for giganticine. *J. Nat. Prod.* **2001**, 64(8), 1114-1116.

2. Vilaivan, T.; **Suparpprom, C.**; Harnyuttanakorn, P.; Lowe, G., Synthesis and properties of novel pyrrolidinyl PNA carrying β-amino acid spacers. *Tetrahedron Lett.* **2001**, *42*, 5533-5536.

3. Vilaivan, T.; **Suparpprom, C.**; Duanglaor, P.; Harnyuttanakorn, P.; Lowe, G., Synthesis and Nucleic Acid Binding Studies of Novel Pyrrolidinyl PNA Carrying an *N*-amino-*N*-methylglycine Spacer. *Tetrahedron Lett.* **2003**, *44*, 1663-1666.

4. **Suparpprom, C.**; Srisuwannaket, C.; Sangvanich, P.; Vilaivan, T., Synthesis and Oligodeoxynucleotide Binding Properties of Pyrrolidinyl Peptide Nucleic Acids Bearing Prolyl-2-aminocyclopentanecarboxylic Acid (ACPC) Backbones. *Tetrahedron Lett.* **2005**, *46*, 2833-2837.